Identification and characterization of a novel capsule-like complex surface antigen of *Francisella tularensis*

Anna Elizabeth Champion

Dissertation submitted to the faculty of the Virginia Polytechnic Institute and State University in partial fulfillment of the requirements for the degree of

Doctor of Philosophy
In
Biomedical and Veterinary Sciences

Thomas Inzana, Chair
Stephen Boyle
Richard Helm
Stephen Melville

November 18, 2014
Blacksburg, VA

Keywords: *Francisella*, capsule, glycoprotein, biofilm, vaccine

Copyright Anna E. Champion, 2014

Identification and characterization of a novel capsule-like complex surface antigen of *Francisella tularensis*

Anna Elizabeth Champion

ABSTRACT

Francisella tularensis is a highly virulent zoonotic pathogen that is the causative agent of tularemia in humans. Two subspecies of *F. tularensis* are the most virulent in humans: *tularensis* (type A) and *holarctica* (type B), with less than 10 organisms via aerosol of a type A strain having the ability to cause fatal infection. Over the last decade much research has been done on the pathogenesis of this unique intracellular bacterium and many different virulence factors have been identified. The goal of this dissertation has been to identify and characterize the capsule-like complex (CLC) surface antigen of *F. tularensis*, and to determine its role in virulence and immunoprotection in a mouse model. In addition, I have investigated the role of CLC in biofilm formation.

The CLC appears as a negatively staining material surrounding *F. tularensis* cells during transmission electron microscopy (TEM). I found that the CLC in the type B live vaccine strain (LVS) could be significantly diminished by deleting two glycosyl transferase genes (LVSΔ1423-22) in the putative polysaccharide locus, FTL_1432-FTL_1421. In addition, I determined that the CLC was not a typical polysaccharide capsule, but was in fact composed of over 50 proteins and glycoproteins including known virulence determinants, such as GroEL, DnaK, and ClpB. Upon further evaluation of the CLC, I determined that it was composed of an increase in production of outer membrane vesicles and tubules (OMV/T). These OMV/T appeared to be

self-aggregating into what I visualized through TEM as the CLC. LVSΔ1423-22 was attenuated in the mouse model, and BALB/c mice immunized with CLC and adjuvant were protected against challenge with LVS. In addition to virulence, the CLC appears to play a role in biofilm formation and development. *F. tularensis* type B strains lacking the surface antigens CLC or CLC and O-antigen, develop a 2-7-fold more robust biofilm than the parent strains. The biofilm matrix contains a glucan-like EPS, proteins, and extracellular DNA, and further characterization may lead to determining if the biofilm acts as an environmental survival mechanism for *F. tularensis*.

In summary, the CLC appears to be a novel surface antigen composed of upregulated OMV/T that is present in type A and B *F. tularensis*. Deficiency in CLC contributes to increased biofilm formation that could contribute to the survival of *F. tularensis* in a wide range of environmental niches. Furthermore, the CLC contributes to virulence of type B strains and elicits a protective immune response to type B challenge. A CLC-deficient type A strain could be a candidate for a new live vaccine strain, and therefore further investigation of such a mutant is warranted.

DEDICATION

I would like to dedicate this work to my parents, Ed Champion and Peggy Layne. Without your invaluable support and love, I would not have been able to accomplish this dream. And to my son, Jack, forever supportive and sometimes helpful, I love you!

ACKNOWLEDGEMENTS

I would like to thank Dr. Tom Inzana for providing me the opportunity to learn and work in his laboratory for the last decade. The colleagues I have had the opportunity to work with and the skills I have gained have made me a better scientist.

I would like to thank my committee members: Dr. Stephen Boyle, Dr. Stephen Melville and Dr. Richard Helm for providing their guidance and input throughout my graduate studies.

I would like to thank my current and previous lab members, especially Dr. Abey Bandara, Cheryl Ryder, Gretchen Berg, Dr. Indra Sandal, Dr. Jane Duncan, Nehal Shah and Dr. Yu Pan for their support in my research and life outside of lab.

I would like to thank the Department of Biomedical Sciences and Pathobiology and everybody at the Veterinary School graduate program, specifically Becky Jones for their support.

Ii would like to thank my parents Ed and Peggy for the opportunity to further my education and their unending support and encouragement throughout the years.

TABLE OF CONTENTS

LIST OF TABLES

LIST OF FIGURES

LIST OF ABBREVIATIONS

2-D:	Two-dimensional
ADH:	adipic acid dihydrazide
Amp:	ampicillin
BCA:	bicinchoninic acid assay
BHI(B/A):	Brain Heart Infusion (broth/agar)
BHI(B/A):	Brain Heart Infusion broth/agar
Bp:	base pairs
BSL:	biosafety level
C:	Celsius
CDC:	Center for Disease Control and Prevention
CDM(A/B):	Chamberlain's defined media (agar/broth)
cDNA:	complementary deoxyribonucleic acid
CFU:	colony forming unit
CLC:	capsule-like complex
CLSM:	confocal laser scanning microscopy
ConA:	Concavalin A
CP:	capsule
CV:	crystal violet
DMEM:	Dulbecco's Modified Eagle Medium
DNA:	deoxyribonucleaic acid
DTT:	dithiothreitol
EDAC:	1-ethyl-3-(3-dimethylaminopropy)carbodiimide
EPS:	exopolysaccharide
FCP:	*Francisella*-containing phagosome
FPI:	*Francisella* Pathogenicity Island
g:	grams
GalNAc:	N-acetyl galactosamine
GC/MS:	gas chromatography/mass spectrometry
Glc:	Glucose
h:	hours
HEPES:	4-2-*hydroxyethyl*)-1-piperazineethanesulfonic acid
HI:	hyperimmune
HMW:	high molecular weight
HRP:	horseradish peroxidase
IFN-γ:	interferon gamma
IN:	intranasal
IP:	intraperitoneal
Kan:	kanamycin
kDa:	kilo dalton
KDO:	3-deoxy-D-*manno*-2-octulosonic acid
KLH:	keyhole limpet hemocyanin
LB(B/A):	Luria-Bertani (broth/agar)
LC-MS/MS:	liquid chromatography mass spectrometry
LPS:	lipopolysaccharide

LVS: Live Vaccine Strain
M: Molar
MAb: monoclonal antibody
MAb: monoclonal antibody
MAC: membrane attack complex
Man: mannose
Mbp: mega base pairs
MDM: monocyte-derived macrophages
MH(B/A): Mueller-Hinton (broth/agar)
Min: minutes
ml: milliliter
mM: millimolar
mRNA: messenger ribonucleic acid
MWCO: molecular weight cut-off
nLC-MS/MS: nano-scale liquid chromatographic tandem mass spectrometry
NMR: nuclear magnetic resonance
O-Ag: O-antigen
OMT: outer membrane tubules
OMV: outer membrane vesicle
ORF: open reading frame
P10: passaged 10 times
PBS: phosphate buffered saline
PCR: polymerase chain reaction
PI: post-infection
PMN: polymorphonuclear leukocytes
PNAG: poly-N-acetyl glucosamine
rDNA: ribosomal DNA
RT-PCR: reverse transcriptase polymerase chain reaction
RT-qPCR: real time-quantitative polymerase chain reaction
SDS-PAGE: sodium dodecyl sulfate-polyacrylamide gel electrophoresis
SDS: sodium dodecyl sulfate
SEM: scanning electron microscopy
SI(S): Sarkosyl soluble(insoluble)
SLP: Surface-Layer Protein
T6SS: type VI secretion system
TEM: transmission electron microscopy
Tfp: type IV pili
Th1/Th2: T helper
TLR: toll-like receptor
TMB: 3.3',5,5'-tetramethylbenzidine
TMS: per-O-trimethylsilyl
TNF-α: tumor necrosis factor alpha
TxS(I): Triton-X 114 soluble(insoluble)

Chapter 1

LITERATURE REVIEW

1.1 History

Francisella tularensis is a Gram-negative, facultative intracellular, pleomorphic coccobacillus; the etiological agent of tularemia, and is capable of infecting a wide variety of mammals and humans [1]. *F. tularensis* has been recognized as a pathogen for a little over 100 years. The first authenticated reports of tularemia came in 1911 from a U.S. Public Health Service researcher named George W. McCoy. He described a novel disease found in California ground squirrels (*Citellus beecheyi*, Richardson), that was characterized by plague-like lesions and transmissible between mammals [2]. However, reports of similar cases had been documented earlier: from Norway in the 1650's and 1890's a disease was described called lemming fever, a case in Utah in 1908, and a case in Japan of Yato-Byo (hare disease) from 1818 [3-6]. *Francisella tularensis* was originally named *Bacterium tularense*, in recognition of where the disease was first discovered, Tulare County, California [7]. Three years later (1914), the first documented case of human disease caused by *Bacterium tularense* occurred in Cincinnati, OH [8]. This case offered the first look into the epidemiology and transmission of tularemia. A meat cutter entered the hospital with inflammation and ulcers of the eye, and 3 days after presentation had swelling of the neck and submaxillary lymph nodes. The causative agent was unculturable on standard diagnostic material. It wasn't until scrapings of infected material were injected into guinea pigs and cultivated on the same egg-yolk that was used by McCoy and Chapin that colonies characteristically phenotypic of *Francisella tularensis* emerged [2,7]. Human cases have now been diagnosed from around the world and in every state in the United States except Hawaii [9].

Some of the earliest work on the pathology of *F. tularensis* came from Dr. Edward Francis [10-13]. Francis began studying *Francisella* in 1919 and was able to show that multiple illnesses, from varying parts of the world, with unknown causes resulted from *F. tularensis* infection [14].

1.2 Taxonomy

Named after Tulare County, California, *Bacterium tularensis* was the original name of *F. tularensis* [15]. Serological analysis during the 1920's indicated it was part of the *Pasteurellaceae* family and thus was renamed *Pasteurella tularensis*, yet during the 1960's DNA hybridization indicated that the genus was not closely related to *Pasteurella* [16]. Decades later, 16S rDNA sequencing revealed that taxonomically, *Francisella* belonged to the γ-subclass of *Proteobacteria*, but had no close genetic relationships to other known genera [17]. In 2007, *Francisella* gained its own recognized family, *Francisella*ceae, in honor of Dr. Edward Frances [18,19]. Early taxonomic classification, done by McCoy and Chapin, were based on the differences in clinical manifestations, hosts, and morphological characteristics [7]. Today, modern genetic analysis and phenotypic differences have defined three species in the genus *Francisella*ceae (**Table 1.1):** *F. philomiragia*, *F. novicida,* and *F. tularensis* [20].

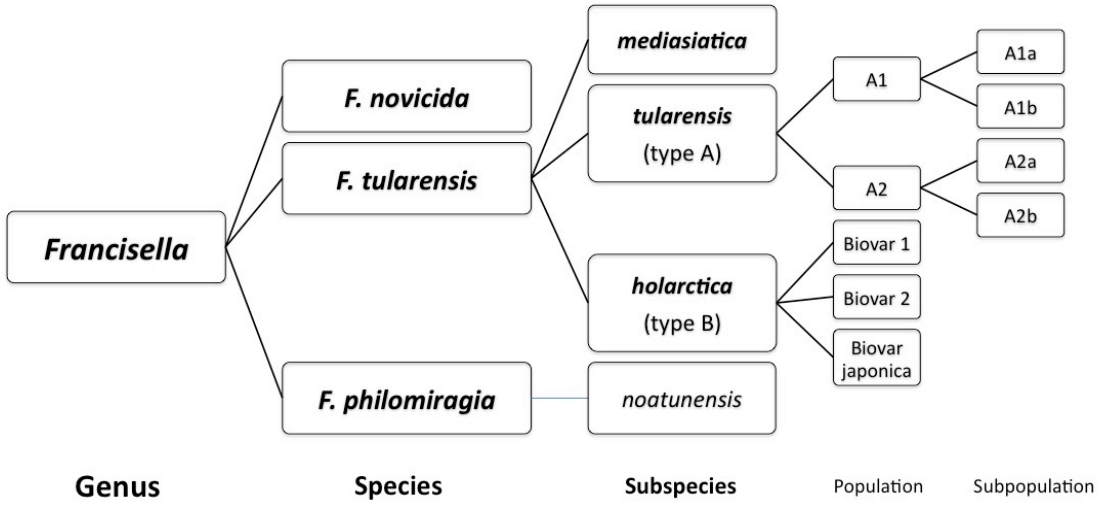

Figure 1.1 Taxonomic organization of the genus *Francisella.*

F. philomiragia, originally designated as *Yersinia philomiragia*, was changed to *Francisella* due to a high 16S rRNA sequence similarity and the unique fatty acid profile associated with *F. tularensis* [19,21]. *F. philomiragia* does not require cysteine for growth and is capable of degrading certain carbohydrates. *F. philomiragia* was originally isolated in Utah, but has since been found worldwide [21]. It is closely associated with water-borne transmission and is much less likely to cause disease than other *Francisella* species [21,22]. *F. novicida* is also closely associated with water-borne disease, and is predominantly found in North America and Australia [19]. Humans can become infected with *F. novicida*, but illness due to this species is considered extremely rare, except in the immuno-compromised. *F. novicida* and *F. tularensis* have a >95% genetic similarity, yet only *F. tularensis* is considered a clinically significant human pathogen [23-25].

F. tularensis is divided into three subspecies: *tularensis* (type A), *holarctica* (type B) and *mediasiatica* [23]. Type A strains are only found in North America, type B strains are common in Europe, Asia, and North America, and *mediasiatica* is found in central Asia and parts of the former Soviet Union [26-28]. Subspecies type A and B are responsible for the majority of tularemia cases around the globe, with infection by *mediasiatica* considered extremely rare and leading only to mild disease [23]. Subspecies *tularensis* can be further divided into two populations: A1 and A2, and those strains can be further divided into subpopulations of A1a/A1b and A2a/A2b, by geographic distribution and virulence characteristics [29]. In 1959, Olsufiev *et al*., recognized that *holarctica* isolates showed distinct virulence differences based on geographic location and host, and in the 1970's those same authors proposed three unique populations of *F. tularensis* type B (biovars I, II, and japonica) [30,31]. More recent studies have used molecular techniques to differentiate type B into as many as 10 biovars, though due to how little genetic diversity there is between biovars and no known difference in virulence, it is highly unlikely these biovars will ever be upgraded to subspecies level [32-34].

1.3 Epidemiology

Francisella is a highly successful pathogen with a low infectious dose, a wide range of vectors and hosts, and vast geographical spread [35]. *F. tularensis* has a wider range of hosts than most other zoonotic pathogens, with natural infections having been found in >100 species [36]. In nature, mammalian infection with the type A subspecies is more commonly found in lagomorphs (hares, rabbits) and infection with type B occurs most often in rodents [37]. Interestingly, dogs appear to be one mammal that while they can be infected and transmit *Francisella*, have very

mild or no clinical symptoms [38-41]. A number of arthropod vectors of *F. tularensis* are also present in nature. Natural infections or bacterial colonization have been found in many different arthropods including, fleas, lice, midge, bedbugs, ticks, mosquitoes, and flies, yet only a few have been identified as important to human transmission, such as hard ticks (*Dermacentor andersoni, D. variailis* and *Amblyomma americanum*), deer flies (*Chrysops discalis*), horse flies, and mosquitoes [35-37,42-44]. There has been no documented case of human-to-human transmission of tularemia [31].

Tularemia was more prevalent and deadly in the first half of the 20th century in the U.S. than it is today. There were 22, 812 diagnosed cases between 1927 and 1948, with the peak year occurring in 1938 with 2,291 cases [45,46]. Today, there averages less than 200 cases reported each year in the U.S., with the highest incidence occurring between May and September [47]. *F. tularensis* type A is found almost exclusively in North America, with subpopulation A1 occurring mostly in the eastern half, while A2 is primarily in the western half [35]. Tularemia infections occurring from A1 strains, including SCHUS4 and TI0902 typically have a higher fatality rate than A2 infections [48]. Type B strains are found throughout North America, Europe, and Asia and can occupy more diverse habitats than type A [49]. Type B strains of *F. tularensis* are endemic throughout Europe and Asia and have caused outbreaks in many countries, such as Bulgaria, Sweden, Norway, Kosovo, France, and Turkey [31,50-52]. Overall the incidence of tularemia cases in the U.S. is decreasing over the last century, with regional outbreaks occurring sporadically [53].

1.4 Ecology

The first insight into natural reservoirs and vectors of *F. tularensis* came from research done by investigators in the former Soviet Union in the mid 1900's. The Soviets found that swamp-flood land and grassland-meadow environments were strongly associated with human tularemia outbreaks [54]. They identified multiple naturally infected arthropod vectors and mammals, which also coincided with human infections [54].

In the United States, tularemia was often referred to as "rabbit fever" due to the fact that most human tularemia cases were believed to be associated with contact with cottontail rabbits [55]. It was later determined that between 1938 and 1948, 56% of human tularemia cases in Arkansas were due to tick bites, while only 31% were due to contact with contaminated rabbits [55]. Contaminated water sources were also determined to be a reservoir for *F. tularensis*. Aquatic mammals, such as muskrats and beavers, as well as mosquito larvae, would feed on the water and could become infectious zoonotic vectors. In Europe, where there is even a stronger correlation between aquatic environments and human tularemia. There is epidemiological data to show that human outbreaks of tularemia strongly correlate with contaminated water sources and mosquito populations [4].

1.5 Disease manifestations and transmission

Human tularemia will manifest in different ways depending on the route of entry, with an incubation period of 3-5 days. If the infection is transmitted through a break in the skin or mucous membrane, the ulceroglandular form of tularemia will occur.

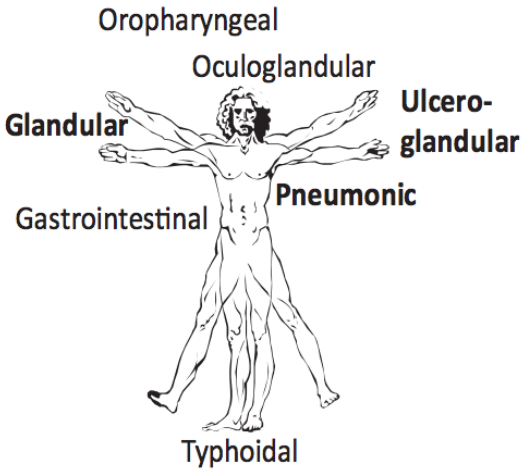

Figure 1.2 Forms of tularemia depending on route of infection. Most common forms in bold. http://commons.wikimedia.org/wiki/File:Vitruvian_man.jpg, Used under fair use, 2014.

Figure 1.3 Skin ulcer from ulceroglandular form of tularemia. http://en.wikipedia.org/wiki/Tularemia#mediaviewer/File:Tularemia_lesion.jpg, Used under fair use, 2014.

The ulceroglandular form occurs most often with vector-borne transmission or contact with an infected animal [4]. The site will develop a primary ulcer subsequently developing into an inflamed pustule, which will heal within a week. The lymph node draining the pustule will enlarge and become tender and antibiotics are normally required to control the infection. This form of tularemia comprises more than 90% of the European cases and the predominant subspecies is *holarctica*. Pneumonic tularemia is the most rare form to occur naturally, but is the most serious. Farmer or lawn workers are at the highest risk. The inhalation of contaminated aerosols is most likely caused by animal carcasses or excretions from infected animals. Pneumonic tularemia most commonly presents as a systemic infection with fever and enlarged lymph nodes. Infection with *holarctica* is normally non-fatal, whereas infection with subspecies

tularensis is potentially life threatening and has a fatality rate of ~30% if left untreated [56]. Treatment with modern antibiotics (aminoglycosides) have reduced the fatality rate to less than 2% in the United States [47]. Other, less common, forms of tularemia include oculoglandular and oropharyngeal.

1.6 Vaccines

Efforts have been underway since the early 1930's to produce a vaccine capable of protecting people against type A *F. tularensis* infection. A myriad of strategies have been applied, including attenuated live, killed whole-cell, and subunit vaccines, yet to date there is no licensed tularemia vaccine.

1.6.1 Killed whole cell vaccines

The earliest vaccines developed to prevent human tularemia employed the use of killed, whole bacterial cells [57]. They were initially developed by Dr. Lee Foshay, and are thus referred to in the literature as "Foshay" vaccines [58]. The Foshay vaccine utilized phenolized or acetone-extracted, killed *F. tularensis* and in a 1930's a vaccine study showed that the killed vaccine offered limited protection against pneumonic tularemia. Approximately 30% of the recipients of the Foshay vaccine still developed severe illness after exposure to a type A *F. tularensis* and required chemotherapeutics [1,57]. The inability of a killed vaccine to fully protect may have to do with a failure to elicit a robust cellular immune response and could have to do with destruction of necessary antigens during processing of the vaccine [59,60].

1.6.2 Live attenuated vaccines

This failure to protect humans with killed whole-cell vaccines led the Soviet Union to focus on developing a live attenuated vaccine. Live attenuated strains were developed by repeatedly passaging a virulent strain of type B *F. tularensis* subsp. *holarctica* on media that contained antiserum. This led to the development of a strain now referred to as the "live vaccine strain" or LVS, and was imported to the U.S. in 1956 [61]. LVS is administered by scarification and was widely used as a vaccine in the Soviet Union, with as many as 60 million people reportedly immunized during a World War II outbreak [62,63]. The U.S. military conducted vaccination studies using LVS and determined there was significant levels of protection against high dose subcutaneous (1,000 cfu) and low dose aerosolized (100 cfu) infection with virulent type A *F. tularensis* SCHUS4 [64,65]. Studies showed increased protection in humans when LVS was administered via aerosol, but a high percentage of volunteers developed significant illness and protection diminished over time [66]. LVS was further characterized by Eigelsbach and Downs and found that the strain could transition to phenotypic variants, including a more mouse-virulent and highly protective "blue" colony type and a less mouse-virulent, less protective "grey" variant [67]. Due to a lack of fully understanding the attenuation and concern over stability, the LVS vaccine is available only to at-risk personnel and lacks federal approval for widespread usage. LVS remains the standard as to which new tularemia vaccines are compared. Recently, Reed *et al*. demonstrated that type A SCHUS4 strains that contained mutations in *guaBA* or *aroD* provided partial protection against aerosol type A challenge in rabbits that surpassed the protection elicited by LVS, which was limited to prolonged time to death [68].

Due to the difficulty in working under bio-safety level 3 conditions and the lack of genetic tools that were available (until recently) for *F. tularensis*, a plethora of *F. novicida* live attenuated strains were developed in the hopes of eliciting a protective immune response [69-77]. These strains showed protection against challenge with *F. novicida*, but were ineffective against type A *F. tularensis*. More recently, tools for genetic manipulation have been made available for use in *F. tularensis* type A and B strains. Numerous attenuated strains of both have been evaluated as vaccine candidates and most have had limited protection against type A challenge in animals [68,78-88]. The same concern over stability, effectiveness, and the ability to cause disease has kept development of these potential vaccines from going further.

1.6.3 Sub-unit vaccines

One way to circumvent the concerns over using killed or attenuated bacteria that has been successful with *Bordetella pertussis*, is to use extracted antigens from the pathogen that are known to stimulate the immune response. Thus far, subunit vaccines produced using various *F. tularensis* components have been ineffective against virulent *F. tularensis* challenge [89-93]. The antigenic molecule that elicits the most effective protection is *F. tularensis* LPS. LPS, when administered with an adjuvant, offers a high degree of protection against type B strains, but minimal protection against type A challenges [89,94]. Other subunit vaccines that were successful against type B challenge used the immunodominant proteins FopA, DnaK, and Tul4, yet protection against type A infection remains minimal [95-97]. Isolated native outer membrane proteins have been found to offer 50% protection against low dose type A infection. Huntley *et al*., showed that Th1 and Th2 antibody responses were generated in response to an extracellular outer membrane preparation, and surviving mice had a reduced bacterial load in the liver, lung,

and spleen [98]. More recently, Richard *et al*., used a novel approach of vaccination with cationic surfactant vesicle vaccines incorporated with *F. tularensis* type A components, which offered partial protection against type A challenge [99]. As to why these vaccines do not offer complete protection, suggestions have included the correct antigen cocktails have not been used and a protective immune response cannot be generated using non live vaccines. The latter was addressed by use of an attenuated *F. tularensis* type A strain in combination with a subunit vaccine, which showed moderate promise against virulent type A infection [100].

1.7 *Francisella* as a Bioweapon

During the 20th century *F. tularensis* attracted the attention of multiple world powers for development as a bioweapon, due to the severity of the disease and ease of transmitting the agent. Japan, the Soviet Union, and the United States all developed programs to weaponize *F. tularensis* [101,102]. During the 1930's, Japan tested numerous biological weapons on prisoners of war, including *F. tularensis* [101]. During the 1950's and 1960's, the U.S. simultaneously investigated payload delivery systems designed to disseminate *F. tularensis* aerosols, as well as vaccine and chemotherapeutic studies in humans [101]. As concern grew around the world about these types of programs, the U.S. ended bioweapons research in 1972 [103]. The Soviet Union continued to develop *F. tularensis*, and reportedly produced drug- and vaccine-resistant strains before officially ending their bioweapons research in the mid 1990's [101,104].

As the number of natural tularemia infections decreased drastically toward the end of the 20th century, the United States Centers for Disease Control and Prevention removed tularemia from the list of notable diseases in the 1980's. However, after the September 11, 2001 terrorist attacks

in the U.S. and the mailed letters that contained *Bacillus anthracis*, there was a renewed interest in studying potentially dangerous pathogens, such as *Francisella*. The CDC classifies *F. tularensis* as a Tier I select agent due to its ease of aerosolization and high infectivity (as few as 10 cells are capable of causing fatal infection). The World Health Organization, estimated that aerosolized dispersal of *F. tularensis* over a population of 5 million people could cause 250,000 to fall ill and 19,000 fatalities [101].

1.8 Physiology

Francisella are small (0.2 – 2.0 μm), Gram-negative pleomorphic coccobacilli. *In vitro* growth on laboratory media requires supplementation with cysteine for all strains except *F. novicida* and *F. philomiragia*. This is thought to be due to a disruption in the sulfate assimilation pathway of subspecies that require such supplementation [105]. *Francisella* is a slow growing bacterium whose optimal growth conditions are 37°C with 5% CO_2. *Francisella* has a relatively small genome size of 1.89 Mbp, with 79% coding proteins and a low G/C content of 33% [105]. Recent developments have lead to many new genetic transformation tools being developed, including chemical transformation, electroporation, and cryostransformation. Multiple mutagenesis vectors and expression vectors have also been constructed and modified for use in *Francisella* [68,106,107]. Transposon mutagenesis has also proved to be a useful tool in *Francisella*, with libraries of *F. novicida*, LVS, and *F. tularensis* SCHUS4 being utilized [108-110].

1.9 Pathogenesis

1.9.1 Intracellular lifestyle

Francisella are facultative intracellular pathogens. *F. tularensis* has the ability to live and multiply in several types of cells in their natural environment and in the host. *Francisella* has been found in waterways and soil, in the environment, and can survive intracellulary in *Acanthamoeba castellanii* [111,112]. Relevant to infection in a mammalian host, *F. tularensis* can live inside a wide range of phagocytic cells, such as monocyte-derived macrophages (MDMs) and polymorphonuclear leukocytes (PMN), as well as non-phagocytic epithelial and endothelial cells and hepatocytes. However, its primary target is the macrophage [113-119]. *F. tularensis* is taken up by phagocytic cells by a process termed "looping phagocytosis", whereby the bacteria are ingested by the host cell via formation of a pseudopod loop that results in the bacteria inside a phagosome [120]. Normal phagosome maturation is modified by the bacterial *igl* proteins, IglABC (FTT_1714-12) that are found in the *Francisella* pathogenicity island (FPI) [121]. *F. tularensis* then prevents phagosome-lysosome fusion, and the *Francisella*-containing phagosome (FCP) becomes decorated with late endosomal markers [122-125]. The bacteria degrade the phagosomal membrane and move into the cytosol and begin to replicate quickly (SCHUS4 doubling time 1h) [122,126,127]. Once the host cell's resources are consumed the cell dies and releases the bacteria into the extracellular environment for the process to be repeated [128,129].

1.9.2 Innate immunity

The ability of *F. tularensis* to cause lethal disease by as few as 10 organisms can be attributed, in part, to its remarkable ability to evade and disrupt the host immune response. Upon entry into the host, bacteria must first circumvent killing by host serum components, such as complement, antibodies, and cationic antimicrobial peptides (CAMP) [130]. *Francisella* has long been known

to be resistant to serum killing [131]. Sandstrom *et al*., suggested the presence of a capsule was the reason *F. tularensis* was resistant to the assembly of the membrane attack complex (MAC) [132]. It is now known *Francisella* uses multiple surface structures such as an O-antigen capsule, lipopolysaccharide (LPS) and capsule-like complex (CLC) to evade killing by the host [133]. Complement-mediated resistance of *Francisella* is highly dependent upon the LPS O-antigen present on the bacterial surface [132,134]. Mutants that are deficient in O-antigen, either by direct mutation of the O-antigen synthesis genes, or by selecting for grey variants, are highly serum-sensitive compared to the wild-type [94]. More recently, it was shown that *F. tularensis* can bind Factor H, which allows cleavage of C3 to the inactive form iC3b [135]. The iC3b leads to ineffective assembly of the MAC, and iC3b opsonizes the bacteria, which targets the cells for phagocytosis by macrophages, dendritic cells, and neutrophils [136]. Another first line of defense *Francisella* utilizes is to prevent interactions with cationic host antimicrobials, such as defensins and cathelicidins [137]. One method by which they can do this, is by increasing the overall surface charge on the bacterium by modifying the LPS lipid A [138]. *Francisella* uses these defenses to prevent lysing of the bacterial cell by the MAC and allowing phagocytosis thus subverting extracellular antimicrobials and promoting intracellular replication.

F. tularensis infection promotes a delayed initial induction of pro-inflammatory and Th1-type cytokines, including interleukin-10 and 12, tumor necrosis factor alpha (TNF-α) and interferon gamma (IFN-γ), where TNF-α and IFN-γ have been shown to be essential for control of infection [91,139-142]. In the murine model, it has been shown that activation of pro-inflammatory cytokines, most importantly IFN-γ, occurs in a toll-like receptor 2 (TLR2)-dependent manner, with *F. tularensis* LPS not inducing the TLR4 response that is seen in other facultative

intracellular bacteria, such as *L. monocytogenes* [143-146]. Two ligands have been identified on the surface of *F. tularensis*, lipoproteins TUL4 (FTT_0901) and FTT_1103 that stimulate the TLR2/TLR1 heterodimer [147]. While IFN-γ activation of phagocytic cells is important for initial containment and control of the infection, macrophages and other phagocytes are the primary target of the bacteria for infection and replication [136]. Therefore, the innate immune response is often enough to control the initial infection, but it is not able to completely resolve the infection [142].

1.9.3 Adaptive immunity

Due to the intracellular lifestyle of *Francisella*, a cell-mediated immune response is important in controlling and resolving the infection. Even early work done by Edward Francis and others showed that patients that recover from tularemia are then immune to further *Francisella* infections [11,13]. In recovered tularemia patients, specific IgG, IgM, and IgA antibodies are detectable 2 weeks after infection, with titers being detectable up to 11 years post-infection [148]. However, antibodies are not believed to contribute much protection against intracellular infections. Passive transfer of immune sera and monoclonal antibodies to surface proteins TUL4 (FTT_0901) and FopA (FTT_0583) and the O-antigen capsule provide protection against type B strains, but only limited protection against type A *F. tularensis* infection [57,92,96,149]. Long-term protective immunity to *Francisella* infection relies primarily on T cells, and this cell-mediated response has been shown to be protective against both type A and B strains of *F. tularensis* [148]. $CD4^+$ T cell- or $CD8^+$ T cell-populations individually are effective in providing survival against *Francisella* infection [150,151]. The $CD4^+$ and $CD8^+$ T cell responses in humans are characterized by production of Th-1 type cytokines including IFN-γ and TNF-α,

which indicate activation of macrophages. However, these cytokines alone are not sufficient for resolution of infection [148,151]. Another important chemokine is IL-17, which plays a critical role during infection and acts in concert with IFN-γ to inhibit *F. tularensis* intracellular growth in macrophages and epithelial cells [152,153]. The host's chemokine response to *Francisella* infections is just beginning to be understood and research continues to elucidate this process.

1.10 Virulence factors

1.10.1 *Francisella* pathogenicity island

The *Francisella* pathogenicity island (FPI) was first discovered in 2004 using bioinformatic analysis of the type A strain SCHUS4 and *F. novicida* strain U112 genomes, and identifying a region that contained a different G/C content [154]. The FPI is comprised of 16-19 ORFs spanning 33-kb, and is present in a single copy in *F. novicida* and *F. philomiragia*, but is duplicated in all the subsp. of *F. tularensis* [32,154]. The critical role played by the FPI in virulence, particularly intracellular replication, has been well documented over the last decade [87,155-162]. The ability of *Francisella* to prevent phagosome-lysosome fusion and escape into the host cytosol is integral to its intracellular lifestyle, and FPI-encoded proteins are essential for this process [126,127]. Together, FPI protein IglC and its regulator MglA have been shown to regulate biogenesis of the phagosome to allow avoidance of lysosomal fusion and escape into the host cytosol [157,163,164]. The two operons located in the FPI (*iglABCD* and *pdp)* are required for intramacrophage growth and virulence [165]. IglG has been shown to be necessary for virulence, but not intracellular growth, while PdpE is not required for either process [159]. Genes in the FPI have also been shown to modulate the host immune response. It has been shown, during infection, that *F. tularensis* signals within the phagosome through TLR2 with a

distinct signaling pattern [166]. Mutants in the *iglC* gene have shown increased expression of TLR2-dependent genes in macrophages, but decreased expression of genes encoding other cytokines (IFN-γ, iNOS, and IP-10) [166]. The roles of other genes in the *igl* operon and the FPI in general, have been elucidated in many studies [162,165-170]. There is also evidence that several of the FPI genes encode for proteins involved in a unique type VI secretion system (T6SS), similar to *Vibrio cholerae* [159]. IcmF-DotU homologs are essential for a functional T6SS, and bioinformatics and functional analyses indicate that the *Francisella* IcmF homolog PdpB, is essential for secretion of IglI [165]. In addition, *Francisella* IglA and IglB are homologs of *V. cholerae* VipA and VipB, and have been shown to be a functional pair; however, it is unknown whether they assemble into the tubular membrane spanning structures in *Francisella* as they do in *Vibrio* [159,171]. PdpE, IglE, IglC, VgrG, IglI, PdpA, IglJ, and IglF are all secreted by the T6SS and localize to the bacterial outer membrane [172].

1.10.2 Lipopolysaccharide

Francisella lipopolysaccharide (LPS) is a well-characterized and important virulence factor during infection. LPS consists of three main components: a lipid A anchor, non-repeating core oligosaccharide, and the repeating O-antigen (O-Ag); *F. tularensis* LPS is unique in each of these components. A typical Gram-negative lipid A molecule contains 6 acyl chains of 12-14 carbons and has phosphate groups that are available to interact with the TLR-4-MD2-CD14 complex to stimulate strong proinflammatory immune responses [173]. In contrast, *F. tularensis* lipid A is asymmetrical, with a β-linked diglucosamine disaccharide that is tetraacylated and has 16-18 carbon fatty acid chains with no endotoxic activity [174-176]. *Francisella* lipid A is not recognized by TLR-4 and does not bind to LPS binding protein [177]. There are also some

differences in the lipid A between *Francisella* species. *F. tularensis* subsp. *holarctica* and *novicida* have a single phosphate on the reducing glucosamine residue (absent in LVS), and in *F. novicida* this is further substituted with a galactosamine [138,176].

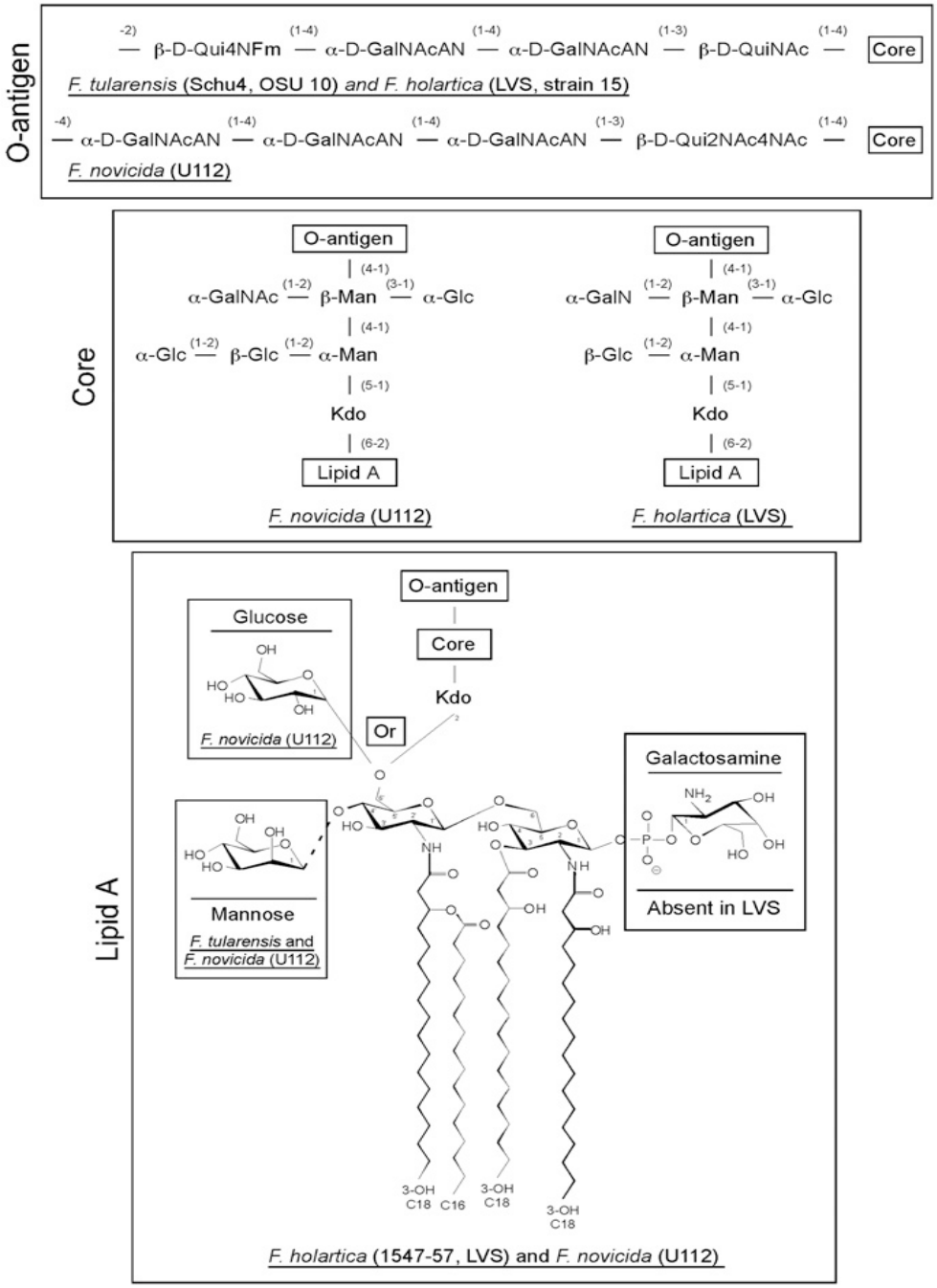

Figure 1.4 Structure of lipid A, core and O-antigen molecules of *F. tularensis* (type A and B) and *F. novicida*. Core: Kdo = 3-deoxy-D-*manno*-2-octulosonic acid; Man = mannose; Glc = Glucose; GalNAc = N-acetyl galactosamine. O-antigen = QuiN4Fm = 4,6-dideoxy-4-

formamido-D-glucose; GalNAcAN = 2-acetamino-2-deoxy-D-galacturonamide; QuiNAc = 2-acetamino-2,6,dideoxy-D-glucose; Qui2NAc4NAc = 2,4,-diacetamino-2,4,6-trideoxy-D-glucose

The core region of LPS links lipid A to the repeating O-Ag polysaccharide, and this linkage occurs through the 8 carbon sugar, 3-deoxy-D-*manno*-2-octulosonic acid (Kdo) [178]. *F. novicida* inner core differs from that of *F. tularensis* by the addition of an α-glucose residue attached to the β-Glc of the primary α-Man [176,178]. NMR structural analysis has been obtained for multiple *Francisella* species, including *F. novicida* and *F. tularensis* type A and B strains [179-181]. *F. tularensis* SCHUS4 and *F. tularensis* subsp. holarctica LVS were found to have identical O-Ag structures consisting of two internal carbohydrate residues (α-D-GalNAcAN--α-D-GalNAcAN) and two outside residues (β-D-Qui4NFm and β-D-QuiNAc), while *F. novicida* O-Ag shares the same two internal residues, but has differing outside residues (α-D-GalNAcAN and β-DQui2NAc4NAc) (Fig. 1.3) [176]. Genomic analysis of the O-Ag gene cluster (*wbt* locus) confirms that while the genetic loci responsible for type A and B O-Ag's are identical, the same locus in *F. novicida* has fewer genes and a lower G+C ratio [182,183].

It was first reported in 1951, that spontaneous colonies of *F. tularensis* SCHUS4 could vary under oblique light [184]. Colonies were categorized as either blue or grey in color, which corresponded to the colony morphology of either smooth (blue) or rough (grey), with the grey variant being typically stable, while the blue variant could spontaneously change to grey [184,185].

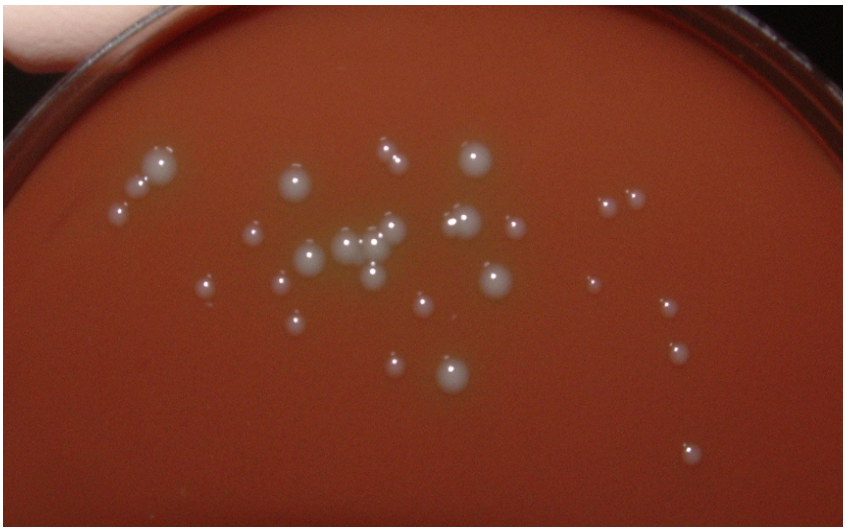

Figure 1.5 Blue and grey colonies of F. *tularensis* LVS.
Larger colonies have an intact O-Ag and are designated as "blue" and smaller colonies are O-Ag deficient and designated as "grey". Transition from blue to grey phenotypes occurred readily in passed LVS and type A strains after 5 day growth on agar. (Photo courtesy of Cheryl Ryder)

The grey variants were found to be less virulent in mice, and were neither immunogenic nor protective in murine challenge studies. Later studies by Cowley *et al*., showed that the grey variant was less capable of surviving in macrophages, was altered in anti-LPS monoclonal antibody reactivity, and stimulated increased nitric oxide production in macrophages [184-186]. It was initially found that the primary modification between blue and grey phenotypes was a considerable decrease in O-Ag polysaccharide, but with no major structural changes [184]. More recent studies by Soni *et al*., have shown that there are structural modifications of the LPS core sugars and lipid A, in addition to decreased O-Ag sugars, on the grey variant [185]. Grey variants have now been reported in *F. tularensis* LVS, SCHUS4, and HN63 and it has been suggested that this is perhaps a common occurrence in wildtype strains [187].

1.10.3 Capsule

Many Gram-negative and Gram-positive bacteria (*Streptococcus pneumoniae, Neisseria meningitides, E. coli*) are surrounded by a layer of material that is either directly or indirectly associated with the outer membrane, called capsule. In most bacteria, this capsular material is composed of high molecular weight polysaccharides, which can vary in structure widely among bacterial species. One exception to this is the poly-glutamic acid capsule of the pathogen, *Bacillus anthracis*. [188]. In pathogenic bacteria, one common role of capsule is to prevent phagocytosis, thus helping the pathogen elude the host immune system. Polysaccharide capsules of Gram-negative bacteria have been divided into four classes based on the biochemical, genetic, serological, and physical properties of *E. coli's* capsular antigens [189]. Of particular comparison to *Francisella*, are the Group 4 capsules. These are often referred to as O-antigen capsules and are synthesized by a Wzy-dependent mechanism that will be discussed further (1.10.3.1).

Until recently, it has long been debated whether *Francisella* did indeed have a capsule or not. Early characterization of a capsular material, performed by Hood, reported a capsule that was composed of mannose, rhamnose, and dideoxy sugars [1]. An putative acapsular mutant strain of *Francisella* LVS was created by Sandstrom *et al*. in 1988, that was reported to be more sensitive to antibody-mediated killing, although further studies were not performed due to the loss of the strain [132]. It is believed by some that this "capsule" mutant was actually a LPS O-antigen mutant. Cherwonogrodzky *et al*., showed through transmission electron microscopy (TEM) and crude extraction, that capsular material could be enhanced through the repeated

passaging of the bacteria in minimal media [190]. The role and existence of capsular antigens on *Francisella* are currently an area of active investigation.

1.10.4 O-antigen capsule

Apicella *et al*., developed a monoclonal antibody (11B7) that recognizes an extracellular substance on the surface of *F. tularensis* by SEM and TEM, and extracted material by western blotting [92]. Apicella *et al*. elucidated the structure of this material and concluded it was a Group 4 capsule that was present on *F. tularensis* type A and B strains [92]. Briefly, bacteria were grown on chocolate agar for 48 hours, the cell pellets were solubilized in Trizma base, SDS, and proteinase K, ethanol precipitated, and phenol-extracted [92]. The capsule was shown to be composed of a polymer of the O-antigen subunit and was between 100-kDa and 250-kDa in size, with no indication of lipid A or core sugar units attached [92]. It was found that O-antigen glycosltransferase mutants do not make a capsule, yet an acyltransferase (*msbB*) and an O-Ag polymerase (FTT_0673-0674) mutant that did not make an O-antigen continued to produce the O-Ag capsule [92]. Passive immunization with 11B7 MAb, and active immunization with purified CP, protected mice against LVS challenge, but not SCHUS4 challenge [92]. *Francisella* SCHUS4 mutants deficient in O-Ag and O-Ag polysaccharide (mutants in FTT1236, FTT1237 and FTT1238) were significantly more sensitive to complement-mediated killing, yet in the absence of complement were phagocytosed more readily and were capable of phagosomal escape, yet were deficient in intracellular growth [191]. Work is still ongoing to determine the novel biosynthetic pathway of this capsule and to elucidate further its role in pathogenesis [88].

1.10.5 Capsule-like complex

The capsule-like complex (CLC) of *F. tularensis* has been partially characterized and reported by our lab. Bandara *et al*., will be discussed further in this dissertation [192]. Briefly, in an effort to ascertain whether *Francisella* did indeed produce a capsule, we enhanced, visually identified, and purified the CLC.

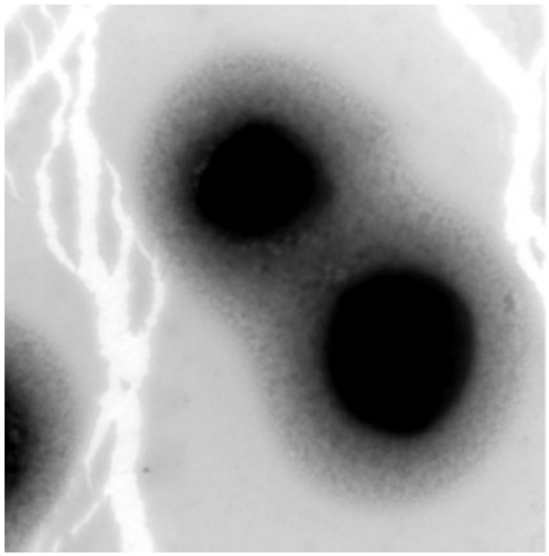

Figure 1.6 *F. tularensis* LVS enhanced for CLC production.
Bacteria passaged in defined media ten times and then grown on defined media agar for 5 days at 32°C. Transmission electron microscopy (TEM), 35000x magnification.

In contrast to the O-Ag capsule preparation, glucose-enhanced minimal media was used, and the bacteria were grown for an extended period of time at lower temperatures. The surface layer only was removed from the bacteria using a chaotropic agent. The only carbohydrates isolated in the CLC were glucose, galactose, and mannose, but there was no evidence of core LPS sugars or O-Ag sugars, and the CLC was isolated from an O-Ag/O-Ag capsule-deficient mutant [192]. The CLC appears to contain glycoproteins and a high molecular weight carbohydrate that presents as multiple bands/smear between 150-kDa and 250-kDa. The genetic locus responsible, in part, for CLC production is conserved across subspecies of *F. tularensis*, has been identified as FTT0789-

FTT0800, and contains glycosyltransferases, ABC transporters, and multiple hypothetical genes [105]. The CLC contributes to the virulence of LVS in mice, with a CLC-deficient mutant being attenuated and protective against challenge with LVS. In addition, active immunization with purified CLC and adjuvant is protective against LVS challenge [192]. Zarrella *et al*., also reported a high molecular weight carbohydrate (>225-kDa) that is present when *Francisella* is grown on brain heart infusion agar (BHI), and is present in *wbt* mutants that cannot produce the O-Ag capsule [193]. BHI has been shown to allow the bacteria to mimic carbohydrate surface structures seen during host infection [193]. The composition of the HMW carbohydrate was not analyzed, but is hypothesized to be related to the CLC. This area is a new and currently evolving research topic that will be further discussed in the following chapters.

1.11 Glycosylation

Glycosylation of proteins was thought to only occur commonly in eukaryotes. However, it is now established that prokaryotes can indeed glycosylate some of their proteins [194]. Glycosylation, is the enzymatic addition of sugars to proteins [195]. The groundbreaking research originally focused on the surface layer (S-layer) glycoproteins of the *Archaea* domain [196,197]. To date, glycoproteins have been found in a number of bacterial species and are primarily surface-associated or secreted proteins, with the best understood bacterial glycoproteins being S-layers, pili, and flagellins [196,198-202]. There are two types of protein glycosylation: O-glycosylation, which is more common in prokaryotes and in which oligosaccharides are attached to the hydroxyl group of serine or threonine, and N-glycosylation, which is rare in bacteria, but has been found in *Campylobacter* and *Archaea* species [202,203].

F. tularensis contains two potential polysaccharide biosynthesis loci, the O-Ag biosynthesis cluster and a second polysaccharide locus, putatively identified as partially responsible for CLC production [105,179]. The proteome of *F. tularensis* reportedly has 20 known glycoproteins, notably, PilA (pilin subunit), Tul4 (DsbA (needed for intracellular survival), and FTH_0069 (needed for intracellular survival and proliferation) included [204,205]. Thomas *et al*., reported that the glycosyl modification of DsbA was an 1156-Da O-linked hexasaccharide comprised of *N*-acetylhexosamines, hexoses, and an unknown monosaccharide [204,205]. Furthermore, deletion of FTT0798 in the putative CLC locus resulted in loss of glycosylation in the F. *tularensis* strain [204]. This link between protein glycosylation and the CLC is currently being examined. Recently, it was also found that both type A and B strains of *F. tularensis* (excluding LVS) produce proteins glycosylated with O-Ag moieties [206,207]. O-antigen protein glycosylation may help the bacteria evade the host immune response.

1.12 Outer membrane vesicles

Outer membrane vesicles (OMV) are bilayer structures commonly shed from the bacterial surface of Gram-negative bacteria. OMV can be used by bacteria to deliver virulence factors distant from the cell itself [208,209]. Investigation into the production of OMV by *Francisella* has recently begun and is focused mainly on *F. novicida,* which were shown to produce both spherical vesicles and tube-shaped vesicles named OMV/T by McCaig *et al*. [210].

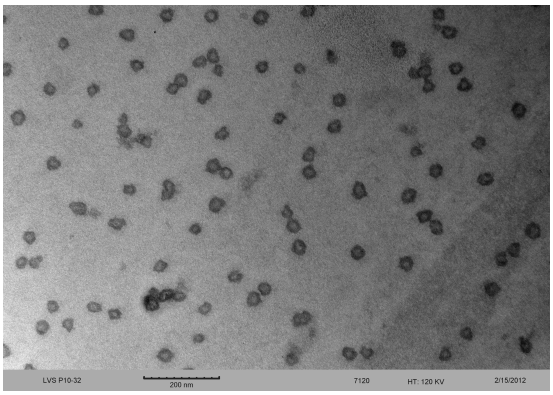

Figure 1.7 OMV isolated from LVS enhanced for CLC production.
TEM, negative stain with uranyl acetate.

The production of tube versus spherical outer membrane vesicles was dependent upon growth medium and phase, and OMV/T were seen during infection of macrophages [210]. Pierson *et al*., reported the ability of *F. novicida* and LVS to produce OMV, and using liquid chromatography mass spectrometry (LC-MS/MS) over 400 proteins were identified from *F. novicida* OMV [211]. The second most commonly identified protein was a hypothetical lipoprotein FTN0714 (homologue to FTT0742) that is a large (~200-kDa) protein that has been observed through SDS-PAGE in the CLC. In addition, genes known to be involved in virulence, such as, FPI proteins IglABC and PdpAB, FopB, TolC and GroEL were also found in the OMV, leading to a hypothesis that OMV could be important delivery systems for virulence factors of *Francisella* [115,154,211]. *F. novicida* OMV have also successfully been used as a novel vaccine against *F. novicida* challenge, which could indicate OMVs have potential as a vaccine against more virulent *Francisella* [211].

1.13 Other Envelope Proteins

Bacterial pathogens such as *Vibrio cholerae* and *Pseudomonas aeruginosa* use type IV pili (Tfp) during host colonization and are an important virulence factor [212,213]. Tfp are strong, flexible

filaments protruding from the bacterial surface, primarily composed of polymeric assemblies of pilin protein, such as PilA in *P. aeruginosa* [214]. Orthologs of the genes required for biogenesis of Tfp (*pil* genes) have been found in *F. tularensis* and pili-like filaments have been detected with TEM on the surface of *Francisella* (Fig. 1.7) [105,215].

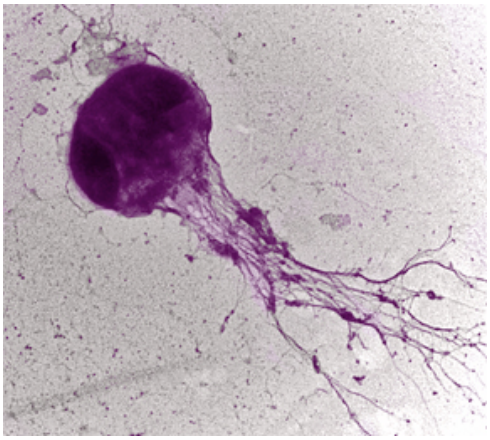

Figure 1.8 LVS exhibiting filamentous pili.
TEM, uranyl acetate negative stain, 35000x magnification

Tfp typically play a role in surface motility, host cell adhesion, and biofilm formation [216]. One role of the Tfp in *F. tularensis* has been to function as a type II-like secretion system. Hager *et al*., reported seven proteins (including: PepO, ChiA, ChiB, CbpA and BglX) were detected in culture supernatant fractions of *F. novicida*, and mutations in the Tfp genes nullified secretion [217]. In addition to nullifying secretion, the filamentous protrusions were no longer visible on the cell surface with TEM [218]. Tfp gene *pilA* and a siderophore uptake protein, *fupA*, were found to be missing or disrupted in LVS, and hypothesized to be the basis for attenuation in LVS [219,220]. Iron uptake is a key virulence factor for intracellular pathogens as it has been documented that upon recognition of infection, the host body will sequester free iron leaving it available only in the phagosome during acidification [221]. This hypothesis was further supported by the expression of a functional *fupA* gene in LVS restoring virulence that equaled a

virulent type B strain [220]. In addition *fupA* works in tandem with the *fsl* operon, that was identified in *Francisella* as responsible for iron uptake, and when inactivated by an internal deletion or deletion of it's regulator *fur*, the bacteria was unable to survive in iron depleted conditions and lost virulence [219,220].

1.14 Biofilm

Biofilms can be defined as a matrix-enclosed bacterial population that are adherent to each other and/or surfaces [222]. Recently it has been demonstrated that *Francisella* form biofilms *in vitro,* with most work focusing on *F. novicida* [223-226]. *F. novicida* will easily form biofilm on a variety of surfaces including plastics, glass, and crab shells, while *F. tularensis* subsp. *tularensis* and subsp. *holarctica* do not form such robust biofilms, but will develop one on plastic 96-well plates [227]. One hypothesis is that *Francisella* form biofilms in order to persist in their natural environment. The fact that *F. philomiragia* has been shown to form biofilms in the aquatic amoeba *Acanthamoeba castellanii* and mosquitoes have been shown to feed on the *F. novicida* biofilm, gives credence to that hypothesis [228,229]. However, a *F. novicida* strain deficient in the Tfp *pilE* gene was found to still fully form biofilm [230]. The *E. coli* two-component quorum sensing system QseBC is known for regulating surface structures and a homolog of the gene for QseC has been found in *F. tularensis* and *F. novicida* [230]. Mutations in *F. novicida qseC* greatly effect biofilm formation [230]. *Francisella* also produce chitinase (ChiA, ChiB, ChiC, ChiD) that has been shown to allow *F. novicida* to form biofilms under nutrient-limiting conditions by using chitin as a carbon source [231]. Matrix composition and exopolysaccharide identification has yet to be elucidated. The role of *Francisella* surface antigens in the development of biofilm is just beginning to be explored.

Chapter 2

Isolation and Molecular Characterization of a Capsule-Like Complex (CLC) from *Francisella tularensis* LVS, and Contribution of the CLC to *F. tularensis* Virulence in Mice

This chapter was adapted from the published work:

Bandara AB, Champion AE, Wang X, Berg G, Apicella MA, et al. (2011) Isolation and mutagenesis of a capsule-like complex (CLC) from *Francisella tularensis*, and contribution of the CLC to F. *tularensis* virulence in mice. PLoS One 6: e19003.

2.1 INTRODUCTION

Francisella tularensis is a Gram-negative coccobacillus, and the etiologic agent of tularemia in a wide variety of animals and humans. *F. tularensis* resides in macrophages, hepatocytes, and a variety of other cells as a facultative intracellular pathogen, but may also be found in the blood during infection [232]. Humans may acquire the agent by handling infected animals, ingesting food or water containing the pathogen, through bites from arthropod vectors (e.g. ticks), or by aerosol, which is the route of exposure of most concern due to intentional release of this agent. The most pathogenic isolates of *F. tularensis* are type A1 strains (subspecies *tularensis*), which may cause human infection with as few as 10 organisms [233,234], and are associated with 30% mortality in the absence of antibiotics following pneumonic tularemia [232,235]. Type B strains (subspecies *holarctica*) are also highly virulent, but are not associated with the same level of mortality as subspecies *tularensis* [233].

Due to their ease of culture and dispersal, persistence in the environment, and high virulence, *F. tularensis* is classified as a Category-A select agent by the CDC [233]. An approved, licensed vaccine for tularemia is not currently available. However, a live vaccine strain (LVS) was developed in the former Soviet Union from a type B strain following extensive passage and testing *in vitro* and in animals [236]. LVS has been used to protect laboratory workers from infection with type A strains [237], but is not currently approved as a vaccine for the general population due to its poor characterization, potential instability, and questionable safety for immuno-compromised individuals [238]. Although attenuated in humans, LVS is antigenically identical to type A strains, and has been used extensively in research as this strain remains highly virulent for mice, particularly by the intraperitoneal (IP) and respiratory routes [239].

Although *F. tularensis* was first isolated nearly 100 years ago [240], relatively little is known regarding its surface components that contribute to virulence. The lipopolysaccharide (LPS) has been well characterized, and is required for resistance of *F. tularensis* to antibody and complement-mediated bactericidal activity and for virulence [86,183,187,241]. Antibodies to the O-antigen provide protection to mice challenged with LVS [242,243], but not against challenge with type A strains [89]. LVS mutants lacking O-antigen induce some protection against challenge with LVS or type B strains, but protection against type A challenge is inadequate [86,182,183,241]. Although individual outer membrane proteins have not provided protection against challenge of mice with type A strains [244], a native outer membrane protein preparation did provide partial protection [98].

An electron-dense surface material resembling a capsule has been demonstrated around types A and B strains of *F. tularensis* by electron microscopy (EM), resulting in the conclusion that these subspecies may be encapsulated [245-248]. Furthermore, a halo-like appearance has been reported around individual *F. tularensis* cells within macrophages [120,249], and it has been hypothesized that once the bacteria are inside the late endosome/phagosome compartment, certain components of the bacterial capsule or membrane are rapidly released leading to the degradation of the membrane and release of the bacteria into the cytoplasm [123]. However, these electron dense surface structures are not always visible, suggesting this capsule-like complex (CLC) is upregulated under specific environmental/growth conditions [250]. A carbohydrate-protein-lipid component distinct from LPS was identified by Hood that is readily removed under hypertonic conditions [251], and its expression can be enhanced by repeated subculture in defined medium [250]. This crude extract from *F. tularensis* strain SCHUS4 contained carbohydrate (including mannose, rhamnose, and two unidentified dideoxy sugars), as well as amino acids, and -OH 14:0 and 16:0 fatty acids. However, a specific component was neither purified nor well characterized. Recently, Apicella et al. [92] described an O-antigen capsular polysaccharide around all *F. tularensis* type A and B strains tested. Mutations in O-antigen glycosyltransferases blocked O-antigen and capsule biosynthesis, but mutations in an O-antigen polymerase or acyltransferase only prevented O-antigen synthesis, not capsule synthesis.

A genetic locus that may encode for proteins involved in synthesis and export of a polysaccharide other than LPS has been identified in the genome sequence of *F. tularensis* LVS (NC_007880), and the same genes are present in type A strain SCHUS4 [105] (NC_006570). This locus contains 12 putative genes in the LVS genome: FTL_1432 through FTL_1421. We

sought to purify and analyze the electron dense CLC that appears to be upregulated under specific growth conditions, with emphasis on the carbohydrate component. Furthermore, to determine if the above locus is involved in synthesis of the carbohydrate component of the LVS CLC, two putative genes encoding for proteins with homology to a galactosyl transferase and a mannosyl transferase were deleted by allelic exchange. The CLC isolated appeared to be a glycoprotein and distinct from the O-antigen capsular polysaccharide. The glycosyl transferase mutant lacked CLC expression, was attenuated in mice, but provided protection against subsequent challenge with the parent.

2.2 MATERIALS AND METHODS

2.2.1 Bacterial strains and growth conditions

The bacterial strains used and their sources are listed in Table 2.1. *Escherichia coli* DH5α was grown in Luria–Bertani (LB) medium (Becton-Dickinson, Franklin Lakes, NJ) at 37°C containing 100 μg ampicillin (Amp)/ml or 50 μg kanamycin (Kan)/ml for selection of recombinant strains. *F. tularensis* strains were cultured from frozen stock suspensions onto brain heart infusion agar (Becton-Dickinson) supplemented with 0.1% L-cysteine hydrochloride monohydrate (Sigma-Aldrich, St. Louis, MO) (BHI agar) and 5% (v/v) sheep blood (BHIB), and incubated at 37°C in 7% CO_2, unless otherwise stated. For culture in broth, *F. tularensis* strains were grown with shaking (175 rpm) in BHI broth at 37ºC, or CDMB [250] with 1.5% glucose (CDMB) at 32°C. For CLC preparation *F. tularensis* LVS was grown on CDMA in petri dishes (150 mm X 15 mm), and incubated at 32°C in 7% CO_2 for 5 days. All experiments with LVS and mutants were carried out in biosafety level (BSL)-2 facilities in an approved biosafety cabinet.

Table 2.1. Bacterial strains and plasmids used in this study.

Bacterial strains	Characterisitcs	Reference or source
E. coli DH5α	F^- ϕ80d *lacZ*ΔM15 Δ(*lacZYA-argF*)*U169 recA1 endA1 hsdR17*(r_K^- m_K^+) *phoA supE44* λ^- *thi-1 gyrA96 relA1*	Invitrogen
LVS	*F. tularensis* subsp. *holarctica* live vaccine strain	Dr. May Chu, CDC
LVS_P17	LVS passed daily for 17 days in CDMB	This work
LVSΔ1423/1422	LVS containing a deletion spanning FTL_1423 to FTL_1422	This work
LVSΔ1423-22 [1423-22+]	LVSΔ1423/1422 containing vector pFTAB-2, expressing the deleted FTL_1423-FTL_1422 region *in trans*	This work
$WbtI_{G191V}$	LVS lacking O-antigen due to a mutation that converts amino acid 191 from a glycine to valline	[241]
$WbtI_{G191V}$_P17	$WbtI_{G191V}$ passed daily for 17 days in CDMB	This work
$WbtI_{G191V}$Δ1423/1422	$WbtI_{G191V}$ containing a deletion spanning FTL_1423-FTL_1422	This work
$WbtI_{G191V}$Δ1423/1422 [1423-22+]	$WbtI_{G191V}$Δ1423/1422 containing vector pFTAB-2, expressing the deleted FTL_1423-FTL_1422 region *in trans*	This work
Plasmids		
pSC-A	PCR Cloning vector, Amp^r	Stratagene
pSC-1423/1422	pSC-A containing the regions flanking FTL_1423/ FTL_1422 region; Amp^r	This work
pSC-1423/1422K	pSC-1423/1422 containing the Kan^r gene; Amp^r; Kan^r	This work
pFNLTP6	*F. tularensis* shuttle vector; Kan^r, Amp^r	This work
pFTAB-1	pFNLTP6 containing the entire FTL_1423-FTL_1422 region; Kan^r, Amp^r	This work
pFATB-2	pFTAB-1 containing *cat* (Cm^r) cassette from pBBR1MCS ligated, Cm^r, Amp^r	This work

2.2.2 Extraction of LPS

LPS was purified from *F. tularensis* LVS by aqueous phenol extraction, enzyme digestion, and ultracentrifugation from killed cells, as described previously [241].

2.2.3 Purification of CLC

The CLC was extracted from O-antigen LVS mutant $WbtI_{G191V}$ that was passed daily 17 times in CDMB ($WbtI_{G191V}$_P17) to avoid contamination with LPS O-antigen. The cells were grown in CDMB to mid-log phase, 500 µl was streaked onto large petri plates of CDMA, and the plates were incubated for 5 days at 32°C in 7% CO_2. Approximately 10 g of bacterial cells (wet weight) were gently resuspended into 200 ml of 0.5% phenol (in water) and incubated at room temperature for 10 min. A thick, foamy extract was obtained and subjected to centrifugation at 10,000 x *g* for 15 min to remove cells, followed by centrifugation of the supernatant again. The crude CLC was precipitated by addition of 60 mM sodium acetate and 5 volumes of cold (-20°C) ethanol, and incubation at -20°C overnight. The precipitate was sedimented by centrifugation at 10,000 x g for 15 min and the pellet suspended in 50 ml of 10 mM Trizma base (pH 7.3) containing 10 mM $CaCl_2$, 10 mM $MgCl_2$, and 0.05% sodium azide . Ten microliters of RiboShredder RNase (Epicentre, Madison, WI) was added, and the mixture incubated for 2 hours at 37°C. Twenty-five µg/ml of DNase (Sigma-Aldrich, St. Louis, MO) was added and the incubation continued for 1 hour. One hundred µg/ml of Proteinase K (Sigma-Aldrich) was added and the mixture incubated for 2 hours at 37°C, followed by incubation at 55°C overnight. Impurities were removed from the semi-purified complex by ultracentrifugation at 100,000 x *g* at 4°C for five hours to overnight. The supernatant was dialyzed in a 50-kDa membrane against four changes of distilled water and lyophilized. In some cases the CLC was further purified by

S-300 column chromatography with water or 0.1% sodium dodecyl sulfate as eluent (15 mm X 252 mm; GE Healthcare Life Sciences, Piscataway, NJ), and the carbohydrate-positive fractions were dialyzed and lyophilized.

2.2.4 CLC compositional analysis

CLC samples were extracted from the same number of cells, as determined by optical density and viable plate count, and analyzed by phenol-sulfuric acid assay [252] for carbohydrate content, KDO assay [253] and Western blotting [241] for LPS, bicinchoninic acid assay (BCA) for protein content (Pierce), and galactose oxidase assay for galactose (Invitrogen). Glycosyl composition was determined by combined GC/MS of the per-O-trimethylsilyl (TMS) derivatives of the monosaccharide methyl glycosides produced from the sample by acidic methanolysis, as described [254].

2.2.5 Electrophoretic analysis and Western blotting

The electrophoretic profile of the CLC was resolved by sodium dodecyl sulfate-polyacrylamide gel electrophoresis (SDS-PAGE) using Novex® 4-12% Pre-Cast bis-Tris gels (Invitrogen, Carlsbad, CA). Following electrophoresis, the gel was fixed in 25% isopropanol/10% acetic acid overnight and stained with 0.25% Stains-All (Sigma-Aldrich, St. Louis, MO) for 2 hours [255]. The bands were visualized on a lightbox, color and size noted, and the gel silver stained as described [255]. Separate gels were stained with Coomassie Blue (Pierce, Rockford, IL), or the samples were transferred to nitrocellulose using an X-Cell II Blot Module Semi-Dry Transfer unit (Invitrogen) for Western blotting. Blots were developed using rabbit polyclonal antiserum to LVS (1:10,400 dilution) [256], followed by anti-rabbit IgG coupled to horseradish peroxidase

(HRP; Jackson ImmunoResearch Labs) (1:2,000 dilution), and developed with 3,3,5,5-tetramethylbenzidine (TMB; Pierce). The presence of carbohydrate in the gel was also examined by staining with Pro-Q Emerald 300 (Molecular Probes, Eugene, OR).

2.2.6 Negative stain electron microscopy

LVS was passed in CDMB to enhance CLC as described for $WbtI_{G191V}$_P17. *F. tularensis* strains were grown on CDMA for 5 days at 32°C. The cells were gently scraped into sodium cacodylate buffer containing 3% glutaraldehyde and turned end-over-end for 2 hours. The cells were washed, suspended in 10 mM sodium cacodylate buffer, adhered to formvar-coated grids, stained with 0.5% uranyl acetate, and viewed with a JEOL 100 CX-II transmission electron microscope [257].

2.2.7 DNA sequence analyses

Annotation of putative *F. tularensis* LVS genes was determined using BLAST [258] and the Smith-Waterman algorithm [259].

2.2.8 DNA manipulation

DNA extraction and manipulation procedures were carried out as described [260]. Restriction enzymes and T4 DNA ligase were obtained from New England BioLabs (Ipswich, MA). Plasmid DNA was extracted using the QIAprep® Spin Miniprep and QIAquick® Gel, as described by the manufacturer (QIAGEN, Valencia, CA). Genomic DNA from *F. tularensis* LVS was purified using the PUREGENE™ DNA Isolation Kit (Gentra Systems, Minneapolis, MN). The StrataClone™ PCR cloning kit (Stratagene™, La Jolla, CA) was used for PCR

cloning. Oligonucleotides were obtained from Integrated DNA Technologies, Inc. (Coralville, IA).

2.2.9 Construction of *F. tularensis* LVS allelic exchange mutants

Open reading frames FTL_1423 and FTL_1422 of strains LVS and $WbtI_{G191V}$_P17 were deleted by allelic exchange. A 1.3-kb region upstream of FTL_1423 was amplified by PCR using the primer pair (containing restriction enzyme sites) FTL1424_F_SalI and FTL1423_R_StuI. A similar size region downstream of FTL_1422 was separately amplified by PCR using the primer pair FTL1422_F_StuI and FTL1421_R (Table 2.2). The two PCR products were ligated to each other by fusion PCR using Taq polymerase, and then cloned into TA cloning vector pSC-A (Stratagene) to produce pSC-1423/1422. This plasmid was isolated from *E. coli* DH5a grown on LB agar containing 100 mg/ml Amp. The Tn*903 npt* gene [261] that confers Kan resistance (Kan^r) was isolated from pUC4K by digestion with *Pvu*II, and cloned into *Stu*I-digested (and blunt ended) plasmid pSC-1423/1422, which resulted in the Kan^r gene being inserted between FTL_1423 and FTL_1422. The resulting plasmid was isolated from *E. coli* DH5a grown on LB agar containing 100 mg/ml Kan, and designated pSC-1423/1422K, which was transformed into *F. tularensis* LVS by cryotransformation [262]. Colonies were collected from the plates and subcultured on BHIB containing 8 μg/ml of Kan for 6 days at 37˚C in 5% CO_2. Deletion of FTL_1423 and FTL_1422 and the presence of the Kan^r gene from selected Kan^r colonies was determined by PCR. Confirmation of the deletion was done by sequencing of the region from FTL_1424 to FTL_1421 at the Virginia Bioinformatics Institute (VBI) core sequencing facility at Virginia Tech. One verified recombinant of each strain was selected and designated LVSΔ1423/1422 (derived from LVS) and $WbtI_{G191V}$_P17Δ1423/1422 (derived from O-antigen

mutant $WbtI_{G191V}$_P17). The *capB* gene from these mutants was amplified by PCR, confirming they were *F. tularensis* and the mutations were non polar (data not shown), as the capB gene is downstream of FTT_1423-22.

For complementation, the entire FTL_1423-FTL_1422 region was amplified by PCR and cloned into expression vector pFNLTP6 [263] to produce pFTAB-1. FTL_1423/1422 was transcribed under the *groE* promoter of pFNLTP6. The *cat* gene encoding resistance to chloramphenicol and transcribed under control of its native promoter was amplified by PCR from plasmid pBBR1MCS [264] and cloned into the *Pst*I site of pFTAB-1 to produce pFTAB-2. This plasmid was introduced into LVSΔ1423/1422 by cryotransformation [262]. Colonies resistant to 10 μg/ml of chloramphenicol were subcultured, and a clone containing the recombinant plasmid (determined by restriction enzyme digestion) was designated LVSΔ1423/1422[1423-22+]. Plasmid pFTAB-2 was also introduced into $WbtI_{G191V}$Δ1423/1422 by cryotransformation to complement that mutant and obtain $WbtI_{G191V}$_P17Δ1423/1422[1423-22+].

Table 2.2 DNA primers used for PCR.

For cloning FTL_1423-FTL_1422 into pSC-A to produce pSC-1423/1422

FTL1424_F_SalI	GCGTCGACTATCAAAGTTGCACCTAG
FTL1423_R_StuI	GAAGGCCTGATTTAGCAAAACGATCC
FTL1422_F_StuI	AATAGATACGCGCTGGCAAGGC
FTL1421_R	ATGTAATCCAACACTCAGATGCAAA

For detection of the Kan^r gene in recombinant mutant strains

Kan_CHK_F	AAGTTGGGTAACGCCAGGGTTTTCC
Kan_CHK_R	ATTAGGCACCCCAGGCTTTACACTT

For verifying the mutation in strain $WbtI_{G191V}$Δ1423/1422

F-FTL-1422	CAGCAACGGTTGGCTGTAATAAGC
R-FTL-1422	CCTACTTATACAATTTAGGTATAA

For cloning FTL_1423-FTL_1422 into pFNLTP6 to produce pFTAB-1

F-FTL1423-EcoRI	CGGGAATTCGAACATTATAAAATCATCAGA
R-FTL1422-XhoI	CGGCTCGAGACTCACTCATTCTCGCCATTT

For cloning *cat* gene into pFTAB-1 to produce pFTAB-2

CAT-Rev	CGGCTGCAGTGACCCGCGACCAGACCACGT
CAT-Forw	CGGCTGCAGCCGGTACCCAGCTTTTGTTCC

2.2.10 Reverse-transcriptase polymerase chain reaction (RT-PCR) and real-time quantitative PCR (RT-qPCR)

RNA was isolated from *F. tularensis* LVS strains using the RNeasy extraction kit following digestion of cells with 400 µg/ml lysozyme, as described (Qiagen, Valencia, CA). RNA integrity values of 9.2-9.8 were obtained using the BioAnalyzer (Agilent, Santa Clara, CA). For RT-PCR, bacteria were grown on CDMA at 37ºC for at least 2 days prior to extraction of RNA. RNA was converted to cDNA and amplified with SuperScript III First Strand Synthesis System (Invitrogen, Carlsbad, CA) using the corresponding primers listed in Table 2.3.

For RT-qPCR, bacteria were cultured on CDMA at 32ºC in 7% CO_2 for 5 days or cultured in BHI broth at 37ºC with shaking overnight to enhance or minimize CLC production, respectively. RNA was converted to cDNA using the random priming method of the High Capacity cDNA Reverse Transcription Kit (Applied Biosystems-AB, Foster City, CA). Real-time PCR reactions were performed in 25 µl reactions using Power Sybr Green (Applied Biosystems) and gene-specific primers (Supplementary Table 3). RT-qPCR reactions were carried out in a 7300 Real-Time PCR System and analyzed using the SDS Software package (Applied Biosystems) using

BHI broth-grown LVS shaking at 37º C as the calibrator and GAPDH as the endogenous control for gene expression. Biological and technical replicates were done in triplicate.

Table 2.3 List of oligonucleotide primers used in RT-PCR assays

Primer	Sequence (5'->3')	Location	Product size (bp)
RT_0789-for	TGGACCGATGGTGCTCAAGGC	807145-807165	974
RT_0790-rev	AGCCTCAGCTTTAGCAAAAAGCCA	808118-808095	
RT_0790-for	GCGGCCAGAGCGACCAGAG	808727-808745	944
RT_0791-rev	ACCAGCACCTACTTGCGCGAC	809670-809650	
RT_0791-for	AGCCGGTGATATTGCAGCGAGT	809919-809940	735
RT_0792-rev	TCGCGAAGGCGGGTATCTCTAA	810653-810632	
RT_0792-for	ACCCGCCTTCGCGAATATGACA	810640-810661	775
RT_0793-rev	GGGATAACAGCTCCAACACCTAGCA	811414-811390	
RT_0793-for	GGGTGGTCAACGCCAAAGGCT	812756-812776	752
RT_0794-rev	TGCAACTCTCATAGCCTCTGCATCA	813507-813483	
RT_0794-for	TGAATGGGTTGGTCCAGCTTGC	814089-814110	345
RT_0795-rev	TCAACAATCCTGTCCCAGATCCAAGA	814433-814408	
RT_0795-for	TCTTGGATCTGGGACAGGATTGTTGA	814408-814433	654
RT_0796-rev	AGAGTTCCTCCATCGATCCAATGCT	815061-815037	
RT_0796-for	AGCATTGGATCGATGGAGGAACTCT	815037-815061	883
RT_0797-rev	ACCTTTGCAAGCATCTAAACCCACA	815919-815895	
RT_0797-for	TGTGGGTTTAGATGCTTGCAAAGGTG	815895-815920	974
RT_0798-rev	TGCCTGCCCAGAGTTTTGCTGA	816868-816847	
RT_0798-for	TCAGAAGCAGCGGTGCGAAA	817442-817461	1000
RT_0799-rev	AGCACAGGAGTACCACAAGCCA	818441-818420	
RT_0799-for	AGCAGCACAAGCGGGGTTGTAT	818472-818493	754
RT_0800-rev	TGTCTGCATACCTAAATGCTTAGCTGG	819225-819199	
RT_0800-for	TCAACTATGCTTGGGATGATGCGTT	818848-818872	2.46 Kbp
RT_0802-rev	TGTGCTACTGGCGTGCCACC	821294-821275	
RT_0802-for	GGTGGCACGCCAGTAGCACA	821275-821294	901

RT_0803-rev	ACGCGCGAACCAGTACCAGC	822175-822156	
RT_0803-for	TTCGCGCGTGCAGCAAGATG	822167-822186	
RT_0804-for	TGCTAGCTCCAGCATGGCTCTT	824670-824691	916
RT_0805-rev	GCACCTGGATCTGGGGTCGC	825585-825566	
RT_0805-for	GCGACCCCAGATCCAGGTGC	825566-825585	640
RT_0806-rev	CAGGAGCCCCCATCTCTAGAGCAAA	826205-826181	

2.2.11 Serum bactericidal assay

The bactericidal activity of 20% fresh guinea pig serum or various dilutions of human serum for LVS and mutants was determined as previously described [265]. Controls included LVS and LVS O-antigen mutant $WbtI_{G191V}$ [241], exposed to 20% fresh serum or 20% heat-inactivated serum.

2.2.12 Survival of *F. tularensis* LVS and mutants in macrophages

The intracellular survival and growth of LVS, LVSΔ1423/1422, LVSΔ1423/1422[1423-22+], and $WbtI_{G191V}$P17Δ1423/1422 was determined in the murine macrophage-like cell line J774A.1 (American Type Culture Collection**,** Manassas, VA) by modification of published methods [266]. The bacteria were mixed with macrophages at a multiplicity of infection of 100:1 (bacteria:macrophages). After 1 h incubation at 37°C in 5% CO_2, extracellular bacteria were removed by washing the cells with PBS, and the medium was replaced with 1 ml of complete Dulbeccos's Modified Eagle Medium (DMEM) containing 50 μg/ml gentamicin. After 45 min incubation, the cells were washed three times with PBS, followed by the addition of complete DMEM without antibiotics. The cells were then incubated at 37°C in 5% CO_2 for 72 h. At 0, 24,

48, and 72 h PI, the J774A.1 cells were washed in PBS, lysed by exposure to water for 5 min, and serial dilutions of the lysate were cultured onto BHIBC agar to determine the number of viable intracellular bacteria. Because the assays were done on different days and involved slightly different numbers of bacteria and macrophages, the slope and standard deviation of bacterial survival for each 24-h time period was calculated.

2.2.13 Virulence of *F. tularensis* LVS mutants in mice

Groups of five C57BL/6 mice (Charles River Laboratories, Wilmington, MA) were inoculated by the intranasal (IN) route with a mixture of 5.9×10^3 CFU/mouse of LVS and 8.0×10^3 CFU/mouse of LVSΔ1423/1422. All doses were confirmed by viable plate count on BHIB agar. Five days PI, the mice were humanely euthanized with excess carbon dioxide, and the liver, lungs, and spleen were harvested and cultured onto BHIB with or without 8 µg/ml of kanamycin, and incubated at 37°C in 5% CO_2 for up to 6 days.

In a separate trial, groups of six-week-old female BALB/c mice (Charles River Laboratories, Wilmington, MA) were inoculated with parent LVS or mutant LVSΔ1423/1422 IN or IP, and survival was monitored for six weeks. The doses used for IN inoculations were about 1.2×10^4 CFU/mouse of LVS or about 1.1×10^4 CFU of LVSΔ1423/1422. The doses used in IP inoculations ranged from 41 to 262 CFU/mouse of LVS, or 39 to 115 CFU of LVSΔ1423/1422. Challenge experiments were done on three different days. Therefore, the doses, determined by viable plate count, varied slightly.

For tissue clearance, BALB/c mice were inoculated IN with 7.9×10^3 CFU of strain LVS or 5.0×10^4 CFU of strain LVSΔ1423/1422. At 2, 4, or 7 days PI, surviving mice were humanely euthanized and the bacteria were cultured from the liver, lungs, and spleen as described above.

All experiments with animals were approved by the Virginia Tech Institutional Animal Care and Use Committee. Following challenge mice were monitored at predetermined intervals and euthanized if they became moribund.

2.2.14 Protective efficacy of *F. tularensis* LVS mutants in mice

BALB/c mice that survived and were healthy for six to seven weeks following IN or IP inoculation with mutant LVSΔ1423/1422 were challenged with 7.9×10^3 or 1.4×10^5 CFU of LVS IN, and mortality and clinical symptoms were recorded. Four weeks after challenge, surviving mice were humanely euthanatized using excess carbon dioxide, and portions of the liver, lungs, and spleen were homogenized and cultured for *F. tularensis*.

2.2.15 Statistical analyses

The student *t* test [267] was used to evaluate the significance in CLC compositional differences between LVS and mutant LVSΔ1423/1422. The analysis of variance was used to analyze the persistence of each strain in mouse macrophage cells (*in vitro*), comparative persistence of *F. tularensis* strains in liver, lungs, and spleen of mice (*in vivo*), and for protective efficacy of each mutant tested in mice and The Fisher's exact test was used to analyze the comparative persistence of *F. tularensis* strains in liver, lungs, and spleen of mice, and for protective efficacy of the mutant in mice [268]. For RT-qPCR the Ct of each replicate was used in an unpaired t test

between samples obtained from bacteria grown to enhance CLC (grown on CDMA at 32°C), or minimize CLC expression (grown in BHI broth at 37°C). Statistical analyses and *P* values were calculated using InStat software (GraphPad, La Jolla, CA).

2.3 RESULTS

2.3.1 Extraction of CLC

Gentle extraction of LVS with 10% NaCl [251] following growth on Chocolate agar for several days yielded a carbohydrate that was distinct from LPS, as determined by gas chromatography/mass spectrometry (GC/MS). However, the yield of this material was poor and many other components were present in the extract, including LPS and a wide variety of proteins. Subsequently, a greater yield of the CLC was obtained from LVS grown on Chamberlain's defined medium agar (CDMA) at 32°C and extracted with 0.5% phenol.

Cherwonogrodzky [250] reported that daily passage of *F. tularensis* LVS in Chamberlain's defined medium broth (CDMB), followed by growth on CDMA, resulted in an increase of the electron dense material surrounding the bacteria. Therefore, to enhance CLC synthesis and minimize contamination with LPS, the LVS O-antigen mutant $WbtI_{G191V}$ [241] was sub-cultured daily in CDMB for seventeen days ($WbtI_{G191V}$_P17), followed by growth at 32°C for 5 days on CDMA in 7% CO_2. Parent strain LVS was passed in the same way to obtain LVS_P17. Negative staining EM confirmed that such passage resulted in an increase in CLC synthesis around LVS_P17 (Fig. 1A). Similar results were obtained with type A strains SCHUS4 and TI0902 (Fig. 1B). In this example, but also in others, the CLC around the cell appeared to aggregate and was more dense than diffuse, possibly due to fixation during EM (Fig. 1B).

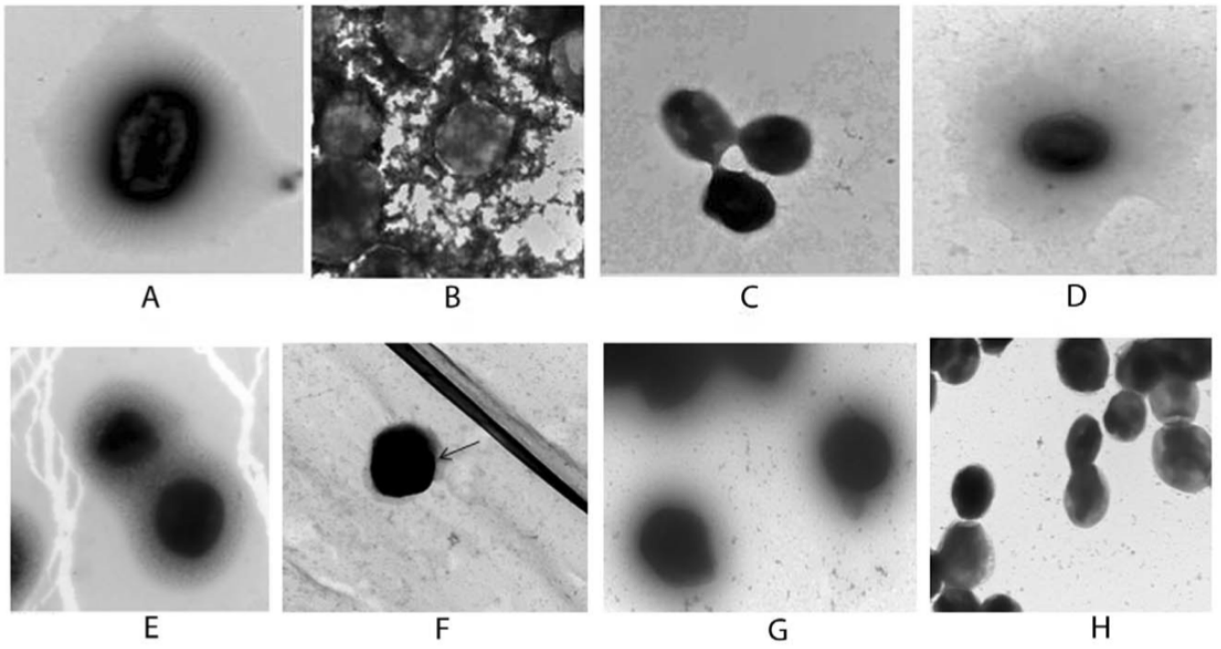

Figure 2.1 Negative stain electron microscopy of the CLC of *F. tularensis*.
Panels A and E: type B strain LVS_P10 grown at 32uC on CDMA; different cultures were examined on different days; Panel B: type A strain TI0902, passed and grown to enhance CLC expression as for LVS. In this and some other cases the CLC appeared to aggregate, which also occurred following isolation of the CLC; Panel C: glycosyl transferase mutant LVSD1423/ 1422_P10; Panel D: complemented strain LVSD1423/1422[1423-22+]_P10; Panel F: LVS not passed in defined medium and grown on CDMA at 37uC; only a small amount of CLC is visible (arrow); Panel G: O-antigen mutant $WbtI_{G191V}$_P17 grown as for LVS_P10; Panel H: O-antigen and CLC double mutant $WbtI_{G191V}$_P17D1423/1422. Strains LVS_P10, $WbtI_{G191V}$_P17, and type A strain TI0902_P10 have an electron dense layer surrounding their cells. This layer is missing in mutants LVSD1423/1422_P10 and $WbtI_{G191V}$_P17D1423/1422, and is restored in complemented strain LVSD1423/ 1422[1423-22+]_P10]. The bacteria were fixed in glutaraldehyde, and stained with uranyl acetate. Magnification is 20,000 X, and the scale bar is 500 nm.

Western blot analysis of LPS from exactly the same number of cells of LVS that were and were not subcultured in CDMB showed there was no increase in the amount of LPS on subcultured cells (Figure 2). Therefore, the enhanced electron dense material around the subcultured cells was not LPS.

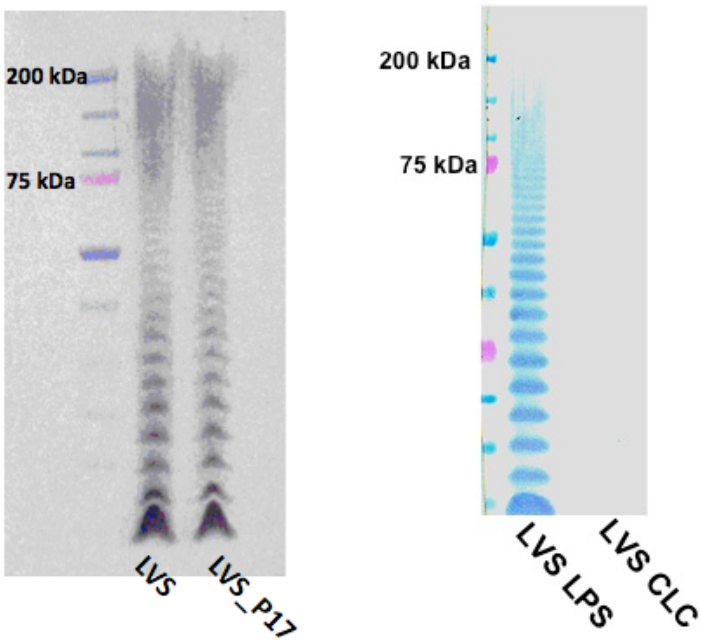

Figure 2.2 Western blot analysis of LVS LPS and CLC.
A: Polyclonal antibody to whole cell LVS on LPS extracted from LVS or LVS enhanced for CLC (LVS_CLC). **B:** MAb to *F. tularensis* O-Ag using LVS LPS or LVS CLC as antigen.

To further enhance CLC synthesis we tested the effect of supplementing CDMA with three carbon sources: 1% glycerol (Gly-CDMA), 1% galactose (Gal-CDMA, and 1% glucose (CDMA). LVS colonies grown on Gly-CDMA appeared similar to LVS grown on CDMA. There was substantially less growth and colony iridescence of bacteria incubated on Gal-CDMA. However, colonies grown on CDMA appeared more mucoid and more iridescent than those on CDMA alone (data not shown). When the CLC was extracted from 10 plates of $WbtI_{G191V}$_P17 grown on each carbon source at 32°C for 5 days there was 10% or more CLC recovered from bacteria grown on CDMA than on media supplemented with the other carbon sources, as

determined by protein and carbohydrate assays (data not shown). Therefore, the bacteria were grown on CDMA for subsequent extraction of CLC.

When $WbtI_{G191V}$_P17 was grown on CDMA as described above, extracted with 0.5% phenol, and the cells removed by centrifugation, the extract was thick, frothed easily, and was slightly yellow in color. Furthermore, this extract became highly insoluble when the phenol was removed or the material concentrated. The solubility of the extracted CLC was greatly improved after ethanol precipitation, digestion with RNase, DNase, and in particular Proteinase K (which also eliminated frothing), and suspension in Trizma buffer. Following ultracentrifugation and dialysis, further purification (primarily to remove ribose) was obtained by gel filtration through Sephacryl S-300 (see Materials and Methods). Approximately 2.8 mg of purified, LPS-free CLC was obtained per gram (wet weight) of $WbtI_{G191V}$_P17 cells grown on CDMA.

2.3.2 Physical and chemical characterization of the CLC

Following electrophoresis the extracted CLC appeared as a large molecular size, heterogeneous smear after staining with StainsAll/Silver stain (though distinct bands were apparent as color initially developed) (Fig. 3B), and by Western blotting with antiserum to whole cells (Fig. 3C). Although purified LPS was clearly observed by Western blotting with antibody to O-antigen, an equivalent amount of *F. tularensis* LPS was not stained by StainsAll/Silver stain, further showing that the CLC was distinct from LPS. Furthermore, as the source of the CLC was an O-antigen negative mutant, the high molecular size material could not be LPS. However, unlike LPS, very little of the material was reactive with the fluorescent stain Pro-Emerald Q (Fig. 3D). The profile of the crude extract obtained following 0.5% phenol extraction showed a wide

variety of peptides. However, a few low molecular size proteins were still present in the CLC following enzyme digestion, as shown by Coomasie Blue staining (Fig. 3A).

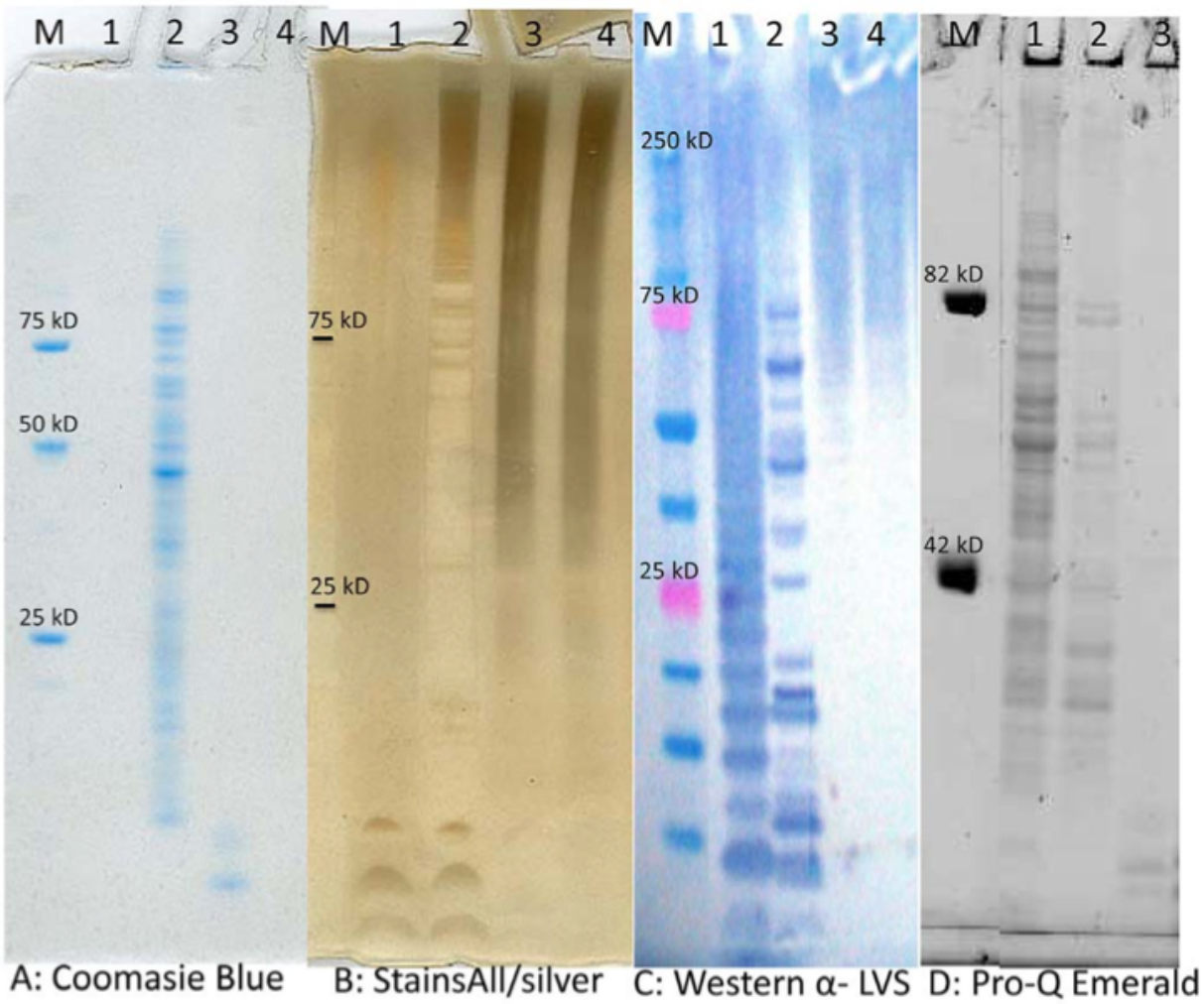

Figure 2.3. Polyacrylamide gel electrophoresis of CLC extracts.
CLC extracts at various stages of purity, or *F. tularensis* LPS as a control, were separated by electrophoresis in a 4–12% separating gel, and the components identified by (A), Coomassie Blue for protein; (B), Stains-All/silver stain for acidic molecules; (C), Western blot with antiserum to LVS whole cells for antigenic components; (D), Pro-Q Emerald stain for carbohydrate. Lanes for panels A-C: M, molecular size standards; 1, LVS LPS (20 mg); 2, crude CLC prior to enzyme digestion (20 mg); 3, CLC extract following enzyme digestion (20 mg); 4, purified CLC (20 mg). Lanes for panel D: M, molecular size standards; 1, crude CLC prior to enzyme digestion (20 mg); 2, CLC extract following enzyme digestion (20 mg); 3, purified CLC (20 mg). The Pro-Q Emerald stain of LPS (not shown here) looks similar to that of the Western blot, and is shown in reference 29.

The composition of the carbohydrate in the CLC was determined by GC/MS. Multiple (>10) analyses consistently indicated that the carbohydrate consisted of neutral residues glucose, mannose, and galactose (Fig. 4). Ribose, xylose, or C18:0 fatty acids were common but inconsistent contaminants, but if present could be removed by column chromatography. Monosaccharide residues unique to LPS, such as KDO or quinovosamine, were not present. In addition, galactose is not present in the LPS of this bacterium [245], further indicating this carbohydrate was distinct from LPS. Purified CLC was readily precipitated by addition of excess cold ethanol, further supporting that the CLC was of large molecular size. These collective results indicated that the CLC on the bacterial surface was a glycoprotein.

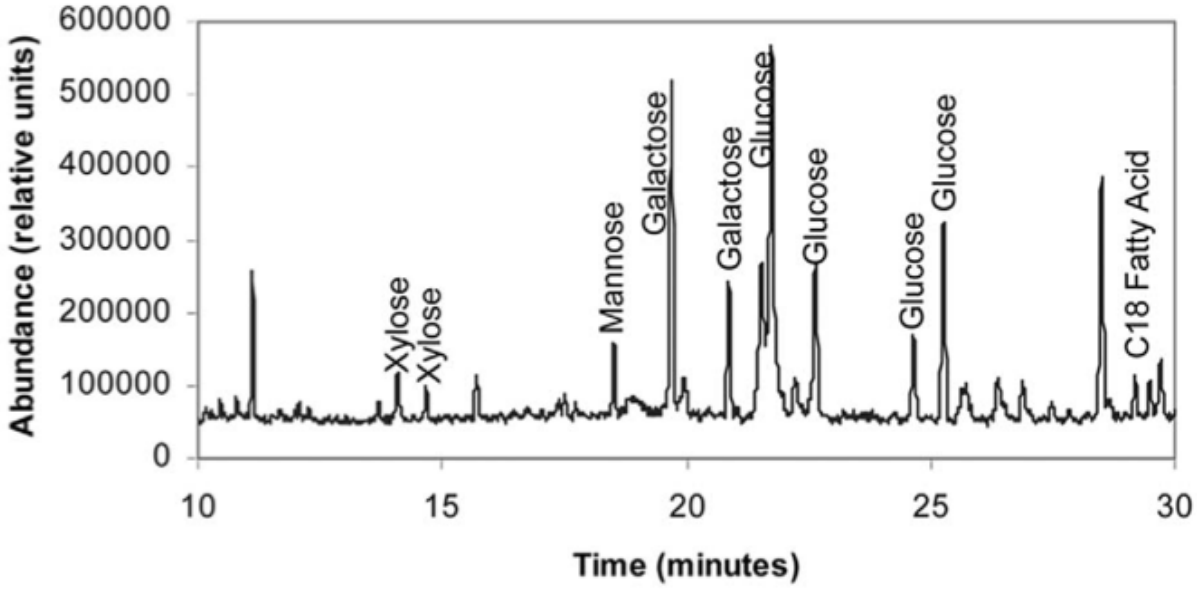

Figure 2.4 Trimethylsilyl (TMS) ethers of the methyl glycosides from purified *F. tularensis* CLC.

TMS derivatives of the glycoses from the CLC were analyzed by GC/MS. All sugars and C18 fatty acids match in both retention time and mass spectrum with known standards.

2.3.3 Identification of the putative genes responsible for CLC carbohydrate biosynthesis

BLAST analysis of the *F. tularensis* LVS genome sequence identified a 12.5 kb locus containing 12 genes (FTL_1432-FTL_1421) with homology to genes that encode for proteins involved in polysaccharide synthesis (Table 2.4).

Table 2.4 Putative genes and gene products that may contribute to F. *tularensis* CLC biosynthesis.

ORF in LVS	ORF in Schu S4	Size (bp)	Product[a]
FTL_1432	FTT_0789	669	D-ribulose-phosphate 3-epimerase
FTL_1431	FTT_0790	1395	Sugar transferase family protein (Glycosyl transferase)
FTL_1430	FTT_0791	1020	UDP-glucose 4-epimerase
FTL_1429	FTT_0792	1230	Glycosyl transferase group 1 family protein
FTL_1428	FTT_0793	1683	ATP-binding membrane transporter
FTL_1427	FTT_0794	1287	Hypothetical protein (Phosphoserine phosphatase)
FTL_1426	FTT_0795	684	Hypothetical protein (protein cfa)
FTL_1425	FTT_0796	762	Hypothetical protein
FTL_1424	FTT_0797	960	Glycosyl transferase family protein (galactosyl transferase)
FTL_1423[b]	FTT_0798	1008	Glycosyl transferase family protein (galactosyl transferase)
FTL_1422[b]	FTT_0799	1014	Glycosyl transferase family protein (mannosyl transferase)
FTL-1421	FTT_0800	663	Haloacid dehalogenase

[a]Determined by Smith-Waterman analysis
[b]Deletion of both of these genes resulted in CLC-deficient mutant LVSΔ1423/1422.

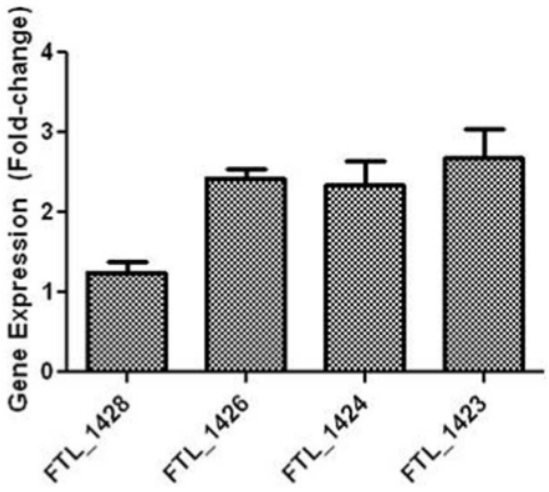

Figure 2.5 RT-qPCR of various regions of the putative CLC locus.

The results are shown as the x-fold change in gene expression using LVS grown in BHI broth to log phase (minimal CLC expression) as the calibrator and GAPDH as the endogenous control for gene expression. The locus tag of each gene from LVS is shown on the X-axis.

Smith-Waterman analysis indicated that FTL_1423 was most similar to a galactosyl transferase from *Streptococcus pneumoniae* (34.5% amino acid identity), and FTL_1422 was most similar (35.5% identity) to a mannosyl transferase from *Salmonella enterica*. Additional evidence that this locus contributed to CLC biosynthesis was obtained by RT-qPCR (Fig. 5). The expression of FTL_1426, FTL_1424, and FTL_1423 within the putative CLC carbohydrate locus was significantly upregulated (P=0.025, 0.023, and 0.031, respectively) up to three-fold when LVS was grown to maximize CLC production (cultured on CDMA at 32°C for 5 days in 7% CO_2) compared to growth conditions that would minimize CLC production (shaking at 200 rpm in brain heart infusion broth supplemented with 0.1% L-cysteine hydrochloride monohydrate) (BHI) broth at 37°C to log phase).

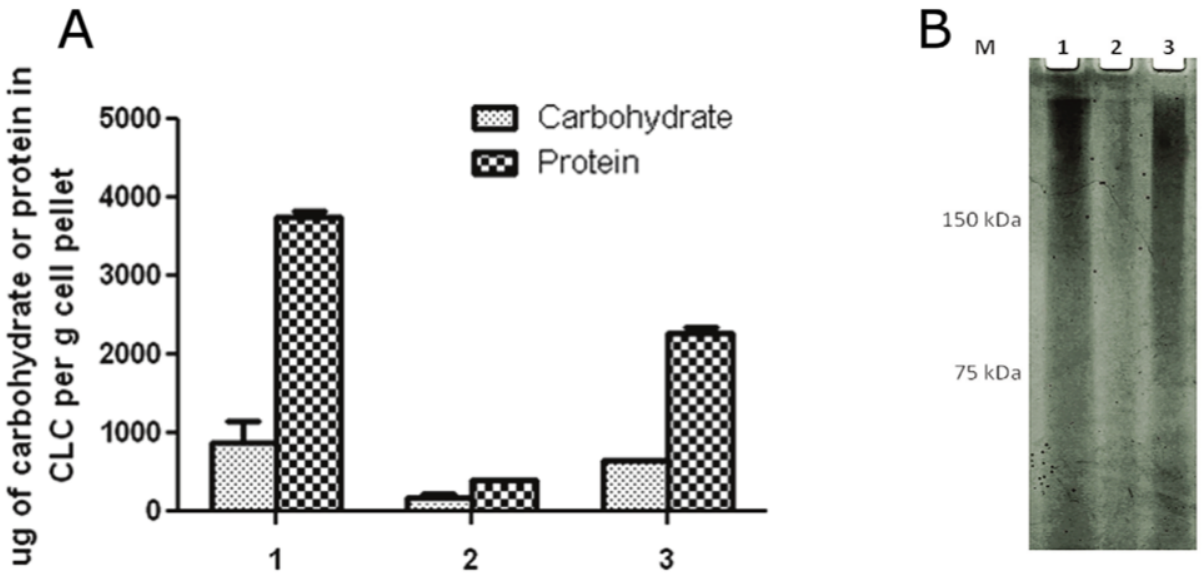

Figure 2.6 CLC content from LVS_P10, LVSΔ1423-22_P10, and LVSΔ1423-22[1423-22+]_P10. Lanes: 1, LVS_P10; 2, LVSΔ1423/ 1422_P10; 3, LVSΔ1423-22[1423-22+]_P10. A) Carbohydrate and protein content of extracted CLC; B) Stains All/silver stain of extracted CLC. The reducing carbohydrate content was measured by phenol sulfuric acid assay [47], and the

protein content was measured by BCA assay. The CLC was extracted from the same number of cells of each strain, as described in Materials and Methods.

2.3.4 Mutagenesis of FTL_1423/1422

FTL_1423 and FTL_1422 were deleted in LVS by allelic exchange (see Materials and Methods). Mutagenesis was confirmed by the inability to amplify either open reading frame (ORF) by polymerase chain reaction (PCR), by identification of the kanamycin resistance gene from the suicide vector in the genome (by PCR and colony blot hybridization), and by sequencing of PCR products (data not shown). Unlike LVS (Fig. 1A), LVSΔ1423/1422 lacked any evidence of a CLC following passage to enhance CLC synthesis (Fig. 1D). Furthermore, significantly less CLC carbohydrate ($P = 0.01$) and protein ($P < 0.01$) was extracted from this mutant with 0.5% phenol than the parent (Fig. 6), and 91% less glucose, galactose, and mannose were present in extracts, as determined by GC/MS (data not shown).

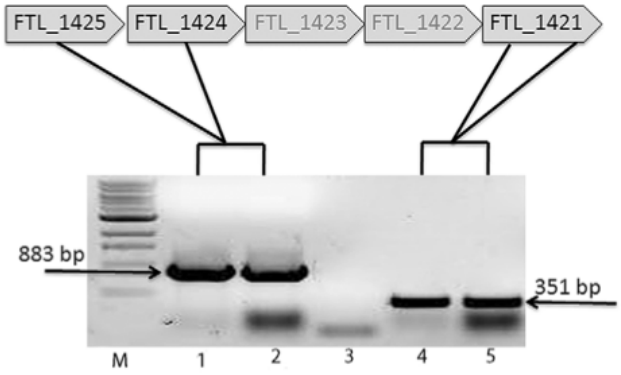

Figure 2.7 RT-PCR of the DNA region FTL_1421 from LVSΔ1423/ 1422.
LVS and LVSD1423/1422 were grown on CDMA for at least 2 days, the RNA isolated, converted to cDNA, and amplified by PCR to determine if a transcript from DNA downstream of the mutation was made. Lanes: M, 1 kb+ DNA molecular size standards; 1, control amplification of FTL_1425-1424 in LVS; 2, amplification of FTL_1425- 1424 upstream of the mutation in LVSΔ1423-22; 3, control amplification of FTL_1425-1424 upstream of the mutation (no bacteria); 4, control amplification of FTL_1421 from LVS; 5, amplification of FTL_1421 immediately downstream of the mutation in LVSD1423/1422. The presence of a normal band of

about 351 bp from LVSΔ1423-22 indicated that the mutation had no polar effect on downstream genes.

To confirm that deletion of FTL_1423/1422 was solely responsible for the absence of the CLC, both ORFs were cloned into expression vector pFNLTP6 [263], which was then introduced into LVSΔ1423/1422 by electroporation. The complemented mutant was restored in CLC synthesis, as shown by electron microscopy (Fig. 1D), and by enhancement of the protein (partially) and carbohydrate content of purified CLC (Fig. 6).

To confirm that the deletion of FTL_1423 and FTL_1422 did not have a polar effect on downstream genes, the DNA region from FTL_1421 through FLT_1418 was subjected to RT-PCR (Fig. 7). The transcript of this region was identical to that of the transcript from LVS, indicating that genes downstream of FTL_1423 and FTL_1422 were not responsible for the loss of CLC in mutant LVSΔ1423-22.

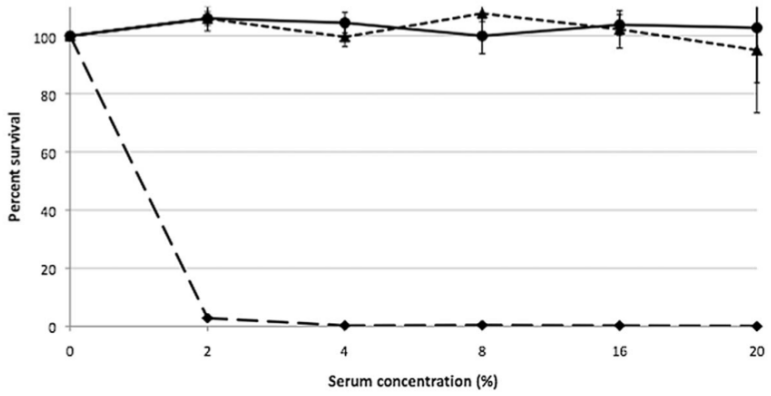

Figure 2.8 Bactericidal assay of LVSΔ1423-22 and control strains in the presence of fresh human serum.

The bacteria were diluted in PBS supplemented with 0.15 mM CaCl2, 0.5 mM MgCl2, and 2%, 4%, 8%, 16%, or 20% fresh, pooled human serum. Aliquots were cultured by viable plate count before and after 60 min. incubation at 37°C. Bacterial strains: LVS, ——•——; LVSΔ1423-22, ---▲---; O-antigen mutant $WbtI_{G191V}$_P17, __ __◆__ __.

2.3.5 *In vitro* growth rate and serum resistance of LVSΔ1423/1422

The generation time for strain LVS in BHI was approximately 2.5 h during log phase. However, mutant LVSΔ1423/1422 grew substantially slower, with a generation time of approximately 6 h. Both parent LVS and mutant LVSΔ1423/1422 were completely resistant to the bactericidal action of up to 20% fresh guinea pig serum and human serum (v/v), whereas there was 0% survival of LVS O-antigen mutant $WbtI_{G191V}$_P17 [241] in as little as 2% human serum (Fig. 8). Therefore, the CLC did not contribute to serum resistance.

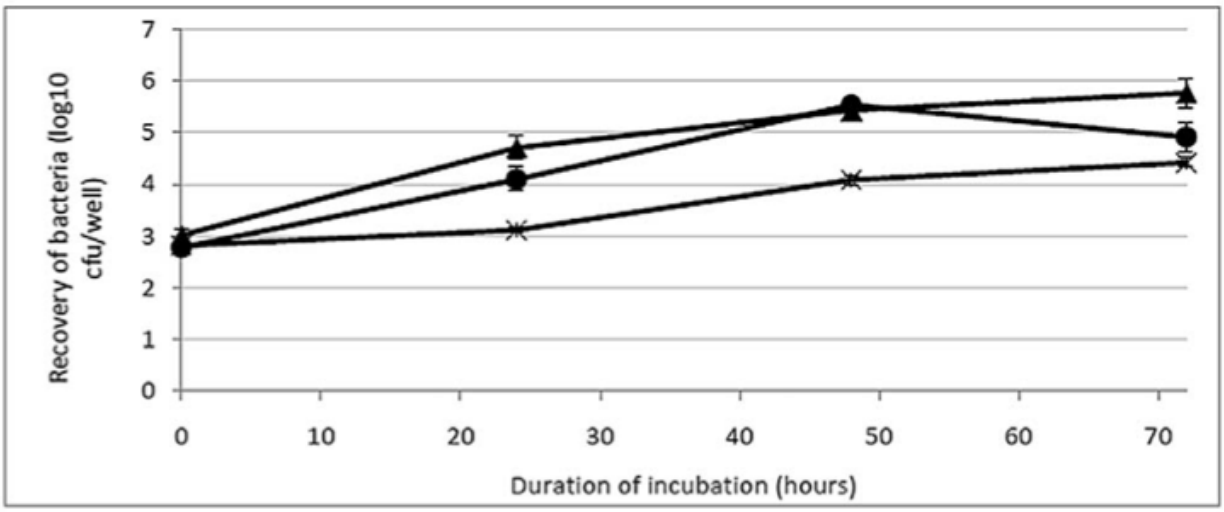

Figure 2.9 Intracellular survival of *F. tularensis* LVSΔ1423-22 in J774A.1 cells.
The J774A.1 monolayer (approximately 4.56105 macrophages/well) was infected with approximately 5.5 x 10^7 CFU/well of strain LVS (●), LVSΔ1423-22 (▲), or LVSΔ1423-22[1423-22+] (✕). Intracellular survival of the bacteria was determined at 0, 24, 48, and 72 h post-infection, as described in Materials and Methods. Data are shown on the log scale as the average number of bacteria recovered from dilutions of lysates of J774A.1 cells. The results shown were from two experiments tested in duplicate at each time point.

2.3.6 Viability of LVSΔ1423/1422, LVSΔ1423/1422[1423-22+], and $WbtI_{G191V}$Δ1423/1422 in macrophages

At 12 and 24 hours after inoculation, there was no significant difference in viability between LVS, LVSΔ1423/1422, and LVSΔ1423/1422[1423-22+] in J774A.1 cells ($P > 0.1$). However, by 48 hours after inoculation the O-antigen mutant in which FTL_1423/1422 was also deleted ($WbtI_{G191V}$Δ1423/1422) had completely lost viability in the J774A.1 macrophages. The slope for intracellular growth of the bacteria as $\log_{10}$ CFU/well between 24 and 48 h for strains LVS, LVSΔ1423/1422, LVSΔ1423/1422[1423-22+], and $WbtI_{G191V}$Δ1423/1422 were +1.44, +0.73, +0.97, and -3.53, respectively (Fig. 9).

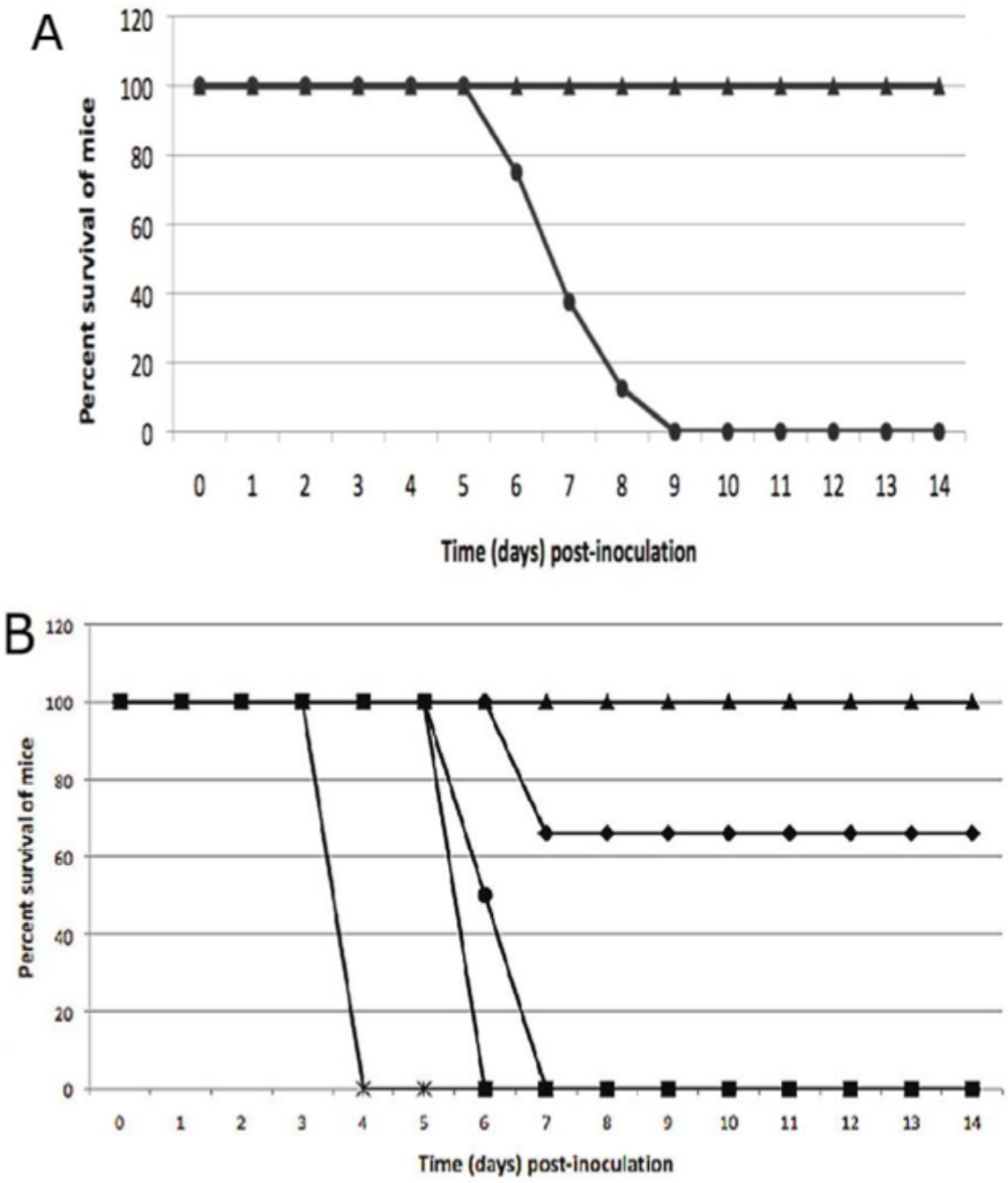

Figure 2.10 Survival of mice inoculated with *F. tularensis* LVSΔ1423-22.
Groups of BALB/c mice were inoculated IN (A) or IP (B), and survival was monitored for six weeks. No mice challenged IN with LVSΔ1423-22 died during the study. The doses and symbols used for IN inoculations were about 1.2 x 10^4 CFU/mouse of LVS (●), and about 1.6 x 10^4 CFU of LVSΔ1423-22 (▲). The doses and symbols used for IP inoculations were 262 CFU/mouse of LVS (●); 3,375 CFU/mouse of LVS (x); 1,124 CFU/mouse of LVSΔ1423-22 (▲); 11,136 CFU/mouse of LVSΔ1423-22 (◆); 33,408 CFU/mouse of LVSΔ1423-22 (■).

2.3.7 Virulence of LVSΔ1423/1422 in mice

BALB/c mice were inoculated by the intranasal (IN) or IP routes with LVS or LVSΔ1423/1422 to evaluate the effect of loss of CLC on F. *tularensis* virulence (Fig. 10). All mice inoculated IN with about $1.26x10^4$ CFU of LVS died or needed to be euthanized in less than 10 days. In contrast, all mice inoculated IN with up to $1.66x10^4$ CFU of LVSΔ1423/1422 survived longer than six weeks and never developed clinical symptoms (Fig. 10A). All BALB/c mice inoculated IP with 41,262 or 3,375 CFU of LVS died within 7 days. In contrast, all mice inoculated IP with 1100 CFU or 2 of three mice inoculated IP with 11,136 CFU of strain LVSΔ1423/1422 survived longer than four weeks. However, all mice inoculated IP with 33,408 CFU of the mutant died or were euthanized within 6 days (Fig.10B). Although the lethal dose of the mutant was lower following IP challenge than IN challenge, the LD50 of the parent was also much lower following IP challenge (~41 CFU) than IN challenge (~200 CFU).

2.3.8 Persistence of LVSΔ1423/1422 in mouse tissues

BALB/c mice were inoculated IN with 7.9×10^3 of LVS or 5.0×10^4 of LVSΔ1423/1422, followed by euthanasia at 2, 4, or 7 days post-inoculation (PI), and the number of bacteria in the lungs, liver, and spleen determined (Fig. 11). LVS numbers increased in all three organs between day-2 and day-7 PI. LVSΔ1423/1422 was recovered from liver (Fig. 11A), lungs (Fig. 11B) and spleen (Fig. 11C) in approximately the same numbers as LVS on day-2 and day-4 PI, but was recovered in significantly fewer numbers from all three organs on day-7 PI ($P < 0.005$ for each organ). These results indicated that expression of the CLC was essential for full virulence of LVS in the respiratory tract were separately compared with LVS. The P values for the differences between the mean values were <0.05 (*) or <0.005 (*).

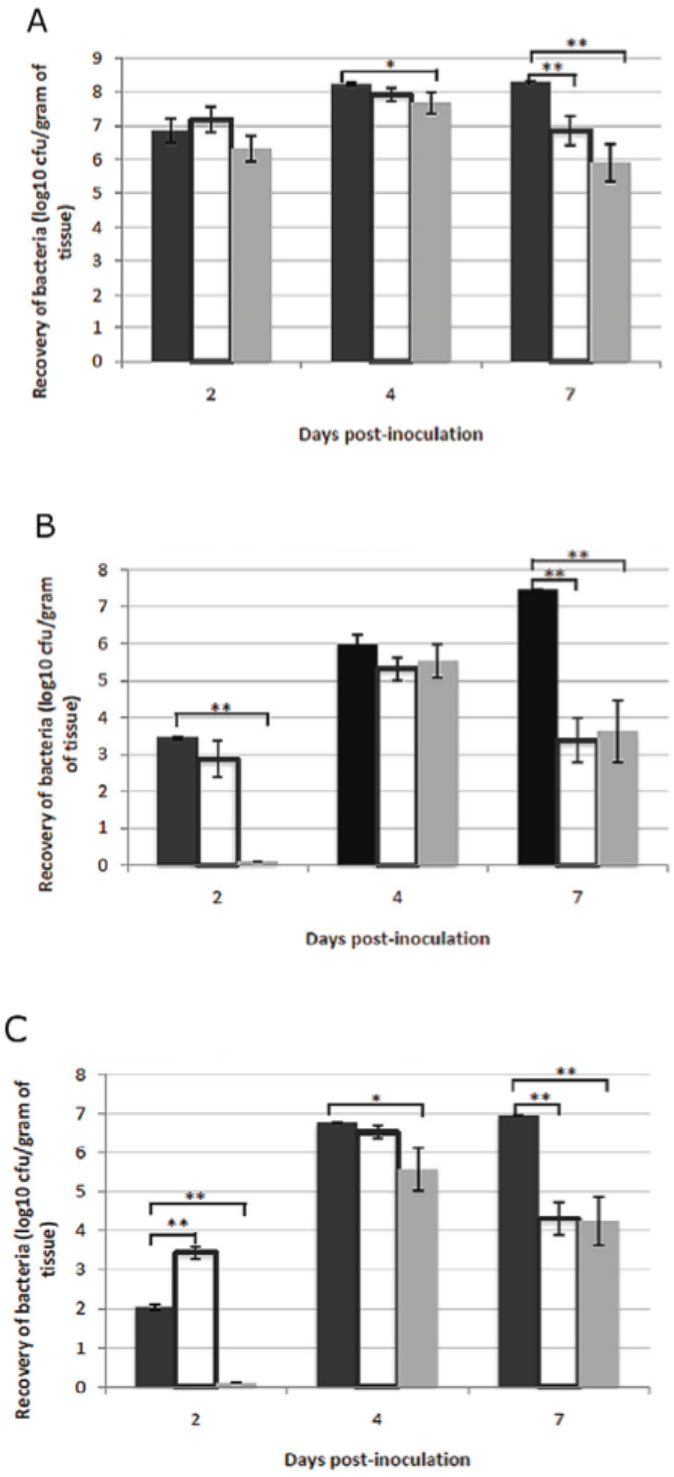

Figure 2.11 Recovery of *F. tularensis* LVSΔ143/1422 from the tissues of mice following IN inoculation.

Groups of BALB/c mice were inoculated IN with 7.9 x 10^3 CFU of strain LVS, 5.0 x 10^4 CFU of strain LVSΔ1423-22 (high dose of mutant), or 1.1 x 10^4 CFU of strain LVSΔ1423-22 (low dose of mutant). At 2, 4, or 7 days PI, mice were euthanized. The lungs (A), liver (B), and spleen (C) were aseptically removed, homogenized in PBS, and the CFU/g of tissue determined. The recovery of bacteria from inoculated mice are shown as dark-filled bars (LVS), open bars (high dose of LVSΔ1423-22), and grey-filled bars (low dose of LVSΔ1423-22). The mean values of the CFUs of each dose of the mutant.

In a separate trial, C57BL/6 mice were inoculated with a mixture of 5.9 × 10^3 CFU/mouse of strain LVS mixed with 8.0 × 10^3 CFU/mouse of mutant LVSΔ1423/1422. Five days PI the mice were euthanized, tissue homogenates were cultured on BHI agar supplemented with 5% (v/v) sheep blood (BHIB), and an average of 1.0 × 10^5, 1.9 × 10^7, and 1.3 × 10^7 of bacteria were present per gram of liver, lungs, and spleen, respectively (Table 3). The same tissue extracts plated on BHIB plates containing kanamycin yielded 0, 0, and 6.1 ×10^2 colonies per gram of liver, lung, and spleen, respectively (Table 2.5). Therefore, LVSΔ1423/1422 was significantly less fit ($P < 0.001$ from each organ) to survive in host tissues than LVS.

Table 2.5 Recovery of LVS and LVSΔ1423-22 following co-inoculation into C57BL/6 mice.

Organ	CFU on BHICB	CFU on BHICB containing Kanamycin
Liver	1.0×10^5	0.00
Lungs	1.9×10^7	0.00[b]
Spleen	1.3×10^7	6.1×10^2

[a]Five mice were inoculated IN with a mixture of 5.9×10^3 CFU of LVS and 8.0×10^3 CFU of LVSΔ1423/1422. Five days PI the mice were euthanized, and tissue extracts were cultured on BHICB with or without Kan. The numbers shown represent the average CFU/g tissue.
[b]A few colonies were isolated from the lungs of one of five mice.

2.3.9 Protective efficacy of LVSΔ1423/1422 in mice

Mice inoculated IN with 6.1×10^3 CFU of LVSΔ1423/1422 were challenged with 1.4×10^5 CFU of LVS IN six weeks PI. All mice survived challenge (Fig. 12) and none developed clinical symptoms, whereas all control mice died or had to be euthanized within 10 days. Thus, LVSΔ1423/1422 lacking CLC was capable of inducing protection in BALB/c mice following IN challenge with a high dose of LVS. Mice previously inoculated IP with 39 CFU of LVSΔ1423/1422 were challenged IN 7 weeks PI with 7.9×10^3 CFU of LVS. The challenged mice developed mild clinical symptoms (reduced activity) until about six days PI, after which time they recovered (data not shown). Therefore, IP inoculation with a low dose of 39 CFU/mouse also induced protection against respiratory tularemia.

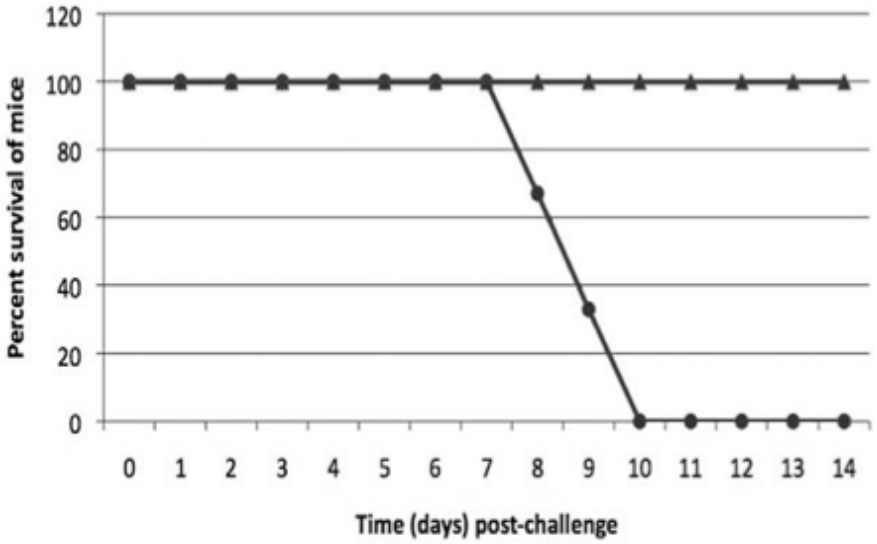

Figure 2.12 Protective efficacy of LVSΔ1423-22 against IN challenge of mice with LVS. Groups of BALB/c mice were injected with PBS (●), or inoculated with 6.1 x 10^3 CFU/mouse of LVSΔ1423-22 (▲). Six weeks PI, the mice were challenged IN with 1.4 x 10^5 CFU/ mouse of LVS, and the mice were monitored for 4 weeks. No mice died or were symptomatic by 10 days post-challenge. The P value for animal survival after 10 days post-challenge was >0.001.

2.4 DISCUSSION

F. tularensis has long been postulated to be encapsulated, based primarily on electron microscopy [245,246,250]. However, the presence of a capsule around *F. tularensis* is not always evident and has not been isolated, raising question as to whether a true capsule actually exists. Cherwonogronsky et al. [250] showed that a CLC can be enhanced by daily passage of *F. tularensis* LVS in CDMB, followed by culture on CDMA, and that bacteria enhanced for this surface material are more virulent in mice. We confirmed by EM and by RT-qPCR that the CLC was upregulated when LVS was passed in CDMB and grown at lower temperature in CO_2 for several days on CDMA, compared with when the bacteria were grown shaking rapidly in complex broth medium. A similar CLC could also be isolated and observed by EM around type A strains SCHUS4 and TI0902.

Analysis by GC/MS, chemical assays, amino acid analysis, and the carbohydrate-specific fluorescent stain Pro-Q Emerald indicated that unlike most bacterial capsules, the predominant component of the CLC was protein, not carbohydrate. Furthermore, following extraction with 0.5% phenol, the CLC foamed and easily became insoluble. These are also features of self-assembling bacterial surface (S)-layer proteins, which are common in bacteria and are often glycosylated (discussed further in Chapter 3) [269]. Proteinase K digestion was used to remove most of the protein to improve solubility and focus on the carbohydrate component, though some proteins were proteinase K resistant. Amino acid analysis indicated that the majority of the amino acids remaining after Proteinase K digestion were glutamic and aspartic acids (unpublished data). Supplementation of the growth medium with glucose, and possibly cations such as Ca^{++} and Mg^{++}, further enhanced CLC synthesis, which is consistent with the effect of

glucose supplementation on cell surface carbohydrate content [270]. Repeated analyses of the carbohydrate component of the CLC consistently yielded glucose, galactose, and mannose. Although the structure of the carbohydrate polymer has not yet been determined, gel electrophoresis and column chromatography confirmed that the material is of large molecular size. Bacterial glycoproteins may have only 150 glycoses, but are attached as a heterogeneous repeating polymer, resulting in a ladder-like banding pattern or smear in polyacrylamide gels [269]. A similar ladder-like/smear profile was observed with the *F. tularensis* CLC following staining with Stains All/silver stain and Western blotting. Therefore, glucose, galactose, and mannose might compose a trisaccharide polymer of a glycosylated protein.

The CLC was distinct from the LPS, as determined by GC/MS, lack of more LPS on cells enhanced for CLC, and the molecular size of CLC isolated from an O-antigen mutant. Apicella et al. [92] recently reported the presence of an O-antigen capsule on *F. tularensis*, which was detected by monoclonal antibody (MAb) binding. This MAb (11B7) bound to the crude CLC initially extracted from the surface of LVS, but not from O-antigen mutant $WbtI_{G191V}$, or from the purified CLC (unpublished data). Therefore, the O-antigen capsule is also distinct from this CLC. "Unencapsulated" mutants of *F. tularensis* LVS have been described that are highly susceptible to complement-mediated killing [246,248]. However, these mutants may also have been O-antigen deficient because *F. tularensis* LVS lacking O-antigen is highly serum-sensitive [86,183,187,241]. In contrast, the CLC mutant generated in this study was resistant to the bactericidal action of guinea pig or human serum.

Loci that are responsible for the synthesis and export of bacterial carbohydrate polymers are about 12-18 kb in size, and contain genes that encode for ABC transporters, glycosyltransferases, membrane spanning proteins, etc. [271,272]. Larrson et al. [105] described a putative polysaccharide locus from the genome sequence of *F. tularensis* strain SCHUS4. To determine if this locus contributed to CLC biosynthesis in LVS, FTL_1423 and FTL_1422 (which have homology to genes encoding for glycosyl transferases) were mutated by allelic exchange. The deletion of these genes appeared adequate to block assembly of the CLC on the bacterial surface, as no CLC could be observed by EM around LVSΔ1423-22, and little CLC could be isolated from this mutant. Therefore, glycosylation of protein may be required for formation of the CLC on the surface. Complementation of LVSΔ1423/1422 *in trans* with both genes restored CLC expression, and RT-PCR indicated that expression of genes downstream of the mutation were not affected, confirming that loss of the CLC was not due to another mutation.

The capability of mutant LVSΔ1423-22 to survive and grow in the mouse macrophage-like cell line J774A.1 for 72 h PI was similar to that of parent strain LVS. However, the O-antigen/CLC double mutant $WbtI_{G191V}$_P17Δ1423/1422 began to decline in intracellular numbers after 24 h PI, and was cleared from the cells by 48 h PI. These results differ from previous results obtained with LVS O-antigen mutant $WbtI_{G191V}$, whose growth was initially delayed in J774A.1 cells, but then grew at the same rate as the parent strain after 48 hours [241]. The inability of the double mutant to grow in macrophages indicated that both O-antigen and the CLC were necessary for intracellular survival. Golovliov et al. [123] suggested that shedding of a capsule-like material from *F. tularensis* following phagocytosis may result in degradation of the membrane and release of bacteria into the cytoplasm. Our results suggest that both the CLC and the O-antigen

may be necessary for phagosomal escape. Additional EM experiments of *F. tularensis* phagocytosis with O-antigen and CLC mutants should help to clarify this issue.

Deletion of both FTL_1423 and FTL_1422 in LVS resulted in significant loss of virulence in mice following IN challenge. These results are consistent with those of Weiss et al. [273], who reported that transposon mutagenesis of *F. novicida* FNN_1213 (equivalent to FTL_1423 of LVS) resulted in moderate attenuation following subcutaneous challenge of mice. However, LVSΔ1423-22 was only slightly less virulent than LVS in mice following IP challenge. Inoculation by the IP route introduces the bacteria directly into the systemic tissues and bypasses many of the innate immune defenses. Therefore, the CLC may be important for protection of *F. tularensis* LVS from the innate immune response, particularly in the respiratory tract. At 2 days and 4 days post-IN inoculation, the presence of LVSΔ1423/1422 in the lungs, liver, and spleen was not significantly different from that of LVS. However, the numbers of this mutant in all three organs dropped significantly by 7 days PI, suggesting that the CLC is necessary for *F. tularensis* LVS to persist in the tissues. Furthermore, when LVS and LVSΔ1423-22 were inoculated concurrently into mice, the mutant was unable to compete with the parent and few mutant cells could be recovered from mouse tissues.

After a single IN inoculation with a high dose of LVSΔ1423/1422 (up to 80× the LVS LD_{50}), mice challenged IN with up to >700 times the LD_{50} with LVS developed no clinical symptoms of tularemia. In addition, mice inoculated IP with LVSΔ1423/1422 were also protected against low dose IN challenge with LVS, demonstrating that systemic immunity to this mutant was adequate for protection in the respiratory tract, though less effectively. Therefore, the generation

of CLC mutants in type A strains is warranted to determine if such mutants are adequately attenuated and capable of inducing a protective immune response against type A strains.

These results showed that the CLC may be a glycoprotein that is upregulated under particular growth conditions, the glycose component of the CLC contained glucose, galactose, and mannose, the loci identified as FTL_1432 through FTL_1421 in LVS contribute to CLC synthesis, and that the CLC is required for full virulence of LVS, but not for inducing protective immunity in mice against LVS.

2.5 Co-Authors' Contributions

Conceived and designed the experiments: Abey Bandara (AB), Anna Champion (AC), Xaishon Wang (XW), Parastoo Azadi (PA) (Complex Carbohydrate Research Center, GA) and Tom Inzana (TJI). Performed the experiments: AB AC XW and Gretchen Berg (GB). Analyzed the data: ABB AEC XW PA and TJI. Contributed reagents/materials/analysis tools: PA. Wrote the paper: AB AC TJI.

CHAPTER 3

Evidence that a component of the CLC could be a surface-layer protein

3.1 Introduction

Surface layers (S-layers) can be found as part of the cell envelope in Gram-positive bacteria and archaea, as well as (less commonly), in Gram-negative bacteria [274]. An S-layer is defined as self-assembled monomolecular crystalline arrays of proteinaceous subunits (Surface-Layer Proteins, SLP) on the surface of the microorganism [275]. These proteins are very commonly glycosylated, water-insoluble and cover much of the bacterial cell surface during various stages of growth [276]. S-layer functions are diverse and vary from species to species including: protection against phagocytosis, resistance against low pH, barrier against enzymatic degradation and adhesion to host cells [275,277]. S-layers have been found in many Gram-negative pathogenic bacterial species, and are commonly associated with the LPS via ionic, carbohydrate-carbohydrate, protein-carbohydrate and/or protein-protein interactions [275]. The specific function of S-layers is still being elucidated for many species, but its designation as a cell-surface antigen has led to research on the role of S-layers in pathogenesis. Many human pathogens, including highly virulent select agents have been found to have SLP's. *Bacillus anthracis* has two SLPs (Sap and EA1) that are proposed to aid in establishing the anthrax infection [278,279]. The S-layer of *Tannerella forsythia* is reported to delay the host immune response as well as aid in adherence to host cells during infection [280,281]. There have been reports of released S-layer structures in O-antigen deficient strains of some Gram-negative S-layer producing bacteria [282]. Generally, S-layers can be extracted with varying chaotropic agents, including urea. After

purification, the SLP subunits will self-assemble into 2-dimensional crystalline arrays [269]. The arrays are either oblique, square, or hexagonal in symmetry [283]. Typically, SLPs are composed of a high proportion of acidic and hydrophobic amino acids, which play an important role in the self-assembly process [284,285]. In addition, Gram-negative bacterial S-layers have been found to act as barriers to protect the bacterial cell against attack by bacterial parasites, such as, *Bdellovibrio bacteriovorus*, and can give the organism a selective advantage in certain conditions such as aquatic habitats [286,287]. *Francisella* has been found in fresh and brackish water, and outbreaks of pathogenic *F. tularensis* and *F. novicida* have been linked to natural water sources [288].

The ability of *Francisella* to persist in a diverse variety of natural habitats as well as the ability of *Francisella* to evade the host immune system and persist during infection, make *F. tularensis* a unique pathogen. During infection of a host, *F. tularensis* surface components (LPS, O-antigen capsule) mask the pathogen and cause a delay in pro-inflammatory cytokines that are necessary for control of the infection [91,139-142]. In the human pathogen, *Tannerella forsythia*, a mutant strain deficient in the glycosylated S-layer was found to induce significantly higher levels of pro-inflammatory IL-1β, TNF-α, and IL-8 than the parent strain [280]. Using *F. tularensis* LVS, it was found that the surface antigen capsule-like complex (CLC) was required for virulence during the intranasal (i.n.) route of infection, but did not affect virulence during the intraperitoneal (i.p.) route [192]. During an i.p. infection, the bacteria are introduced directly into the host tissues and therefore bypass much of the innate immune system, suggesting the CLC might be a factor of importance in protecting the bacteria from the host innate immune response [91,139-142]. The CLC of *F. tularensis* was initially characterized as being composed of highly insoluble

glycoprotein(s), decorated with glucose, galactose, and mannose residues [192]. The extraction procedures used yielded a low amount of the glycoprotein that was hard to manipulate due to high insolubility. Parallels in the role of the CLC to known roles of S-layers as well as the biochemical and biophysical similarities of CLC components to known SLPs, led us to hypothesize whether or not the CLC or a component of the CLC was in fact a novel S-layer-like glycoprotein.

3.2 Materials and Methods

3.2.1 Bacterial strains and growth conditions

F. tularensis strains used in this study were derived from the type B Live Vaccine Strain (LVS). $WbtI_{G191V}$_P10 is an O-antigen (O-Ag) deficient mutant of LVS and $WbtI_{G191V}\Delta$1423-22 is the O-Ag deficient mutant of LVS that is also deficient in CLC production due to the deletion of two glycosyl transferases [67,94,192]. *F. tularensis* strains were cultured from frozen stock suspensions onto brain heart infusion agar (Becton-Dickinson) supplemented with 0.1% L-cysteine hydrochloride monohydrate (Sigma-Aldrich, St. Louis, MO) (BHIA) or Chamberlain's defined media [250] with 1.5% glucose agar (CDMA) and incubated at 37°C in 7% CO_2, unless otherwise stated. For culture in broth, *F. tularensis* strains were grown with shaking (175 rpm) in BHI broth (BHIB) at 37°C, or CDM broth (CDMB) at 32°C. For selection of recombinant strains 15 μg kanamycin (Kan)/ml was added to the stated medium. For enhancement of surface CLC/SLP, the bacteria were passaged in CDMB ten times and is indicated by a "P10" on the strain name. For CLC preparation, *F. tularensis* was grown on CDMA in petri dishes (150 mm X 15 mm), and incubated at 32°C in 7% CO_2 for 5 days. All experiments with LVS and mutants were carried out in biosafety level (BSL)-2 facilities in an approved biosafety cabinet.

3.2.2 Reverse-transcriptase PCR

Annotation of putative *F. tularensis* LVS genes were determined using BLAST and the Smith-Waterman algorithm [258,259]. For reverse transcriptase-PCR (RT-PCR), RNA was isolated from LVS strains using the RNeasy extraction kit following digestion of cells with 400 µg/ml lysozyme. Bacteria were grown on CDMA at 37ºC for at least 2 days prior to extraction of RNA. RNA was converted to cDNA and amplified with SuperScript III First Strand Synthesis System) using overlapping primers progressively down the locus **(Table 3.1)**.

Table 3.1 Reverse-transcriptase primers for potential SLP locus.

Gene		Sequence (5'->3')	Start	Stop
FTT_0789	Forward	TGGACCGATGGTGCTCAAGGC	807145	807165
FTT_0790	Reverse	AGCCTCAGCTTTAGCAAAAAGCCA	808118	808095
	Product length	974		
FTT_0790	Forward	GCGGCCAGAGCGACCAGAG	808727	808745
FTT_0791	Reverse	ACCAGCACCTACTTGCGCGAC	809670	809650
	Product length	944		
FTT_0791	Forward	AGCCGGTGATATTGCAGCGAGT	809919	809940
FTT_0792	Reverse	TCGCGAAGGCGGGTATCTCTAA	810653	810632
	Product length	735		
FTT_0792	Forward	ACCCGCCTTCGCGAATATGACA	810640	810661
FTT_0793	Reverse	GGGATAACAGCTCCAACACCTAGCA	811414	811390
	Product length	775		
FTT_0793	Forward	GGGTGGTCAACGCCAAAGGCT	812756	812776
FTT_0794	Reverse	TGCAACTCTCATAGCCTCTGCATCA	813507	813483
	Product	752		

	length			
FTT_0794	Forward	TGAATGGGTTGGTCCAGCTTGC	814089	814110
FTT_0795	Reverse	TCAACAATCCTGTCCCAGATCCAAGA	814433	814408
	Product length	345		
FTT_0795	Forward	TCTTGGATCTGGGACAGGATTGTTGA	814408	814433
FTT_0796	Reverse	AGAGTTCCTCCATCGATCCAATGCT	815061	815037
	Product length	654		
FTT_0796	Forward	AGCATTGGATCGATGGAGGAACTCT	815037	815061
FTT_0797	Reverse	ACCTTTGCAAGCATCTAAACCCACA	815919	815895
	Product length	883		
FTT_0797	Forward	TGTGGGTTTAGATGCTTGCAAAGGTG	815895	815920
FTT_0798	Reverse	TGCCTGCCCAGAGTTTTGCTGA	816868	816847
	Product length	974		
FTT_0798	Forward	TCAGAAGCAGCGGTGCGAAA	817442	817461
FTT_0799	Reverse	AGCACAGGAGTACCACAAGCCA	818441	818420
	Product length	1000		
FTT_0799	Forward	AGCAGCACAAGCGGGGTTGTAT	818472	818493
FTT_0800	Reverse	TGTCTGCATACCTAAATGCTTAGCTGG	819225	819199
	Product length	754		

3.2.3 Surface-layer extractions

$WbtI_{G191V}$ or $WbtI_{G191V}\Delta 1423\text{-}22$ was enhanced for CLC production by repeated passage in CDMB [192]. CLC-enhanced bacteria was either grown on CDMA for 5 days or shaken in CDMB overnight. The media was removed by centrifugation of broth grown bacteria, and both plate- and broth-grown cells were washed twice in 10 mM HEPES (4-2-*hydroxyethyl*)-1-piperazineethanesulfonic acid) before SLP extraction. Equal amounts of bacteria (2×10^{10} colony forming units [CFU]) were resuspended in 1 ml of various SLP chaotropic agents (ex. low/high pH, urea, phenol, guanidine, neutral buffers) for 15 minutes at room temperature **(Table 3.2)**. Cells were removed from solution by centrifugation at 10,000 x g for 10 minutes. Samples with acidic pH were adjusted to pH 7 with 5 N NaOH. Supernatants containing potential SLPs were either used directly or excess ethanol added to precipitate large molecular size components. Carbohydrate content was determined by phenol sulfuric acid assay and protein content was determined by bicinchoninic acid assay (BCA) (Pierce) [289].

Table 3.2 Chaotropic extraction buffers for potential SLP

Extraction buffer	Modification
1X PBS	pH 7
10 mM ethylenediaminetetraacetic acid (EDTA)	
10 mM ethylene glycol tetraacetic acid (EGTA)	
100 mM HEPES	pH 2, 4, 6, 7.5, 8 and 12
100 mM Tris buffer	pH 7.2
200 mM glycine-HCl	pH 2, 3, 4
0.5% β-mercaptoethanol in 10 mM NaCl	
10 mM $CaCl_2$	
100 mM HEPES	+10 minute, 65°C incubation

1 M urea	
1 M guanidine-HCl	
10 mM NaCl	

3.2.4 Putative SLP SDS-PAGE visualization

Sodium dodecyl sulfate-polyacrylamide gel electrophoresis (SDS-PAGE) was performed with 10 µl of extracted material on 8% SDS-PAGE or 4-12% NuPAGE gels (Invitrogen) and run according to manufacturer's instructions. Gels that were silver stained only were stained with the SilverSnap kit (Pierce) according to manufacturer's instructions. Alcian blue/silver stain was performed according to a modified method of Min and Cowman using a Bio-Rad silver stain kit [290]. StainsAll/silver stain was performed according to the method outlined in Bandara et al [192].

3.2.5 Transmission electron microscopy (TEM)

Samples were prepared for TEM one of two ways before being adhered to formvar-coated slot grids, stained with 0.5% uranyl acetate for 10s and viewed with a JEOL 100 CX-II transmission electron microscope [257]. Briefly, the extracted SLP was either placed directly on the grid in the chaotropic buffer solution, or the SLP solution was dialyzed against sterile distilled water or ethanol precipitated and then resuspended in distilled water before being placed on the grid. Adherence of SLP to the grid was facilitated by air drying before staining.

3.2.6 Amino acid composition

Amino acid analysis was performed by UC-Davis Proteomics Institute [291,292]. Briefly, extracted SLP was treated with performic acid, hydrolyzed with 6M HCl (24 h, 110°C), and run

on a L-8800 Hitachi analyzer that uses ion-exchange chromatography to separate amino acids followed by a "post-column" ninhydrin reaction detection system.

3.2.7 Polysaccharide composition

Ion pairing normal-phase liquid chromatography (IP-NPLC) was used for enrichment and identification of glycopeptides from the urea-extracted CLC of $WbtI_{G191V}$_P10 as described previously [204].

3.3 Results

3.3.1 Genomic analysis

A second polysaccharide synthesis locus was initially identified during full genome sequencing of *F. tularensis* type A strain SCHUS4 [105]. The 12.5-kb locus of 12 genes, FTT0789-FTT0800, was hypothesized, at the time, as potentially encoding for the, as yet unknown, *F. tularensis* capsule. Our previous publication by Bandara et al., showed the relationship between two glycosyltransferases in this locus (FTT0798-99) and production of the CLC [192]. Upon further inspection and comparison to known S-layer protein loci, we hypothesized that this *F. tularensis* loci could be a SLP operon. SLP loci typically contain genes for biosynthesis of enzymes for glycan transfer, assembly, and export, and upon further annotation, this highly conserved, putative *F. tularensis* SLP loci contained homologs of these genes (Table 3.3) [269,293]. Using reverse transcriptase-PCR, this putative locus was determined to be transcribed in a single polycistronic, mRNA transcript using the *F. tularensis* strain LVS [192].

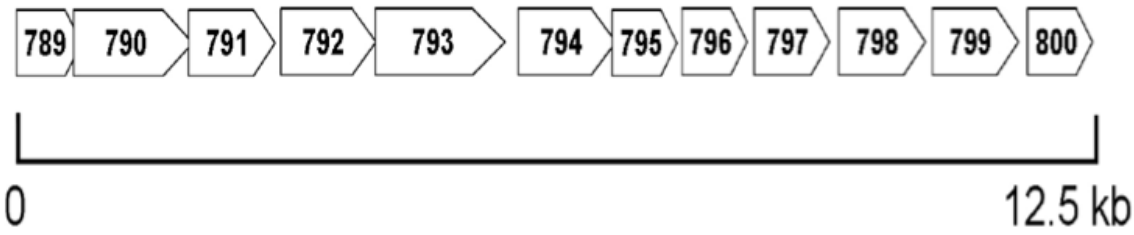

ORF Name	Size (bp)	Putative Product
FTT_0789 or FTL_1432	669	D-ribulose-phosphate 3-epimerase
FTT_0790 or FTL_1431	1395	Glycosyltransferase
FTT_0791 or FTL_1430	1020	UDP-glucose 4-epimerase
FTT_0792 or FTL_1429	1230	Glycosyltransferase
FTT_0793 or FTL_1428	1683	ATP-binding membrane transporter
FTT_0794 or FTL_1427	1287	Phosphoserine phosphatase
FTT_0795 or FTL_1426	684	SAM-dependent methyltransferase
FTT_0796 or FTL_1425	762	LPS cholinephosphotransferase
FTT_0797 or FTL_1424	960	Galactosyl transferase
FTT_0798 or FTL_1423	1008	Galactosyl transferase
FTT_0799 or FTL_1422	1014	Second mannosyl transferase
FTT_0800 or FTL_1421	663	Haloacid dehalogenase

Table 3.3 Annotation of a putative *F. tularensis* glycosylation locus
SLP loci usually contain genes for biosynthesis of monosaccharide/glycan transfer, assembly, and export. The putative SLP locus of *F. tularensis* shown above contains homologs of these genes, and this region is conserved within *Francisella*.

3.3.2 Putative SLP extraction via chaotropic agent

The putative SLP extracted with 1M urea stained only faintly with silver stain, but with the addition of a cationic dye (Alcian blue or StainsAll) and silver stain a band of ~170-kDa was readily visible in the O-antigen mutant $WbtI_{G191V}$, but visably reduced in the O-antigen CLC double mutant $WbtI_{G191V}$Δ1423-22 **(Figure 3.1)**. The electrophoretic profile of the putative SLP was similar to results obtained from cells extracted with 0.5% phenol, with the exception that the 0.5% phenol extract stained stronger with the cationic dye alone then did the extract with 1M

urea. However, sample components in the 1M urea extract stained stronger after addition of silver. This is somewhat expected as the 0.5% phenol extraction method also contains an enzyme digestion step, and the proteins left are only those that are resistant to Proteinase K. In addition to the ~170-kDa band there was an additional HMW band (>250-kDa) in the 1M urea-extracted sample that was absent in the phenol-extracted sample and greatly reduced in the CLC-deficient mutant $WbtI_{G191V}\Delta 1423\text{-}22$.

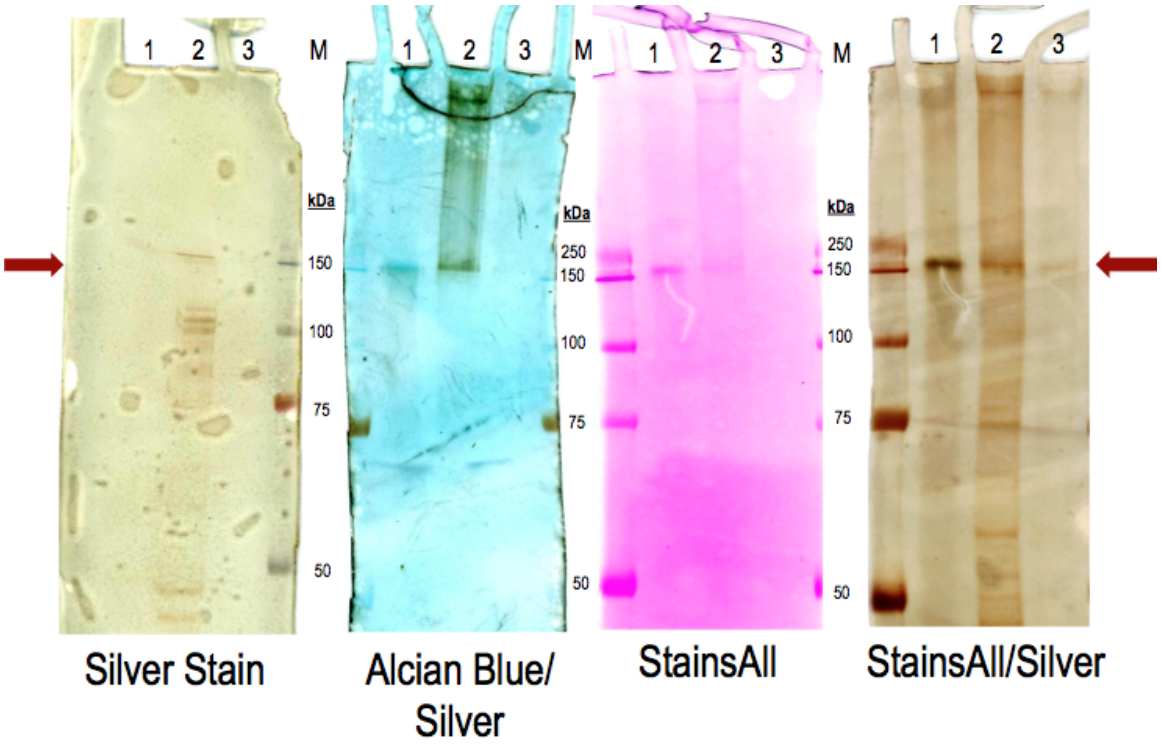

Figure 3.1 Electrophoretic profile of putative SLP extractions from $WbtI_{G191V}$ and $WbtI_{G191V}\Delta 1423\text{-}22$

1: SLP extracted from $WbtI_{G191V}$ with 0.5% phenol and enzyme digested, 2: SLP extraction of 10^9 cfu $WbtI_{G191V}$ with 1M urea, 3: SLP extraction of 10^9 CFU of $WbtI_{G191V}\Delta 1423\text{-}22$ with 1M urea. Red arrow indicates the putative glycoprotein.

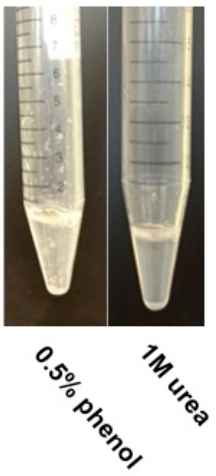

Figure 3.2. Solubility of putative SLP extracted with 0.5% phenol or 1M urea. Putative SLP was extracted from LVS_P10 via 0.5% phenol or 1M urea extraction, and immediately visualized for comparison. The putative SLP in 1M urea had no insoluble material while the phenol extracted putative SLP was highly insoluble.

3.3.3 Visualization of the putative surface-layer protein

Extraction of the putative SLP with 1M urea greatly increased the solubility of the material, compared to extraction with 0.5% phenol (Figure 3.2). The extracted SLP remained soluble until diluted to a concentration of 0.5M urea, at which point some insoluble material was observed. When the urea was completely removed by dialysis with distilled water, or the SLP was concentrated through a 100-kDa filter greater than 2-fold, the material would aggregate and fall out of solution. When visualized under negative staining TEM, the SLP in a chaotropic agent (1M urea) had a disorganized arrangement, but when the disrupting agent was removed, self-aggregation was evident. Due to technical restrictions, we were not able to confirm visualization of a crystalline lattice structure, but there was a discernable pattern **(Figure 3.3)**.

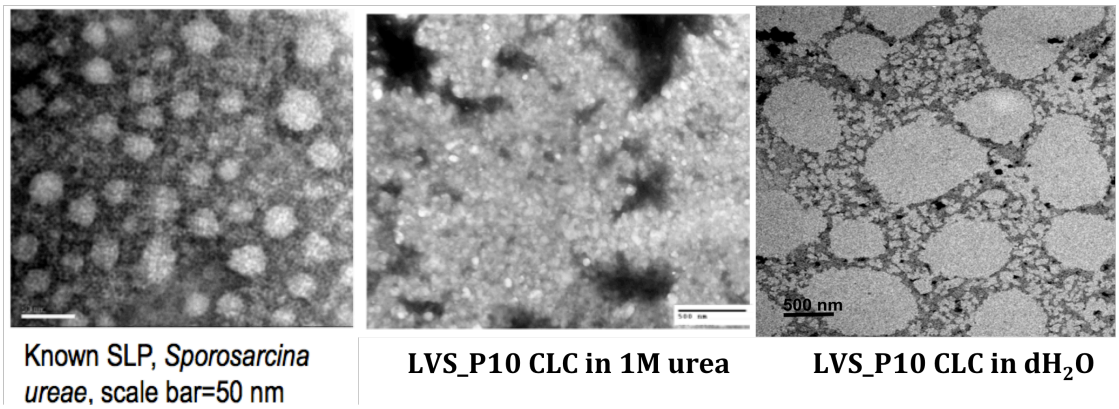

Figure 3.3 Negative-stained TEM of *F. tularensis* CLC (putative SLP) compared to known SLP of *S. ureae*.

CLC extracted from LVS_P10 using 1M urea and either directly visualized with uranyl acetate under TEM or dialyzed to remove urea and visualized with TEM.

3.3.4 Composition of putative SLP

Analysis of the HMW putative SLP yielded an amino acid composition similar to that of known bacterial surface layer proteins **(Table 3.4)**. A large percentage of acidic and hydrophobic amino acids were present, which is indicative of proteins that will self-aggregate and be highly insoluble in water. In addition, a 420-Da repeating glycose unit was observed in the 200-kDa band **(Figure 3.4)** and in the ~170-kDa band, with the number of 420-Da units/chain length being variable. There was evidence of a 420-Da unit in the band/smear greater than 250-kDa, but the longer chains were not observed. The addition and loss of a 17-Da ammonia was also observed in the MS spectrum. Amino acid sequencing and identification of the protein components was unsuccessful, potentially due to the high level of glycosylation present in these bands. Further analysis of the protein components is discussed in detail in Chapter 4.

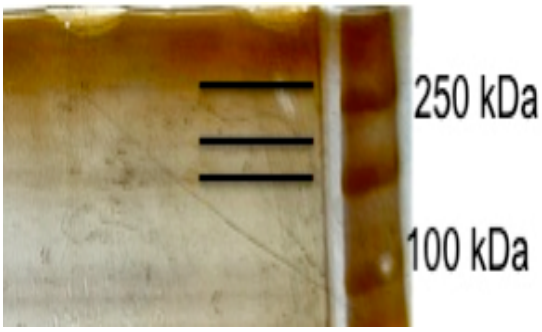

Figure 3.4 8% SDS-PAGE of WbtI$_{G191V}$_P10 CLC 1M urea extract.
Extract was concentrated through a 100-kDa filter and bands indicated by black lines were excised and sent for MS analysis.

Table 3.4 Amino acid composition of CLC extract from LVS.
Amino acid composition of the CLC (putative SLP) extract from LVS revealed characteristics of known surface-layer proteins, with a high percentage of acid and hydrophobic amino acids.

Amino Acid Type	Percent
Acidic	28.98
Basic	8.60
Hydrophobic	30.66
Uncharged Polar	7.69

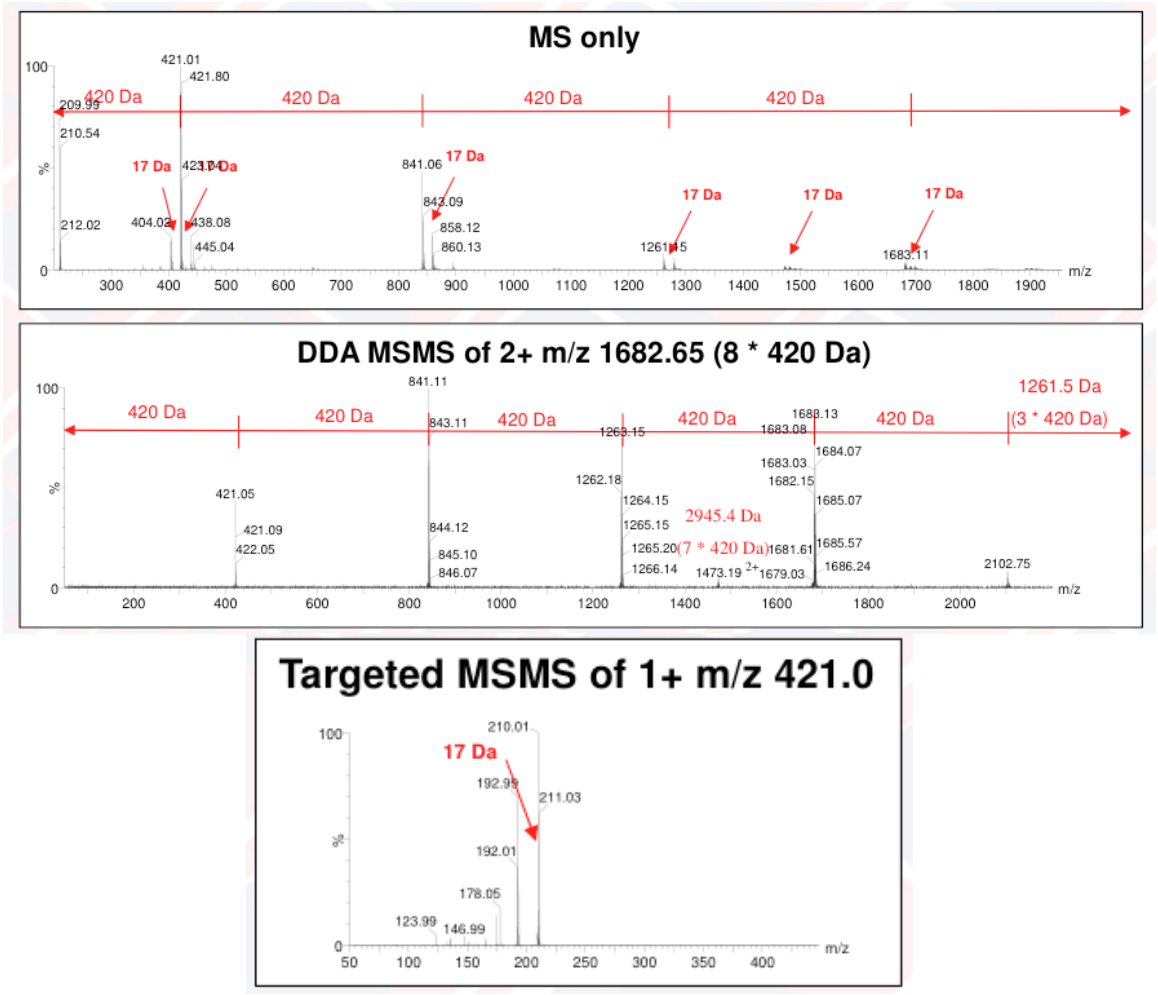

Figure 3.5 Mass-spectrometry of high molecular size putative SLP bands excised from LVSΔWbtI_P10 1M urea extract.

A 420-Da repeating unit was observed in the 200-kDa band **(Figure 3.4)** and in the ~170-kDa band, with the number of 420-Da units/chain length being variable. There was evidence of a 420-Da unit in the band/smear greater than 250-kDa, but the longer chains were not observed. The addition and loss of a 17-Da ammonia was also observed in the MS spectrum. DDA = data dependent acquisition.

3.4 Discussion

Many bacterial surface components of pathogenic bacteria are important virulence factors during infection. At the time of this research, the surface components of *F. tularensis* were just beginning to be elucidated, as was their role in pathogenesis. The initial characterization of the

capsule-like complex of *F. tularensis* LVS found that it contained a mixture of proteinase-resistant proteins, some of which may be glycosylated [192]. There was a distinct correlation between virulence and the presence of the CLC in type B *F. tularensis*, which would indicate that one or more of the components of the CLC is important during infection. The specific components of the CLC are still under investigation. We hypothesize that one of these components could be a glycoprotein with characteristics similar to known surface-layer proteins. S-layers are defined as two-dimensional crystalline arrays that coat the cell and are composed of one or more (glyco)proteins [294]. The SLP's can self-assemble and form regularly spaced arrays on the surface of the bacteria; these S-layers have been found to perform multiple functions in pathogenesis and environmental persistence [278,286,294,295]. SLP in other human pathogens, such as *A. salmonicida* and *B. cereus*, help to shield the bacteria from the bactericidal activity of host complement as well as regulate bacterium-phagocyte interactions [296-298]. *Francisella* is also a facultative intracellular bacterium that is completely resistant to the bactericidal action of serum. While a mutant strain of LVS that is deficient in CLC is still serum resistant, an interesting question is whether or not the singular putative surface glycoprotein enhances serum resistance as well.

Chemical analyses of bacterial S-layers show that they are predominately composed of a single glycoprotein subunit, with a relatively high molecular weight (HMW) of up to 200-kDa [269]. CLC isolated from *F. tularensis* LVS and type A strain SCHUS4 contains a HMW banding pattern of potential glycoprotein(s) beginning at ~170-kDa, as well as may other smaller molecular weight proteins ranging from 10-150-kDa (discussed further in Chapter 4). Identification of the amino acid sequence of the HMW bands (>170-kDa) was inconclusive,

potentially due to the high amount of glycosylation present. However, since chains of the same 420-Da repeating glycose was observed in all bands greater than ~170 kDa, it can be hypothesized that these are polymers or aggregates of the same glycoprotein or glycan.

The O-antigen capsule identified by Apicella et al., is a polysaccharide found in this same HMW region, but is not seen in O-antigen deficient mutants. In contrast, the putative SLP electrophoretic banding pattern was equally present in O-antigen mutants, and such mutants were used for its isolation to prevent contamination with LPS O-antigen [92]. The glycan structure of typical SLP's contain O-linked units that consist of 2-6 sugars and have up to 50 repeating units [294]. The putative SLP locus conserved in all *Francisella* species is consistent with glycosylation operons associated with known surface layer glycoproteins [299]. During the course of this research, the putative SLP locus in *F. tularensis* was found to glycosylate an essential virulence factor, DsbA with an O-linked, 1156-Da hexasaccharide repeating unit [204]. This is not the same sized glycan that was found on the putative HMW SLP bands nor contains the same monosaccharides, but the 1156-Da glycose has been found on other glycoproteins in the CLC (discussed in Chapter 4). While there is no indication that the FTT_0789-FTT0800 locus can produce two distinct glycans, there is the possibility that the 420-Da glycan may be produced by a bifunctional glycosyltransferse in this locus that attaches the sugar directly to the protein.

The amino acid composition of SLP from various bacteria and archaea have been shown to be similar [275,276,284,286]. SLP generally have a high percentage of hydrophobic and acidic amino acids, and typically a low content of arginine, histidine, methionine, and cysteine [300].

The amino acid composition of the CLC material greater than 100-kDa revealed that almost 60% were either acidic or hydrophobic amino acids with very low levels of arginine, histidine, methionine, and cysteine. The high acidic amino acid content could explain why normal silver staining techniques either stained the HMW material faintly or not at all [255]. It was not until the silver stained gel was overlaid with a cationic dye (Alcian Blue or StainsAll) that the SLP material was clearly seen. The unique amino acid composition also explains the high insolubility of the CLC material in water, as SLP that consist of this unique amino acid readily self-assemble into crystalline lattices [301]. We were able to increase the solubility and decrease the self-aggregation of the putative SLP with the addition of 1M urea, which acted as a disrupting agent. Urea is a common chaotropic agent used during SLP extractions in bacteria such as *Clostridium difficile* and *Bacillus anthracis* [302-304]. Despite the overall similarity in amino acid composition and glycoses that have been observed for various SLP's, genomic sequence identities among SLP genes are extremely rare [305]. However, within the last 15 years, it has been observed that high sequence identities between the N-terminal region of SLP proteins exist [286]. These three tandem ~55 amino acid repeats are called surface-layer homology (SLH) domains, and they aid in enabling the SLP to attach to the bacterial envelope through non-covalent interactions [306]. To date, no such SLH domain has been identified by proteome analysis of *F. tularensis* type A SCHUS4 and type B LVS strains. This does not negate the existence of an SLP, as there have been proteins capable of S-layer formation without an SLH domain, such as the SLP of *Geobacillus stearothermophilus* [307].

The biological function of S-layers is varying among species and is not completely understood, yet due to the high metabolic cost of producing them, they must be necessary for survival. In

Clostridium difficile and *Campylobacter fetus* the S-layer has been shown to protect the bacteria from the host innate immune response by inhibiting phagocytosis and preventing killing by serum complement [308,309]. In *F. tularensis* the LPS O-Antigen plays the key role in preventing complement-mediated killing, while LVS deficient in CLC is still serum resistant [192]. However, multiple surface structures have been shown to play a role in phagocytosis and intracellular survival of *F. tularensis* [92,133,192]. We had suggested, the capsule-like material shed from around *F. tularensis* upon phagocytosis seen by Golovliov *et al*. and during our studies, could be S-layer material [123]. A proposed function of glycoprotein S-layers is adhesin and there is some evidence that this SLP could also have that function. In the Gram-negative bacterium *Tannerella forsythia*, an argument has been established that S-layer glycosylation plays a role in biofilm formation [299]. A mutant with a deletion of the *wecC* gene, involved in glycosylation, formed more cell aggregates and developed a more robust biofilm than the weak biofilm-forming parent strain [299]. This result is similar to what we see with biofilm formation by *F. tularensis* after the removal of the CLC (discussed in Chapter 5). Briefly, we have observed that the parent LVS strain, with an intact O-antigen and CLC, does not form a robust biofilm. On the other hand when LVS is deficient in O-antigen and CLC (i.e. $WbtI_{G191V}\Delta 1423$-22), the bacteria form a robust biofilm with a 3-D structure readily evident by SEM. One hypothesis is that the change is cell surface hydrophobicity may allow better surface attachment. In addition, the removal of polysaccharides from the surface might expose adhesin sites on the putative S-layer.

A common method to confirm identification of an SLP is to use a TEM technique called freeze-etching to visualize the crystalline lattice structure [301]. Our university is not equipped to do

this technique. Therefore, complete certainty of a crystalline lattice structure assembled by a glycoprotein component of the CLC is unconfirmed. However, circumstantial evidence is abundant to the potential presence of an S-layer-like glycoprotein, yet we have not currently determined the putative gene responsible for the actual SLP. Usually this gene lies directly upstream of the glycosylation locus, and in *Francisella* there are several hypothetical genes with no determined function directly upstream of the FTT_0789-0801 putative locus. With amino acid sequencing of the purified SLP we hoped to determine which of these genes it might be. *Francisella* has a long history of novel structures with unique characteristics (i.e. LPS), so it is not unrealistic to hypothesize the presence of a novel S-layer-like surface structure as yet undiscovered in other prokaryotes.

3.5 Co-Authors' Contributions

UC-Davis Proteomics Institute performed the amino acid analysis. Susan Twine from the National Research Council of Canada performed the amino acid sequencing and glycoprotein identification. Experimental design was conceived by Anna Champion and Tom Inzana.

CHAPTER 4

Further characterization of the *Francisella tularensis* capsule-like complex (CLC)

4.1 Introduction

Francisella tularensis, the etiological agent of tularemia, is a Gram-negative coccobacillus capable of causing disease in animals and humans [54]. Infection can occur through several routes including: the lungs (inhalation), ingestion of contaminated water or food (gastrointestinal), or a break in the skin and mucous membranes (ulcero-gandular) [20,31]. *F. tularensis* is classified as a Tier I select agent by the U.S. Center for Disease Control, due to the ease of dispersal, persistence in the environment and the high infectivity and lethality of the pathogen [233]. *F. tularensis* subspecies *tularensis* (type A) is the most virulent biotype and found mostly in North America. Subspecies *tularensis* is capable of causing lethal disease in up to 30% of untreated cases with as few as 10 organisms (via inhalation) [46,310]. *F. tularensis* subspecies *holarctica* (type B), is less virulent for humans, but is the culprit for most tularemia outbreaks in Europe and can cause death if untreated [50,311]. Over the last decade, much research has focused on characterizing the pathogenesis of this facultative intracellular pathogen and on the development of a vaccine [312]. Currently there is no approved, licensed vaccine for tularemia. However, a live attenuated strain of subspecies *holarctica* (LVS) was identified by researchers in the Soviet Union that conferred protection against aerosol challenge with virulent type A strains [64]. This protection was better than from killed strains, but was still not protective against high dose respiratory exposure. Due to that and the lack of a full understanding of the attenuation of LVS and concern over the stability of the strain, it is not

approved for general use. Given the intracellular nature of *F. tularensis* and the success of LVS as a vaccine, a live attenuated type A strain with a defined mutation would logically be the most efficacious to induce protective immunity against infection. Targeted mutations that have been successful in attenuating *F. tularensis* and other intracellular bacteria have included surface components such as the LPS and outer membrane proteins [83,182,313].

Research into the surface components of *F. tularensis* has markedly increased over the last five years. The known surface components include: lipopolysaccharide (LPS), O-antigen capsule, glycoproteins, outer membrane vesicles and tubes (OMV/T), and the capsule-like complex (CLC). The LPS is well characterized and its role in virulence and resistance to complement-mediated bactericidal activity well documented [86,183,187,241]. Deletion of the O-antigen in type A and B strains results in a highly attenuated mutant that offers protection against challenge with type B strains, but not type A infection [86,182,183,241]. In addition, a capsule comprised of O-Ag sugars was found in type A and B strains, characterized and found to be necessary for intracellular growth [92]. While an O-Ag capsule deficient mutant was attenuated, it did not provide adequate protection against type A *F. tularensis* [92,191]. Outer membrane vesicles (OMV), common to Gram-negative bacteria, have also been found in *Francisella*, with most work focusing on *F. novicida* [210,211]. *F. novicida* was shown to produce both OMV and outer membrane tubules (OMT), which contain similar outer membrane proteins, yet predominant proteins vary depending on whether it is vesicle or tubule shaped. These differences could be enhanced by growth conditions and growth phase [210]. Known virulence factors, such as the *Francisella* pathogenicity island (FPI) proteins, IGlABC and PdpAB, FopB, TolC, and GroEL were found in the OMV [115,154,211]. *F. novicida* OMV have successfully

been used as a vaccine against challenge with *F. novicida*, but that is no indication that OMVs could work against the more virulent *F. tularensis* type A and B strains [211]. It has been noted by Golovliov *et al*., that a capsular/vesicular material surround phagocytized *Francisella* and could possibly be shed during infection as a way to mask the bacteria from the host [123].

Another novel surface component that has been identified in *F. tularensis* is the CLC [192]. The CLC is regulated by specific growth conditions and appears as an electron dense material around the cell when visualized by transmission electron microscopy. However, after purification of the CLC less than 10% carbohydrate is present [192]. No evidence of O-antigen sugars or core LPS sugars have been found in the CLC, and when analyzed specifically for carbohydrate, only glucose, galactose, and mannose monosaccharides were identified [192]. However, the CLC appears to contain many proteinase-resistant proteins, glycoproteins, and possibly a high molecular weight carbohydrate that present as multiple bands or a smear between 150-250 kDa. These proteinase-resistant proteins have some similarities to other bacterial surface-layer proteins, as was discussed in Chapter 3. Identification of novel glycoproteins present in the CLC or the presence of previously identified *F. tularensis* glycoproteins, such as DsbA or the Pil proteins, has not yet been established. The high molecular weight carbohydrate was found to be dependent on the growth medium. For example, only when *F. tularensis* was grown in medium that mimicked host conditions (Brain Heart Infusion, BBL), was the HMW carbohydrate evident [193]. A definitive link between the HMW carbohydrate, described by Zarrella *et al*., and the CLC has yet to be established [193]. The CLC appears conserved between type A and B strains. The locus responsible for glycosylation of virulence factor proteins, such as DsbA (FTT0789-FTT0800) in *F. tularensis* type A and B strains, also plays a role in the production of CLC

[105,192] [204,205]. It was found that when two glycosyl transferases (FTT0798-99) were deleted in LVS, CLC production was significantly diminished and the strain was highly attenuated [192]. In LVS, this CLC-deficient strain was also protective against homologous LVS challenge.

We previously determined there is no antigenic similarity or cross-reactivity between the LPS and O-Ag capsule and the CLC, yet similarity of the CLC to other surface components, such as the OMV/T has yet to be determined. Identification of at least some of the many individual components of the CLC could result in a better understanding of the CLC's role in virulence and help elucidate potential genetic targets that could be useful for vaccine development. In this study we further characterized *F. tularensis* CLC from both type A and LVS strains. We took a closer look at the regulation of the CLC and the similarities seen between CLC and OMV. We were able to show that a protective immune response to a type B strain was generated upon immunization with purified CLC, and we were able to identify a complex list of proteins that comprise the CLC. Some of these proteins were glycosylated with the known 1156 Da hexassaccharide, previously published [204]. In addition, a novel 420-Da glycose was found identified in the higher molecular weight bands greater than 170-kDa. This in depth analysis of the CLC and its components could prove advantageous in elucidating the role of CLC in pathogenesis.

4.2 Materials and Methods

4.2.1 Bacterial strains and growth conditions

The bacterial strains used and their sources are listed in Table 4.1. *F. tularensis* strains were cultured from frozen stock suspensions onto brain heart infusion agar (Becton-Dickinson) supplemented with 0.1% L-cysteine hydrochloride monohydrate (Sigma-Aldrich, St. Louis, MO) (BHIA) or Chamberlain's defined media (CDM) [250] with 1.5% glucose agar (CDMA) and incubated at 37°C in 7% CO_2, unless otherwise stated. For culture in broth, *F. tularensis* strains were grown with shaking (175 rpm) in BHI broth (BHIB) at 37°C, or CDM broth (CDMB) at 32°C. For selection of recombinant strains 15 µg kanamycin (Kan)/ml was added to the stated medium. For enhancement of surface CLC, the bacteria were passaged in CDMB ten times and is indicated by a "P10" on the strain name. For CLC preparation, *F. tularensis* was grown on CDMA in petri dishes (150 mm X 15 mm), and incubated at 32°C in 7% CO_2 for 5 days. All experiments with LVS and mutants were carried out in biosafety level (BSL)-2 facilities in an approved biosafety cabinet. All experiments with type A strains, TI0902 and SCHUS4 were carried out in a biosafety level-3 facility in an approved biosafety cabinet.

Table 4.1 *Francisella tularensis* bacterial strains used in this study

Strain	LPS/O-Ag	O-Ag capsule	CLC	Attenuated	Source
LVS	+	+	+	N	[67]
LVS_P10	+	+	+++	N	[192]
LVSΔ1423-22	+	+	-	Y	[192]
$WbtI_{G191V}$	-	-	+	Y	[94]
$WbtI_{G191V}$_P10	-	-	+++	Y	[192]
$WbtI_{G191V}$Δ1423-22	-	-	-	Y	[192]
SCHU_S4_P10	+	+	+++	N	[105]
TI0902_P10	+	+	+++	N	[314]

4.2.2 CLC extraction

Bacterial strains were enhanced for CLC production by repeated passage in CDMB [192]. CLC-enhanced bacteria were then grown on CDM agar plates for 5 days at 32°C and 6% CO_2. CLC was extracted by one of two methods. CLC was extracted by phenol as described previously

[192], or by urea extraction. Briefly, bacteria were scraped off plates and resuspended in 1M urea at a concentration of ~1 agar plate lawn of bacteria to 5-10 mls 1M urea. After cells were suspended, incubated at room temperature for 15 minutes, and harvested by centrifugation (10k*g for 15 min) and the supernatant was saved. For type A strains experiments were carried out in a Biosafety-level 3 facility and therefore cell death had to be verified before removal of any antigens. After urea extracted supernatants were harvested sodium acetate was added to 30 mM and CLC was precipitated with 5 volumes of cold 95% ethanol. A portion of this crude supernatant was concentrated 5 to 10-fold by ultrafiltration through a 100-kDa Centriprep filter (Millipore, Darmstadt, Germany).

4.2.3 Visualization of CLC urea extracts

Sodium dodecyl sulfate-polyacrylamide gel electrophoresis (SDS-PAGE) was performed with 10 µl of extracted material on either 4-8% NuPAGE or 4-12% NuPAGE gels (Invitrogen, Grand Island, NY)); electrophoresis was carried out according to the manufacturer's instructions. Gels that were silver stained only were stained with the SilverSnap kit (Pierce,, Rockford, IL) according to manufacturer's instructions. StainsAll/silver stain was performed according to the method described by Bandara *et al*. [192]. Fluorescent carbohydrate visualization was performed on urea extracts run on NuPAGE gels using the Pro-Emerald Q 300 stain kit (Life Technologies, Grand Island, NY).

4.2.4 Extraction of CLC from various media

$WbtI_{G191V}$_P10 was grown in either CDM, BHI, or Mueller-Hinton (MH) broth (100 ml) with shaking at 180 rpm, or on agar plates (2 plates) for 5-10 days at 32°C. After shaking, the cells were removed by centrifugation (10,000 x *g* for 15 min) and the supernatant was removed and 5

volumes of 95% ethanol was added and held at -20°C overnight. The resulting precipitate was harvested and resuspended in 5-10 ml of sterile water and lyophilized. The cell pellet was resuspended in 20 ml of 1M urea and extracted for CLC, as described above. The bacteria grown on plates were resuspended in 20 ml of 1M urea and extracted for CLC. As a control, excess 95% cold ethanol was added to media without bacterial growth and analyzed. Equal amounts (10 μg) of sample was electrophoresed on a 4-12% NuPAGE gel (Invitrogen) and stained with silver stain or StainsAll/Silver.

4.2.5 Generation of hyperimmune rabbit serum

Antiserum to $WbtI_{G191V}$_P10 CLC was raised in a New Zealand white rabbit by subcutaneous immunization with 100 μg phenol-extracted purified CLC mixed 1:1 in Freund's complete adjuvant, injected into 6 sites. Two weeks later, the immunization was repeated with 100 μg phenol-extracted purified CLC in Freund's incomplete adjuvant. Two weeks after this injection, the rabbit was immunized intravenously with 500 μg CLC at weekly intervals until hyperimmune serum (enzyme-linked immunosorbent assay [ELISA] titer greater than 1:6,400) was obtained.

4.2.6 Murine Immune Response to CLC

To test the murine immune response to CLC, female C57 Black/6 or CD1 mice were immunized twice, 2 weeks apart, with 50 μg of CLM preparations at various stages of purity. The first and second immunizations contained Freund's Complete and Freund's Incomplete adjuvant, respectively. After an initial pre-immunization bleed, mice were bled at 2-weeks post immunizations (2 and 4 weeks). Serum samples were collected and stored at -20°C until testing. A sandwich ELISA was performed in HBX high-binding 96-well plates (Immulon, Waltham,

MA) using 1 μg of CLC per well as described [315]. Briefly, immune serum was added to the ELISA plate wells, any remaining reactive sites blocked with 4% skim milk in phosphate-buffered saline, pH 7.4 (PBS)-0.05% Tween 20,followed by goat anti-mouse IgG1, IgG2, or IgM (source), and anti-goat antibody conjugated to horseradish peroxidase (HRP). Wells were washed between incubations with PBS-Tween 20, which was also used for dilution of reagents. Color was developed using TMB (3.3',5,5'-tetramethylbenzidine) substrate as per the manufacture's instructions (Pierce, Rockford, IL). Sera from mice immunized with PBS served as a negative control baseline.

4.2.7 CLC-protein conjugates and mouse challenge

CLC was purified from LVS enhanced for CLC production as previously described [192]. The purified CLC was conjugated to keyhole limpet hemocyanin (KLH) or purified *Salmonella* flagellin protein through an adipic acid dihydrazide (ADH) spacer as described by Schneerson *et al*. [316]. Briefly, the immunogenic protein carrier was conjugated to ADH at pH 4.7 with 1-ethyl-3-(3-dimethylaminopropy)carbodiimide (EDAC). Reactive groups on the glycose moiety of the CLC were generated with cyanogen bromide at pH 10.5, and conjugated to either KLH or flagellin through ADH at pH 8.5. The CLC-conjugate was eluted through a Sepharose S-300 size exclusion column and collected in the void volume. Fractions were tested for protein (absorbance at 280 nm), pooled, dialyzed against distilled water, and lyophilized. After lyophilization, some insolubility was observed, but samples were sonicated to regain clarity. To confirm conjugation was successful, CLC conjugates were analyzed by SDS-PAGE on 4-12% bis-tris gels with unconjugated CLC and the protein carrier as a control.

To test the CLC's level of protection against LVS challenge, groups of 6 BALB/C mice were immunized intradermally with CLC-KLH and CLC-flagellin protein conjugates every 2 weeks for 6 weeks. The first and second immunizations were administered along with Freund's Complete and Incomplete adjuvant, respectively. Mice were challenged with 5 x LD_{50} of LVS intranasally (5000 cfu.) or intradermally (2 x 10^7 cfu.). Blood samples were collected from mice post-vaccination (at 6 weeks) and post-challenge (3 days). Serum samples were cryo-preserved at -80°C until cytokine analysis could be performed.

4.2.8 CLC fractionation with GelFree, Triton X-114, and Sarcosyl Extractions

Urea-extracted CLC (100 μg) from $WbtI_{G191V}$_P10 was fractionated on the GELFREE 8100 (Expedeon, San Diego, CA) protein fractionation system. This system uses a technology termed Gel Elution Liquid Fraction Entrapment Electrophoresis (GELFREE), for molecular weight-based fracionation of intact proteins with liquid phase recovery. Urea-extracted CLC was desalted by Zeba spin desalting columns (7K MWCO) (Pierce, Rockford, IL) prior to fractionation and lyophilized. One-hundred micrograms of desalted CLC sample was resuspended in 112 μl sterile distilled water, and 8 μl of 1M DTT (dithiothreitol) and 30 μl of provided sample buffer was added. The sample was heated at 50°C for 10 minutes and cooled to room temperature. Fractionation into 12 fractions was performed on the GelFree 8100 following manufactures' instructions for the high molecular weight 5% tris-acetate cartridge.

Various methods of fractionating and further purifying the CLC were tested to identify the specific components of the material. To resolve insolubility that commonly occurred following concentration of urea-extracted CLC, purified CLC from $WbtI_{G191V}$_P10 and $WbtI_{G191V}$Δ1423-22

was fractionated using the non-ionic detergent Triton X-114 and/or Sarkosyl [317]. Equal amounts (5 mg) of urea-extracted CLC from the parent and the CLC-deficient mutant were suspended in 5 ml of distilled water and Triton X-114 (Sigma) was added to a final concentration of 5% (v/v). The samples were vortexed for 1 minute and placed on ice at 4°C overnight. Samples were then incubated at 37°C for 2 hours, then centrifuged at 3000 x *g* at room temperature for 10 minutes to separate the aqueous (TxS-A) and detergent phases (TxS-D). Both phases were removed carefully, so as not to disturb the insoluble pellet, and dialyzed against distilled water and lyophilized. The Triton X-114 insoluble pellet was resuspended in 1 ml of 1% N-lauryolsarcosine (Sarkosyl) and incubated at room temperature for 15 minutes. The samples were then centrifuged at 5000 x *g* for 10 minutes at room temperature, the soluble supernatant was removed, and the insoluble pellet was resuspended in 1 ml of distilled water, constituting the Sarkosyl-soluble (TxI-SS) and Sarkosyl-insoluble (TxI-SI) fractions. All fractions were analyzed on a 4-12% bis-tris NuPAGE gel (Invitrogen) and visualized by SilverSnap (Pierce, Rockford, IL) silver stain per manufacturers instructions.

4.2.9 OMV extraction

Outer membrane vesicles were purified from *F. tularensis* strains by one of two procedures. A method described for OMV and outer membrane tubules (OMT) purification from *F. novicida* was slightly modified and used for purification of OMV/T from *F. tularensis* strains [210]. Briefly, bacterial cultures were grown in CDMB for ~5 hours, with appropriate antibiotic, as required, to exponential phase (Klett meter optical density of 95), and bacteria were removed by successive, differential low-speed centrifugation (5,000 x *g*, followed by 7500 x *g*, for 30 min each), and the supernatant was passed through a 0.45 μm syringe filter (Nalgene). Sodium azide was added to a concentration of 0.05%. The media supernatant was concentrated from 1L to

about 50ml using an Amicon tangential flow filtration unit with a 100-kDa molecular mass cutoff membrane (Millipore, Darmstadt, Germany). The concentrated cell-free media was then ultracentrifuged (100,000 x *g* for 1 hr at 4°C). The OMV/T pellet was resuspened in 10 mM HEPES (pH7.5) containing 0.05% sodium azide, and ultracentrifuged again, as done previously. The pelleted OMV/T was then resuspened in 1-2ml of HEPES buffer with sodium azide and stored at either 4°C or -20°C, depending on future use.

The second OMV method used more closely mimics the CLC extraction procedure, and was modified from a previously published method [318,319]. Overnight cultures of *F. tularensis* strains in CDMB were grown on 5 CDMA plates with appropriate antibiotic, as required per strain. Bacteria were scraped off the agar plates and suspended in 100 ml sterile PBS (pH 7.3). The bacterial cells were removed by centrifugation at 10,000 x *g* for 30 min. The supernatant was passed through a 0.45 μm filter (Millipore) and sodium azide was added to 0.05%, final concentration. The supernatant was ultracentrifuged at 100,000 x *g* for 2 hours at 4°C. The OMV pellet was washed twice with PBS and the OMV suspended in 1ml of sterile PBS. The OMV were aliquoted and stored at -20°C. Total protein concentrations of OMV for each method were determined using the BCA protein kit (Pierce), as per manufacturer's instructions.

4.2.10 CLC protein identification

CLC was extracted from *F. tularensis* LVS using 1M urea, as described above. The CLC was concentrated using a 100-kDa Centriprep filter unit (Millipore, Darmstadt, Germany), and the sample separated into soluble and insoluble fractions. Trypsin digests of the fractions were analyzed by nano-liquid chromatography-MS/MS using a 'CapLC' (capillary chromatography

system) (Waters) coupled to a 'QTOF Ultima' hybrid quadrupole time-of-flight mass spectrometer (Waters). Peptide extracts were injected into a 75-μm internal diameter × 150-mm PepMap C_{18} nanocolumn (Dionex/LC packings), and resolved by gradient elution (5–75% acetonitrile, 0.l2% formic acid in 30 min, 350 nL/min). MS/MS spectra were acquired on doubly, triply, and quadruply charged ions.

Peak lists were automatically generated by ProteinLynx (Waters) with the following parameters: smoothing—four channels, two smoothes, Savitzky Golay mode; centroid—minimum peak width at half height of four channels, centroid top 80%. Tryptic peptides were analyzed by nLC–MS/MS and resulting spectra searched against the NCBInr (NCBInr 20050724; 2693904 sequences) and *F. tularensis* LVS genome sequence using MASCOT 2.0.1 (Matrix Science, UK) to identify protein homologues. The following parameters were used for mass spectral identification: peptide tolerance of 1.5 Da, MS/MS tolerance of 0.8 Da, possible one missed cleavage site, variable modifications including carbamidomethylation of cysteine residues, oxidation of methionine, formation of pyroglutamate at N-terminal glycine, and N-terminal acetylation. Peptide identifications were accepted if they met all of the following criteria: MASCOT peptide score >25, mass accuracy <100 ppm. In addition, all MS/MS spectra were manually assessed for data quality and high confidence identification, requiring a clear series of high mass y ions and correct charge state assignment for all fragments. However, proteins that were heavily glycosylated would not be identified using this method.

In addition to this method, purified urea-extracted CLC from $WbtI_{G191V}$ and $WbtI_{G191V}\Delta$1423-22 was also run on 4-12% bis-tris NuPAGE gels and the proteins stained with Coomasie.

Differences in electrophoretic banding patterns were noted, and the differing band excised for protein identification as described in Miller et. al. [320]. This method produced few results, as most proteins proved difficult to elute from the polyacrylamide gel.

4.2.11 Transmission Electron Microscopy

LVS and type A strains were passed in CDMB to enhance the CLC as described previously [192]. *F. tularensis* strains were grown on CDMA (with appropriate antibiotic when necessary) for 5 days at 32°C. The cells were gently scraped into 0.1M sodium cacodylate buffer (pH 7.5) containing 3% glutaraldehyde and turned end-over-end for 2 hours. Type A strains were left in the fixative at 4°C overnight and for up to 5 days while cell death was verified by streaking 50 μl aliqots of fixed cells onto CDMA and incubating for 5 days. If no growth occurred after this time period the cells were removed from the BSL-3 facility. The cells were then washed, suspended in 100 mM sodium cacodylate buffer, adhered to formvar-coated grids, stained with 0.5% uranyl acetate, and viewed with a JEOL 100 CX-II transmission electron microscope [257]. Approximately 20 μl of purified OMV/T from each method was placed onto formvar-coated copper grids and allowed to adhere for 10 minutes. Grids were dried with filter paper and stained briefly with 0.5% uranyl acetate, rinsed with distilled water and dried. Grids were viewed using a JEOL 100 CX-11 transmission electron microscope as described above.

4.2.12 Type A CLC

To determine the protective efficacy of type A CLC to type A lethal challenge, we immunized groups of 5 mice with either crude CLC or concentrated HMW CLC extracted from SCHUS4 using 1M urea. Mice were immunized with 50 μg of CLC intradermally, every 2 weeks for 10

weeks, with the first and second immunizations containing Freund's complete and Freund's incomplete adjuvant, respectively. Mice were intranasally challenged with 500 or 1500 cfu of *F. tularensis* SCHUS4.

4.2.13 Carbohydrate Analysis

Glycose composition of type A CLC was determined by combined GC/MS of the per-O-trimethylsilyl (TMS) derivatives of the monosaccharide methyl glycosides produced from the sample by acidic methanolysis, as described [254]. Ion pairing normal-phase liquid chromatography (IP-NPLC) was used for enrichment and identification of glycopeptides from the urea-extracted CLC of $WbtI_{G191V}$_P10 as described previously [204].

4.2.14 Statistics

Statistical analyses were performed using Microsoft Excel software (Redmond, WA) and GraphPad software (La Jolla, CA). Data was compared using student t-test and expressed as the mean $\pm$ standard deviation. Results with a p value of less than 0.05 was considered statistically significant.

4.3 Results

4.3.1 Comparison of urea and phenol extracted CLC

Extraction of the CLC with urea greatly enhanced the analysis of the CLC by additional assays. However, it needed to be confirmed that the material extracted by urea and phenol were the same antigen. Hyperimmune sera to CLC extracted via phenol and to CLC extracted via urea were generated in mice. Western blot analysis using phenol-extracted CLC as the antigen and

immune serum to either antigen yielded similar profiles. The high molecular weight smear was evident in the purified CLC using sera to either extracted antigen, and a similar banding patterns of proteins were seen in the crude extracts. One slight difference between the two Western blot banding patterns was the evidence of multiple faint bands in the pure CLC when using the serum produced from CLC extracted with urea (Figure 4.1). This could be due to the CLC being digested more from the more harsh phenol extraction. Overall, the electrophoretic and immunological analysis indicated the preparations extracted with urea or phenol were the same. All further extractions of CLC from *F. tularensis* were performed using the urea-extraction material.

Figure 4.1 Western blot of urea- and phenol-extracted CLC using immune mouse sera. Primary antibody to phenol-extracted CLC. C: crude CLC, P: purified CLC, M: marker (250, 150, 100, 75, 50, 37, 25, 20, 15, 10-kDa). Similar high molecular weight (>150-kDa) electrophoretic western blot profiles were obtained using immune sera to phenol-extracted CLC antigen extracted by either phenol or urea method.

Table 4.2 Protein Concentrations of Triton X-114 and Sarkosyl fractions

	protein (μg/ml)
$WbtI_{G191V}$_P10	
TxS-A	352
TxS-D	364
TxI-SS	302
TxI-SI	20
$WbtI_{G191V}$Δ1423-22	
TxS-A	426
TxS-D	392
TxI-SS	775
TxI-SI	330

TxS: Triton X-114 soluble,
TxI: Triton X-114 insoluble
A: aqueous
D: detergent
SS: Sarkosyl soluble
SI: Sarkosyl insoluble

4.3.2 CLC fractionation

Approximately the same amount of soluble protein was found in the Triton X-114 aqueous (TxS-A) and detergent (TxS-D) fractions of CLC from both LVS and the LVS mutants (Table 4.2). However, the Triton X-114 insoluble (TxI) material from the CLC of $WbtI_{G191V}$_P10 CLC was far more soluble (~15:1) in 1% Sarkosyl (TxI-SS) than the Triton X-114 insoluble material from the CLC of $WbtI_{G191V}$Δ1423-22 (~2:1). When these fractions were analyzed by SDS-PAGE using StainsAll/Silver, equivalent amounts of protein in the Triton X-114-soluble, aqueous and detergent phases were not evident in the CLC preparations of the $WbtI_{G191V}$_P10 or $WbtI_{G191V}$Δ1423-22 (Figure 4.2). The proteins found in the TxS detergent phase were not stained with StainsAll/Silver. The increased amount of proteinaceous material solubilized by sarkosyl was visualized with StainsAll/Silver and the difference was clearly apparent (Figure 4.2). Overall there was a greater amount of protein found in the CLC of $WbtI_{G191V}$Δ1423-22 compared to the parent. As discussed in Chapter 2, the CLC-deficient strain made much less CLC than the parent, but when compared 1:1 by weight, the CLC extracted from the mutant appeared to contain more protein than the parent and fractionates differently. This could be due to the lack of high molecular size polysaccharide that is present in CLC of the parent strain.

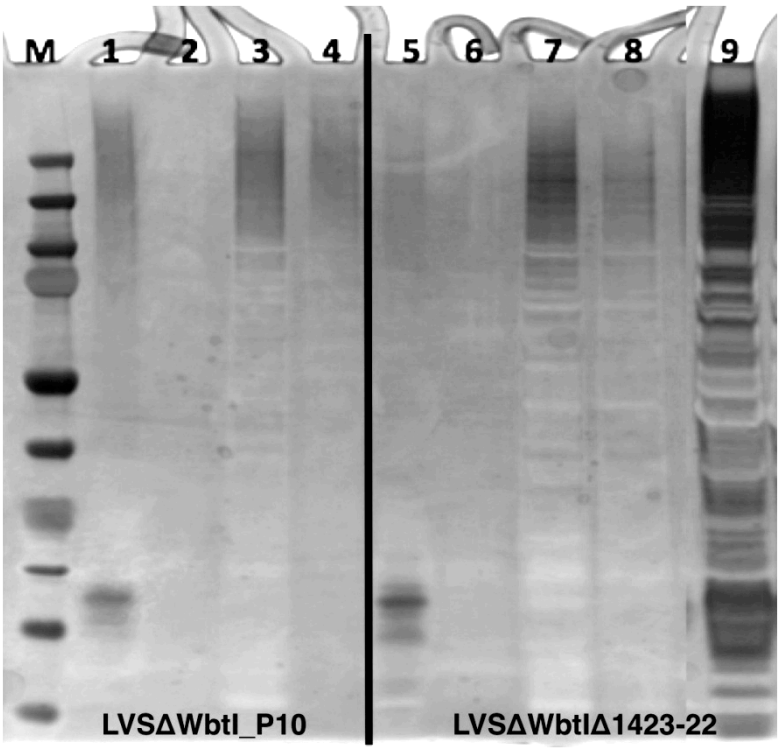

Figure 4.2 CLC fractionation using Triton X-100 and Sarcosyl detergents.
CLC from the parent strain fractioned predominantly into the TxS (was Tsx defined)-A phase and the TxI-SS phase. The CLC deficient strain showed little to no CLC in the TxS phase, but the TxI-SS phase appeared to contain more material than the parent.

1. TxS-A
2. TxS-D
3. TxI-SS
4. TxI-SI
5. Δ1423-22 TxS-A
6. Δ1423-22 TxS-D
7. Δ1423-22 TxI-SS
8. Δ1423-22 TxI-SI
9. Whole CLC 1M urea extract

Due to the HMW material still appearing as a smear after detergent fractionation, another method was employed. The GelFree 8100 fractionation system separates analytes based on electrophoretic mobility. Since we know the CLC appears as a high molecular weight smear in SDS-PAGE gels, this method was used to determine if the specific bands/components of the HMW portion of the CLC could be better resolved. Figure 4.3A shows phenol and urea extracted CLC before fractionation and the collected fractions from the GelFree 8100. Multiple proteins

are evident in both the phenol- and urea-extracted CLC, including the HMW band/smear. Interestingly, there were no bands or smear above 150-kDa after fractionation. The larger protein bands last appeared faintly in fraction 9; a smaller 45-kDa band appeared in fraction 6-8 and 11-12. This 45-kDa band is also the only band evident on a Western blot of the CLC using immune serum absorbed with the CLC-deficient mutant (Figure 4.3B). Unfortunately, protein identification using mass spectrometry failed to produce a positive identification.

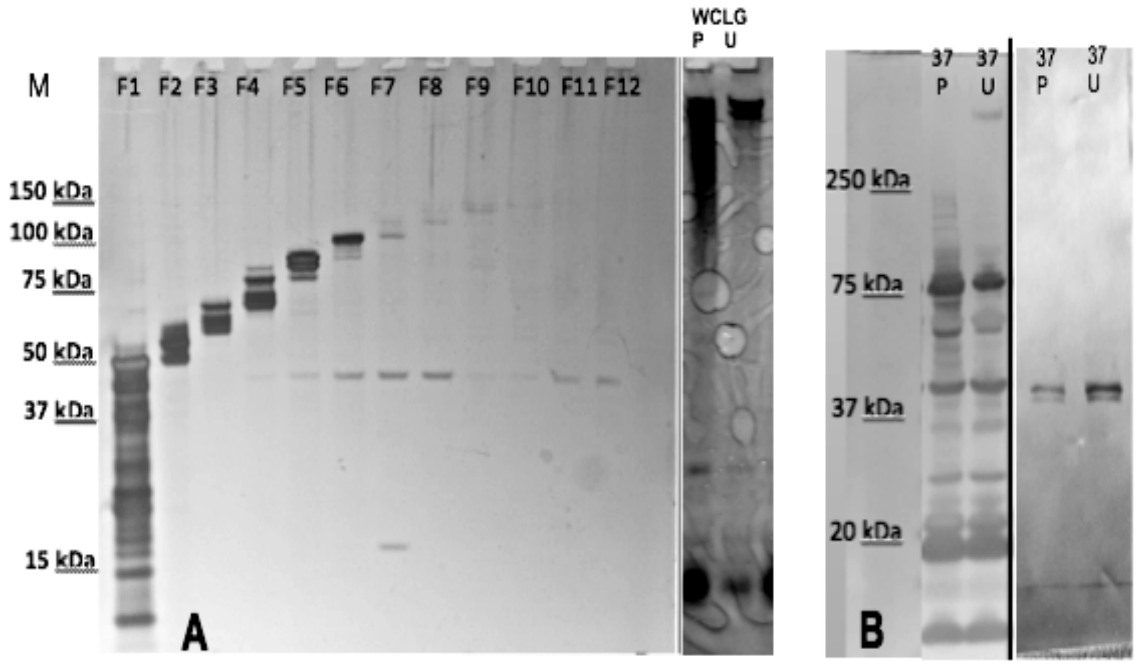

Figure 4.3 Fractionation of WbtI$_{G191V}$ CLC.

A: Silver stained fractionation of 100 µg of CLC urea extract using the GelFree 8100.
F1-F12: fraction 1-12. WCLG: whole CLC is evident as a smear above 250 kDa. P, phenol. U,urea. Before fractionation, staining of the CLC is evident as a smear above 150-kDa, but after fractionation, the highest molecular weight material is gone and in fractions 6-8 and 11-12, a 45-kDa band appears.

B: Western blot of CLC.
Left-right: Hyperimmune (HI) rabbit serum to CLC and HI sera-adsorbed with CLC-deficient strain, WbtI$_{G191V}$Δ1423-22. P: phenol extracted, U: urea extracted. Multiple proteins are evident in both the phenol- and urea-extracted CLC, including the HMW band clearly evident in the urea extracted when rabbit HI sera to CLC was used. After the CLC HI sera was adsorbed with the

CLC-deficient strain only one band/doublet was evident. This band was 45-kDa and is the same size as the band seen during fractionation with the GelFree8100.

4.3.3 Impact of growth media and method on CLC

CLC is normally extracted from bacteria that have been grown for an extended period of time on defined media agar. To determine if CLC was produced/upregulated under any other growth conditions, we grew $WbtI_{G191V}$_P10 in CDMB/A, BHIB/A, and MHB/A. We found that CLC and the HMW band/smear was highly expressed upon growth of bacteria on CDMA (as described in Chapter 2-3) and BHIA (though less expressed than with CDMA). When *F. tularensis* grown for 5-10 days in CDMB/BHIB, no evidence of the release of CLC into the broth media was observed. However, when $WbtI_{G191V}$_P10 was grown for 10 days in MHB, the high molecular weight CLC band/smear appeared to be released into the broth supernatant (Figure 4.4). When the bacterial cells that were removed from the 10-day growth were extracted for CLC using urea, only faint evidence of the HMW band appeared upon silver stain. It can by hypothesized that depending upon the growth media, the CLC is either retained by the cell or it is shed into the surrounding broth.

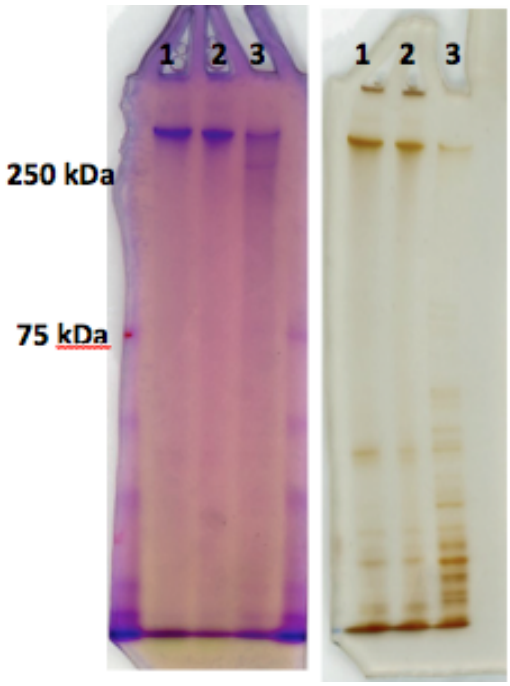

Figure 4.4 Ethanol precipitate of 10-day broth culture after the bacteria were removed by centrifugation. Left: StainsAll, Right: Silver stain

Lane **1:** Ethanol precipitate from MH broth after growth of $WbtI_{G191V}$_P10, **2:** Ethanol precipitate of MH broth after growth of $WbtI_{G191V}$_P10, **3**: Urea extract of MH broth following growth of $WbtI_{G191V}$_P10 CLC.A band/smear larger than 250 kDa was present from the ethanol precipitate of MH broth after growth of CLC-enhanced *F. tularensis* for 10 days. The CLC does not appear to be tightly adherent to the cell, based on the faintly staining HMW band after 1M urea extraction of CLC.

4.3.4 Murine antibody response to CLC

Two and four weeks post-immunization mice that were immunized with purified CLC or CLC/Freund's adjuvant had a stronger immune response than those that received only crude CLC (Figure 4.5). In CD1 mice, after the first immunization IgG1, IgG2, and IgM levels were the same for PBS-immunized mice as for those mice immunized with crude or purified CLC. After the initial immunization, an increase in IgG and IgM levels occurred only in CD1 mice immunized with Freund's adjuvant and purified CLC. The IgG1, IgG2, and IgM levels of immunized C57Black/6 mic were increased over those of mice inoculated with PBS only, in groups inoculated with crude CLC and pure CLC with adjuvant (Figure 4.5A). There was no

significant difference between IgM levels between these two groups, indicating an adjuvant is not necessary in C57Black/6 mice for a good IgM response. Initially, as expected, IgM was the predominant antibody response in all groups exhibiting a response after initial immunization. Two weeks after the second immunization, the predominant antibody response was IgG1 and IgG2, particularly in the presence of Freund's adjuvant. Although all mice immunized made an antibody response, CD1 mice produced a more dominant long-term response to CLC (higher IgG levels) than either C57 Black/6 or BALB/c mice (data not shown for the latter) (Figure 4.5B). Also of interest, is the lack of an IgG1 response in C57 Black/6 mice immunized with only crude CLC, and the predominantly IgG1 response in C57 Black/6 mice following immunization with pure CLC plus Freund's adjuvant. Therefore, the potential immune response to CLC is dependent upon both the mouse strain and the adjuvant given.

A.

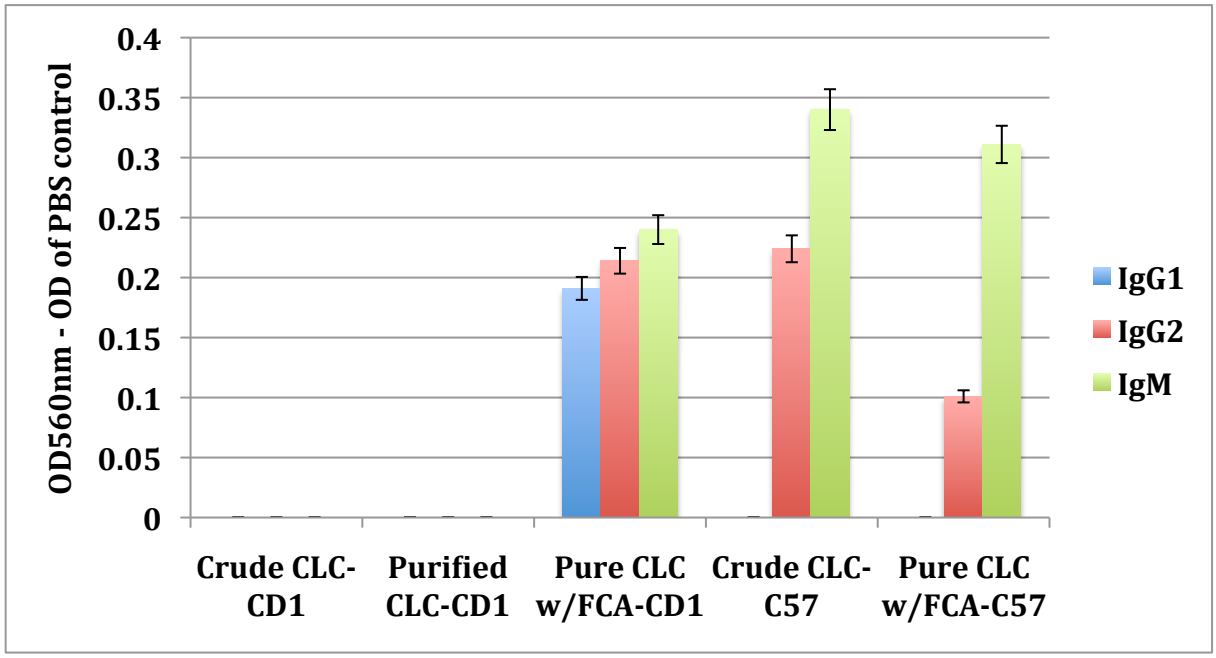

B.

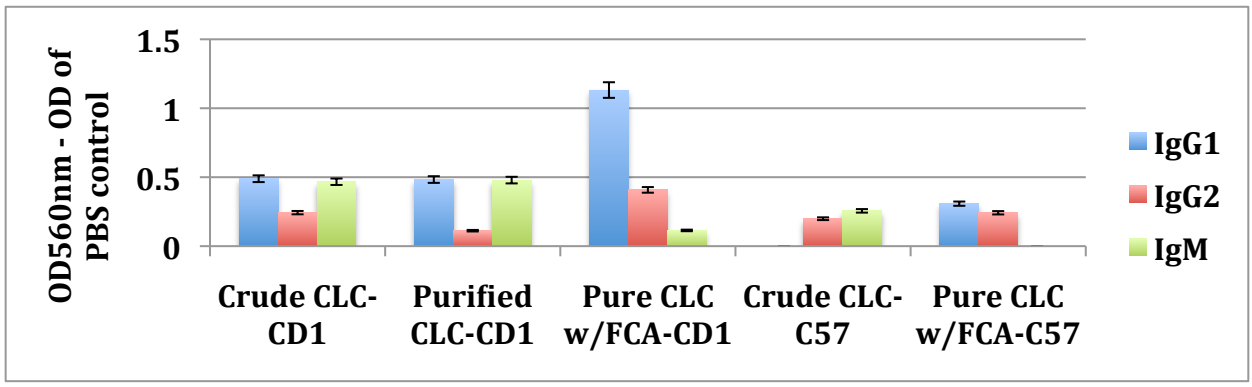

Figure 4.5 Murine antibody response to CLC

A. IgG1, IgG2, and IgM responses of CD-1 or C57 Black/6 mice 14 days after the initial immunization with crude CLC, purified CLC, or purified CLC with Freund's Complete Adjuvant (CFA). CD1 (CD1 mice), C57 (C57 Black/6 mice). **B.** IgG1, IgG2, and IgM responses of mice 14 days after a second immunization with crude CLC, purified CLC, or pure CLC in Freunds Incomplete Adjuvant (FIA).

4.3.5 Protective efficacy of CLC

Conjugation of CLC to either KLH or flagellin proteins was confirmed by SDS-PAGE. Gels were stained with Coomasie Blue, and conjugated CLC appeared as a band/smear above 200-kDa (Figure 4.6B). All CLC conjugates provided some protection against lethal LVS challenge in the BALB/c mouse model, but no significant protection occurred for the flagellin-CLC group challenged intranasally. The extent of protection in mice challenged intranasally was less than that of mice challenged intradermally. Mice immunized with the flagellin-CLC conjugate, followed by intranasal challenge, were the least protected, with only 33% of mice surviving (Figure 4.6A). Mice immunized with CLC conjugated to KLH were more protected (66%) after intranasal challenge. Complete protection against mortality only occurred in the KLH- and flagellin-conjugate groups that were immunized and challenged intradermally. The LVS challenge dose was 5 x LD_{50}, which was ~5000 CFU for intranasal and ~$2x10^7$ CFU for intradermal challenge.

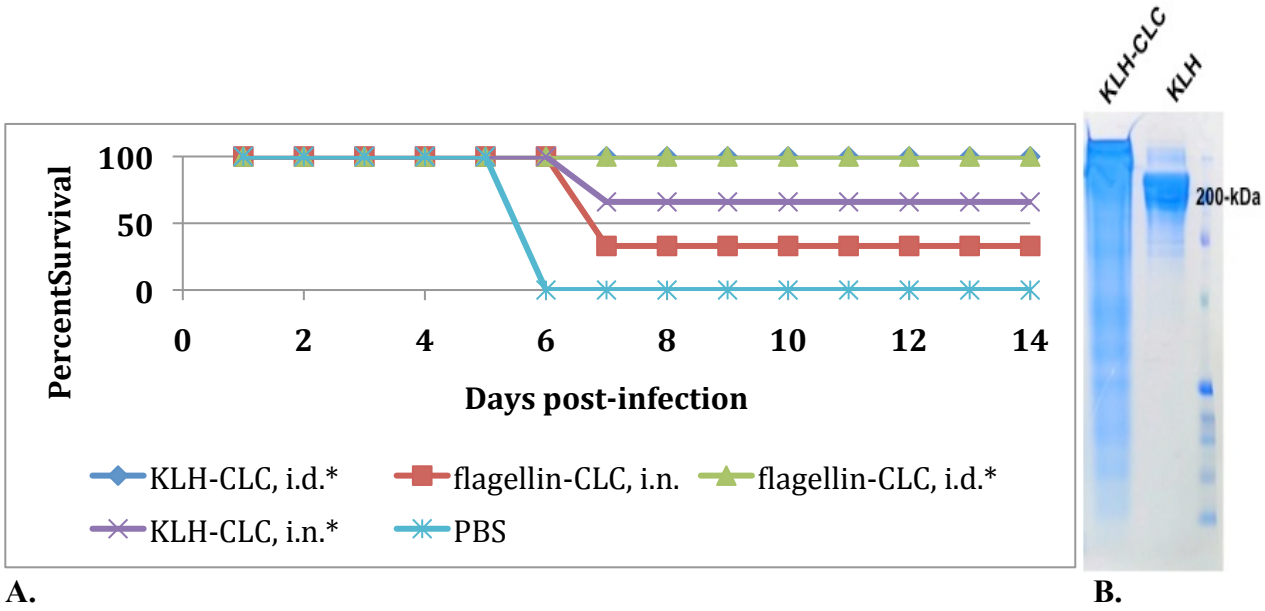

Figure 4.6 Protective efficacy of CLC-conjugate in BALB/c mouse immunization study
A. BALB/c mice were 100% protected from intradermal challenge with 5 x LD_{50} of LVS after intradermal immunization with 50 μg of KLH- or flagellin-conjugated CLC. Significant protection was also found in KLH- conjugated CLC after intranasal challenge with 5 x LD_{50} of LVS, but was not 100%. Mice immunized with PBS all died by day 6. **B.** SDS-PAGE showing the increase in size of conjugated KLH-CLC versus unconjugated KLH. *, $p<0.05$.

Sera was collected from immunized BALB/c mice pre- and post-challenge and tested for cytokine levels. There was no significant difference in the cytokine response (IL-2, IL-4, IL-5, GM-CSF, and TNF-α) of BALB/c mice immunized by either route with CLC-protein conjugates after challenge with LVS compared to mice immunized with PBS (data not shown). IL-12 was increased in both KLH-CLM and flagellin-CLM immunized mice, compared to the PBS control. Mice that made a greater response to IL-10, IL-12, and IFN-γ after challenge were better protected than mice in which that response did not occur, such as the PBS control, and to a lesser degree, flagellin-CLC following intranasal challenge (Figure 4.7)

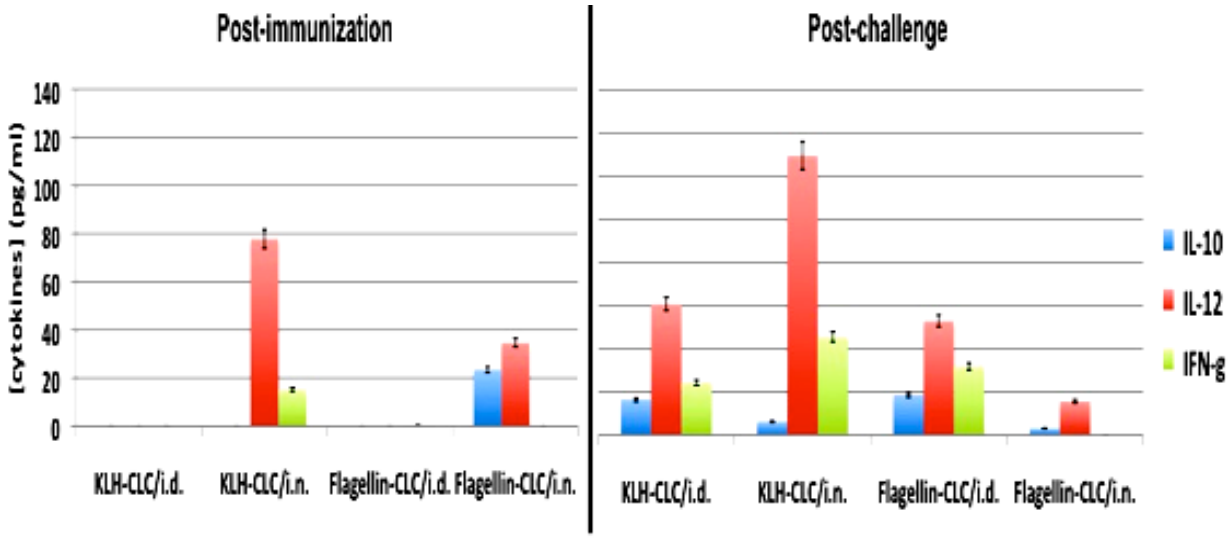

Figure 4.7 Murine cytokine response of BALB/C mice immunized with CLC-protein conjugates and challenged with 5 x LD_{50} of LVS (i.n: intranasal, i.d.: intradermal).
Post-immunization sera collected 2 weeks after the final immunization, post-challenge sera collected 3 days post-challenge Cytokine concentration expressed as ([cytokine] of immunized mice -[cytokine] of PBS control mice).

4.3.6 Isolation of OMV/T and electron microscopy

OMV/T were extracted using methods for both broth-grown and agar-grown bacteria. There was a significant size difference ($p<0.0055$) between OMV and OMT from LVS_P10 and LVSΔ1423-22 versus $WbtI_{G191V}$_P10 and $WbtI_{G191V}$Δ1423-22 (Figure 4.9). The average size of the OMV extracted from LVS ranged from 20-200 nm in diameter, while the average OMV extracted from $WbtI_{G191V}$ was 10-40 nm in diameter. The average size of the OMT extracted from plate-grown LVS_P10 was much larger than the vesicular form, with an average length of 500 nm, which was equivalent to OMT occasionally seen in the $WbtI_{G191V}$ strain.

There were distinct differences in regards to shape and type of OMV/T observed between the two methods of OMV/T extraction. When OMV/T were extracted from bacteria grown in broth media, the vesicles were more circular appearance. This included both LVS_P10 and

$WbtI_{G191V}$_P10 strains and their CLC-deficient mutants. When the OMV/T were extracted from bacteria grown on solid agar, the LVS_P10 strain had an approximately even distribution of circular vesicles and tubes, while OMV/T from the LVSΔ1423-22 CLC-deficient mutant were predominantly tubular in shape (Figure 4.9A-D). When the O-antigen deficient strain $WbtI_{G191V}$ and it's CLC-deficient mutant, $WbtI_{G191V}$Δ1423-22 were grown on solid agar, the OMV/T that were extracted were entirely circular in shape (Figure 4.9E-F). Another difference observed between strains LVS and $WbtI_{G191V}$ and their CLC-deficient mutants were the marked decrease in OMV/T and the negatively staining material that was observed between the OMV/T in both parent strains. This decrease in darker staining material was most evident in $WbtI_{G191V}$ versus $WbtI_{G191V}$Δ1423-22 (Figure 4.9E/G). However, upon closer magnification of the OMV/T present in the $WbtI_{G191V}$ CLC-deficient strain, the material between the OMV/T looked similar to that of the parent strain. Therefore, this material appeared to be deficient in CLC mutants rather than missing entirely. When OMV/T were extracted from bacteria grown in broth media, the shape differences observed in the plate-extracted OMV/T were not evident. Figure 4.8 shows images of OMV/T extracted from broth; the images shown are from $WbtI_{G191V}$ and it's CLC-deficient mutant, but are representative of LVS and it's CLC-deficient mutant as well. The OMV/T were mostly circular in nature for both parent and mutant. However, the negatively stained material observed in between the OMV/T was markedly less in the CLC-deficient mutant, $WbtI_{G191V}$Δ1423-22 (Figure 4.8A/B). Interestingly, protein concentrations of purified OMV/T increased in the CLC-deficient mutants in both strains when bacteria were grown in broth. However, when bacteria were grown on agar, similar to CLC-extraction, the protein content decreased in the $WbtI_{G191V}$Δ1423-22 mutant when compared to

the $WbtI_{G191V}$ parent (Table 4.3). The same results were not obtained for the LVS strains with an intact O-antigen.

Table 4.3 Average protein concentrations of OMV/T preparations

OMV/T	[Protein] μg/ml
LVS_P10/broth	**158**
LVSΔ1423-22/broth	**213**
LVS_P10/plates	**400**
LVSΔ1423-22/plates	**678**
$WbtI_{G191V}$ _P10/broth	**73**
$WbtI_{G191V}$Δ1423-22/broth	**290**
$WbtI_{G191V}$ _P10 OMV/plates	**610**
$WbtI_{G191V}$Δ1423-22 OMV/plates	**450**

McCaig et. al. suggested that a heat sensitive factor, such as protein, is responsible for the structuring of outer membrane vesicles into tubes [210]. The two glycosyl transferases responsible for CLC-deficiency in LVS do not appear to be involved in the hypothetical protein responsible for structuring the OMT, because LVSΔ1423-22, when grown on plates, produces almost exclusively tubule shaped-OMV (Figure 4.9A-D). Rarely were OMT seen in the mutants lacking O-Ag or O-Ag/CLC, indicating the O-Ag may play a role in tubule formation (Figure 4.9E-H).

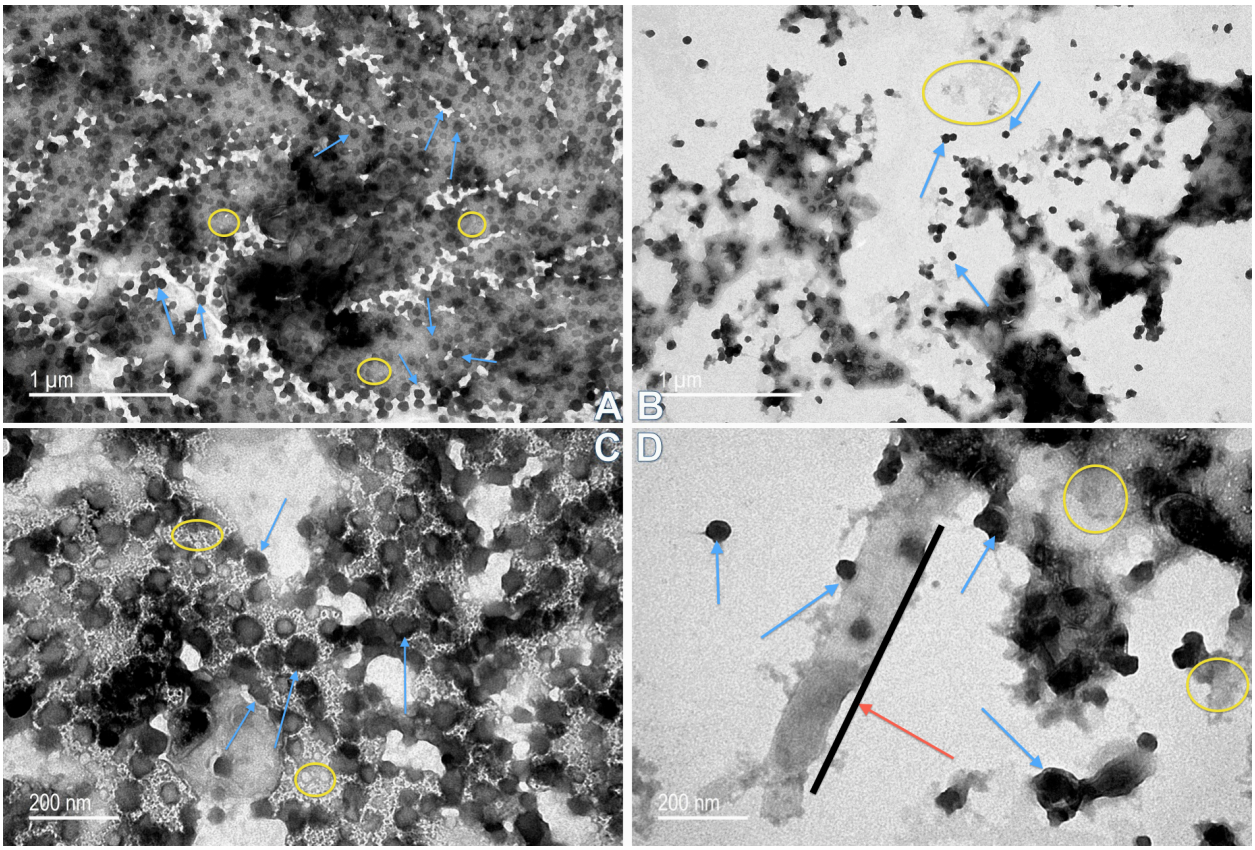

Figure 4.8 Transmission electron microscopy of OMV/T purified from *F. tularensis* strains grown in broth

A. WbtI$_{G191V}$_P10 (50k mag.), **B**. WbtI$_{G191V}$Δ1423-22 (50k mag.), **C**. WbtI$_{G191V}$_P10 (120k mag.), **D**. WbtI$_{G191V}$Δ1423-22 (120k mag.). OMV/T were purified from WbtI$_{G191V}$_P10 or WbtI$_{G191V}$Δ1423-22 using the modified *F. novicida* broth-grown method. Spherical OMV were found in both the parent (WbtI$_{G191V}$_P10) and, to a lesser extent, the CLC deficient mutant (WbtI$_{G191V}$Δ1423-22). A major distinction between parent and CLC mutant was the lack of lighter staining material found between OMV. The material is clearly seen as a slightly granular grey material at both 50k and 120k magnifications. At the higher magnification WbtI$_{G191V}$Δ1423-22 appears to be forming an OMT in addition to OMV. This was something that was not commonly seen in the WbtI$_{G191V}$ strains. Red arrows/black lines: OMT, Blue arrows: OMV, Yellow circles: material in between OMV/T.

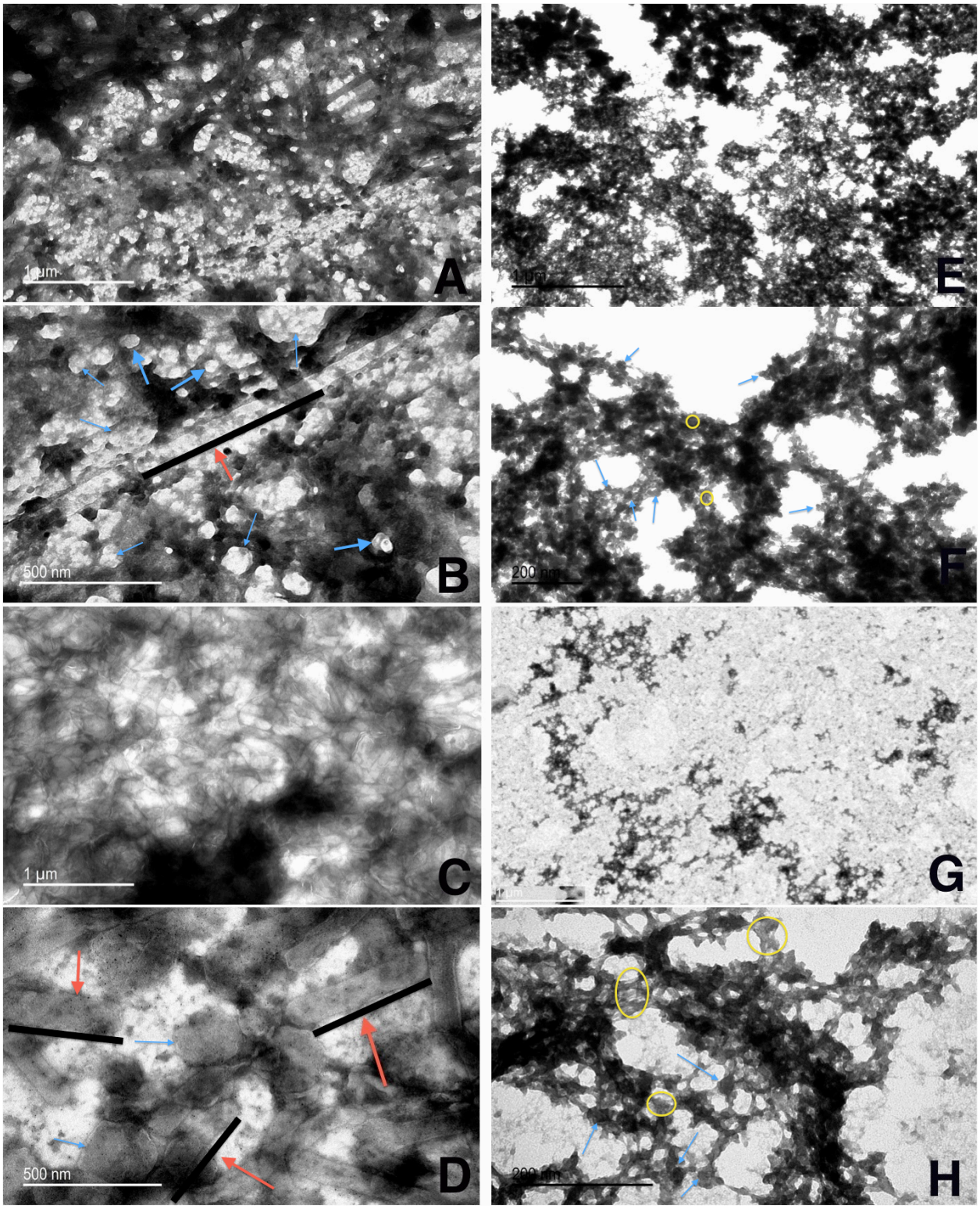

Figure 4.9 Transmission electron microscopy of OMV/T purified from *F. tularensis* strains grown on agar plates

OMV/T were purified from LVS_P10, WbtI$_{G191V}$Δ1423-22, WbtI$_{G191V}$_P10 or WbtI$_{G191V}$Δ1423-22 grown on CDM agar following a modified protocol used for *Brucella*. **A-B:** LVS_P10 (50k

mag., 120k mag.), **C-D**: $WbtI_{G191V}$Δ1423-22 (50k mag., 120k mag.), **E-F**: $WbtI_{G191V}$_P10 (50k mag., 120k mag.), **G-H:** $WbtI_{G191V}$Δ1423-22 (50k mag., 120k mag.). Red arrows/black lines: OMT, Blue arrows: OMV, Yellow circles: material inbetween OMV/T.

4.3.7 Protein composition of CLC

The carbohydrate content of the insoluble and soluble fractions of the CLC were similar, yielding just over 10% carbohydrate/mg of CLC (soluble: 112 µg carb/mg CLC, insoluble: 138 µg carb/mg CLC). Therefore, the protein composition was also analyzed. A total of 68 proteins were identified in the urea-extracted CLC from LVS. Twelve of these proteins were identified in the soluble material (Table 4.4) and 56 proteins were identified in the insoluble material (Table 4.5). Two of the top 20 proteins identified in OMV by Pierson *et. al*., were found in the soluble portion of the CLC; specifically chaperone proteins DnaK and GroEL (FTL_1191 and FTL_1714) [211]. GroEL was also found in the insoluble portion of the CLC along with 5 other top 20 OMV proteins (FTL_1146, FTL_1743 and FTL_1592, FTL_1442, FTL_1772) as described by Pierson et. al. [211]. Overall, out of the 12 proteins identified in the CLC soluble fraction, 4 were novel to the CLC (FTL_1474, FTL_1907, FTL_0014 and FTL_0227), and out of the 56 proteins identified in the CLC insoluble fraction, 18 were novel to the CLC (listed in Table 4.5). Nine proteins found in the CLC and in OMV/T (noted in Tables 4.4 and 4.5) have previously been associated with pathogenesis [82]. The soluble portion of the CLC, which contains the HMW smear, was also tested for glycosylation of proteins using nLC-MS/MS (Figure 4.10). While the specific amino acid sequence of the protein was not able to be identified due to heavy glycosylation, a glycan of 1157-Da was observed that corresponds to the previously reported hexasaccharide modification of proteins in *F. tularensis* (Figure 4.11) [204].

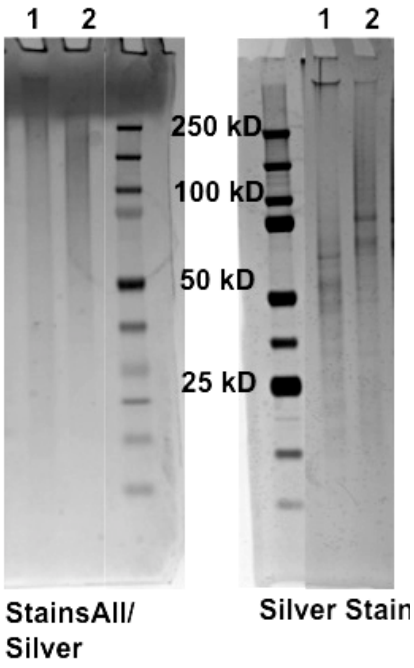

Figure 4.10 Insoluble and soluble fractions of LVS CLC 4-12% bis-tris SDS-PAGE
1: LVS CLC soluble – 10 μg, **2**: LVS CLC insoluble – 10 μg.
The soluble fraction contains the majority of the HMW band, while the insoluble fraction visualizes as a smear in StainsAll/Silver gels. Both insoluble and soluble fractions of the CLC appear to have lower molecular weight protein bands along with the HMW material when stained with silver.

Table 4.4 Proteins identified in the soluble fraction of CLC from LVS

SOLUBLE					
Identifier	**Found in:**	**Description**	**prot_score**	**Mass (Da)**	**pep_exp**
FTL_1191	T20, P,C	Chaperone protein dnaK (heat shock protein family 70 protein)	**222**	69140	0.00046
FTL_0009	E, S	outer membrane protein	**122**	19465	8.40E-05
FTL_1474	N	transcriptional elongation factor	**73**	17692	1.50E-07
FTL_0225	S	protein chain elongation factor EF-Ts	**68**	30940	6.70E-07
FTL_1592	N	Acetyl-CoA carboxylase, biotin carboxyl carrier protein subunit	**60**	16394	3.40E-06
FTL_1907	N	cell division protein	**52**	39720	2.10E-05
FTL_1461	P, C	purine nucleoside phosphorylase	**50**	26848	2.50E-05
FTL_0113	S	intracellular growth locus, subunit C	**47**	22119	6.60E-05
FTL_0014	N	Single-strand binding protein	**43**	17512	0.00014
FTL_1494	P, E, S	hypothetical protein	**41**	18147	0.00033
FTL_1714	T20, P, S, C	Chaperone protein, groEL (Yaron S, E coli 2000)	**39**	57367	0.00026
FTL_0227	N	ribosome recycling factor	**38**	20540	0.00043

T20 = Top 20 proteins found in *F. novicida* OMV [211]
P = OMV proteins previously associated with pathogenesis [82]
E = Proteins found in exponential phase OMV/T [210]
S = Proteins found in early stationary phase OMV/T [210]
C = Proteins found in culture filtrate [321]
N = Novel to this work

Table 4.5 Proteins identified in the insoluble fraction of CLC from LVS

INSOLUBLE					
Identifier	**Found in:**	**Description**	**prot_score**	**Mass (Da)**	**pep_expect**
FTL_1751	E, S	elongation factor Tu (EF-Tu)	**969**	43363	2.00E-05
FTL_1714	T20, P, C	Chaperone protein, groEL	**802**	57367	2.90E-06
FTL_1191	P, C	Chaperone protein dnaK (heat shock protein family 70 protein)	**394**	69140	1.10E-07
FTL_1907	E, S	cell division protein	**381**	39720	3.10E-08
FTL_0113	N, P	intracellular growth locus, subunit C	**368**	22119	1.30E-05
FTL_0234	E, S	elongation factor G (EF-G)	**250**	77681	2.00E-05
FTL_0112	P, S	intracellular growth locus, subunit B	**226**	57881	2.50E-13
FTL_1795	E, S	ATP synthase beta chain	**224**	49834	3.40E-07
FTL_0891	N	trigger factor (TF) protein (peptidyl-prolyl cis/trans isomerase)	**190**	49540	1.70E-10
FTL_0094	P, E, S	ClpB protein	**178**	95987	1.00E-07
FTL_0225	N	protein chain elongation factor EF-Ts	**177**	30940	1.40E-06
FTL_1146	T20, C	Glyceraldehyde-3-phosphate dehydrogenase	**161**	35391	0.0003
FTL_0267	P, S	Chaperone Hsp90, heat shock protein HtpG	**151**	72326	1.00E-07
FTL_1791	N, C	superoxide dismutase	**148**	21926	9.30E-07
FTL_1912	E, S	30S ribosomal protein S1	**145**	61631	0.00017
FTL_1461	N, C	purine nucleoside phosphorylase	**132**	26848	0.0007
FTL_0436	N	Isoleucyl-tRNA synthetase	**127**	106904	6.00E-13
FTL_0572	E, S	hypothetical protein	**113**	51945	1.10E-11
FTL_0260	S	30S ribosomal protein S4	**107**	23222	8.10E-11
FTL_0597	N	NAD dependent epimerase	**105**	36427	1.80E-07
FTL_0895	N, C	Histone-like protein HU form B	**105**	9468	1.20E-10
FTL_1190	N	Chaperone protein grpE (heat shock protein family 70 cofactor)	**102**	22022	2.50E-06
FTL_0166	S	universal stress protein	**102**	30202	2.10E-06
FTL_1746	S	50S ribosomal protein L10	**101**	18720	1.90E-10
FTL_0949	N	Ribose-phosphate pyrophosphokinase	**97**	34887	2.70E-06

FTL_0987	S	lactate dehydrogenase	**94**	34055	5.90E-07
FTL_0588	N	isocitrate dehydrogenase	**93**	82332	7.70E-05
FTL_0834	S	Rhodanese-like family protein	**88**	27847	4.90E-09
FTL_1553	P, S	Succinyl-CoA synthetase beta chain	**87**	41516	1.30E-06
FTL_1527	S	Enolase (2-phosphoglycerate dehydratase)	**85**	49480	4.30E-09
FTL_1701	P	GlpX protein	**83**	34820	1.90E-08
FTL_0923	S	Glutaredoxin 2	**83**	25135	1.30E-08
FTL_1224	N	Thioredoxin 1	**78**	12194	6.60E-08
FTL_1743	T20,P, S,E	DNA-directed RNA polymerase, β subunit	**77**	157289	6.20E-08
FTL_1591	S	Acetyl-CoA carboxylase, biotin carboxylase subunit	**76**	50019	7.50E-08
FTL_0097	N	hypothetical protein	**76**	13785	6.10E-05
FTL_1780	N, C	triosephosphate isomerase	**76**	27638	5.80E-08
FTL_0232	S	30S ribosomal protein S12	**69**	13806	9.70E-07
FTL_1350	N	Glycyl-tRNA synthetase beta subunit	**66**	77973	4.80E-07
FTL_1140	N	malonyl coA-acyl carrier protein transacylase	**62**	33480	2.30E-06
FTL_0233	S	30S ribosomal protein S7	**61**	17796	2.60E-06
FTL_1138	N	acyl carrier protein	**61**	10653	2.30E-06
FTL_1240	S	Phospho-2-dehydro-3-deoxyheptonate aldolase	**60**	40853	1.80E-06
FTL_1747	S	50S ribosomal protein L1	**57**	24626	4.70E-06
FTL_1275	N	dethiobiotin synthetase	**55**	24487	9.70E-06
FTL_1592	T20	Acetyl-CoA carboxylase, biotin carboxyl carrier protein subunit	**53**	16394	1.60E-05
FTL_1334	N	L-serine dehydratase 1	**52**	49977	2.70E-05
FTL_0387	N	aspartate transaminase	**52**	44355	2.60E-05
FTL_1442	T20, S	Enoyl-[acyl-carrier-protein] reductase (NADH)	**49**	27757	4.10E-05
FTL_0916	E, S	Ketol-acid reductoisomerase	**46**	37855	7.30E-05
FTL_1797	N	ATP synthase alpha chain	**46**	55502	5.20E-05
FTL_0311	S	dihydrolipoamide dehydrogenase	**44**	50495	9.90E-05
FTL_1772	T20, S	aconitate hydratase	**44**	102639	0.00028
FTL_1784	E	2-oxoglutarate dehydrogenase E1 component	**39**	105613	0.00029
FTL_0739	N	glucose inhibited division protein A	**36**	69721	0.00053

FTL_1022	N	Coproporphyinogen III oxidase	**36**	35854	0.00053

T20 = Top 20 proteins found in *F. novicida* OMV [211]
P = OMV proteins previously associated with pathogenesis [82]
E = Proteins found in exponential phase OMV/T [210]
S = Proteins found in early stationary phase OMV/T [210]
C = Proteins found in culture filtrate [322]
N = Novel to this work

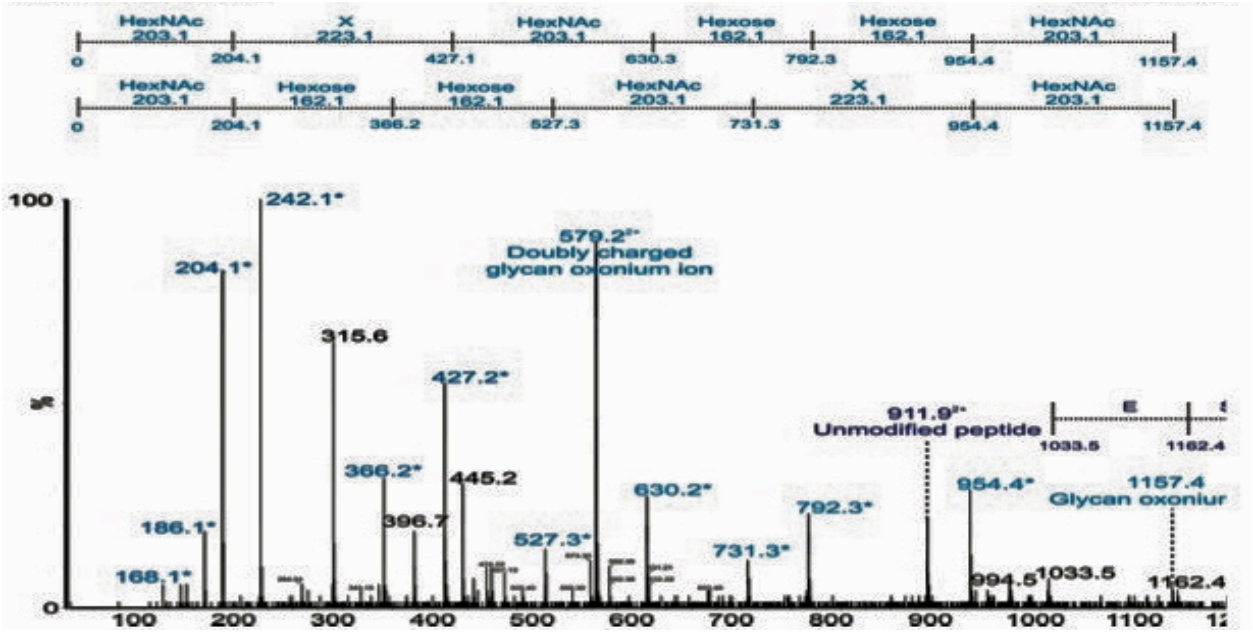

Figure 4.11 Detection of glycopeptides in soluble capsule extract

nLC-MS/MS spectrum of a triply protonated glycopeptide at m/z 993.7, enriched from soluble fraction using ion-pairing normal phase liquid chromatography (IP-NPLC). Relative ion abundance is shown on the y axis, and m/z is shown on the x axis. The spectrum is dominated in the low-m/z region by a glycan related ions, indicated in light blue and with an asterisk. In particular, a glycan-related oxonium ion was visible at m/z 1157, corresponding to a previously reported hexasaccharide modification of proteins in *Francisella tularensis*. The doubly charged form of this oxonium ion is also observed at m/z 579. From this, carbohydrate related fragment ions were observed as neutral losses of monosaccharides in the sequence 203-223-203-162-162-203 or 203-162-162-203-223-203 (total mass of glycan is 1156 Da). These masses plausibly represent monosaccharides such as HexNAc (203) and hexose (162). The loss of 223 does not correspond to a known monosaccharide and is indicated as X in the figure. A doubly charged ion at m/z 911 likely corresponds to the unmodified form of the peptide, giving a predicted peptide mass of 1823. This corresponds to the total glycopeptide mass of 2977, less the 1156 Da hexasaccharide moiety. The intensity of the carbohydrate ions obscured peptide related y and b type fragment ions, making sequencing of the peptide challenging. A short peptide sequence was determined from putative type y ions in the high m/z region of the spectrum, corresponding to the amino acid sequence (Q/K)(I/L)VSE. The sequence is not sufficient to identify the complete peptide, therefore the identity of the protein from which this glycopeptides was derived is currently unknown.

4.3.8 Relationship between CLC and OMV/T

The CLC and extracted OMV/T were similar in electrophoretic appearance by SDS-PAGE (Figure 4.12). The OMV/T extracted using the broth-grown method yielded a more intact, high

molecular size smear/band (>200-kDa) when compared with the agar-grown OMV/T, which yielded a high molecular weight smear and protein banding from 150-kDa down to 10-kDa. Both of these phenotypes have been seen with extracted CLC, particularly when comparing phenol-extracted CLC (compare to OMV/T agar-extracted phenotype) and urea-extracted CLC (compare to OMV/T broth-extracted phenotype). Figure 4.13A shows an intact $WbtI_{G191V}$_P10 cell enhanced for CLC and the subsequent 1M urea CLC extraction of the negatively staining surrounding material (Figure 4.13B-D). When visualized using TEM, lower magnification showed the electron dense material surrounding the bacteria cell, but upon higher magnification of the CLC extracted from the bacterial cell with urea, individual circular vesicles were able to be visualized (Figure 4.13E).

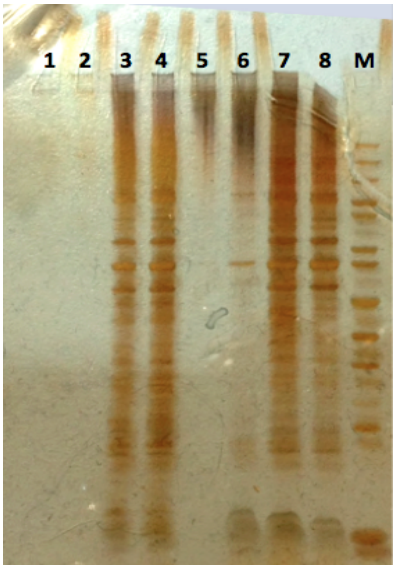

Figure 4.12 SDS-PAGE Silver Stain of OMV/T extracted from broth or agar grown LVS and mutants

OMV/T had a similar appearance to CLC when run on SDS-PAGE. OMV/T extracted from plates yielded a HMW smear and many lower protein bands, while the OMV/T extracted from broth yielded mostly a HMW smear, particularly evident in the $WbtI_{G191V}$ strains.

1. LVS_P10 OMV – broth
2. LVSΔ1423-22 OMV – broth
3. LVS_P10 OMV – plate
4. LVSΔ1423-22 OMV – plate
5. $WbtI_{G191V}$_P10 OMV – broth
6. $WbtI_{G191V}$Δ1423-22 OMV – broth
7. $WbtI_{G191V}$_P10 OMV – plate
8. $WbtI_{G191V}$Δ1423-22 OMV - plate

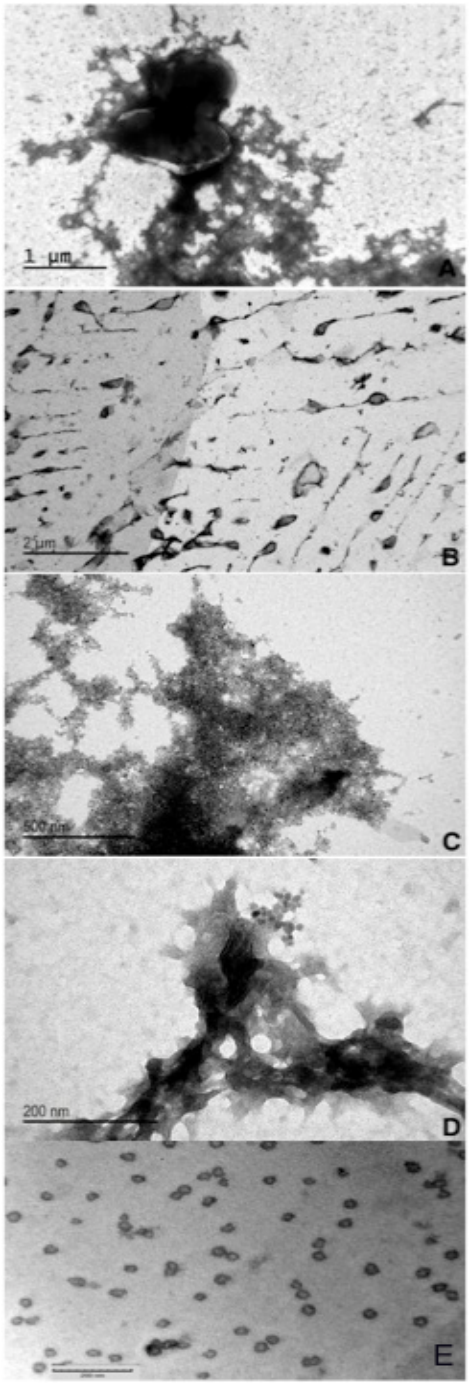

Figure 4.13 TEM *F. tularensis* $WbtI_{G191V}$ enhanced for CLC and urea extracted CLC.
A. Whole cell bacteria, **B-E.** Urea extracted CLC.
Whole cells were fixed with glutaraldehyde before staining and all samples were negatively stained with 0.5% uranyl acetate. Panel B, gives an overview of urea extracted CLC; panels C-E are a higher magnification. The circular OMV are clearly seen in panel E, while panel C shows groups of what appear to be OMV clustered together.

4.3.9 Type A Capsule-like Complex

Francisella tularensis type A strains SCHUS4 and clinical isolate TI0902 exhibited a more mucoid and iridescent surface appearance when passaged in CDM and grown at 32°C or 37°C on CDMA than the unpassaged parent strains. These results were similar to those with type B LVS CLC. Initial efforts to visualize the CLC on the surface of the bacteria using negative stain TEM techniques were less successful than with the type B CLC. We hypothesized this was due to the extended period of time the bacteria had to remain in fixative and at 4°C during the time required to verify that no viable cells remained in the culture and were safe to remove from the Biosafety-level 3 laboratory. With slight modifications we were able to visualize a darker staining electron dense material surrounding both SCHUS4_P10 and TI0902_P10 cells that was greatly diminished in the unpassaged parents (Figure 4.14). This material stained noticeably darker and appeared more granular than material visualized from the type B strains. This could be due to the slight modification of the TEM preparation procedure needed for the biosafety level 3 laboratory. CLC extraction with either phenol or urea appeared very similar to the CLC extracted from type B strains (Figure 4.15B). Phenol extracted CLC stained with StainsAll/Silver yielded a HMW smear in addition to some lower banding. The urea-extracted CLC was a less diffuse HMW band/smear by SDS-PAGE, similar to LVS CLC, and also included the additional lower molecular weight bands. In addition, the type A CLC antigens were immunologically similar to the type B CLC (phenol and urea extractions) and reacted with HI sera to LVS CLC generated in a rabbit (Figure 4.15A). Similar to the type B CLC, the type A CLC appeared sensitive to proteinase K digestion, yet resistant protein bands in the western blot and the HMW smear in the StainsAll/Silver gel remain after digestion. Carbohydrate composition analysis of purified CLC from *F. tularensis* SCHUS4 yielded similar results to type

B CLC: there was less than 5% carbohydrate, which consisted of glucose, galactose, and mannose. Interestingly, the CLC extracted from O-Ag deficient TI0902 strain, TIGB03 stained blue with StainsAll which is indicative of a more pure polysaccharide than the purple color CLC stains from all other type A and B F. *tularensis*. Once the mutation in TIGB03 was complemented and O-Ag was restored to the strain, the CLC electrophoretic profile reverted back to that of the parent (Figure 4.16). Further studies are ongoing to characterize this anomaly.

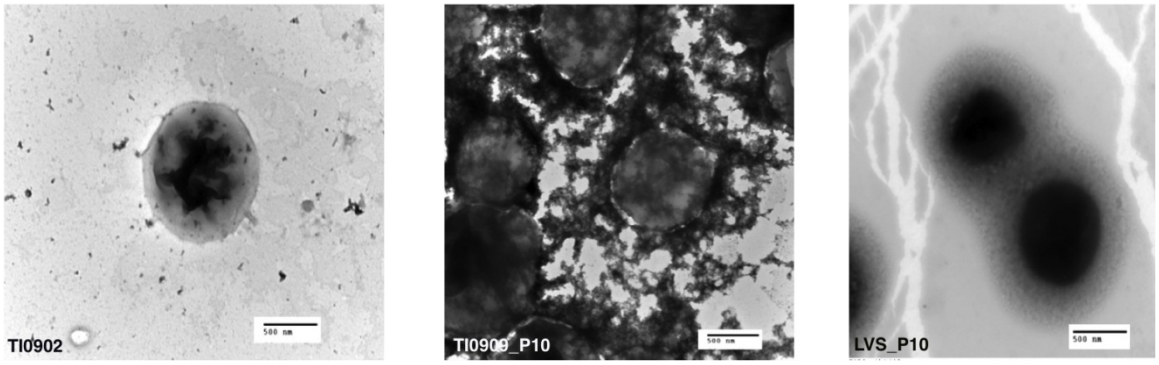

Figure 4.14 TEM of *F. tularensis* Type A strain clinical isolate TI0902
Bacteria were fixed in glutaraldehyde buffer overnight and stained with 0.5% uranyl acetate. The CLC material visualized surrounding type A strains SCHUS4 (not shown) and TI0902 (left) was upregulated by repeated passage (middle) and were darker staining and more granular (circular) than the CLC from LVS (right).

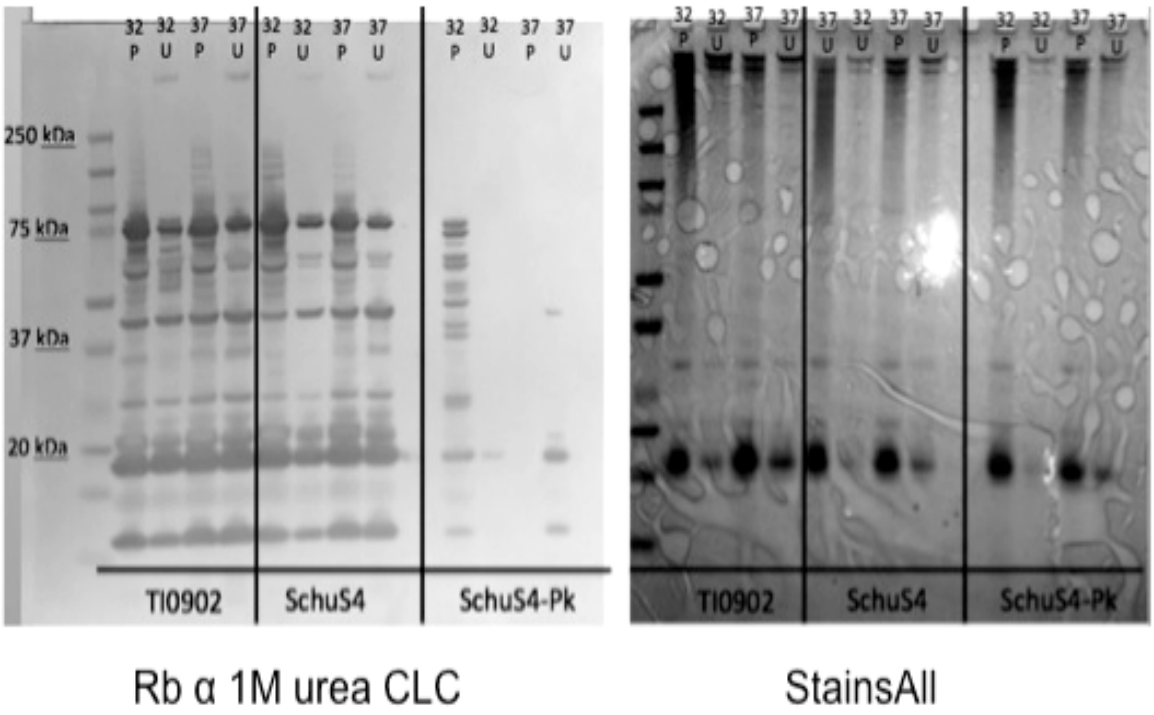

Figure 4.15 CLC extracted from Type A strains TI0902 and SCHUS4 **by either phenol or urea extraction methods at 32°C or 37°C**

P: phenol extraction, **U**: urea extraction, **Pk**: proteinase K treated.

The western blot using rabbit HI sera to urea-extracted type B CLC also reacted with the type B CLC Western blots performed (Figure 4.3). Some proteins were still reactive after proteinase K digestion and the HMW smear was evident after staining with StainsAll. Thus, the CLC extracts from type B and type A cells were similar in appearance and antigenically.

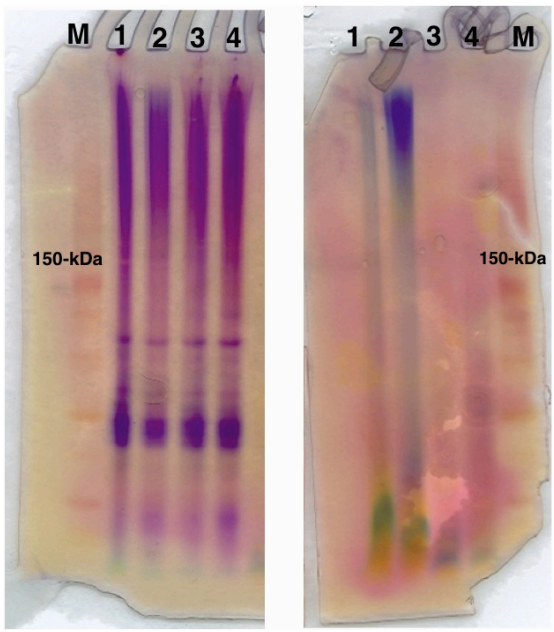

Figure 4.16 Electrophoretic profile of CLC extracted from type A strains stained with StainsAll.

Left gel is 0.5% phenol extracted crude CLC. Right gel is 0.5% phenol extracted CLC after concentration through a 100-kDa Centriprep filter. M: marker, 1: TI0902, 2: TIGB03, 3-4: TIGB03[+] complemented.

4.4 Discussion

The capsule-like complex of *Francisella tularensis* remains a novel and elusive antigen, proven to be necessary during pathogenesis [192]. One of the complexities of working with the CLC antigen is the high insolubility that occurs upon purification. By changing the chaotropic extraction buffer from 0.5% phenol to 1M urea while studying the surface-layer protein like qualities of the CLC, a marked increase in solubility and ease of manipulation was obtained. Initially, it needed to be determined that extraction of the CLC with 1 M urea resulted in the same antigen extracted with phenol [192]. SDS-PAGE electrophoretic profiles of the CLC extracted by both methods and stained with StainsAll/Silver showed that these antigens were similar in HMW smear/banding pattern. Due to the more concise banding pattern of the urea-extracted CLC, further testing was needed to confirm the CLC antigens were the same. Immune sera generated using type B CLC extracted with either phenol or urea cross-reacted with CLC

antigen extracted by either method from both type A and B strains. In addition, CLC antigens from type A and B exhibited similar Western blot electrophoretic profiles in the pure CLC (smear greater than 200-kDa) and in the crude CLC (HMW smear and multiple lower weight bands), and neither reacted to monoclonal antibodies to O-antigen or O-antigen capsule [92]. This led us to conclude that CLC antigens from type A and type B strains were identical, regardless of the extraction method.

Previously published results indicated the CLC contained no more than 10% carbohydrate and consisted mostly of (glyco)proteins [192]. In this study, we aimed to further characterize the CLC components. Initially, we attempted to fractionate the CLC and increase its solubility using Triton X-114. The *F. tularensis* O-antigen capsular polysaccharide can be purified from the aqueous phase of a Triton X-114 extraction [92]. Therefore, in addition to separating the proteins, we hypothesized the HMW carbohydrate would also be fractionated into the TxS-A phase. However, the HMW material from the parent strain partitioned into the TxS-A phase and the TxI-SS phase equally. These results suggest that the HMW polysaccharide component of the CLC and/or glycoproteins associated with the CLC partitioned into the hydrophilic TxS-A phase, while the integral membrane proteins, OMP, and lipoproteins partitioned into the TxS-D phase, as is well documented [317,323,324]. Analysis of the CLC extracted from $WbtI_{G191V}\Delta 1423\text{-}22$ further confirmed the possibility of a HMW carbohydrate/glycoprotein component of the CLC, as the TxS-A fraction of the glycosyl transferases-deletion mutant did not yield a HMW smear as did the parent strain. However, the TxI-SS fraction did yield a darker staining HMW smear/bands by SDS-PAGE and silver staining which is probable evidence of differing (glyco)protein components than the parent CLC. We have previously reported that the double

transferase mutant of LVS and $WbtI_{G191V}$ is deficient in, but continues to produce, a low amount of CLC [192]. There was no significant difference in the amount of protein isolated in the TxS-A and TxS-D phases of the CLC from either the parent or mutant strain. The difference in protein content between parent and CLC-deficient mutant was evident in the ratio of TxI-SS:TxI-SI fractions. The CLC from $WbtI_{G191V}$_P10 had a ratio of 15:1 (TxI-SS:TxI-SI vs. 2:1 for CLC from mutant (Table 4.2). The higher protein concentration found in the sarkosyl-insoluble fraction of $WbtI_{G191V}\Delta$1423-22 could be the result of more inner membrane proteins present due to the lack of CLC coating and protecting the surface of the cell during urea extraction.

The individual components of the HMW smear remained unidentified at the start of the study. If the HMW CLC was an aggregate of glycoproteins or a mixture of (glyco)proteins and polysaccharide, individual components should be resolved using a size exclusion system based on electrophoretic mobility. The GelFree 8100 cartridge is capable of fractionating components up to 500-kDa, however, the largest band visualized from CLC extract by silver stain was just under 150-kDa after fractionation, and no HMW smear was visualized at all with StainsAll/Silver. Thus, the HMW CLC smear observed was likely due to aggregates of surface (glyco)proteins, and the HMW aggregate smear was separated into individual components during GelFree fractionation. The 45-kDa band that appeared in the highest molecular weight GelFree fractions (>100-kDa) was also the only antigen reactive after HI sera to CLC was absorbed with CLC-deficient mutant cells. Thus, the 45-kDa protein could be involved in maintaining the aggregation of the CLC or OMV/T. The 45-kDa protein has also been recognized as an immunoreactive protein in mouse sera following immunization with OMP's [98]. Unfortunately, identification of this band was unsuccessful following concentration of the fractions and mass

spectrometry. We identified 56 proteins in CLC extracted from $WbtI_{G191V}$_P10, and found many surface proteins and proteins involved in virulence (including FPI proteins). Sixty-percent of these proteins have previously been identified in OMV of *F. novicida* [210], suggesting that the (glyco)protein content of the CLC was due to enhanced OMV production. Proteins identified previously in OMV and OMV/T have numbered in the hundreds [210,211]. The CLC extract analyzed in this study consisted of substantially fewer proteins, which may be due to the enzymatic treatment of the CLC used during the purification process.

An effective vaccine for *F. tularensis* is proposed to require both cell-mediated and humoral responses [68,148,325,326]. Multiple research groups have previously isolated OMP, OMV, and OMV/T from *F. novicida* and LVS [98,210,211], and have shown that OMP and OMV/T induce a pro-inflammatory response from host cells, which also occurs after immunization with the CLC. [98,210]. Immunization of mice with the CLC produced increased levels of IgG_1, IgG_2, and IgM, as well as an increase in pro-inflammatory cytokines, TNF-α and IFN-γ. As previously reported, the murine antibody response depended on mouse strain as well as purity of the CLC, and our overall increased levels of IgG and IgM antibody response correlates with previously published results [311]. In the BALB/c mouse model, CLC conjugated to an immunogenic protein was protective against a lethal LVS challenge. Complete protection (100% survival) was obtained using either KLH or flagellin as the immunogenic protein, when mice were challenged intradermally. Protection against *F. novicida* challenge has also been established using OMV, but the protection was incomplete and did not lead to 100% survival of OMV vaccinated mice [211]. However, a vaccine for tularemia needs to protect against the aerosolized route of infection due to the potential for use as a bioweapon, and be protective against the more virulent

type A strains. BALB/c mice intradermally immunized multiple times with type A CLC and Freund's Complete adjuvant were not protected against intranasal challenge with a lethal dose of *F. tularensis* SCHUS4. The challenge does of SCHUS4 given to the mice (500 c.f.u.) in our study was ~10 times higher than the challenge dose given by Huntley *et. al.* who reported a 50% survival rate with outer membrane protein (OMP) immunizations [98]. Differences in OMP preparation versus CLC preparation and differences in challenge c.f.u. could account for the differences in protection between studies, as well as our CLC antigen does not contain any detectable LPS, whereas Huntley et. al. reported LPS contamination in their study and indicated that it might have an immunomodulatory implication [98]. Therefore, CLC by itself may not be a viable choice for a vaccine, but still could have potential as part of a subunit vaccine, or it may well protect against a lower challenge dose of virulent type A *F. tularensis*, and future studies may be useful.

McCaig *et al*. previously reported that OMT of *F. novicida* appeared to initiate contact with host macrophages and may trigger phagocytosis [210]. The CLC-deficient mutant of LVS produced almost exclusively OMT when grown on CDMA, and LVSΔ1423-22 was not defective in uptake and growth in macrophages [192]. Giving credence to McCaig's hypothesis that OMT trigger phagocytosis, $WbtI_{G191V}$Δ1423-22 was defective in growth in macrophages and produced almost exclusively OMV in spherical form, no tubules [192]. Therefore, regulation of OMV/T could have an impact on the intracellular nature of *Francisella*. In addition, we have reported what appears to be CLC surrounding the bacterial cell, before and during macrophage uptake, and that the CLC is shed in the *Francisella*-containing vacuole (FCV) (Appendix I). This phenomenon has also been reported by other groups that have observed vesicle-like material

associated with phagocytized bacteria [117,123]. An important question remains as to whether the CLC consists only of upregulated OMV/T or if an additional component is present to form the negatively staining material seen in TEM during upregulation of CLC and during infection. The production of a HMW carbohydrate in conjunction with the CLC has previously been established [192]. Zarrella *et al*., found that bacteria grown in BHI medium allow the bacterial surface to mimic adaptations usually seen during host infection, while growth in MH medium did not [193]. An important observation is that the presence of a HMW carbohydrate (>200-kDa) appears to be the same HMW carbohydrate associated with the CLC. However, Zarrella *et al*. did not observe this carbohydrate surface modification after growth of LVS in CDM [193]. The discrepancy between our results and Zarrella et al. could possibly be due to our technique to enhance CLC production [193]. After CLC enhancement, the HMW carbohydrate is present after growth on CDMA and could be due to upregulation [190]. To investigate the role this HMW carbohydrate may play in the formation of CLC, we grew CLC-enhanced LVS strains in MH media to evaluate the CLC/OMV production. Of interest was that the MH grown bacteria did indeed produce HMW carbohydrate, yet instead of retaining this material on the bacterial surface, it was shed into the media. This could indicate that the CLC/HMW carbohydrate is retained by the bacterial cell in CDM and BHI because it is used during host infection. This theory is supported by the inability of the CLC-deficient mutant $WbtI_{G191V}\Delta 1423\text{-}22$ to replicate and survive in macrophages, unlike parent strain $WbtI_{G191V}$ [94,192]. Golovliov *et al*. suggested that shedding of a capsule-like material from *F. tularensis* following phagocytosis may result in degradation of the membrane and release of the bacteria into the cytoplasm [123]. Interestingly, our research has shown that deficiency in CLC alone is not enough to prevent *F. tularensis* replication in macrophages, but that an additional deficiency in O-antigen is also required.

However, TEM of infected macrophages revealed negatively staining material being shed from both LVS and $WbtI_{G191V}$. Therefore, deficiency of only one surface antigen (O-Ag or CLC) alone does not effect formation of this vesicular material. One hypothesis is that the HMW/CLC protects the bacteria from degradation until it enters the phagosome, where it sheds the material and replication/escape occurs [123]. Another possibility is that the HMW/CLC promotes host phagocytosis, and once the bacteria are phagocytized the CLC is no longer needed. The observation by McCaig *et al*., that OMT initiate contact with macrophages, gives credence to this theory [210].

McCaig *et al*. found that *F. novicida* produced markedly fewer OMV/T when grown in MH or CDM broth or agar [210]. The lack of production of OMV/T in MH could correspond to what we have seen in regards to CLC production in MH. However, the lack of OMV/T on bacteria grown in CDM does not support this theory. *F. tularensis* LVS produced OMV/T when grown in CDM, and the disparity between our results and others may lie in the passage of our LVS strains in order to increase CLC production [190]. *F. tularensis* LVS appears to shed a HMW material, similar to what occurs during CLC extraction when bacteria are grown in MH broth to late stationary phase. One hypothesis is that the HMW material shed during growth in MHB is part of the CLC and is attached to the cell when grown on CDMA. The MHB-shed HMW material correlates with the HMW carbohydrate described by Zarrella *et al.* that is "missing" during bacterial growth in MHB, but is present when the bacteria are grown in BHI, which results in production of carbohydrates to ones similar to those seen during host infection [192,193]. Evidence of negatively staining material occurring between the OMV/T found after the CLC was extracted using urea could be the unknown HMW material/carbohydrate described

by Bandara *et. al*. and Zarella *et al*. [192,193]. In addition to the 1156-Da hexose found to glycosylate various proteins in *F. tularensis*, we identified a novel 420-Da glycose polymer also found in the CLC (Chapter 3)[204]. This 420-Da carbohydrate polymer, found in the CLC smear greater than 170-kDa, could function to help aggregate the (glyco)proteins. If the bacteria lack the ability to produce OMV/T when grown in MHB, then the HMW carbohydrate may be shed indiscriminately into the media. This hypothesis would correspond to why we see the band during urea extraction of bacteria grown in CDMB or BHI, but not released into the media. TEM pictures of urea-extracted CLC from $WbtI_{G191V}$_P10 and $WbtI_{G191V}\Delta$1423-22 (Figure 4.8) show the lack of inter-vesicle material in the mutant, and therefore, substantiate this hypothesis.

During the course of this research, Thomas *et al*.(ref) reported that deleting glycosyltransferase FTT_0798 resulted in the loss of an O-linked 1156-Da glycan moiety on DsbA, but virulence was not affected [204]. We previously showed that deletion of the LVS homologue, FTL_1423, and another glycosyl transferase, FTL_1422, significantly decreased the CLC material ($p = 0.01$) and attenuated the strain in mice, while deleting only one glycosyl transferase had little effect on either [192]. This same 1156-Da glycan moiety has been identified in the CLC extracted with urea, as well as an unknown 420-Da polysaccharide chain. The 420-Da repeating polysaccharide unit (discussed in Chapter 3) was found in the CLC band/smear greater than 170-kDa to >250-kDa, and may be the link to the material we observed between the OMV/T after CLC extraction that potentially is the unknown HMW carbohydrate. Further characterization and identification of the HMW carbohydrate is needed.

In conclusion, we present evidence that the CLC is composed of OMV/T in *F. tularensis* type A and B strains: (i) the CLC upon visualization with TEM appears to contain OMV and OMT that are differentially regulated depending on O-antigen and CLC (glycosyl transferase) deficiencies, (ii) 60% of the proteins identified in the CLC match previously identified OMV/T proteins in *F. novicida,* and (iii) visualization on SDS-PAGE gels of CLC and OMV/T have similar phenotypes when stained with silver and StainsAll/silver. Several pieces of data circumstantially indicate the HMW carbohydrate component of the CLC is somehow related to the aggregation of this antigen, and could potentially be regulated by growth condition. Future research into the material found between OMV/T after upregulation of CLC is needed. Could the 420-Da glycan moiety be part of this cohesive material? The differential regulation of CLC, OMV and OMT appears to be connected and more insight into this phenomenon could help elucidate a new virulence factor of *Francisella tularensis*.

4.5 Co-Authors' Contributions

Parastoo Azadi (Complex Carbohydrate Research Center, GA) did compositional analysis of the purified carbohydrate. Susan Twine from the NRCC performed the amino acid sequencing and glycoprotein identification. Mutants used were constructed by Abey Bandara. Experimental design was conceived by Anna Champion and Tom Inzana.

CHAPTER 5

The Role of *F. tularensis* Surface Antigens on Biofilm Development

5.1 Introduction

In the last decade, there has been an upsurge in interest in studying the zoonotic pathogen *Francisella tularensis*. *F. tularensis* is a Gram-negative, facultative, intracellular bacteria that can infect numerous mammals, arthropods and other eukaryotes, and is the causative agent of tularemia or "rabbit fever" [4,245,327]. The virulent *F. tularensis* subsp. *tularensis* is categorized by the Center for Disease Control (CDC) as a Tier I select agent, due to the high infectivity and historical weaponization and, as such, much of the current research has focused on mammalian infection and vaccine development. While that is indeed important, other facets of pathogenesis should also be investigated so that we may have a detailed understanding of this microbe.

Each year in the U.S. there are approximately 200 cases of naturally occurring tularemia, with the majority of transmissions occurring through ticks. *F. tularensis* subsp. holarctica, is less virulent to humans, but is more common in Europe where there are thousands of human cases during active years. The route of infection for the majority of these cases in northern Europe is suspected to be mosquito-borne, as most of the patients were near water and had mosquito bites. It has been shown that mammals typically die from infection or clear the bacteria completely [31], so *F. tularensis* must be persisting in nature in other ways. Studies, using molecular typing methods, have shown that *F. tularensis* persist in environmental samples of water and mud [111,328,329] leading investigators to ask, "how".

Francisella is a rather fastidious organism, requiring supplementation of cysteine and other nutrients to grow in vitro. A common life strategy for terrestrial and aquatic habitats, especially where nutrients might be limited, is for bacteria to form a biofilm. A biofilm is an aggregated microbial community that produces an extracellular polymeric substance, usually composed of exopolysaccharide, extracellular DNA (eDNA) and proteins. Recently it has been demonstrated that *Francisella* form biofilms *in vitro,* with most work focusing on *F. tularensis* novicida. *F. novicida* will easily form biofilm on a variety of surfaces including plastics, glass and crab shells, while *F. tularensis* subsp. *tularensis* and subsp. holarctica do not form as robust biofilms, but will develop one on plastic 96-well plates.

Despite their genetic similarity, a key difference between the less virulent *F. novicida* and the type A and B strains lie in the polysaccharide surface components. *F. tularensis* type A and B strains have a LPS that consists of a non-endotoxic lipid A, core oligosaccharide that contains mannose and an O-antigen (O-Ag) composed entirely of dideoxyglycoses [178,330]. The outermost portion of LPS is the surface-exposed O-Ag. *F. tularensis* SCHUS4 and *F. tularensis* subsp. holarctica LVS were found to have identical O-Ag structures consisting of two internal carbohydrate residues (α-D-GalNAcAN--α-D-GalNAcAN) and two outside residues (β-D-Qui4NFm and β-D-QuiNAc), while *F. novicida* O-Ag shares the same two internal residues, but has differing outside residues (α-D-GalNAcAN and β-DQui2NAc4NAc) [176]. Genomic analysis of the O-Ag gene cluster (*wbt* locus) confirms that while type A and B are identical, *F. novicida* has fewer genes and a lower G+C ratio [182,183]. LPS is an important virulence factor for all subspecies, as it protects the bacteria against innate host defenses [176]. Subspecies

tularensis and holarctica also produce an antigenicly distinct O-Ag capsule that when removed does not effect complement susceptibility [92]. Type A and B strains are also reported to have a novel capsule-like complex containing proteins (some glycosylated) and a high molecular weight carbohydrate [92,192]. To date, *F. novicida* has been reported to be unencapsulated, yet unpublished data from our lab suggests a similar CLC is present upon upregulation. The question remains whether these surface components affect the formation of biofilm or development of the matrix.

We proposed to explore the ability of the more virulent type A and B strains to form biofilms and hypothesized that some of the differences we see may be due to the differences in surface antigens between *F. novicida* and the virulent *F. tularensis* subspecies. The objectives of this study were to i) determine the role of surface polysaccharide components in the formation of biofilm and matrix development, ii) elucidate the components of the biofilm matrix and the exopolysaccharide (EPS). We hypothesize that the purpose of biofilm development could be to aid persistence of *F. tularensis* whilst in the natural environment.

5.2 Materials and Methods

5.2.1 Bacterial strains and growth conditions

Strains used in this study are described in Table 5.1. Strains were cultured on either Chamberlain's defined medium with 1.5% glucose (CDM), Brain Heart Infusion (BHI) (BBL, FisherSci) or Mueller-Hinton (MH) supplemented with 0.1% cysteine at 37°C in 5% CO_2 [190]. CLC enhancement was achieved with subsequent passing in CDM broth for 10 passages then 5 days on CDM agar at 32°C in 5% CO_2, as previously described [192]. Recombinant strains were

grown in CDM with 15 μg/ml kanamycin (Kan). All experiments with LVS and mutants were carried out in biosafety level (BSL)-2 facilities in an approved biosafety cabinet

Table 5.1: Strains used in this study with description.

Strain	LPS/O-Ag	O-Ag capsule	CLC	Attenuated	Source/Reference
LVS	+	+	+	N	[67]
LVS_P10	+	+	+++	N	[192]
LVSΔ1423-22	+	+	-	Y	[192]
WbtI$_{G191V}$	-	-	+	Y	[94]
WbtI$_{G191V}$_P10	-	-	+++	Y	[192]
WbtI$_{G191V}$Δ1423-22	-	-	-	Y	[192]

(+: present, +++:enhanced, -: not present)

5.2.2 Attachment assay

Triplicate cultures of all strains were grown shaking (180 rpm) overnight at 37°C to stationary phase. Cultures were transferred (200 μl) to 96-well polystyrene plates and allowed to adhere for 1, 2 or 4 hours statically at 37°C. Media was removed and crystal violet staining was performed as described above. Statistical analyses were performed on triplicate samples and significant differences noted.

5.2.3 Static biofilm formation.

Overnight cultures of *F. tularensis* strains were grown at 37°C. Stationary phase bacteria were diluted 1:4 in either CDM or Mueller-Hinton (MH) broth and 200 μl were plated in triplicate into a 96-well polystyrene microtiter plate (Nunc, Rochester, NY). The samples were incubated for 5, 10, 15, 20 or 25 days at 37°C, with fresh media replacing old every 5 days. Biofilms were visualized with crystal violet (CV) staining. Media and non-adhered cells were carefully removed by pipeting and 100 μl of 0.1% CV was added to each well. After 15 minutes, the wells

were carefully washed three times with sterile distilled water. The attached biofilm was quantitated by solubilizing the CV with 95% ethanol, and the absorbance at 560 nm was determined. For plates with sample absorbance readings greater than 4.0, a dilution was made as indicated (1:3-1:10) of all samples on plate and absorbances reported as such.

5.2.4 CLSM and image analysis

Biofilms were statically grown for 5, 10 or 15 days in 8-well chambered glass coverslips coated with poly-L-lysine (Lab-Tek II/Thermo Scientific, Waltham, MA). Media and non-adherent cells were replaced with fresh media every 5 days. At each time point, media was removed from the well, the coverslip was washed with sterile saline twice, and 40 μM/ml Syto9 in sterile saline from the BacLight stain (Molecular Probes, Inc., Eugene, OR) or 50 μg/ml FITC-labeled ConA in saline was added. After 15 min of incubation at room temperature in the dark, the coverslip wells were washed in saline and visualized with confocal laser scanning microscopy (CLSM). CLSM was performed by using a ZEISS LSM 510 laser-scanning microscope, mounted on an inverted Axio Observer Z1 (Carl Zeiss, Jena, Germany). LSM image browser software was used for analysis of the biofilm images, including collection of z-stacks, three-dimensional reconstruction and data analysis. Images were acquired from the center of the coverslip at 1.1-μm sections through the biofilm and number of sections varied depending on thickness of biofilm.

5.2.5 Exopolysaccharide analysis

Glycosyl composition analysis was performed by combined gas chromatography/mass spectrometry (GC/MS) of the per-*O*-trimethylsilyl (TMS) derivatives of the monosaccharide methyl glycosides produced from the sample by acidic methanolysis. Three hundred micrograms

of sample was taken and added to a test tube with 20 μg of Inositol as internal standard. Methyl glycosides were then prepared from the dry sample following the mild acid treatment by methanolysis in 1 M HCl in methanol at 80 °C (16 hours), followed by re-*N*-acetylation with pyridine and acetic anhydride in methanol (for detection of amino sugars). The sample was then per-*O*-trimethylsilylated by treatment with Tri-Sil (Pierce) at 80 °C (0.5 hours). These procedures were carried out as previously described in Merkle and Poppe [254]. GC/MS analysis of the TMS methyl glycosides was performed on an Agilent 7890A GC interfaced to a 5975C MSD, using Agilent DB-1 fused silica capillary column (30m × 0.25 mm ID).

5.2.6 Enzymatic detachment assays

Biofilms were grown in CDMB for 10 days in 96-well plates as described above. Wells were washed once with PBS (pH 7.2) and biofilm disruption by Proteinase K (100 μg/ml, 10 mM Tris-HCl pH 7.5) (Sigma-Aldrich), sodium m-periodate (40 mM in dH_2O) or DNase I (100 μg/ml in 150 mM NaCl/1 mM $CaCl_2$) (Sigma-Aldrich) was assayed. Enzymes were added to designated wells at a concentration of 50 μg/ml in 200 μl of PBS (pH 7.2) and incubated at room temperature for 2 hours. Enzyme solutions were removed and wells were washed once with PBS and then stained with crystal violet as described above. All bacterial strains and conditions were performed in at least triplicate unless otherwise stated.

5.2.7 CLC/HMW carbohydrate isolation

F. tularensis strains were grown shaking at 37°C overnight in either CDMB or MH and 500 μl was used to inoculate 10 ml of broth in 50 ml conical tubes (Corning). Tubes were held stationary at 37°C for 10 days. Each tube was separated into 3 parts: biofilm (attached cells), planktonic (non-adherent cells that were centrifuged from media) and broth (supernatant media

with cells removed). Surface components of the biofilm and planktonic cells were extracted with 1M urea. Briefly, cells were resuspended in 1-5 ml of 1M urea and allowed to rest at room temperature for 15 minutes. Cells were removed with centrifugation (6,000xg for 15 minutes) and extractions were stored at -20°C until needed. The surface components that may have been shed into the media or secreted from the bacteria were isolated by ethanol precipitation from the cell-free media supernatant and precipitate was resuspended in 1-5 ml distilled water. Samples were visualized on 4-12% NuPAGE gels (Invitrogen), run according to manufacturers instructions, and gels were stained for proteins with silver stain (Pierce, Rockford, IL), for carbohydrates with Pro-Q Emerald 300 (Molecular Probes, Grand Island, NY) or for CLC/HMW carbohydrate with StainsAll/silver stain (Pierce, Rockford, IL/SigmaAldrich, St. Louis, MO) [192].

5.2.8 Electron microscopy

For scanning electron microscopy (SEM), strains were grown as biofilm on 10 mm diameter silicone disks in CDM broth for 5 days, statically at 32°C. After removal of media, biofilms were fixed in 2% glutaraldehyde, followed by 1% osmium tetraoxide for 30 minutes each. Samples were dehydrated in a sequential series of ethanol solutions (increasing from 10%-100%). Disks were critical point dried, sputter-coated with carbon and visualized in a Zeiss EVO40 scanning electron microscope.

5.2.9 Statistical analysis

Statistical analyses were performed using Microsoft Excel software (Redmond, WA) and GraphPad Prism software (San Diego, CA). Data was compared using student t-test and

expressed as the mean ± standard deviation. Results with a p value of less than 0.05 was considered statistically significant unless otherwise stated.

5.3 Results

5.3.1 Biofilm development

Most previous studies of biofilm formation by *F. novicida* and *F. tularensis* strains have allowed the biofilm to grow for seven days or less [226,230,231]. We have found that *F. tularensis* needs at least 10 days growth to differentiate biofilm development between parent (LVS) and surface structure mutants in O-Ag or CLC mutants ($WbtI_{G191V}$, LVSΔ1423-22 and $WbtI_{G191V}$Δ1423-22). Static attachment of *F. tularensis* LVS occurs after 2 hours (Figure 5.1), microcolony and some multi-layering of cells occurs at 5 days (Figure 5.2), yet the ability to differentiate between parent and surface antigen mutants is not evident until day 7-10. A mature biofilm appears to develop by ~15 days post-incubation and the differences between the parent and $WbtI_{G191V}$, LVSΔ1423-22 and $WbtI_{G191V}$Δ1423-22 are fully evident. After 15 days incubation dispersal occurs and at ~20 days the biofilm cycle begins again and reattachment of cells and biofilm formation reoccurs (Figure 5.4). This elongated biofilm cycle was able to occur only by changing the media every 5 days with fresh media.

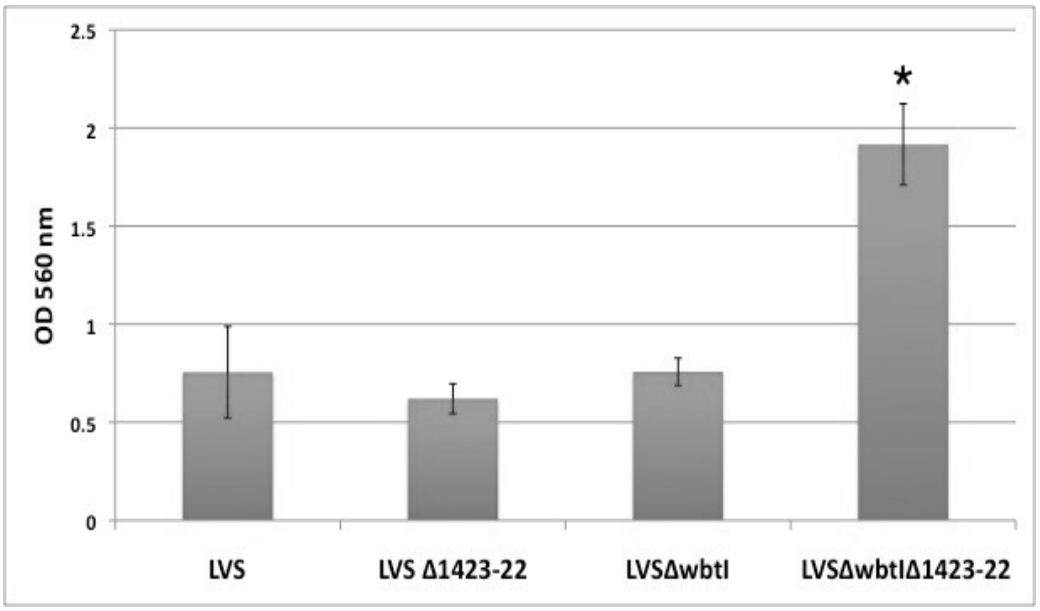

Figure 5.1: Crystal violet attachment assay of LVS and surface antigen mutants.
Cells grown to stationary phase were inoculated into 96-well plates in triplicate, incubated for 1 hour at 37°C, washed and stained with CV. Absorbance read at 560nm after solubilization of CV with 95% ethanol * = *p* value <0.005

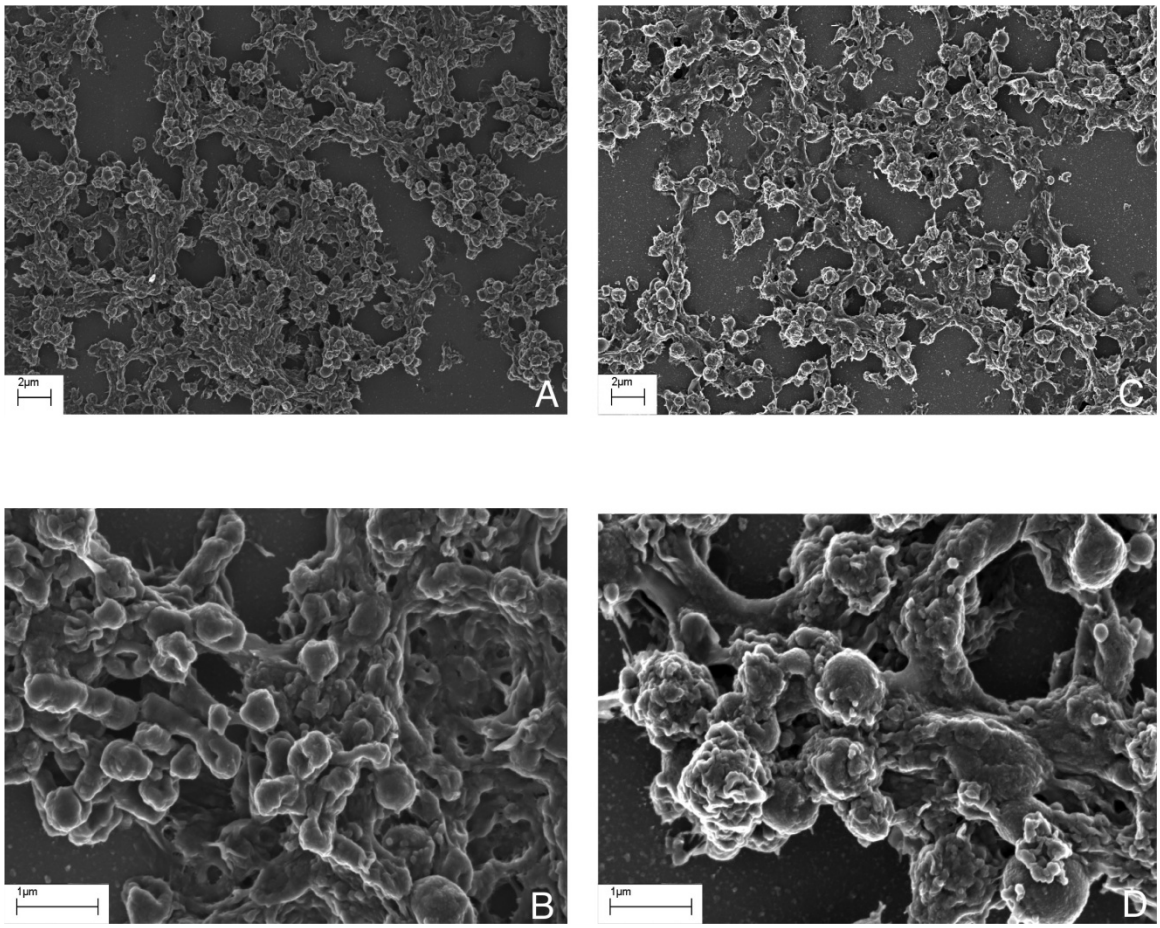

Figure 5.2 TEM of LVS and LVSΔ1423-22 biofilm after 5 days incubation. A-B. LVS, C-D. LVSΔ1423-22

Biofilms were grown on silicone disks and carbon-coated before visualization. After 5 days growth, no difference was seen in overall attachment or formation. At an increased magnification the surface of LVSΔ1423-22 appeared more granular than the parent, which could be the result of CLC deficiency.

5.3.2 Effects of bacterial surface components on biofilm development

Attachment of LVS to the polyvinyl surface of a 96-well plate was not significantly increased or inhibited by the loss of only one surface antigen. Incubation time for attachment to occur was also not a significant factor for any strains as bacteria incubated for 1, 2 or 4 hours showed no difference in attachment. $WbtI_{G191V}$Δ1423-22 attached significantly better ($p = 0.0101$) (~2-fold)

compared to the parent strain and to the strains deficient in only O-Ag (p = 0.0025) or CLC (p = 0.0019) (Figure 5.1).

All strains with deletions in FTL_1423-22 polysaccharide locus formed 2-15-fold more biofilm than their respective parent strain by day 15 (Figure 5.4). The amount of biofilm formed by CLC-enhanced strain LVS_P10 was 46% less than that of the parent LVS strain (Table 5.2). $WbtI_{G191V}$ also developed 2 to 4-fold more biofilm than the parent after 15 days of growth. $WbtI_{G191V}\Delta$1423-22, deficient in LPS/O-Ag, O-Ag capsule and CLC, formed 15-fold more biofilm than the LVS parent during a 96-well static incubation assay. All results using the crystal violet biofilm assay were calculated and compared to the parent strain and blank control in the same 96-well plate to eliminate technical bias. Furthermore, these differences in biofilm formation were also evident using CLSM. Figure 5.3 shows the formation of biofilm by LVS and the surface antigen mutants after 15 days of development when the differences between strains were fully evident. LVS and LVS_P10 developed more sparse microcolonies, whereas the surface antigen mutants, particularly $WbtI_{G191V}\Delta$1423-22, developed more confluent, thicker biofilms.

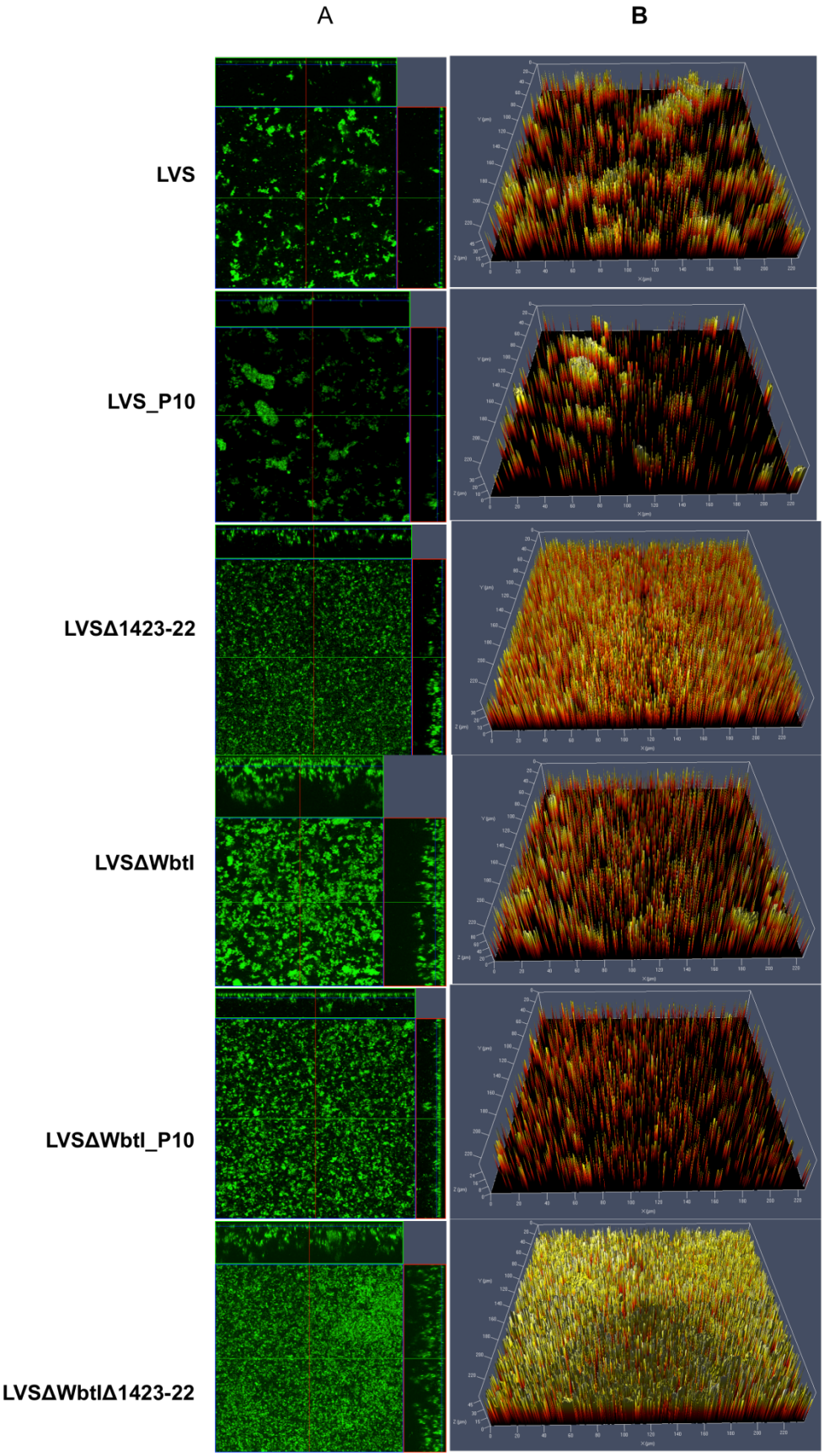
A
B
LVS
LVS_P10
LVSΔ1423-22
LVSΔWbtI
LVSΔWbtI_P10
LVSΔWbtIΔ1423-22

Figure 5.3 Comparison of biofilm formation by *F. tularensis* LVS and O-Ag and CLC mutants.

Panel A contains orthogonal sections showing horizontal (z) and side views (x and y) of reconstructed three-dimensional biofilm images at a magnification of 25x. Biofilms were stained with Syto9 showing both live and dead bacterial cells. Panel B shows topographical images of biofilm growth of the parent LVS and surface structure mutants.

5.3.3 Effects of growth media on biofilm development.

Growth curves of *F. tularensis* strains grown in CDMB and MHB indicated neither medium affected growth between parent and mutant strains (data not shown). Overall, biofilm development was enhanced when the bacteria were grown in CDMB compared to MHB for all strains by day 15 (Figure 5.4). However, the degree of enhancement was markedly increased for strains lacking both O-Ag and CLC, particularly after day 15 of biofilm maturity. Furthermore, biofilm formation was increased 15.3-fold in CDMB and 5.5-fold in MHB when compared with the parent strain (Table 5.2). LVSΔWbtI was deficient in biofilm when compared to the parent after 10 days incubation in MHB, but by day 15, the O-Ag mutant had developed a 45-fold more robust biofilm. However, this large increase in biofilm was somewhat misleading because when the amount of biofilm in CDMB was clearly greater than the amount of biofilm when the same strains were grown in MHB (Table 5.3). By day 15, the mutant lacking O-Ag and CLC developed 81-fold more biofilm in CDMB than in MHB, while the mutant lacking only O-Ag developed just 1.47-fold more biofilm in CDMB than MHB. This difference strongly indicates a correlation between missing the bacterial surface components, O-Ag and CLC, and growth medium to biofilm development.

Table 5.2 Fold-difference of biofilm development in CDM or MH compared to LVS

	Day 10		Day 15	
	CDM	**MH**	**CDM**	**MH**
LVS	1	1	1	1
LVS P10	1.5 ±0.20	-2.5 ±0.01	-1.8 ±0.4	1.3 ±0.75
LVSΔ1423-22	2.1 ±0.16	-2.5 ±0.01	1.8 ±0.1	1.56 ±0.91
$WbtI_{G191V}$	4.6 ±0.17*	-2.7 ±0.01	2.3 ±0.1	45.2 ±0.138*
$WbtI_{G191V}$Δ1423-23	4.9 ±0.10*	1.2 ±0.1	15.3 ±0.5*	5.5 ±0.34*

* indicates $p < 0.01$

Table 5.3 Fold-difference in biofilm development of CDM compared to MH

	Day 10	**Day 15**
LVS	-1.2 ±.08	29.2 ±0.36*
LVS P10	2.7 ±0.4	12.4 ±0.58*
LVSΔ1423-22	3.9 ±0.4*	35.5 ±0.69*
$WbtI_{G191V}$	9.7 ±0.4*	1.47 ±0.56
$WbtI_{G191V}$Δ1423-23	3.3 ±0.8*	81.0±0.15*

* indicates $p < 0.01$

A.

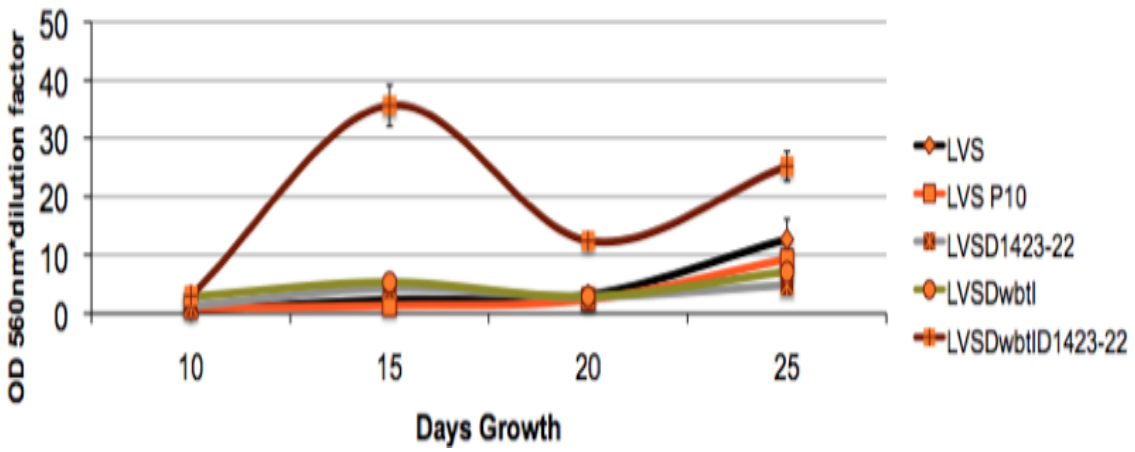

B.

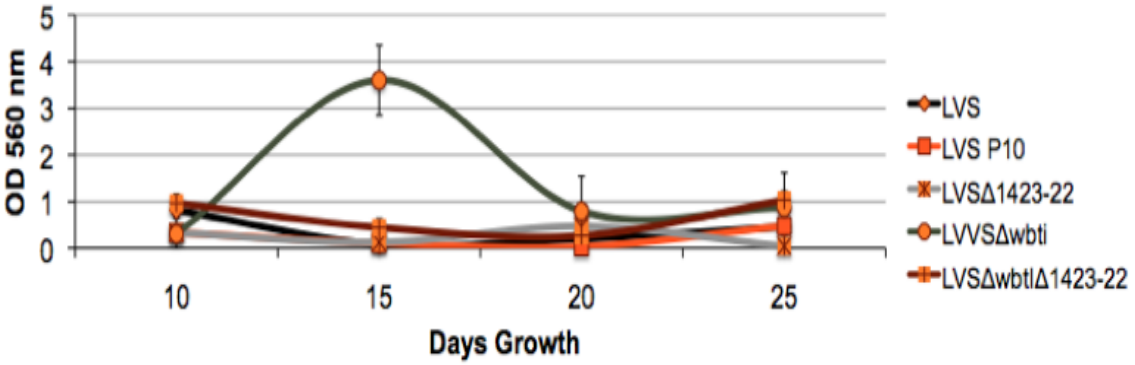

Figure 5.4 Static 96-well plate biofilm development.
A. Chamberlains defined media (CDMB), **B.** Mueller-Hinton broth (MH). A marked increase in biofilm formation by $WbtI_{G191V}$Δ1423-22 occurred in CDMB medium that was not seen in MH.

5.3.4 Surface extraction of CLC from biofilm cells

In order to elucidate the role of the CLC in biofilm formation, we attempted to extract CLC from biofilm cultures. LVS and LVS_P10 cells that were attached to the plastic surface as biofilms both produced CLC, as determined by the presence of high molecular weight (HMW) bands/smear (Figure 5.5). These HMW bands were not seen in extracts from LVSΔ1423-22, $WbtI_{G191V}$, or $WbtI_{G191V}$Δ1423-22 attached cells. As expected, no HMW band/smears were present in any of the strains that were non-adherent or were planktonic cells (Figure 5.5). A

decrease in silver stained bands was seen in the O-Ag and O-Ag/CLC planktonic cells compared to the LVS parent, suggesting that O-Ag and O-Ag/CLC deficient strains make more biofilm and that there are fewer unattached, planktonic cells. CLC did not appear to be secreted/released into the broth supernatant during biofilm development when the bacteria were grown in CDMB.

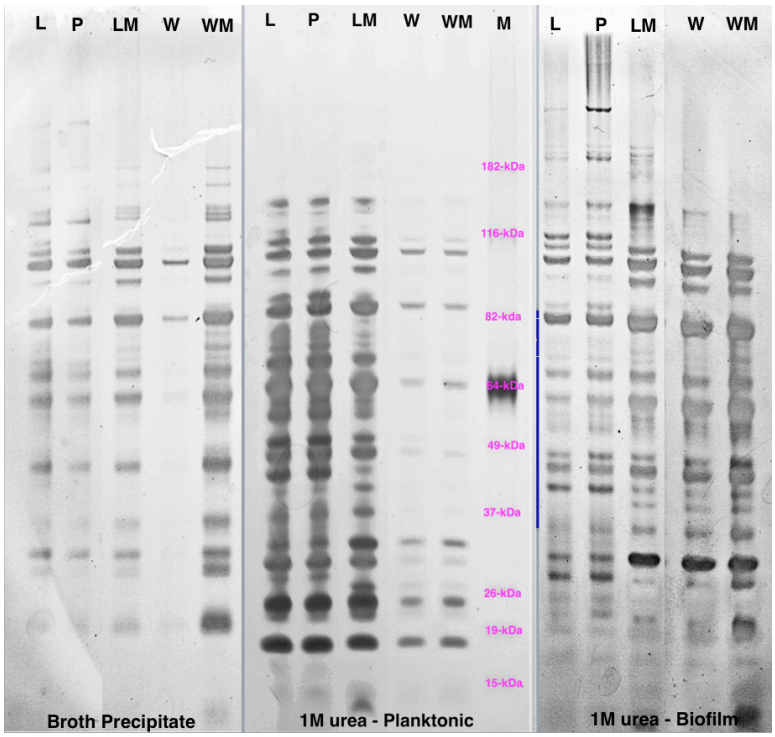

Figure 5.5 Surface and broth extractions of LVS strains grown as biofilms. Bacteria were grown in CDMB for 25 days and samples analyzed by SDS-PAGE on 4-12% gels, stained with silver. L: LVS, P: LVS_P10, LM: LVSΔ1423-22, W: $WbtI_{G191V}$, WM: $WbtI_{G191V}$Δ1423-22, M: Ladder

5.3.5 Composition of the extracellular matrix

Exopolysaccharide (EPS) was extracted from $WbtI_{G191V}$Δ1423-22, which made the most robust biofilm, using phenol. Extracted EPS could be visualized by Pro-Q Emerald 300 fluorescent carbohydrate stain and included HMW bands (>200-kDa) (Figure 5.6). Initially it was determined that the extracted polysaccharide reacted in an assay for amino sugars, and Cywes-

Bentley *et al.* have proposed that *F. tularensis* makes poly-N-acetyl glucosamine [331]. Upon carbohydrate composition analysis it was found that the purified EPS was 99.9 Mole% glucose and 0.1 Mole% mannose. The absence of PNAG was confirmed by lack of reactivity by immunoblotting and fluorescence microscopy with wheat germ agglutinin (lectin to PNAG) (data not shown). Concanavalin A (ConA) conjugated to fluorescein (Sigma), binds to α-D-mannosyl and α-D-glucosyl groups and reacted strongly with the *F. tularensis* biofilm by fluorescence microscopy. Figure 5.7C shows a CLSM full side view of LVS, $WbtI_{G191V}$, and $WbtI_{G191V}$Δ1423-22. An increase in EPS/matrix (red) is evident in both mutants. CLSM, in conjunction with ConA, to visualize the matrix was difficult due to the thickness of the matrix. The laser beam was not strong enough to get full images of the biofilm thickness, and in addition, some biofilm broke off from the coverslip which also made imaging more difficult. This breaking off of biofilm structures is shown in Figure 5.7 panel B LVSΔ1423 where the 2-D overview of the z-stack three-dimensional image is blocked by a ConA staining mass. This occurred sporadically and is not representative of the full slide.

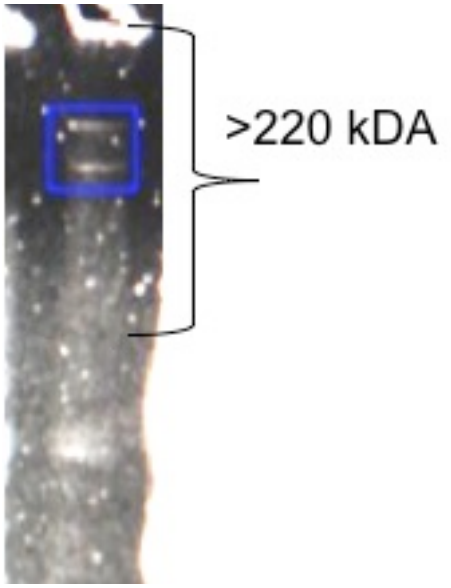

Figure 5.6 Fluorescent carbohydrate stain of EPS extracted from $WbtI_{G191V}$Δ1423-22. HMW carbohydrate was not evident in LVS_P10, lower molecular weight bands did stain in all strains.

Enzymatic detachment of biofilm using sodium *m*-periodate showed that only $WbtI_{G191V}$ ($p = 0.0246$) and $WbtI_{G191V}\Delta 1423\text{-}22$ ($p = 0.0055$) had a significant in biofilm remaining after treatment when compared to treatment with PBS (Figure 5.8). Detachment with m-periodate, which oxidizes polysaccharides, indicates these strains may produce more EPS in their biofilms compared with the parent strain. The $WbtI_{G191V}$ biofilm was significantly diminished in biofilm after treatment with DNase ($p = 0.019$) and was the only strain affected as such. $WbtI_{G191V}\Delta 1423\text{-}22$ was the only strain whose biofilm was significantly decreased after treatment with Proteinase K ($p = 0.0162$). These differences indicate that changes in the surface antigen structures on *Francisella* impact the composition of the matrix in addition to the amount of biofilm produced.

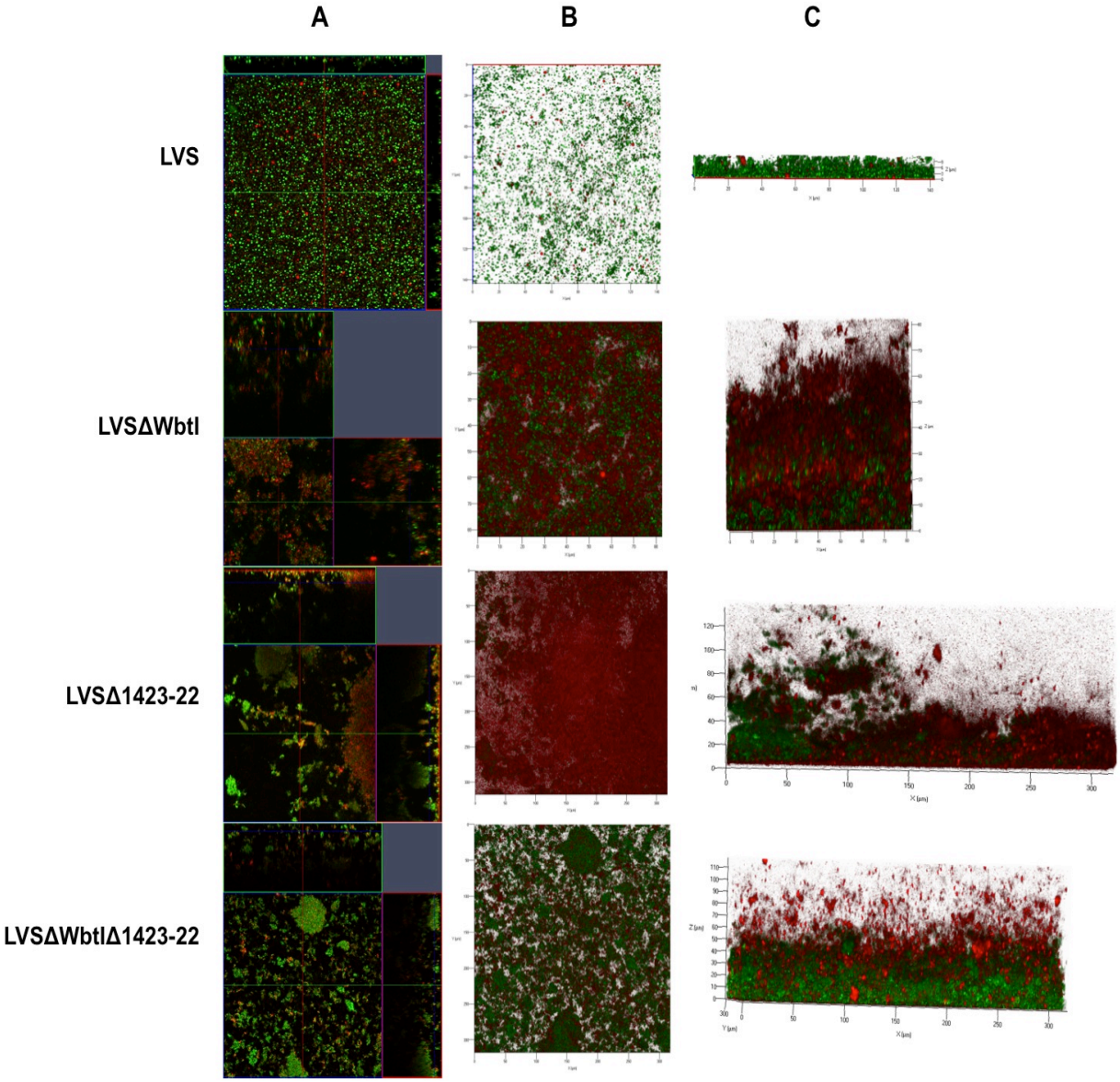

Figure 5.7 Comparison of the biofilm matrix development of *F. tularensis* LVS and its surface structure mutants.

Panel A shows orthogonal sections of horizontal (z) and side views (x and y) of reconstructed three-dimensional biofilm images at a magnification of 25x. Bacterial cells are stained with Syto9 (green) and the matrix EPS is stained with fluorescently tagged ConA-Texas Red (red). Panel B is an overview (x and y) view of the reconstructed three-dimensional z-stack of each biofilm growth on the coverslip. Panel C is the side view of the three-dimensional z-stack. Each picture was obtained from biofilm grown for 15 days.

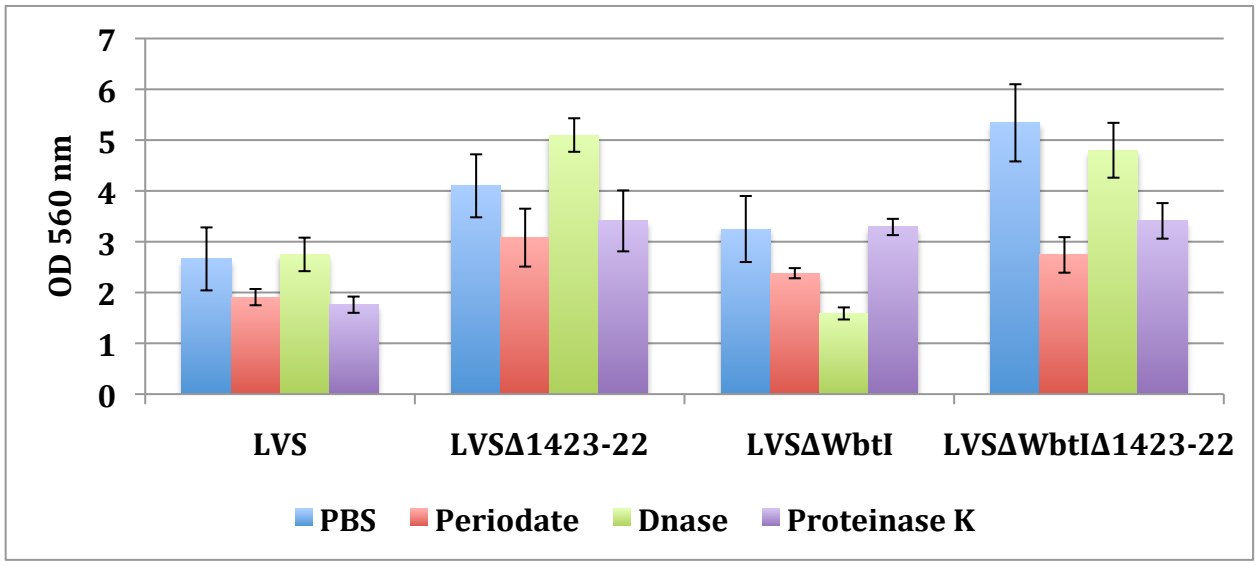

Figure 5.8 Enzymatic detachment assay of LVS biofilms.
Ten day old biofilms were treated with sodium m-periodate, DNase, Proteinase K, or PBS for two hours at 37°C, washed with distilled water and left to dry overnight before crystal violet staining. Only $WbtI_{G191V}$ and $WbtI_{G191V}$Δ1423-22 were significantly different in biofilm remaining after periodate treatment when compared to the untreated biofilm. This indicates these strains may produce more EPS in their biofilms compared with the LVS parent strain. $WbtI_{G191V}$ biofilm was significantly diminished in biofilm after treatment with DNase and was the only strain to do so. $WbtI_{G191V}$Δ1423-22 biofilm had the only significant difference in biofilm after treatment with Proteinase K.

5.3.6 Biofilm by Type A *F. tularensis*

Overall, type A strains developed less crystal violet stainable biofilm than the type B strains. In addition, by 15-days incubation, the bacteria seemed to have detached and new/continued growth of biofilm was not detected even with addition of fresh media. This could indicate that type A strains have a shorter biofilm cycle than type B. The type A strain, TIGB03, is deficient in O-Ag and like its type B counterpart, develops more biofilm than parent strain TI0902 (Figure 5.9). This occurred in both MHB and CDMB media by day 5. However, this was only seen when bacteria were grown in MHB by day 10. When biofilms were formed in CDMB, more biofilm developed, but by day 10, there was no significant difference between strains ($p = 0.78$). After 5 days growth in CDMB, TIGB03 ($p = 0.0321$) and SCHUS4ΔDsbA ($p = 0.0015$) produced

significantly more biofilm (~2-fold and ~3-fold, respectively) than their parent strains, TI0902 and SCHUS4. A CLC-deficient mutant of type A was not available at the time of this study, but SCHUS4ΔDsbA is a mutant in a gene affected by the CLC glycosylation locus, FTT_0789-FTT_0800 [204].

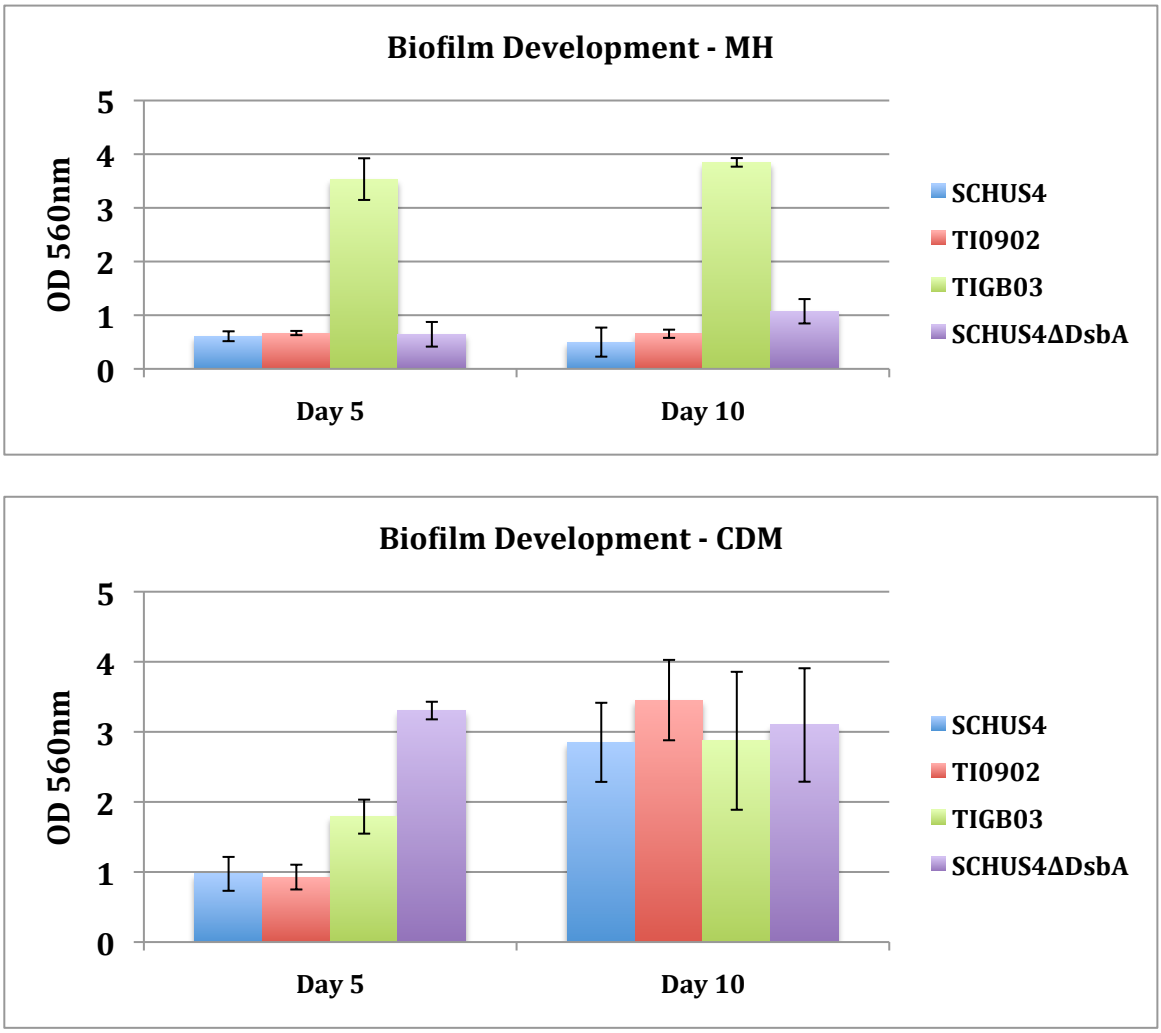

Figure 5.9 Static biofilm development by *F. tularensis* type A strains in MH or CDM. Differences between surface antigen mutants and their parents were not significant ($p = 0.78$) by day 10 in CDM. However, after 5 days incubation there was an increase in biofilm development by TIGB03 ($p = 0.0321$) and SCHUS4ΔDsbA ($p = 0.0015$)in CDM. Biofilm development in MH showed a significant increase in only the O-Ag mutant TIGB03 compared to the parent strain. Significance determine by unpaired *t* test.

5.3.7 *F. novicida* biofilm

The distinct differences in biofilm development observed between type A and B strains and their surface antigen mutants grown in CDMB versus MHB was not seen with *F. novicida* and the CLC deficient mutant F.n.Δ1412-12. The *F. novicida* double transferase mutant, which is deficient in CLC, did not produce more biofilm than the parent in either medium (Figure 5.10). However, there was a significant difference between biofilm development when cells were grown in MHB compared to CDMB ($p = 0.0050$) ~2-fold greater biofilm in CDMB). An O-Ag mutant was not available at the time of this work. The HMW/CLC band was present only in the planktonic *F. novicida* cells when grown in CDMB, but could be found secreted into the broth in MH and on the planktonic cells (Figure 5.11). The extraction of *F. novicida* biofilm cells with 1M urea yielded far fewer proteins than was seen in the type B extractions. *F. novicida* also attached more uniformly to the glass coverslip than type A or B strains, and increased CLC production (*F. novicida*_P10) negatively effected biofilm formation (Figure 5.12).

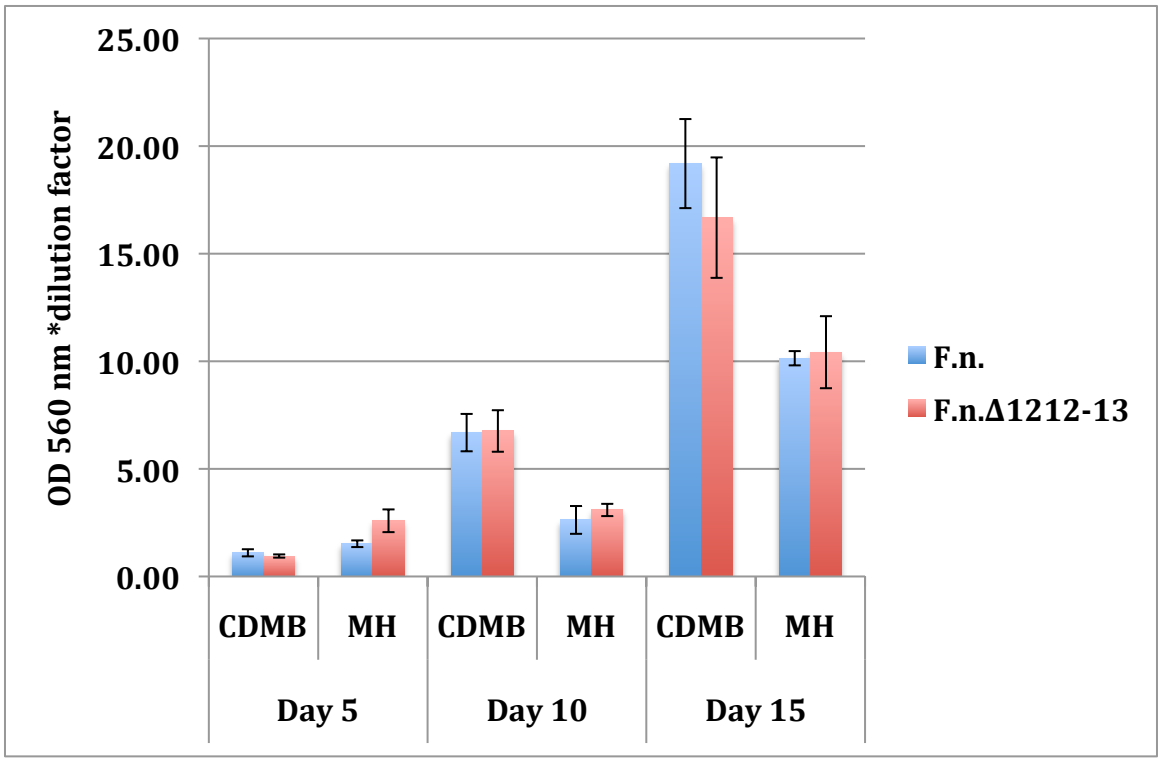

Figure 5.10 Comparison of biofilm development of *F. novicida* and CLC-deficient mutant in CDMB and MHB.

No significant differences were seen between parent and mutant biofilm development in either media. Like type B strains, biofilm development peaked at ~15 days.

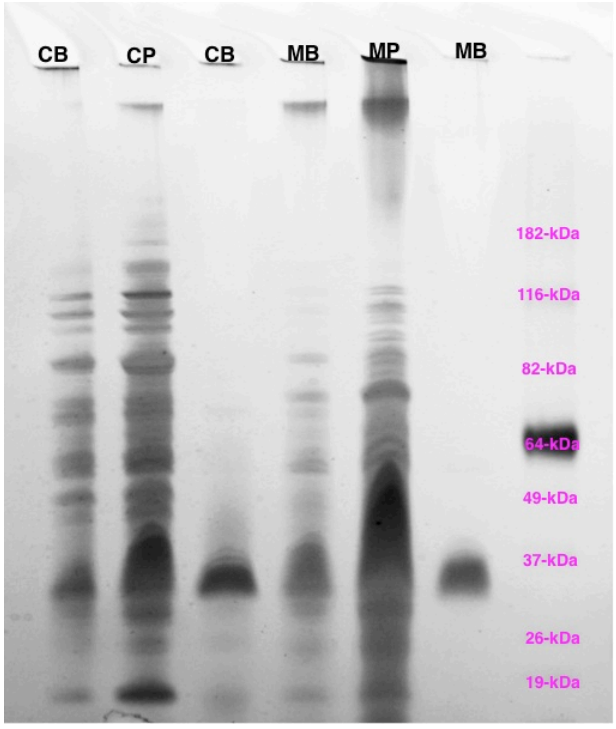

Figure 5.11 Surface and broth extractions of *F. novicida* biofilm.
F. novicida biofilms were grown for 25 days before extraction. The HMW/CLC band was present only in the planktonic *F. novicida* cells when grown in CDM, but could be found secreted into the broth in MH and on the planktonic cells. The extraction of *F. novicida* biofilm cells yielded far fewer proteins than was seen in the type B extractions. CB: CDM broth precipitate (ppt), CP: CDM planktonic, CB: CDM biofilm, MB: MH broth ppt, MP: MH planktonic, MB: MH biofilm

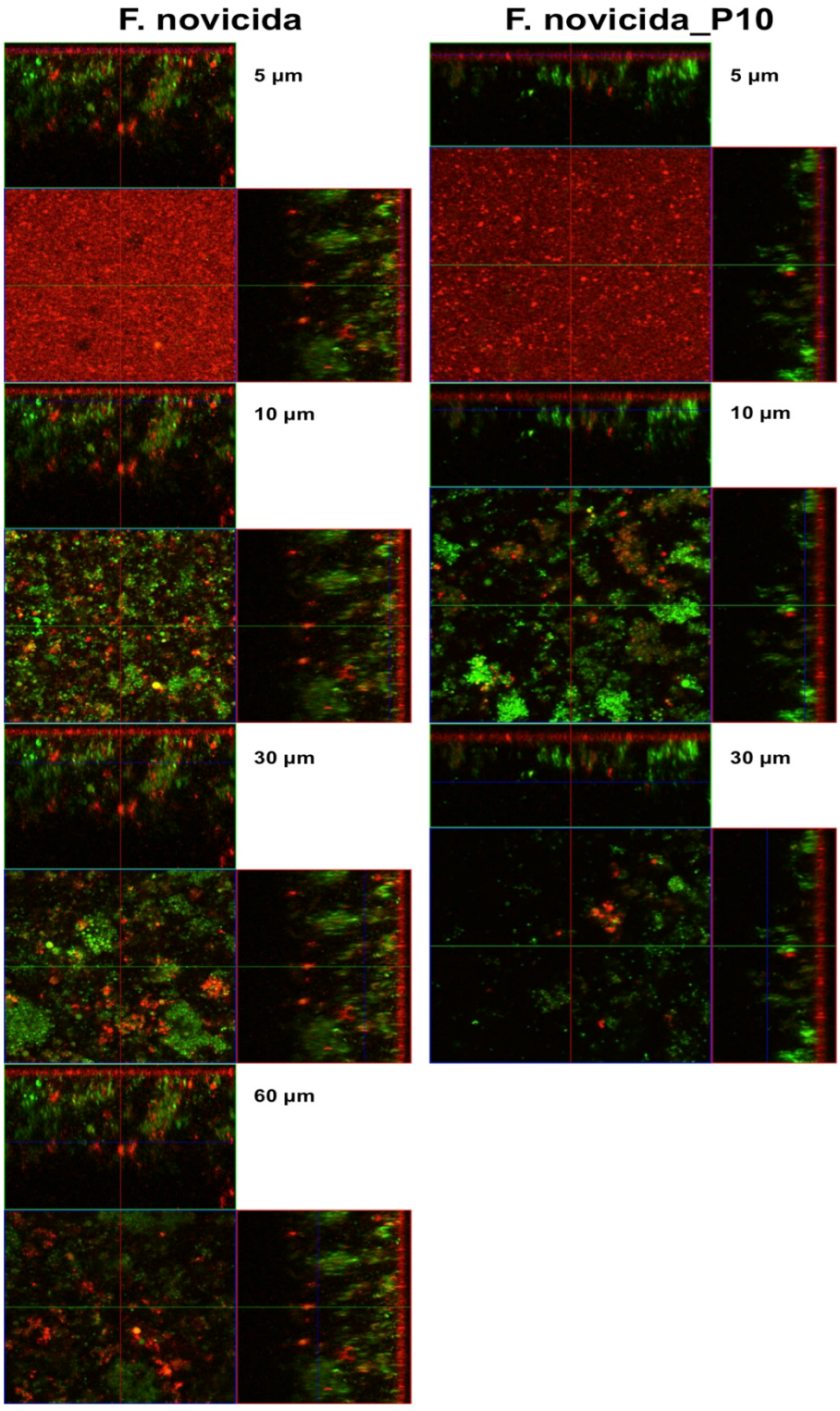

Figure 5.12 Comparison of *F. novicida* and the CLC-enhanced *F. novicida*_P10 in CDM. Passage of *F. novicida* to increase CLC production resulted in a les robust biofilm formation by day 10. Initial attachment did not appear to be affected. Large, dense aggregates of cells were evident by day 10.

5.4 Discussion

The ability of *Francisella* species to form biofilms has been confirmed in subspecies *tularensis*, *holarctica,* and *novicida*, yet the question remains as to the role of biofilm in *F. tularensis* pathogenesis or survival in the environment or hosts. *Francisella* is a unique intracellular pathogen with an extremely low infectious dose and there are a few considerations for what role biofilm has in pathogenesis. The hypothesis that biofilm plays a role in environmental survival of *Francisella* is the most documented [223,225,228]. *F. tularensis* can survive in a wide range of environmental conditions, from hot, dry and arid, to cold waterways, and even intracellularly in amoebae, thus protection from their surroundings is necessary [111,112,228]. The shorter biofilm cycle and overall less biofilm formed by type A strains compared to type B strains could be an indicator of the differing environmental niches that these two biotypes inhabit. Type A strains are found mostly in dry, arid environments while type B strains are commonly found in waterways, particularly in Europe, but also in the U.S. [20,36,332]. Attachment and structural stability of type B biofilms may need to be more robust than type A in order to survive the shear force of flowing water and the natural predation that occurs in waterways from amoebae species and vectors, such as, mosquito larvae [4,111,112]. However, it should be noted that mosquito larvae are still able to feed on LVS when in a biofilm [229]. Formation of biofilm by *F. novicida* has been hypothesized to aid in survival when inside of arthropod vectors [223]. *Y. pestis* survives inside the flea gut in biofilm form, and recently it has been demonstrated that *F. novicida* will form biofilms on chitin surfaces [231,333]. Chitin is found in many arthropod vector exoskeletons, and we have found that *F. tularensis* type A and B strains will form biofilms (data not shown), albeit not as robust, at room temperature (~22°C), which is similar to the internal temperature of a tick [231,334].

Another question that remains is the role of *Francisella* biofilm during infection in a mammalian host. Our studies show that O-Ag deficient strains of *F. tularensis* type A and B develop a more robust biofilm than their respective parent strains. Mutants in the O-Ag locus (*wbt*) develop 2-5-fold more robust biofilms than their more virulent parent strains, yet are highly attenuated in both type A and B strains [88,94,335]. This could indicate that biofilm does not play a role in host virulence. Previous studies in *Francisella* have found that surface properties may be linked to adhesion and invasion of host cells [113,218,223,336]. Studies in *F. novicida* demonstrated increased bacterial adhesion of macrophages by *chi* mutants with enhanced biofilm formation, and that the EPS may play a role in bacterial invasion of the host [223]. Enhancement of biofilm in attenuated strains seems to negatively correlate host cell invasion with biofilm formation. O-antigen and CLC LVS mutants are highly attenuated in the mouse model, but enhanced in biofilm formation. Therefore, the increase in biofilm formation observed under host-adapted growth conditions indicates that biofilm is most likely not involved in host virulence [94,192], which correlates with the hypothesis that biofilm is used by *Francisella* species as a way to survive in the environment rather than as a virulence mechanism in the host.

Researchers have shown in other bacteria that a change in bacterial surface properties, many times, includes a change in cell surface charge and altered cell surface hydrophobicity [337,338]. Particulary, changes in cell hydrophobicity have been found in many bacteria when alterations occur in the LPS or O-Ag [337]. In *E. coli*, *hld* mutants (rough LPS) demonstrated an increase in biofilm formation and expression of several surface bacterial factors effecting virulence [339]. Altered cell surface charge has also been shown in *Pseudomonas* and *Bradyrhizobium* when the

bacteria lack O-polysaccharide [340,341]. *F. tularensis* has a unique O-Ag consisting of two proximal carbohydrate residues (α-D-GalNAcAN--α-D-GalNAcAN) and two distal residues (β-D-Qui4NFm and β-D-QuiNAc), while *F. novicida* O-Ag shares the same two proximal residues, but has different distal glycoses (α-D-GalNAcAN and β-DQui2NAc4NAc) [176]. The difference in O-Ag surface carbohydrates between the two species could explain the differences evident in biofilm formation between the parent strains of *F. novicida* and *F. tularensis*. While *F. novicida* formed a uniform film across the surface, *F. tularensis* attached in nonuniform clumps (Figure 5.7 and 5.12). Removal of the dideoxy O-Ag sugars in *F. tularensis* ($WbtI_{G191V}$) allowed for more uniform attachment across the surface, although the biofilm was still was not comparable to that of *F. novicida*. *F. tularensis* has the ability to phase vary from smooth (blue, O-Ag positive) to rough (grey, O-Ag negative) colony phenotypes and one hypothesis for this phenomenon could be to increase viability in the environmental niches by removing O-Ag and increasing biofilm capability [185].

When CLC is not upregulated *in F. tularensis*, LPS O-Ag and the O-Ag capsule are the two most surface exposed polysaccharides. When bacteria are passed in CDMB, the CLC is upregulated and therefore could be masking the O-Ag and its effects on surface hydrophobicity and biofilm development [190,192]. When CLC is upregulated there is a slight decrease in biofilm formation, which commonly occurs in encapsulated bacteria [342]. Interestingly, mutants deficient in CLC due to mutagenesis of two glycosyltransferases increased biofilm formation compared to the parent strain, but the biofilm was not as robust as the biofilm from the O-Ag deficient mutant. However, biofilm formation was increased 7-fold in *F. tularensis* mutants lacking both O-Ag and CLC (Figure 5.4). The CLC is composed of multiple glycoproteins, and

is negatively affected by deletion of two glycosyltransferases in a proposed O-linked protein glycosylation locus (FTT_0789-0800) [192,204]. Similar results have been shown in *Acinetobacter baumannii* lacking PglC, the initiating glycosyltransferases (iGT) in a glycan synthesis locus [343]. The proposed iGT of the *F. tularensis* CLC locus, FTT_0790, and the iGT of the O-Ag locus, *wbtB* are homologous to *pglC* in *A. baumannii* and could indicate *en bloc* glycan synthesis is involved in CLC O-glycosylation as well [344]. Deletion of the downstream glycosyltransferases (FTT_0798-99) that add the remaining sugars to the glycan, could impact CLC production and therefore allow for a more robust biofilm to develop.

Deletions in the only two polysaccharide loci, so far identified in *Francisella*, positively correlate with biofilm production, and that leads to the question of what is producing the exopolysaccharide (EPS) of the matrix. *F. tularensis* biofilm is susceptible to enzymes that degrade DNA, proteins, and polysaccharide and therefore likely have each of these components. Cywes-Bentley *et al.* have reported antibody to β-(1→6)-linked poly-N-acetyl-d-glucosamine (PNAG) reacts with *F. tularensis* [331]. However, our attempts to detect PNAG on the *F. tularensis* biofilm using a fluorescent-tagged wheat germ agglutinin lectin (WGA) (specific to PNAG) were unsuccessful. Extracts from *F. tularensis* biofilm as well as CLC were also incubated with fluorescein-tagged WGA, but no fluorescence was detected (data not shown). Phenol extraction of the EPS from the most robust biofilm-forming strain, $WbtI_{G191V}\Delta 1423\text{-}22$, and subsequent carbohydrate composition indicated the EPS consisted of 99.9% glucose, suggesting that the EPS was a form of common glucan. The *F. tularensis* gene FTT_1629c, annotated as a hypothetical gene, has 25.8% identity to the *Streptococcus pneumoniae tts* gene, which is solely responsible for producing the type 37 capsule which is comprised of (1→3)-B-

glucan. FTT_1629c also includes a DXD motif (glycose binding domain), which indicates it is likely a glycosyltransferase. Further investigation into the structure of this polysaccharide is ongoing. Future considerations could include examining the EPS of the parent LVS strain as well. It is reasonable to consider that there may be more than one EPS, and the predominant EPS of the $WbtI_{G191V}$Δ1423-22 mutant is different from the parent. One of the glycosyl transferases deleted in $WbtI_{G191V}$Δ1423-22, FTL_1423, has homology to the *Y. pestis hmr* gene, which is similar to *icaA*, an *N*-glycosyltransferase used for PNAG production [345].

Lack of O-Ag and CLC is not the only factor involved in the ability of *F. tularensis* to form a more robust biofilm. Growth conditions were a key contributing factor in whether or not the phenotypes described above were evident. Zarrella *et. al*. [193] demonstrated that *F. tularensis* undergoes host-adaptation that includes changes in multiple surface polysaccharides, and that these changes can be reproduced by growing *F. tularensis* in growth media. Zarrella *et. al*. demonstrated that *F. tularensis* grown in BHIB expresses the same surface polysaccharides as when growing in the host, whereas growth in MHB and CDMB does not. We have found that CDMB does indeed produce the HMW carbohydrate demonstrated by Zarrella *et. al*. in BHI-grown cells and considered to be part of the CLC by Bandara *et. al*. [192,193]. Biofilm formation was also affected when the bacteria were grown in CDMB (host-adapted) versus MHB (not host-adapted), and indicated an increase in biofilm formation occurs in all surface antigen mutants when grown in media that mimics the host. A significant increase in biofilm formation in $WbtI_{G191V}$Δ1423-22 occurred only when the bacteria were grown in BHIB and CDMB. The phenotype of the mutants that made a more robust biofilm did not increase in surface coverage as much as it increased in the formation of dense aggregates that adhered to the surface, as well as

floating pellicles. Overall less biofilm was present when the bacteria were grown in MH, and the differences observed in the CLC-deficient mutant when host-adapted, were not found in MH-grown $WbtI_{G191V}$Δ1423-22.

Unpublished data from our lab indicated that *F. novicida* also produces a CLC that is similar to the types A and B CLC. *F. novicida* strains that have been passed and enhanced for the CLC show a less robust biofilm phenotype than the parent (Figure 5.12), and deletion of the same two glycosyltransferases (FTL_1423-22) reduces CLC production. However, CLC-deficient mutants have the same biofilm phenotype as the parent *F. novicida*. Furthermore, the *F. novicida* CLC-mutant demonstrated no change in biofilm formation based on growth medium (MH, CDM, or BHI), but *F. novicida* and the CLC-mutant produced the most robust biofilms in CDM and BHI. Interestingly, an *F. novicida* mutant that cannot make the secreted protein ΔFTN-0714 was inhibited in attachment and static biofilm formation, yet remained virulent [231]. This putative lipoprotein has also been identified in OMV/T and has been visualized on SDS-PAGE gels of the CLC from *F. tularensis* and *F. novicida* [210]. Previous studies have allowed *F. tularensis* biofilms to develop for less than 12 hours before describing the amount of biofilm formed. We have found that this amount of time is inadequate for representative biofilm formation by *Francisella* species, perhaps due to the slow growth rate of this bacterium. There was no apparent increase in biofilm formation by *F. novicida* ΔFTN-0714 compared to the parent, yet visually an increase in bacterial aggregates and floating pellicles was evident. This dichotomy has also been observed in *A. baumannii*, and demonstrates the limited use of static 96-well assays for biofilms that do not adhere very well [343]. Therefore, while initial attachment may be attenuated, the ability of *F. novicida* to produce biofilm appears to be positively affected by

deletion of the lipoprotein encoded by FTN-0714, and in previous studies the biofilm may not have been given enough time to develop or was removed in the supernatant. FTN_0714 is conserved across *Francisella* species and, in *F. novicida*, correlates to the increase in biofilm formation we see with LVS strains that are CLC-deficient. If the CLC is, in part, upregulated OMV/T, then it may be hypothesized that since this lipoprotein is a component of OMV/T it is in the CLC as well. A deletion of this lipoprotein in type B and type A strains was not available during this study due to technical difficulties of producing a mutagenesis plasmid containing the large sized gene, but it may be worthwhile in future studies to see if the trend of increased biofilm formation continues with deletion of this OMV lipoprotein.

In conclusion, the surface antigens LPS, O-Ag capsule, and CLC affect the ability of *F. tularensis* to form biofilms *in vitro*. We have demonstrated that under specific growth conditions strains lacking one or all of these surface antigens, will form a more robust biofilm than the parent strain. For the first time, we have shown the extended biofilm development cycle *F. tularensis* type A and B strains. In addition, the biofilm formed by type A and B strains and mutants lacking surface polysaccharides or glycoproteins have been compared to the well-characterized biofilm of *F. novicida*.

5.5 Co-Authors' Contributions

I was assisted on confocal microscopy at Virginia Tech by Kristi DeCourcy. Mutants used were constructed by Abey Bandara (VT).

CHAPTER 6

FINAL CONCLUSIONS AND FUTURE DIRECTIONS

6.1 Conclusions

Francisella tularensis is a highly virulent, unique pathogen that has the ability to survive in a wide range of hosts and environmental niches both intracellulary and extracellulary. Multiple virulence factors and adaptations contribute to the potency of this pathogen, and due to the relatively small genome, it can be assumed gene expression is differentially regulated to allow the bacteria to adapt to various environmental conditions [126,193]. Adaptations to the surface of *Francisella* include LPS, O-Ag capsule, pili, OMV/T and, the particular focus of this dissertation, the novel capsule-like complex (CLC). The overall goals of this research were to identify and characterize the components of the CLC, elucidate the role of CLC in pathogenesis and determine the protective efficacy of the CLC to virulent *F. tularensis*.

6.1.1 Characterization of the CLC

I have visually shown that the CLC is present in type A and B strains of *F. tularensis* through TEM, and have proven that extraction of the CLC via chaotropic agent is possible in both biotypes. I determined through this work that growth conditions including: temperature, days grown, passage and media all influence expression of the CLC. Before the start of this work, *Francisella* was hypothesized to be encapsulated based on TEM images of a darker staining material surrounding the bacterial cell and a crude capsular extract by Hood et al. [1,132,190]. The capsule extract by Hood contained multiple sugars including: mannose, glucose and rhamnose in addition to proteins. Polysaccharide capsules are a common feature and virulence

factor of many bacterial species, and I first approached identifying the *Francisella* capsule as if it were composed of polysaccharide. This initially complicated the extraction process as the CLC material extracted via phenol was highly insoluble and did not react strongly in phenol-sulfuric acid assays for carbohydrates or standardized protein assays [289]. I was not able to visualize the CLC on SDS-PAGE gels stained with silver stain or fluorescent carbohydrate stain, and a high molecular weight smear was only faintly visible after Western blot using polyclonal antibody to whole cell *Francisella* LVS. These difficulties were later found to be due to the fact that the CLC was not a standard polysaccharide capsule and the upregulated material we were visualizing through TEM was a mixture of (glyco)proteins (Chapter 4). Extracts of the CLC material were found to contain less than 10% carbohydrate, and so came the term capsule-like complex (CLC). During the course of my graduate study, a fully polysaccharide capsule was identified on *F. tularensis* type A and B strains, and was determined to be composed of O-Ag sugars [92]. I was able to conclusively determine that the CLC and O-Ag capsule were two separate surface antigens by extracting CLC from O-Ag deficient mutants that did not produce the O-Ag capsule. Carbohydrate composition also differentiated the CLC from O-Ag, as the CLC was originally found to contain only glucose, galactose and mannose [192]. In addition, lack of O-Ag on *F. tularensis* results in bacteria that are highly sensitive to complement-mediated killing, yet strains deficient in CLC are still serum-resistant [94,192].

With the knowledge that the CLC was composed primarily of proteinaceous material, the extraction process was modified to eliminate denaturation of proteins (Chapter 3). This facilitated further characterization of the CLC material through amino acid composition, which aided in our understanding of the self-aggregating (high insolubility) tendencies of the CLC. A

high percentage of hydrophobic and acidic amino acids is common in self-assembling surface-layer proteins and led to the hypothesis that a CLC component may have S-layer-like properties, as the CLC amino acid composition contained ~60% acid and hydrophobic amino acids [278,286,294,295]. This unique amino acid composition would also explain the difficulty I had in visualizing this material using SDS-PAGE, and led to my discovery of the cationic stain StainsAll overlaid with silver stain as a way of visualizing this unique combination of (glyco)proteins in the CLC, and greatly facilitated the ease in working with this antigen [192].

Through amino acid sequencing of the CLC components we identified over 50 proteins in the extracted CLC (Chapter 4). More than 60% of these identified proteins have also been found in outer membrane vesicles and tubules (OMV/T) of *F. novicida* [210,211]. Several known virulence factor proteins were also identified in the CLC and OMV/T including: GroEL, DnaK, ClpB and Tul4 [82]. This led us to suggest that the CLC was in fact upregulated outer membrane vesicles and could play a role in the delivery of virulence factors, which is common for OMV [208,209].

6.1.2 Glycosylation and the CLC-deficient mutant

The ability of *Francisella* to upregulate a surface antigen/CLC production in response to growth conditions has been noted on multiple occasions [190,192]. This indicates that the CLC material is most likely regulated in some way in *F. tularensis*, yet the specific regulatory pathway has not yet been elucidated. I have however identified a genetic locus at least partially responsible for CLC production in *F. tularensis* [192]. This locus, FTT_0789-FTT_0800, was originally annotated as a potential second polysaccharide locus and is conserved in *F. tularensis* biotypes,

later discovered by Thomas *et. al.* to be responsible for glycosylation of the essential virulence factor, DsbA [105,204]. DsbA is glycosylated with an O-linked 1156-Da hexasaccharide that has been identified on several other proteins in *Francisella*, including on proteins identified as components in the CLC [207]. I have found that upon deleting two glycosyl transferases (FTT_0798-0799) in the locus, the CLC is greatly diminished via TEM and after extraction [192]. This indicates glycosylation of at least some of the CLC components is necessary for the negatively staining surface aggregates we visualize with TEM.

In addition to this known 1156-Da glycose, a 420-Da glycose repeating polymer was identified on high molecular weight bands of the CLC after SDS-PAGE (Chapter 3). Amino acid sequencing and identification of the protein components was unsuccessful, potentially due to the high level of glycosylation present in these bands. While there is no indication that the FTT_0789-FTT0800 locus can produce two distinct glycans, there is the possibility that the 420-Da glycan may be produced by a bifunctional glycosyltransferase in this locus that attaches the sugar directly to the protein, which would explain the reduced amount CLC antigen we can extract from *F. tularensis* containing mutations in the FTT0789-0800 locus.

6.1.3 OMV/T and CLC

Much evidence from protein composition and TEM led me to conclude the surface antigen CLC is partially composed of upregulated outer membrane vesicles and tubules (Chapter 4). The amount of circular- shaped versus tubular-shaped OMV/T was found to be regulated by growth conditions and mutations in the two CLC glycosyl transferases (FTL_1423-22). OMV/T purified from *F. tularensis* grown in broth contained almost exclusively small circular OMV.

OMV/T purified from plate-grown methods, similar to that of CLC extractions, had differential results between LVS and $WbtI_{G191V}$ strains that were deficient in CLC production. CLC-deficient LVS resulted in almost exclusively OMT, while O-Ag and O-Ag/CLC deficient mutants resulted in OMV. McCaig et al. found the OMT shape to be heat labile and inferred that a specific protein may be involved in forming the OMT shape [210]. If that hypothesis is accurate, my studies have shown that the OMT-shaping protein is missing or inactive after removal of O-Ag and the two glycosyl transferases. In addition to the shape differences, less OMV were found in O-Ag/CLC mutants than in the parent. Irregardless of OMV/T extraction method, an inter-vesicular material was distinctly missing from the CLC-deficient mutants. Hypothetically, this material could be the HMW material (>170-kDa) that is deficient in glycosyl transferase mutants, more investigation into this hypothesis is needed.

6.1.4 Role of CLC in Pathogenesis

Typically bacteria will not expend the metabolic energy to produce and regulate a complex antigen, such as CLC, unless said antigen is necessary for either environmental survival or host virulence. I sought to determine the role of CLC in *Francisella* pathogenesis. Using *F. tularensis* type B, I was able to determine that the CLC is necessary for virulence in mice through the intranasal route of infection. LVSΔ1423-22 infected intranasally resulted in a complete loss of virulence as opposed to the intraperitoneal (IP) route of infection, which was only slightly less virulence than the parent LVS [192]. The IP route bypasses much of the bodies innate immune defenses and therefore, the CLC may be important for protection of *F. tularensis* LVS from the innate immune response, particularly in the respiratory tract. Purified CLC initiates a protective immune response in the BALB/c mouse model after immunization only

with the addition of an adjuvant, and 100% survival of immunized mice is only seen after conjugation of the CLC to an immunogenic protein and challenge through the intradermal route. This protective immune response from purified CLC is not seen when the challenged via the intranasal route with type B or the challenge strain is from the more virulent type A *F. tularensis*.

As stated above, the CLC appears to contain copious amounts of OMV/T, which have previously been shown to offer some protection upon immunization in mice [98]. My studies mimicked that protection when using the type B strains, but did not see protection with type A challenge. Our studies used approximately 10 times the challenge dose of Huntley et. al., which could account for the differences in partial protection that we saw, and is not indicative of the CLC material being different from previously extracted OMV.

6.1.5 Surface Antigen Role in Biofilm Formation

Plentiful circumstantial evidence points to a role for *Francisella* biofilm formation in environmental survival. My research using type B *F. tularensis* LVS strains has shown that strains that are attenuated in mice due to deficiencies in surface antigens (O-Ag and CLC) form a more robust biofilm than the virulent parent (Chapter 5). This alone can make one conclude that biofilm formation is not necessary for *Francisella* once it has infected a host. *F. tularensis* has the ability to survive in a wide range of environmental conditions that include: dry and arid, waterways and intracellulary in amoebae, therefore protection from their environment is key to survival [111,112,228]. We found that while both CLC and CLC/O-Ag mutants are enhanced in biofilm formation, only the CLC/O-Ag mutant, which makes the most robust biofilm, is attenuated in bacterial invasion and replication in macrophages [192]. Enhancement of biofilm in

attenuated strains seems to negatively correlate host cell invasion with biofilm formation. O-antigen and CLC LVS mutants are highly attenuated in the mouse model, but enhanced in biofilm formation. Therefore, the increase in biofilm formation observed under host-adapted growth conditions indicates that biofilm is most likely not involved in host virulence [94,192], which correlates with the hypothesis that biofilm is used by *Francisella* species as a way to survive in the environment rather than as a virulence mechanism in the host.

6.2 Summary and Future Directions

Further characterization of the glycosylated proteins in the CLC, particularly the HMW portion is key to a complete understanding of the CLC. In addition, identification of potential stand-alone glycosyltransferases that may produce the 420-Da glycose polymer and identification of the specific protein component that is glycosylated in this HMW material would be a novel contribution. Analysis of whether or not a type A mutant in FTT_0798-99 produces CLC, is attenuated or is protective is an ideal next step to undertake. Translation of the properties of type B mutants to similar type A mutants is not always identical. Very often, mutations in type B that are attenuated will still be highly virulent in the type A strains, for example the CapB mutants [81]. A live attenuated type A strain is the ideal vaccine candidate for this intracellular pathogen, and what much research has strived for. How much potential the CLC surface antigen has to be a useful vaccine candidate still remains to be discovered. Furthermore, continued research into the role of biofilms in *F. tularensis* pathogenesis is still needed. In addition to the exopolysaccharide glucan that we discovered, what other matrix components are found in *F. tularensis* biofilm and are they specifically effected by CLC deficiency?

In summary, my work has elucidated the identity of a novel surface antigen of *F. tularensis*, the capsule-like complex (CLC). I found that the CLC is upregulated by growth conditions and can be found in type A and B biotypes. The type B CLC is necessary for virulence in mice and offers protection against lethal type B challenge. Partial identification of the protein and glycoprotein components has been completed and two of the carbohydrate components have been identified. The known glycosylation locus (FTT0789-0800) has been identified as necessary for upregulated CLC production, formation of OMV/T and implicated in biofilm formation. This dissertation brings novel insight into the role of CLC in pathogenesis of the unique intracellular bacteria *Francisella tularensis*.

REFERENCES CITED

1. Hood AM (1977) Virulence factors of Francisella tularensis. J Hyg (Lond) 79: 47-60.

2. McCoy GW, Chapin CW (1911) Tuberculosis among Ground Squirrels (Citellus Beecheyi, Richardson). J Med Res 25: 189-198.

3. Pearse RA (1911) Insect bites. Northwest Med 3: 81-82.

4. Morner T (1992) The ecology of tularaemia. Rev Sci Tech 11: 1123-1130.

5. Ohara S (1954) Studies on yato-byo (Ohara's disease, tularemia in Japan). I. Jpn J Exp Med 24: 69-79.

6. Scheel Oea (1992) [Tularemia in Norway. A clinical and epidemiological review]. Tidsskr Nor Laegeforen 112: 635-670.

7. McCoy GWaCWC (1912) Further observations on a plague-like disease of rodents with a preliminary note on the causative agent, Bacterium tularense. The Journal of Infectious Diseases 10: 61-72.

8. Wherry WBBHL (1914) Infection of man with Bacterium tularense. J Infect Dis 15: 331-340.

9. (1998) Summary of notifiable disease. United States Centers for Disease Control and Prevention: 71-80.

10. Francis E, A.C. Evans, and United States. (1926) Agglutination, cross-agglutination and agglutinin absorption in tularaemia. Government printoff. Washington DC.

11. Francis E (1929) A summary of present knowledge of tularaemia. Harvey Lectures 23: 25-48.

12. Francis E (1942) Fermentation of sugars by bacterium tularense. J Bacteriology 43: 343-346.

13. Francis E (1947) Streptomycin in treatment of tularemia. Trans Assoc Am Physicians 60: 181-186.

14. Francis E (1919) Deer-fly fever or Pahvant Valley plague. In: printoff Ug, editor. Washington DC.

15. Francis E (1919) Deer-fly fever - a disease of hitherto unknown etiology. Public Health Report. 2061-2062 p.

16. Ritter DB, Gerloff RK (1966) Deoxyribonucleic acid hybridization among some species of the genus Pasteurella. J Bacteriol 92: 1838-1839.

17. Forsman M, Sandstrom G, Sjostedt A (1994) Analysis of 16S ribosomal DNA sequences of Francisella strains and utilization for determination of the phylogeny of the genus and for identification of strains by PCR. Int J Syst Bacteriol 44: 38-46.

18. Olsufjev NG (1970) Taxonomy and characteristic of the genus Francisella Dorofeev, 1947. J Hyg Epidemiol Microbiol Immunol 14: 67-74.

19. Sjostedt A (2005) Francisella. In: DJ Brenner JSaGG, editor. The Proteobacteria, Part B, Bergey's Manual of Systemic Bacteriology. 2nd ed. New York, NY: Springer. pp. 200-210.

20. Keim P, Johansson A, Wagner DM (2007) Molecular epidemiology, evolution, and ecology of Francisella. Ann N Y Acad Sci 1105: 30-66.

21. Jensen WI, Owen CR, Jellison WL (1969) Yersinia philomiragia sp. n., a new member of the Pasteurella group of bacteria, naturally pathogenic for the muskrat (Ondatra zibethica). J Bacteriol 100: 1237-1241.

22. Wenger JD, Hollis DG, Weaver RE, Baker CN, Brown GR, et al. (1989) Infection caused by Francisella philomiragia (formerly Yersinia philomiragia). A newly recognized human pathogen. Ann Intern Med 110: 888-892.

23. Champion MD, Zeng Q, Nix EB, Nano FE, Keim P, et al. (2009) Comparative genomic characterization of Francisella tularensis strains belonging to low and high virulence subspecies. PLoS Pathog 5: e1000459.

24. Rohmer L, Fong C, Abmayr S, Wasnick M, Larson Freeman TJ, et al. (2007) Comparison of Francisella tularensis genomes reveals evolutionary events associated with the emergence of human pathogenic strains. Genome Biol 8: R102.

25. Tarnvik A, Sandstrom G, Sjostedt A (1996) Epidemiological analysis of tularemia in Sweden 1931-1993. FEMS Immunol Med Microbiol 13: 201-204.

26. Griffin KF, Oyston PC, Titball RW (2007) Francisella tularensis vaccines. FEMS Immunol Med Microbiol 49: 315-323.

27. Sjostedt A (2003) Virulence determinants and protective antigens of Francisella tularensis. Curr Opin Microbiol 6: 66-71.

28. Titball R, A. Johansson and M Forsman (2003) Will the enigma of Francisella tularensis virulence soon be solved. Trends in Microbiology 11: 118-123.

29. Kugeler KJ, Mead PS, Janusz AM, Staples JE, Kubota KA, et al. (2009) Molecular Epidemiology of Francisella tularensis in the United States. Clin Infect Dis 48: 863-870.

30. Olsufjev NGaIM (1983) Subspecific taxonomy of Francisella tularensis. International Journal of Systematic Bacteriology 33: 872-874.

31. Sjostedt A (2007) Tularemia: history, epidemiology, pathogen physiology, and clinical manifestations. Ann N Y Acad Sci 1105: 1-29.

32. Larsson P, Elfsmark D, Svensson K, Wikstrom P, Forsman M, et al. (2009) Molecular evolutionary consequences of niche restriction in Francisella tularensis, a facultative intracellular pathogen. PLoS Pathog 5: e1000472.

33. Vogler AJ, Birdsell D, Price LB, Bowers JR, Beckstrom-Sternberg SM, et al. (2009) Phylogeography of Francisella tularensis: global expansion of a highly fit clone. J Bacteriol 191: 2474-2484.

34. Johansson A, Petersen JM (2010) Genotyping of Francisella tularensis, the causative agent of tularemia. J AOAC Int 93: 1930-1943.

35. Petersen JM, Mead PS, Schriefer ME (2009) Francisella tularensis: an arthropod-borne pathogen. Vet Res 40: 7.

36. Hopla CE (1974) The ecology of tularemia. Adv Vet Sci Comp Med 18: 25-53.

37. JF B (1977) Tularemia. Boca Raton: CRC. 161-193 p.

38. Feldman KA (2003) Tularemia. J Am Vet Med Assoc 222: 725-730.

39. Feldman KA, Stiles-Enos D, Julian K, Matyas BT, Telford SR, 3rd, et al. (2003) Tularemia on Martha's Vineyard: seroprevalence and occupational risk. Emerg Infect Dis 9: 350-354.

40. Feldman KA, Enscore RE, Lathrop SL, Matyas BT, McGuill M, et al. (2001) An outbreak of primary pneumonic tularemia on Martha's Vineyard. N Engl J Med 345: 1601-1606.

41. Calhoun EL, Mohr CO, Alford HI, Jr. (1956) Dogs and other mammals as hosts of tularemia and of vector ticks in Arkansas. Am J Hyg 63: 127-135.

42. Brown RN LRaDD (2005) Geographic distribution of tick-borne diseases and their vectors. In: Goodman JL DDaSD, editor. Tick-borne diseases of humans. Washington DC: ASM Press. pp. 363-367.

43. Triebenbach AN, Vogl SJ, Lotspeich-Cole L, Sikes DS, Happ GM, et al. (2010) Detection of Francisella tularensis in Alaskan mosquitoes (Diptera: Culicidae) and assessment of a laboratory model for transmission. J Med Entomol 47: 639-648.

44. Eliasson H, Lindback J, Nuorti JP, Arneborn M, Giesecke J, et al. (2002) The 2000 tularemia outbreak: a case-control study of risk factors in disease-endemic and emergent areas, Sweden. Emerg Infect Dis 8: 956-960.

45. Sanford JP (1983) Landmark perspective: Tularemia. JAMA 250: 3225-3226.

46. Brooks GF, Buchanan TM (1970) Tularemia in the United States: epidemiologic aspects in the 1960s and follow-up of the outbreak of tularemia in Vermont. J Infect Dis 121: 357-359.

47. (2014) Tularemia, Statistics. Centers for Disease Control and Prevention.

48. Molins CR, Carlson JK, Coombs J, Petersen JM (2009) Identification of Francisella tularensis subsp. tularensis A1 and A2 infections by real-time polymerase chain reaction. Diagn Microbiol Infect Dis 64: 6-12.

49. Petersen JM, Molins CR (2010) Subpopulations of Francisella tularensis ssp. tularensis and holarctica: identification and associated epidemiology. Future Microbiol 5: 649-661.

50. Kantardjiev T, Ivanov I, Velinov T, Padeshki P, Popov B, et al. (2006) Tularemia outbreak, Bulgaria, 1997-2005. Emerg Infect Dis 12: 678-680.

51. Meric M MS, D Dundar and A Willke (2010) Tularemia outbreaks in Sakarya, Turkey: case-control and environmental studies. Singapore Med J 51: 655-659.

52. Siret V, Barataud D, Prat M, Vaillant V, Ansart S, et al. (2006) An outbreak of airborne tularaemia in France, August 2004. Euro Surveill 11: 58-60.

53. Boyce JM Recent Trends in the Epidemiology of Tularemia. In: Prevention TCfDCa, editor. Atlanta, GA. pp. 196-197.

54. Olsufjev A (1966) Tularemia. In: Y. P, editor. In human diseases with natural foci. Moscow: Foreign Languages Publishing House.

55. Washburn AM, Tuohy JH (1949) The changing picture of tularemia transmission in Arkansas; a study of 704 case histories. South Med J 42: 60-62.

56. Dienst FT, Jr. (1963) Tularemia: a perusal of three hundred thirty-nine cases. J La State Med Soc 115: 114-127.

57. Foshay L, W.H. Hesselbrock, H.J. Wittenberg and A. H. Rodenberg (1942) Vaccine prophylaxis against tularemia in man. Am J Public Health Nations Health 32: 1131-1145.

58. Conlan JWaPO (2007) Vaccines against Francisella tularensis. Ann N Y Acad Sci.

59. Tarnvik A (1989) Nature of protective immunity to Francisella tularensis. Rev Infect Dis 11: 440-451.

60. Gordon M, Donaldson DM, Wright GG (1964) Immunization of Mice with Irradiated Pasteurella Tularensis. J Infect Dis 114: 435-440.

61. Tigertt WD (1962) Soviet viable Pasteurella tularensis vaccines. A review of selected articles. Bacteriol Rev 26: 354-373.

62. Sjostedt A, Tarnvik A, Sandstrom G (1996) Francisella tularensis: host-parasite interaction. FEMS Immunol Med Microbiol 13: 181-184.

63. Cross AS, Calia FM, Edelman R (2007) From rabbits to humans: the contributions of Dr. Theodore E. Woodward to tularemia research. Clin Infect Dis 45 Suppl 1: S61-67.

64. Saslaw S, Eigelsbach HT, Prior JA, Wilson HE, Carhart S (1961) Tularemia vaccine study. II. Respiratory challenge. Arch Intern Med 107: 702-714.

65. Saslaw S, Eigelsbach HT, Wilson HE, Prior JA, Carhart S (1961) Tularemia vaccine study. I. Intracutaneous challenge. Arch Intern Med 107: 689-701.

66. Hornick RB, Eigelsbach HT (1966) Aerogenic immunization of man with live Tularemia vaccine. Bacteriol Rev 30: 532-538.

67. Eigelsbach HT, Downs CM (1961) Prophylactic effectiveness of live and killed tularemia vaccines. I. Production of vaccine and evaluation in the white mouse and guinea pig. J Immunol 87: 415-425.

68. Reed DS, Smith LP, Cole KS, Santiago AE, Mann BJ, et al. (2014) Live attenuated mutants of Francisella tularensis protect rabbits against aerosol challenge with a virulent type A strain. Infect Immun 82: 2098-2105.

69. Cong Y, Yu JJ, Guentzel MN, Berton MT, Seshu J, et al. (2009) Vaccination with a defined Francisella tularensis subsp. novicida pathogenicity island mutant (DeltaiglB) induces protective immunity against homotypic and heterotypic challenge. Vaccine 27: 5554-5561.

70. Kanistanon D, Hajjar AM, Pelletier MR, Gallagher LA, Kalhorn T, et al. (2008) A Francisella mutant in lipid A carbohydrate modification elicits protective immunity. PLoS Pathog 4: e24.

71. Mohapatra NP, Soni S, Bell BL, Warren R, Ernst RK, et al. (2007) Identification of an orphan response regulator required for the virulence of Francisella spp. and transcription of pathogenicity island genes. Infect Immun 75: 3305-3314.

72. Mohapatra NP, Balagopal A, Soni S, Schlesinger LS, Gunn JS (2007) AcpA is a Francisella acid phosphatase that affects intramacrophage survival and virulence. Infect Immun 75: 390-396.

73. Pammit MA, Raulie EK, Lauriano CM, Klose KE, Arulanandam BP (2006) Intranasal vaccination with a defined attenuated Francisella novicida strain induces gamma interferon-dependent antibody-mediated protection against tularemia. Infect Immun 74: 2063-2071.

74. Quarry JE, Isherwood KE, Michell SL, Diaper H, Titball RW, et al. (2007) A Francisella tularensis subspecies novicida purF mutant, but not a purA mutant, induces protective immunity to tularemia in mice. Vaccine 25: 2011-2018.

75. Shen H, Chen W, Conlan JW (2004) Mice sublethally infected with Francisella novicida U112 develop only marginal protective immunity against systemic or aerosol challenge with virulent type A or B strains of F. tularensis. Microb Pathog 37: 107-110.

76. Tempel R, Lai XH, Crosa L, Kozlowicz B, Heffron F (2006) Attenuated Francisella novicida transposon mutants protect mice against wild-type challenge. Infect Immun 74: 5095-5105.

77. West TE, Pelletier MR, Majure MC, Lembo A, Hajjar AM, et al. (2008) Inhalation of Francisella novicida Delta mglA causes replicative infection that elicits innate and

adaptive responses but is not protective against invasive pneumonic tularemia. Microbes Infect 10: 773-780.

78. Conlan JW, Shen H, Golovliov I, Zingmark C, Oyston PC, et al. (2010) Differential ability of novel attenuated targeted deletion mutants of Francisella tularensis subspecies tularensis strain SCHU S4 to protect mice against aerosol challenge with virulent bacteria: effects of host background and route of immunization. Vaccine 28: 1824-1831.

79. Forestal CA, Gil H, Monfett M, Noah CE, Platz GJ, et al. (2008) A conserved and immunodominant lipoprotein of Francisella tularensis is proinflammatory but not essential for virulence. Microb Pathog 44: 512-523.

80. Meibom KL, Dubail I, Dupuis M, Barel M, Lenco J, et al. (2008) The heat-shock protein ClpB of Francisella tularensis is involved in stress tolerance and is required for multiplication in target organs of infected mice. Mol Microbiol 67: 1384-1401.

81. Michell SL, Dean RE, Eyles JE, Hartley MG, Waters E, et al. (2010) Deletion of the Bacillus anthracis capB homologue in Francisella tularensis subspecies tularensis generates an attenuated strain that protects mice against virulent tularaemia. J Med Microbiol 59: 1275-1284.

82. Pechous RD, McCarthy TR, Mohapatra NP, Soni S, Penoske RM, et al. (2008) A Francisella tularensis Schu S4 purine auxotroph is highly attenuated in mice but offers limited protection against homologous intranasal challenge. PLoS One 3: e2487.

83. Qin A, Scott DW, Thompson JA, Mann BJ (2009) Identification of an essential Francisella tularensis subsp. tularensis virulence factor. Infect Immun 77: 152-161.

84. Qin A, Scott DW, Mann BJ (2008) Francisella tularensis subsp. tularensis Schu S4 disulfide bond formation protein B, but not an RND-type efflux pump, is required for virulence. Infect Immun 76: 3086-3092.

85. Santiago AE, Cole LE, Franco A, Vogel SN, Levine MM, et al. (2009) Characterization of rationally attenuated Francisella tularensis vaccine strains that harbor deletions in the guaA and guaB genes. Vaccine 27: 2426-2436.

86. Sebastian S, Dillon ST, Lynch JG, Blalock LT, Balon E, et al. (2007) A defined O-antigen polysaccharide mutant of Francisella tularensis live vaccine strain has attenuated virulence while retaining its protective capacity. Infect Immun 75: 2591-2602.

87. Twine S, Bystrom M, Chen W, Forsman M, Golovliov I, et al. (2005) A mutant of Francisella tularensis strain SCHU S4 lacking the ability to express a 58-kilodalton protein is attenuated for virulence and is an effective live vaccine. Infect Immun 73: 8345-8352.

88. Rasmussen JA, Post DM, Gibson BW, Lindemann SR, Apicella MA, et al. (2014) Francisella tularensis Schu S4 lipopolysaccharide core sugar and O-antigen mutants are attenuated in a mouse model of tularemia. Infect Immun 82: 1523-1539.

89. Conlan JW, Shen H, Webb A, Perry MB (2002) Mice vaccinated with the O-antigen of Francisella tularensis LVS lipopolysaccharide conjugated to bovine serum albumin develop varying degrees of protective immunity against systemic or aerosol challenge with virulent type A and type B strains of the pathogen. Vaccine 20: 3465-3471.

90. Fulop M, Manchee R, Titball R (1995) Role of lipopolysaccharide and a major outer membrane protein from Francisella tularensis in the induction of immunity against tularemia. Vaccine 13: 1220-1225.

91. Golovliov I, Ericsson M, Akerblom L, Sandstrom G, Tarnvik A, et al. (1995) Adjuvanticity of ISCOMs incorporating a T cell-reactive lipoprotein of the facultative intracellular pathogen Francisella tularensis. Vaccine 13: 261-267.

92. Apicella MA, Post DM, Fowler AC, Jones BD, Rasmussen JA, et al. (2010) Identification, characterization and immunogenicity of an O-antigen capsular polysaccharide of Francisella tularensis. PLoS One 5: e11060.

93. Gregory SH, Chen WH, Mott S, Palardy JE, Parejo NA, et al. (2010) Detoxified endotoxin vaccine (J5dLPS/OMP) protects mice against lethal respiratory challenge with Francisella tularensis SchuS4. Vaccine 28: 2908-2915.

94. Li J, Ryder C, Mandal M, Ahmed F, Azadi P, et al. (2007) Attenuation and protective efficacy of an O-antigen-deficient mutant of Francisella tularensis LVS. Microbiology 153: 3141-3153.

95. Ashtekar AR, Katz J, Xu Q, Michalek SM (2012) A mucosal subunit vaccine protects against lethal respiratory infection with Francisella tularensis LVS. PLoS One 7: e50460.

96. Savitt AG, Mena-Taboada P, Monsalve G, Benach JL (2009) Francisella tularensis infection-derived monoclonal antibodies provide detection, protection, and therapy. Clin Vaccine Immunol 16: 414-422.

97. Hickey AJ, Hazlett KR, Kirimanjeswara GS, Metzger DW (2011) Identification of Francisella tularensis outer membrane protein A (FopA) as a protective antigen for tularemia. Vaccine 29: 6941-6947.

98. Huntley JF, Conley PG, Rasko DA, Hagman KE, Apicella MA, et al. (2008) Native outer membrane proteins protect mice against pulmonary challenge with virulent type A Francisella tularensis. Infect Immun 76: 3664-3671.

99. Richard K, Mann BJ, Stocker L, Barry EM, Qin A, et al. (2014) Novel catanionic surfactant vesicle vaccines protect against Francisella tularensis LVS and confer significant partial protection against F. tularensis Schu S4 strain. Clin Vaccine Immunol 21: 212-226.

100. Jia Q, Bowen R, Sahakian J, Dillon BJ, Horwitz MA (2013) A heterologous prime-boost vaccination strategy comprising the Francisella tularensis live vaccine strain capB mutant and recombinant attenuated Listeria monocytogenes expressing F. tularensis IglC induces potent protective immunity in mice against virulent F. tularensis aerosol challenge. Infect Immun 81: 1550-1561.

101. Dennis DT, Inglesby TV, Henderson DA, Bartlett JG, Ascher MS, et al. (2001) Tularemia as a biological weapon: medical and public health management. JAMA 285: 2763-2773.

102. Harris S (1992) Japanese biological warfare research on humans: a case study of microbiology and ethics. Ann N Y Acad Sci 666: 21-52.

103. Evans F (1997) Tularemia. Textbook of Military Medicine Aspects of Chemical and Biological Warfare. Washington D.C.: Medical Research Institute of Chemical Defense.

104. Wheelis M, L. Rozsa and M. Dando (2006) Deadly cultures: biological weapons since 1945. Cambridge, MA: Harvard University Press.

105. Larsson P, Oyston PC, Chain P, Chu MC, Duffield M, et al. (2005) The complete genome sequence of Francisella tularensis, the causative agent of tularemia. Nat Genet 37: 153-159.

106. Golovliov I, Twine SM, Shen H, Sjostedt A, Conlan W (2013) A DeltaclpB mutant of Francisella tularensis subspecies holarctica strain, FSC200, is a more effective live vaccine than F. tularensis LVS in a mouse respiratory challenge model of tularemia. PLoS One 8: e78671.

107. Kuoppa K, Forsberg A, Norqvist A (2001) Construction of a reporter plasmid for screening in vivo promoter activity in Francisella tularensis. FEMS Microbiol Lett 205: 77-81.

108. Kawula TH, Hall JD, Fuller JR, Craven RR (2004) Use of transposon-transposase complexes to create stable insertion mutant strains of Francisella tularensis LVS. Appl Environ Microbiol 70: 6901-6904.

109. Maier TM, Casey MS, Becker RH, Dorsey CW, Glass EM, et al. (2007) Identification of Francisella tularensis Himar1-based transposon mutants defective for replication in macrophages. Infect Immun 75: 5376-5389.

110. Qin A, Mann BJ (2006) Identification of transposon insertion mutants of Francisella tularensis tularensis strain Schu S4 deficient in intracellular replication in the hepatic cell line HepG2. BMC Microbiol 6: 69.

111. Abd H, Johansson T, Golovliov I, Sandstrom G, Forsman M (2003) Survival and growth of Francisella tularensis in Acanthamoeba castellanii. Appl Environ Microbiol 69: 600-606.

112. El-Etr SH, Margolis JJ, Monack D, Robison RA, Cohen M, et al. (2009) Francisella tularensis type A strains cause the rapid encystment of Acanthamoeba castellanii and survive in amoebal cysts for three weeks postinfection. Appl Environ Microbiol 75: 7488-7500.

113. Hall JD, Craven RR, Fuller JR, Pickles RJ, Kawula TH (2007) Francisella tularensis replicates within alveolar type II epithelial cells in vitro and in vivo following inhalation. Infect Immun 75: 1034-1039.

114. McCaffrey RL, Allen LA (2006) Francisella tularensis LVS evades killing by human neutrophils via inhibition of the respiratory burst and phagosome escape. J Leukoc Biol 80: 1224-1230.

115. Oyston PC (2008) Francisella tularensis: unravelling the secrets of an intracellular pathogen. J Med Microbiol 57: 921-930.

116. Lindemann SR, Peng K, Long ME, Hunt JR, Apicella MA, et al. (2010) F. tularensis Schu S4 mutants in O-antigen and capsule biosynthesis genes induce early cell death in human macrophages. Infect Immun.

117. Anthony LD, Burke RD, Nano FE (1991) Growth of Francisella spp. in rodent macrophages. Infect Immun 59: 3291-3296.

118. Lauriano CM, Barker JR, Yoon SS, Nano FE, Arulanandam BP, et al. (2004) MglA regulates transcription of virulence factors necessary for Francisella tularensis

intraamoebae and intramacrophage survival. Proc Natl Acad Sci U S A 101: 4246-4249.

119. Moreland JG, Hook JS, Bailey G, Ulland T, Nauseef WM (2009) Francisella tularensis directly interacts with the endothelium and recruits neutrophils with a blunted inflammatory phenotype. Am J Physiol Lung Cell Mol Physiol 296: L1076-1084.

120. Clemens DL, Lee BY, Horwitz MA (2005) Francisella tularensis enters macrophages via a novel process involving pseudopod loops. Infect Immun 73: 5892-5902.

121. Asare R, Abu Kwaik Y (2010) Molecular complexity orchestrates modulation of phagosome biogenesis and escape to the cytosol of macrophages by Francisella tularensis. Environ Microbiol 12: 2559-2586.

122. Clemens DL, Lee BY, Horwitz MA (2004) Virulent and avirulent strains of Francisella tularensis prevent acidification and maturation of their phagosomes and escape into the cytoplasm in human macrophages. Infect Immun 72: 3204-3217.

123. Golovliov I, Baranov V, Krocova Z, Kovarova H, Sjostedt A (2003) An attenuated strain of the facultative intracellular bacterium Francisella tularensis can escape the phagosome of monocytic cells. Infect Immun 71: 5940-5950.

124. Checroun C, Wehrly TD, Fischer ER, Hayes SF, Celli J (2006) Autophagy-mediated reentry of Francisella tularensis into the endocytic compartment after cytoplasmic replication. Proc Natl Acad Sci U S A 103: 14578-14583.

125. Santic M, Molmeret M, Klose KE, Abu Kwaik Y (2006) Francisella tularensis travels a novel, twisted road within macrophages. Trends Microbiol 14: 37-44.

126. Chong A, Wehrly TD, Nair V, Fischer ER, Barker JR, et al. (2008) The early phagosomal stage of Francisella tularensis determines optimal phagosomal escape and Francisella pathogenicity island protein expression. Infect Immun 76: 5488-5499.

127. Clemens DL, Lee BY, Horwitz MA (2009) Francisella tularensis phagosomal escape does not require acidification of the phagosome. Infect Immun 77: 1757-1773.

128. Lai XH, Golovliov I, Sjostedt A (2001) Francisella tularensis induces cytopathogenicity and apoptosis in murine macrophages via a mechanism that requires intracellular bacterial multiplication. Infect Immun 69: 4691-4694.

129. Celli J, Zahrt TC (2013) Mechanisms of Francisella tularensis intracellular pathogenesis. Cold Spring Harb Perspect Med 3: a010314.

130. Rus H, Cudrici C, Niculescu F (2005) The role of the complement system in innate immunity. Immunol Res 33: 103-112.

131. Lofgren S, Tarnvik A, Bloom GD, Sjoberg W (1983) Phagocytosis and killing of Francisella tularensis by human polymorphonuclear leukocytes. Infect Immun 39: 715-720.

132. Sandstrom G, Lofgren S, Tarnvik A (1988) A capsule-deficient mutant of Francisella tularensis LVS exhibits enhanced sensitivity to killing by serum but diminished sensitivity to killing by polymorphonuclear leukocytes. Infect Immun 56: 1194-1202.

133. Jones CL, Napier BA, Sampson TR, Llewellyn AC, Schroeder MR, et al. (2012) Subversion of host recognition and defense systems by Francisella spp. Microbiol Mol Biol Rev 76: 383-404.

134. Clay CD, Soni S, Gunn JS, Schlesinger LS (2008) Evasion of complement-mediated lysis and complement C3 deposition are regulated by Francisella tularensis lipopolysaccharide O antigen. J Immunol 181: 5568-5578.

135. Ben Nasr A, Klimpel GR (2008) Subversion of complement activation at the bacterial surface promotes serum resistance and opsonophagocytosis of Francisella tularensis. J Leukoc Biol 84: 77-85.

136. Bosio CM (2011) The subversion of the immune system by francisella tularensis. Front Microbiol 2: 9.

137. Cederlund A, Gudmundsson GH, Agerberth B (2011) Antimicrobial peptides important in innate immunity. FEBS J 278: 3942-3951.

138. Wang X, Ribeiro AA, Guan Z, McGrath SC, Cotter RJ, et al. (2006) Structure and biosynthesis of free lipid A molecules that replace lipopolysaccharide in Francisella tularensis subsp. novicida. Biochemistry 45: 14427-14440.

139. Collazo CM, Sher A, Meierovics AI, Elkins KL (2006) Myeloid differentiation factor-88 (MyD88) is essential for control of primary in vivo Francisella tularensis LVS infection, but not for control of intra-macrophage bacterial replication. Microbes Infect 8: 779-790.

140. Stenmark S, Sunnemark D, Bucht A, Sjostedt A (1999) Rapid local expression of interleukin-12, tumor necrosis factor alpha, and gamma interferon after cutaneous Francisella tularensis infection in tularemia-immune mice. Infect Immun 67: 1789-1797.

141. Elkins KL, Rhinehart-Jones T, Nacy CA, Winegar RK, Fortier AH (1993) T-cell-independent resistance to infection and generation of immunity to Francisella tularensis. Infect Immun 61: 823-829.

142. Elkins KL, Rhinehart-Jones TR, Culkin SJ, Yee D, Winegar RK (1996) Minimal requirements for murine resistance to infection with Francisella tularensis LVS. Infect Immun 64: 3288-3293.

143. Cole LE, Shirey KA, Barry E, Santiago A, Rallabhandi P, et al. (2007) Toll-like receptor 2-mediated signaling requirements for Francisella tularensis live vaccine strain infection of murine macrophages. Infect Immun 75: 4127-4137.

144. Telepnev M, Golovliov I, Grundstrom T, Tarnvik A, Sjostedt A (2003) Francisella tularensis inhibits Toll-like receptor-mediated activation of intracellular signalling and secretion of TNF-alpha and IL-1 from murine macrophages. Cell Microbiol 5: 41-51.

145. Inoue S, Itagaki S, Amano F (1995) Intracellular killing of Listeria monocytogenes in the J774.1 macrophage-like cell line and the lipopolysaccharide (LPS)-resistant mutant LPS1916 cell line defective in the generation of reactive oxygen intermediates after LPS treatment. Infect Immun 63: 1876-1886.

146. Farrell A (2012) NO means yes to Listeria infections. Nature Medicine 18.

147. Thakran S, Li H, Lavine CL, Miller MA, Bina JE, et al. (2008) Identification of Francisella tularensis lipoproteins that stimulate the toll-like receptor (TLR) 2/TLR1 heterodimer. J Biol Chem 283: 3751-3760.

148. Elkins KL, Cowley SC, Bosio CM (2007) Innate and adaptive immunity to Francisella. Ann N Y Acad Sci 1105: 284-324.

149. Stenmark S, Lindgren H, Tarnvik A, Sjostedt A (2003) Specific antibodies contribute to the host protection against strains of Francisella tularensis subspecies holarctica. Microb Pathog 35: 73-80.

150. Yee D, Rhinehart-Jones TR, Elkins KL (1996) Loss of either CD4+ or CD8+ T cells does not affect the magnitude of protective immunity to an intracellular pathogen, Francisella tularensis strain LVS. J Immunol 157: 5042-5048.

151. Cowley SC, Sedgwick JD, Elkins KL (2007) Differential requirements by CD4+ and CD8+ T cells for soluble and membrane TNF in control of Francisella tularensis live vaccine strain intramacrophage growth. J Immunol 179: 7709-7719.

152. Lin Y, Ritchea S, Logar A, Slight S, Messmer M, et al. (2009) Interleukin-17 is required for T helper 1 cell immunity and host resistance to the intracellular pathogen Francisella tularensis. Immunity 31: 799-810.

153. Cowley SC, Meierovics AI, Frelinger JA, Iwakura Y, Elkins KL (2010) Lung CD4-CD8-double-negative T cells are prominent producers of IL-17A and IFN-gamma during primary respiratory murine infection with Francisella tularensis live vaccine strain. J Immunol 184: 5791-5801.

154. Nano FE, Zhang N, Cowley SC, Klose KE, Cheung KK, et al. (2004) A Francisella tularensis pathogenicity island required for intramacrophage growth. J Bacteriol 186: 6430-6436.

155. Santic M, Molmeret M, Barker JR, Klose KE, Dekanic A, et al. (2007) A Francisella tularensis pathogenicity island protein essential for bacterial proliferation within the host cell cytosol. Cell Microbiol 9: 2391-2403.

156. Santic M, Akimana C, Asare R, Kouokam JC, Atay S, et al. (2009) Intracellular fate of Francisella tularensis within arthropod-derived cells. Environ Microbiol 11: 1473-1481.

157. Bonquist L, Lindgren H, Golovliov I, Guina T, Sjostedt A (2008) MglA and Igl proteins contribute to the modulation of Francisella tularensis live vaccine strain-containing phagosomes in murine macrophages. Infect Immun 76: 3502-3510.

158. Ludu JS, de Bruin OM, Duplantis BN, Schmerk CL, Chou AY, et al. (2008) The Francisella pathogenicity island protein PdpD is required for full virulence and associates with homologues of the type VI secretion system. J Bacteriol 190: 4584-4595.

159. Broms JE, Sjostedt A, Lavander M (2010) The Role of the Francisella Tularensis Pathogenicity Island in Type VI Secretion, Intracellular Survival, and Modulation of Host Cell Signaling. Front Microbiol 1: 136.

160. Robertson GT, Child R, Ingle C, Celli J, Norgard MV (2013) IglE is an outer membrane-associated lipoprotein essential for intracellular survival and murine virulence of type A Francisella tularensis. Infect Immun 81: 4026-4040.

161. Faron M, Fletcher JR, Rasmussen JA, Long ME, Allen LA, et al. (2013) The Francisella tularensis migR, trmE, and cphA genes contribute to F. tularensis pathogenicity island gene regulation and intracellular growth by modulation of the stress alarmone ppGpp. Infect Immun 81: 2800-2811.

162. Long ME, Lindemann SR, Rasmussen JA, Jones BD, Allen LA (2013) Disruption of Francisella tularensis Schu S4 iglI, iglJ, and pdpC genes results in attenuation for

growth in human macrophages and in vivo virulence in mice and reveals a unique phenotype for pdpC. Infect Immun 81: 850-861.

163. Santic M, Molmeret M, Klose KE, Jones S, Kwaik YA (2005) The Francisella tularensis pathogenicity island protein IglC and its regulator MglA are essential for modulating phagosome biogenesis and subsequent bacterial escape into the cytoplasm. Cell Microbiol 7: 969-979.

164. Lindgren H, Golovliov I, Baranov V, Ernst RK, Telepnev M, et al. (2004) Factors affecting the escape of Francisella tularensis from the phagolysosome. J Med Microbiol 53: 953-958.

165. Barker JR, Chong A, Wehrly TD, Yu JJ, Rodriguez SA, et al. (2009) The Francisella tularensis pathogenicity island encodes a secretion system that is required for phagosome escape and virulence. Mol Microbiol 74: 1459-1470.

166. Cole LE, Santiago A, Barry E, Kang TJ, Shirey KA, et al. (2008) Macrophage proinflammatory response to Francisella tularensis live vaccine strain requires coordination of multiple signaling pathways. J Immunol 180: 6885-6891.

167. Gavrilin MA, Bouakl IJ, Knatz NL, Duncan MD, Hall MW, et al. (2006) Internalization and phagosome escape required for Francisella to induce human monocyte IL-1beta processing and release. Proc Natl Acad Sci U S A 103: 141-146.

168. Parsa KV, Butchar JP, Rajaram MV, Cremer TJ, Gunn JS, et al. (2008) Francisella gains a survival advantage within mononuclear phagocytes by suppressing the host IFNgamma response. Mol Immunol 45: 3428-3437.

169. Lindgren M, Eneslatt K, Broms JE, Sjostedt A (2013) Importance of PdpC, IglC, IglI, and IglG for modulation of a host cell death pathway induced by Francisella tularensis. Infect Immun 81: 2076-2084.

170. Lindgren M, Broms JE, Meyer L, Golovliov I, Sjostedt A (2013) The Francisella tularensis LVS DeltapdpC mutant exhibits a unique phenotype during intracellular infection. BMC Microbiol 13: 20.

171. Bonemann G, Pietrosiuk A, Mogk A (2010) Tubules and donuts: a type VI secretion story. Mol Microbiol 76: 815-821.

172. Broms JE, Meyer L, Sun K, Lavander M, Sjostedt A (2012) Unique substrates secreted by the type VI secretion system of Francisella tularensis during intramacrophage infection. PLoS One 7: e50473.

173. Tan Y, Kagan JC (2014) A cross-disciplinary perspective on the innate immune responses to bacterial lipopolysaccharide. Mol Cell 54: 212-223.

174. Cole LE, Elkins KL, Michalek SM, Qureshi N, Eaton LJ, et al. (2006) Immunologic consequences of Francisella tularensis live vaccine strain infection: role of the innate immune response in infection and immunity. J Immunol 176: 6888-6899.

175. Hajjar AM, Harvey MD, Shaffer SA, Goodlett DR, Sjostedt A, et al. (2006) Lack of in vitro and in vivo recognition of Francisella tularensis subspecies lipopolysaccharide by Toll-like receptors. Infect Immun 74: 6730-6738.

176. Gunn JS, Ernst RK (2007) The structure and function of Francisella lipopolysaccharide. Ann N Y Acad Sci 1105: 202-218.

177. Sandstrom G, Sjostedt A, Johansson T, Kuoppa K, Williams JC (1992) Immunogenicity and toxicity of lipopolysaccharide from Francisella tularensis LVS. FEMS Microbiol Immunol 5: 201-210.

178. Vinogradov E, Perry MB, Conlan JW (2002) Structural analysis of Francisella tularensis lipopolysaccharide. Eur J Biochem 269: 6112-6118.

179. Prior JL, Prior RG, Hitchen PG, Diaper H, Griffin KF, et al. (2003) Characterization of the O antigen gene cluster and structural analysis of the O antigen of Francisella tularensis subsp. tularensis. J Med Microbiol 52: 845-851.

180. Thirumalapura NR, Goad DW, Mort A, Morton RJ, Clarke J, et al. (2005) Structural analysis of the O-antigen of Francisella tularensis subspecies tularensis strain OSU 10. J Med Microbiol 54: 693-695.

181. Vinogradov E, Conlan WJ, Gunn JS, Perry MB (2004) Characterization of the lipopolysaccharide O-antigen of Francisella novicida (U112). Carbohydr Res 339: 649-654.

182. Thomas RM, Titball RW, Oyston PC, Griffin K, Waters E, et al. (2007) The immunologically distinct O antigens from Francisella tularensis subspecies tularensis and Francisella novicida are both virulence determinants and protective antigens. Infect Immun 75: 371-378.

183. Raynaud C, Meibom KL, Lety MA, Dubail I, Candela T, et al. (2007) Role of the wbt locus of Francisella tularensis in lipopolysaccharide O-antigen biogenesis and pathogenicity. Infect Immun 75: 536-541.

184. Eigelsbach HT, Braun W, Herring RD (1951) Studies on the variation of Bacterium tularense. J Bacteriol 61: 557-569.

185. Soni S, Ernst RK, Muszynski A, Mohapatra NP, Perry MB, et al. (2010) Francisella tularensis blue-gray phase variation involves structural modifications of lipopolysaccharide o-antigen, core and lipid a and affects intramacrophage survival and vaccine efficacy. Front Microbiol 1: 129.

186. Cowley SC, Myltseva SV, Nano FE (1996) Phase variation in Francisella tularensis affecting intracellular growth, lipopolysaccharide antigenicity and nitric oxide production. Mol Microbiol 20: 867-874.

187. Hartley G, Taylor R, Prior J, Newstead S, Hitchen PG, et al. (2006) Grey variants of the live vaccine strain of Francisella tularensis lack lipopolysaccharide O-antigen, show reduced ability to survive in macrophages and do not induce protective immunity in mice. Vaccine 24: 989-996.

188. Ezzell JW, Welkos SL (1999) The capsule of bacillus anthracis, a review. J Appl Microbiol 87: 250.

189. Nickerson CAaMS (2006) Molecular Paradigms of Infectious Disease: A Bacterial Perspective; Nickerson CAaMS, editor. Washington DC: Springer.

190. Cherwonogrodzky JW, Knodel MH, Spence MR (1994) Increased encapsulation and virulence of Francisella tularensis live vaccine strain (LVS) by subculturing on synthetic medium. Vaccine 12: 773-775.

191. Lindemann SR, Peng K, Long ME, Hunt JR, Apicella MA, et al. (2011) Francisella tularensis Schu S4 O-antigen and capsule biosynthesis gene mutants induce early cell death in human macrophages. Infect Immun 79: 581-594.

192. Bandara AB, Champion AE, Wang X, Berg G, Apicella MA, et al. (2011) Isolation and mutagenesis of a capsule-like complex (CLC) from Francisella tularensis, and contribution of the CLC to F. tularensis virulence in mice. PLoS One 6: e19003.

193. Zarrella TM, Singh A, Bitsaktsis C, Rahman T, Sahay B, et al. (2011) Host-adaptation of Francisella tularensis alters the bacterium's surface-carbohydrates to hinder effectors of innate and adaptive immunity. PLoS One 6: e22335.

194. Messner P (2004) Prokaryotic glycoproteins: unexplored but important. J Bacteriol 186: 2517-2519.

195. Spiro RG (2002) Protein glycosylation: nature, distribution, enzymatic formation, and disease implications of glycopeptide bonds. Glycobiology 12: 43R-56R.

196. Schaffer C, Messner P (2004) Surface-layer glycoproteins: an example for the diversity of bacterial glycosylation with promising impacts on nanobiotechnology. Glycobiology 14: 31R-42R.

197. Mescher MF, Strominger JL (1976) Purification and characterization of a prokaryotic glucoprotein from the cell envelope of Halobacterium salinarium. J Biol Chem 251: 2005-2014.

198. Castric P, Cassels FJ, Carlson RW (2001) Structural characterization of the Pseudomonas aeruginosa 1244 pilin glycan. J Biol Chem 276: 26479-26485.

199. Stimson E, Virji M, Makepeace K, Dell A, Morris HR, et al. (1995) Meningococcal pilin: a glycoprotein substituted with digalactosyl 2,4-diacetamido-2,4,6-trideoxyhexose. Mol Microbiol 17: 1201-1214.

200. Verma A, Schirm M, Arora SK, Thibault P, Logan SM, et al. (2006) Glycosylation of b-Type flagellin of Pseudomonas aeruginosa: structural and genetic basis. J Bacteriol 188: 4395-4403.

201. Schirm M, Arora SK, Verma A, Vinogradov E, Thibault P, et al. (2004) Structural and genetic characterization of glycosylation of type a flagellin in Pseudomonas aeruginosa. J Bacteriol 186: 2523-2531.

202. Dell A, Galadari A, Sastre F, Hitchen P (2010) Similarities and differences in the glycosylation mechanisms in prokaryotes and eukaryotes. Int J Microbiol 2010: 148178.

203. Young NM, Brisson JR, Kelly J, Watson DC, Tessier L, et al. (2002) Structure of the N-linked glycan present on multiple glycoproteins in the Gram-negative bacterium, Campylobacter jejuni. J Biol Chem 277: 42530-42539.

204. Thomas RM, Twine SM, Fulton KM, Tessier L, Kilmury SL, et al. (2011) Glycosylation of DsbA in Francisella tularensis subsp. tularensis. J Bacteriol 193: 5498-5509.

205. Balonova L, Hernychova L, Mann BF, Link M, Bilkova Z, et al. (2010) Multimethodological approach to identification of glycoproteins from the proteome of Francisella tularensis, an intracellular microorganism. J Proteome Res 9: 1995-2005.

206. Jones BD, Faron M, Rasmussen JA, Fletcher JR (2014) Uncovering the components of the Francisella tularensis virulence stealth strategy. Front Cell Infect Microbiol 4: 32.

207. Balonova L, Mann BF, Cerveny L, Alley WR, Jr., Chovancova E, et al. (2012) Characterization of protein glycosylation in Francisella tularensis subsp. holarctica:

identification of a novel glycosylated lipoprotein required for virulence. Mol Cell Proteomics 11: M111 015016.

208. Bomberger JM, Maceachran DP, Coutermarsh BA, Ye S, O'Toole GA, et al. (2009) Long-distance delivery of bacterial virulence factors by Pseudomonas aeruginosa outer membrane vesicles. PLoS Pathog 5: e1000382.

209. Unal CM, Schaar V, Riesbeck K (2011) Bacterial outer membrane vesicles in disease and preventive medicine. Semin Immunopathol 33: 395-408.

210. McCaig WD, Koller A, Thanassi DG (2013) Production of outer membrane vesicles and outer membrane tubes by Francisella novicida. J Bacteriol 195: 1120-1132.

211. Pierson T, Matrakas D, Taylor YU, Manyam G, Morozov VN, et al. (2011) Proteomic Characterization and Functional Analysis of Outer Membrane Vesicles of Francisella novicida Suggests Possible Role in Virulence and Use as a Vaccine. Journal of Proteome Research 10: 954-967.

212. Fullner KJ, Mekalanos JJ (1999) Genetic characterization of a new type IV-A pilus gene cluster found in both classical and El Tor biotypes of Vibrio cholerae. Infect Immun 67: 1393-1404.

213. Mattick JS, Whitchurch CB, Alm RA (1996) The molecular genetics of type-4 fimbriae in Pseudomonas aeruginosa--a review. Gene 179: 147-155.

214. Craig L, Pique ME, Tainer JA (2004) Type IV pilus structure and bacterial pathogenicity. Nat Rev Microbiol 2: 363-378.

215. Gil H, Benach JL, Thanassi DG (2004) Presence of pili on the surface of Francisella tularensis. Infect Immun 72: 3042-3047.

216. Hobbs M, Mattick JS (1993) Common components in the assembly of type 4 fimbriae, DNA transfer systems, filamentous phage and protein-secretion apparatus: a general system for the formation of surface-associated protein complexes. Mol Microbiol 10: 233-243.

217. Hager AJ, Bolton DL, Pelletier MR, Brittnacher MJ, Gallagher LA, et al. (2006) Type IV pili-mediated secretion modulates Francisella virulence. Mol Microbiol 62: 227-237.

218. Chakraborty S, Monfett M, Maier TM, Benach JL, Frank DW, et al. (2008) Type IV pili in Francisella tularensis: roles of pilF and pilT in fiber assembly, host cell adherence, and virulence. Infect Immun 76: 2852-2861.

219. Ramakrishnan G, Meeker A, Dragulev B (2008) fslE is necessary for siderophore-mediated iron acquisition in Francisella tularensis Schu S4. J Bacteriol 190: 5353-5361.

220. Sen B, Meeker A, Ramakrishnan G (2010) The fslE homolog, FTL_0439 (fupA/B), mediates siderophore-dependent iron uptake in Francisella tularensis LVS. Infect Immun 78: 4276-4285.

221. Pan X, Tamilselvam B, Hansen EJ, Daefler S (2010) Modulation of iron homeostasis in macrophages by bacterial intracellular pathogens. BMC Microbiol 10: 64.

222. Costerton JW, Zbigniew Lewandowski, Douglas E. Caldwell, Darren R. Korber and Hilary M Lappin-Scott (1995) Microbial Biofilms. Annual Review of Microbiology 49: 711-745.

223. Chung MC, Dean S, Marakasova ES, Nwabueze AO, van Hoek ML (2014) Chitinases Are Negative Regulators of Francisella novicida Biofilms. PLoS One 9: e93119.

224. Dean RE, Ireland PM, Jordan JE, Titball RW, Oyston PC (2009) RelA regulates virulence and intracellular survival of Francisella novicida. Microbiology 155: 4104-4113.

225. van Hoek ML (2013) Biofilms: An advancement in our understanding of Francisella species. Virulence 4.

226. Zogaj X, Wyatt GC, Klose KE (2012) Cyclic di-GMP stimulates biofilm formation and inhibits virulence of Francisella novicida. Infect Immun 80: 4239-4247.

227. van Hoek ML (2013) Biofilms An advancement in our understanding of Francisella species. Virulence 4: 833-846.

228. Verhoeven AB, Durham-Colleran MW, Pierson T, Boswell WT, Van Hoek ML (2010) Francisella philomiragia biofilm formation and interaction with the aquatic protist Acanthamoeba castellanii. Biol Bull 219: 178-188.

229. Mahajan UV, Gravgaard J, Turnbull M, Jacobs DB, McNealy TL (2011) Larval exposure to Francisella tularensis LVS affects fitness of the mosquito Culex quinquefasciatus. FEMS Microbiol Ecol 78: 520-530.

230. Durham-Colleran MW, Verhoeven AB, van Hoek ML (2010) Francisella novicida forms in vitro biofilms mediated by an orphan response regulator. Microb Ecol 59: 457-465.

231. Margolis JJ, El-Etr S, Joubert LM, Moore E, Robison R, et al. (2010) Contributions of Francisella tularensis subsp. novicida chitinases and Sec secretion system to biofilm formation on chitin. Appl Environ Microbiol 76: 596-608.

232. Ellis J, Oyston PC, Green M, Titball RW (2002) Tularemia. Clin Microbiol Rev 15: 631-646.

233. Dennis DT, Inglesby TV, Henderson DA, Bartlett JG, Ascher MS, et al. (2001) Tularemia as a biological weapon: medical and public health management. JAMA 285: 2763-2773.

234. Staples JE, Kubota KA, Chalcraft LG, Mead PS, Petersen JM (2006) Epidemiologic and molecular analysis of human tularemia, United States, 1964-2004. Emerg Infect Dis 12: 1113-1118.

235. Penn RL (2005) *Francisella tularensis* (Tularemia). In: Mandell GL, Bennett JE, Dolin R, editors. Mandell, Douglas, and Bennett's Principals and Practice of Infectious Diseases. 6th ed. Philadelphia: Elsevier Churchill Livingstone. pp. 2674-2685.

236. Tigertt WD (1962) Soviet viable Pasteurella tularensis vaccines. A review of selected articles. Bacteriol Rev 26: 354-373.

237. Conlan J, Oyston P (2007) Vaccines against *Francisella tularensis*. Ann N Y Acad Sci 1105: 325-350.

238. Conlan JW (2004) Vaccines against Francisella tularensis--past, present and future. Expert Rev Vaccines 3: 307-314.

239. Fortier AH, Slayter MV, Ziemba R, Meltzer MS, Nacy CA (1991) Live vaccine strain of Francisella tularensis: infection and immunity in mice. Infect Immun 59: 2922-2928.

240. McCoy GW, Chapin CW (1912) Further observations on a plague-like diseases of rodents with a preliminary note on the causative agent, *Bacterium tularensis*. . J Infect Dis 10: 61-72.

241. Li J, C. Ryder, M. Mandal, F. Ahmed, P. Azadi, D.S. Snyder, R.D. Pechous, T. Zahrt, and T.J. Inzana. (2007) Attenuation and protective efficacy of an O-antigen-deficient mutant of *Francisella tularensis* LVS. Microbiol 153: 3141-3153.

242. Cole LE, Yang Y, Elkins KL, Fernandez ET, Qureshi N, et al. (2009) Antigen-specific B-1a antibodies induced by Francisella tularensis LPS provide long-term protection against F. tularensis LVS challenge. Proc Natl Acad Sci U S A 106: 4343-4348.

243. Dreisbach VC, Cowley S, Elkins KL (2000) Purified lipopolysaccharide from Francisella tularensis live vaccine strain (LVS) induces protective immunity against LVS infection that requires B cells and gamma interferon. Infect Immun 68: 1988-1996.

244. Fulop M, Manchee R, Titball R (1996) Role of two outer membrane antigens in the induction of protective immunity against Francisella tularensis strains of different virulence. FEMS Immunol Med Microbiol 13: 245-247.

245. McLendon MK, Apicella MA, Allen LA (2006) Francisella tularensis: taxonomy, genetics, and Immunopathogenesis of a potential agent of biowarfare. Annu Rev Microbiol 60: 167-185.

246. Sandström G, Löfgren S, Tärnvik A (1988) A capsule-deficient mutant of *Francisella tularensis* LVS exhibits enhanced sensitivity to killing but diminished sensitivity to killing by polymorphonuclear leukocytes. Infect Immun 56: 1194-1202.

247. Sjöstedt A (2005) Family III. *Francisellaceae*, *fam. nov.* In: D. J. Brenner NRK, and J. T. Staley, editor. Bergey's Manual of Systematic Bacteriology second edition. New York: Springer. pp. 199-210.

248. Sorokin VM, Pavlovich NV, Prozorova LA (1996) Francisella tularensis resistance to bactericidal action of normal human serum. FEMS Immunol Med Microbiol 13: 249-252.

249. Clemens DL, Horwitz MA (2007) Uptake and intracellular fate of Francisella tularensis in human macrophages. Ann N Y Acad Sci 1105: 160-186.

250. Cherwonogrodzky JW, Knodel MH, Spence MR (1994) Increased encapsulation and virulence of *Francisella tularensis* live vaccine strain (LVS) by subculturing on synthetic medium. Vaccine 12: 773-775.

251. Hood AM (1977) Virulence factors of *Francisella tularensis*. J Hyg (Lond) 79: 47-60.

252. Dubois M, Hamilton, A, Rebers, PA and Smith, F (1956) Anal Chem 28: 350-356.

253. Karkhanis Y, Zeltner, JA, Jackson, JJ and Carlo, DJ (1978) Anal Biochem 85: 595-601.

254. Merkle RK, Poppe I (1994) Carbohydrate composition analysis of glycoconjugates by gas-liquid chromatography/mass spectrometry. Methods Enzymol 230: 1-15.

255. Goldberg HA, Warner KJ (1997) The staining of acidic proteins on polyacrylamide gels: enhanced sensitivity and stability of "Stains-all" staining in combination with silver nitrate. Anal Biochem 251: 227-233.

256. Inzana TJ, Glindemann GE, Snider G, Gardner S, Crofton L, et al. (2004) Characterization of a wildtype strain of *Francisella tularensis* isolated from a cat. J Vet Diagn Invest 16: 374-381.

257. Ward CK, Inzana TJ (1994) Resistance of Actinobacillus pleuropneumoniae to bactericidal antibody and complement is mediated by capsular polysaccharide and blocking antibody specific for lipopolysaccharide. J Immunol 153: 2110-2121.

258. Altschul S, Gish, W, Miller, W, Myers, EW, Lipman DJ (1990) Basic local alignment search tool. J Mol Biol 215: 403-410.

259. Smith TF, Waterman MS (1981) Identification of common molecular subsequences. J Mol Biol 147: 195-197.

260. Sambrook J, Fritsch EF, Maniatis T (1989) Molecular cloning: a laboratory manual. Cold Spring Harbor, N.Y.: Cold Spring Harbor Laboratory.

261. Ried JL, Collmer A (1987) An nptI-sacB-sacR cartridge for constructing directed, unmarked mutations in gram-negative bacteria by marker exchange-eviction mutagenesis. Gene 57: 239-246.

262. Pavlov VM, Mokrievich AN, Volkovoy K (1996) Cryptic plasmid pFNL10 from *Francisella novicida*-like F6168: the base of plasmid vectors for *Francisella tularensis*. FEMS Immunol Med Microbiol 13: 253-256.

263. Maier TM, Havig A, Casey M, Nano FE, Frank DW, et al. (2004) Construction and characterization of a highly efficient Francisella shuttle plasmid. Appl Environ Microbiol 70: 7511-7519.

264. Kovach ME, Elzer PH, Hill DS, Robertson GT, Farris MA, et al. (1995) Four new derivatives of the broad-host-range cloning vector pBBR1MCS, carrying different antibiotic-resistance cassettes. Gene 166: 175-176.

265. Inzana TJ, Anderson P (1985) Serum factor-dependent resistance of *Haemophilus influenzae* type b to antibody to lipopolysaccharide. J Infect Dis 151: 869-877.

266. Cowley SC, Elkins KL (2003) Multiple T cell subsets control Francisella tularensis LVS intracellular growth without stimulation through macrophage interferon gamma receptors. J Exp Med 198: 379-389.

267. Ott LR (1993) An Introduction to Statistical Analysis. Fourth edition Duxbury Press: 260-290.

268. Lentner M, Bishop, T. (1993) Experimental Design and Analysis. Valley Book Company, Blacksburg, VA.

269. Messner P, Steiner K, Zarschler K, Schaffer C (2008) S-layer nanoglycobiology of bacteria. Carbohydr Res 343: 1934-1951.

270. Anderson P, Pitt J, Smith DH (1976) Synthesis and release of polyribophosphate by Haemophilus influenzae type b in vitro. Infect Immun 13: 581-589.

271. DeShazer D, Waag DM, Fritz DL, Woods DE (2001) Identification of a Burkholderia mallei polysaccharide gene cluster by subtractive hybridization and demonstration that the encoded capsule is an essential virulence determinant. Microb Pathog 30: 253-269.

272. Ward CK, Inzana TJ (1997) Identification and characterization of a DNA region involved in the export of capsular polysaccharide by Actinobacillus pleuropneumoniae serotype 5a. Infect Immun 65: 2491-2496.

273. Weiss DS, Brotcke A, Henry T, Margolis JJ, Chan K, et al. (2007) In vivo negative selection screen identifies genes required for Francisella virulence. Proc Natl Acad Sci U S A 104: 6037-6042.

274. Sleytr UB, Messner P, Pum D, Sara M (1993) Crystalline bacterial cell surface layers. Mol Microbiol 10: 911-916.

275. Sara M, Sleytr UB (2000) S-Layer proteins. J Bacteriol 182: 859-868.

276. Sleytr UB, Egelseer EM, Ilk N, Pum D, Schuster B (2007) S-Layers as a basic building block in a molecular construction kit. FEBS J 274: 323-334.

277. Schneitz C, Nuotio L, Lounatma K (1993) Adhesion of Lactobacillus acidophilus to avian intestinal epithelial cells mediated by the crystalline bacterial cell surface layer (S-layer). J Appl Bacteriol 74: 290-294.

278. Fouet A (2009) The surface of Bacillus anthracis. Mol Aspects Med 30: 374-385.

279. Mesnage S, Tosi-Couture E, Mock M, Gounon P, Fouet A (1997) Molecular characterization of the Bacillus anthracis main S-layer component: evidence that it is the major cell-associated antigen. Mol Microbiol 23: 1147-1155.

280. Sekot G, Posch G, Messner P, Matejka M, Rausch-Fan X, et al. (2011) Potential of the Tannerella forsythia S-layer to delay the immune response. J Dent Res 90: 109-114.

281. Sakakibara J, Nagano K, Murakami Y, Higuchi N, Nakamura H, et al. (2007) Loss of adherence ability to human gingival epithelial cells in S-layer protein-deficient mutants of Tannerella forsythensis. Microbiology 153: 866-876.

282. Awram P, Smit J (2001) Identification of lipopolysaccharide O antigen synthesis genes required for attachment of the S-layer of Caulobacter crescentus. Microbiology 147: 1451-1460.

283. Sleytr UBS, M; Pum, D; Schuster, B; Messner, P; Schaffer, C. (2002) Biopolymers; Steinbuchel AF, S.R., editor. Weinheim: Wiley-VCH.

284. Sara M, Sleytr UB (1996) Biotechnology and biomimetic with crystalline bacterial cell surface layers (S-layers). Micron 27: 141-156.

285. Schaffer C, Wugeditsch T, Neuninger C, Messner P (1996) Are S-layer glycoproteins and lipopolysaccharides related? Microb Drug Resist 2: 17-23.

286. Beveridge TJ, Pouwels PH, Sara M, Kotiranta A, Lounatmaa K, et al. (1997) Functions of S-layers. FEMS Microbiol Rev 20: 99-149.

287. Koval SF (1997) The effect of S-layers and cell surface hydrophobicity on prey selection by bacterivorous protozoa. FEMS Microbiol Rev 20: 138-142.

288. Leblebicioglu H, Esen S, Turan D, Tanyeri Y, Karadenizli A, et al. (2008) Outbreak of tularemia: a case-control study and environmental investigation in Turkey. Int J Infect Dis 12: 265-269.

289. Dubois M HA, Rebers PA, Smith F (1956) Colorimetric method for determination of sugars and related substances. Anal Chem 28: 350-356.

290. Min H, Cowman MK (1986) Combined alcian blue and silver staining of glycosaminoglycans in polyacrylamide gels: application to electrophoretic analysis of molecular weight distribution. Anal Biochem 155: 275-285.

291. Cooper C, Packer, N. and Williams, K. (2000) Amino Acid Analysis Protocols. Methods in Molecular Biology. Totawa, NJ: Humana Press.

292. Ozols J (1990) Amino acid analysis. In: Deutscher MP, editor. Guide to Protein Purification, Methods in Enzymology. San Diego, CA: Academic Press. pp. 587-601.

293. Kuen B, Sara M, Lubitz W (1996) Heterologous expression and self-assembly of the S-layer protein SbsA of Bacillus stearothermophilus in Escherichia coli. Mol Microbiol 19: 495-503.

294. Fagan RP, Fairweather NF (2014) Biogenesis and functions of bacterial S-layers. Nat Rev Microbiol 12: 211-222.

295. Auger S, Ramarao N, Faille C, Fouet A, Aymerich S, et al. (2009) Biofilm formation and cell surface properties among pathogenic and nonpathogenic strains of the Bacillus cereus group. Appl Environ Microbiol 75: 6616-6618.

296. Garduno RA, Phipps BM, Kay WW (1995) Physical and functional S-layer reconstitution in Aeromonas salmonicida. J Bacteriol 177: 2684-2694.

297. Kotiranta A (1997) Function of the S-layer of some Gram-positive bacteria in phagocytosis. FEMS Microbiol Rev 20: 110-114.

298. Kotiranta A, Haapasalo M, Kari K, Kerosuo E, Olsen I, et al. (1998) Surface structure, hydrophobicity, phagocytosis, and adherence to matrix proteins of Bacillus cereus cells with and without the crystalline surface protein layer. Infect Immun 66: 4895-4902.

299. Honma K, Inagaki S, Okuda K, Kuramitsu HK, Sharma A (2007) Role of a Tannerella forsythia exopolysaccharide synthesis operon in biofilm development. Microb Pathog 42: 156-166.

300. Sara M, Sleytr UB (1996) Crystalline bacterial cell surface layers (S-layers): from cell structure to biomimetics. Prog Biophys Mol Biol 65: 83-111.

301. Schaffer C, Messner P (2001) Glycobiology of surface layer proteins. Biochimie 83: 591-599.

302. Chitlaru T, Ariel N, Zvi A, Lion M, Velan B, et al. (2004) Identification of chromosomally encoded membranal polypeptides of Bacillus anthracis by a proteomic analysis: prevalence of proteins containing S-layer homology domains. Proteomics 4: 677-691.

303. Takeoka A, Takumi K, Koga T, Kawata T (1991) Purification and characterization of S layer proteins from Clostridium difficile GAI 0714. J Gen Microbiol 137: 261-267.

304. Takumi K, Susami Y, Takeoka A, Oka T, Koga T (1991) S layer protein of Clostridium tetani: purification and properties. Microbiol Immunol 35: 569-575.

305. Kuen BaLW (1996) Analysis of S-layer proteins and genes. In: Sleytr UB, Messner P., Pum D., Sara M., editor. Crystalline bacterial cell surface proteins. Austin, TX: Academic Press, Landes Company. pp. 77-102.

306. Mesnage S, Fontaine T, Mignot T, Delepierre M, Mock M, et al. (2000) Bacterial SLH domain proteins are non-covalently anchored to the cell surface via a conserved mechanism involving wall polysaccharide pyruvylation. EMBO J 19: 4473-4484.

307. Pavkov T, Egelseer EM, Tesarz M, Svergun DI, Sleytr UB, et al. (2008) The structure and binding behavior of the bacterial cell surface layer protein SbsC. Structure 16: 1226-1237.

308. Ryan A, Lynch M, Smith SM, Amu S, Nel HJ, et al. (2011) A role for TLR4 in Clostridium difficile infection and the recognition of surface layer proteins. PLoS Pathog 7: e1002076.

309. Blaser MJ, Smith PF, Repine JE, Joiner KA (1988) Pathogenesis of Campylobacter fetus infections. Failure of encapsulated Campylobacter fetus to bind C3b explains serum and phagocytosis resistance. J Clin Invest 81: 1434-1444.

310. McCrumb FR (1961) Aerosol Infection of Man with Pasteurella Tularensis. Bacteriol Rev 25: 262-267.

311. Chen W, Shen H, Webb A, KuoLee R, Conlan JW (2003) Tularemia in BALB/c and C57BL/6 mice vaccinated with Francisella tularensis LVS and challenged intradermally, or by aerosol with virulent isolates of the pathogen: protection varies depending on pathogen virulence, route of exposure, and host genetic background. Vaccine 21: 3690-3700.

312. Oyston PC, Sjostedt A, Titball RW (2004) Tularaemia: bioterrorism defence renews interest in Francisella tularensis. Nat Rev Microbiol 2: 967-978.

313. Meibom KL, Barel M, Charbit A (2009) Loops and networks in control of Francisella tularensis virulence. Future Microbiol 4: 713-729.

314. Inzana TJ, Glindemann GE, Snider G, Gardner S, Crofton L, et al. (2004) Characterization of a wild-type strain of Francisella tularensis isolated from a cat. J Vet Diagn Invest 16: 374-381.

315. Inzana TJ, Champion A (2007) Use of an inhibition enzyme-linked immunosorbent assay for quantification of capsular polysaccharide or proteins in vaccines. Clin Vaccine Immunol 14: 323-327.

316. Schneerson R, Barrera O, Sutton A, Robbins JB (1980) Preparation, characterization, and immunogenicity of Haemophilus influenzae type b polysaccharide-protein conjugates. J Exp Med 152: 361-376.

317. Bordier C (1981) Phase separation of integral membrane proteins in Triton X-114 solution. J Biol Chem 256: 1604-1607.

318. Avila-Calderon ED, Lopez-Merino A, Jain N, Peralta H, Lopez-Villegas EO, et al. (2012) Characterization of outer membrane vesicles from Brucella melitensis and protection induced in mice. Clin Dev Immunol 2012: 352493.

319. Gamazo C, Winter AJ, Moriyon I, Riezu-Boj JI, Blasco JM, et al. (1989) Comparative analyses of proteins extracted by hot saline or released spontaneously into outer membrane blebs from field strains of Brucella ovis and Brucella melitensis. Infect Immun 57: 1419-1426.

320. Miller D, O'Brien K, Xu H, White RH (2014) Identification of a 5'-deoxyadenosine deaminase in Methanocaldococcus jannaschii and its possible role in recycling the radical S-adenosylmethionine enzyme reaction product 5'-deoxyadenosine. J Bacteriol 196: 1064-1072.

321. Konecna K, Hernychova L, Reichelova M, Lenco J, Klimentova J, et al. (2010) Comparative proteomic profiling of culture filtrate proteins of less and highly virulent Francisella tularensis strains. Proteomics 10: 4501-4511.

322. Cervenka R, Zelinkova H, Konecna M, Komarek J (2010) Electrochemical modification of a graphite platform for a solid sampling electrothermal atomic absorption spectrometry of mercury. Anal Sci 26: 989-993.

323. Tandon NN, Lipsky RH, Burgess WH, Jamieson GA (1989) Isolation and characterization of platelet glycoprotein IV (CD36). J Biol Chem 264: 7570-7575.

324. Nallaparaju KC (2008) The Role of a Novel Outer Membrane Protein of Francisella tularensis in Host-pathogen Interactions: ProQuest.

325. Eyles JE, Hartley MG, Laws TR, Oyston PC, Griffin KF, et al. (2008) Protection afforded against aerosol challenge by systemic immunisation with inactivated Francisella tularensis live vaccine strain (LVS). Microb Pathog 44: 164-168.

326. Kirimanjeswara GS, Olmos S, Bakshi CS, Metzger DW (2008) Humoral and cell-mediated immunity to the intracellular pathogen Francisella tularensis. Immunol Rev 225: 244-255.

327. Nigrovic LE, Wingerter SL (2008) Tularemia. Infect Dis Clin North Am 22: 489-504, ix.

328. Eliasson H, Back E (2007) Tularaemia in an emergent area in Sweden: an analysis of 234 cases in five years. Scand J Infect Dis 39: 880-889.

329. Petersen JM, Schriefer ME, Gage KL, Montenieri JA, Carter LG, et al. (2004) Methods for enhanced culture recovery of Francisella tularensis. Appl Environ Microbiol 70: 3733-3735.

330. Vinogradov EV, Shashkov AS, Knirel YA, Kochetkov NK, Tochtamysheva NV, et al. (1991) Structure of the O-antigen of Francisella tularensis strain 15. Carbohydr Res 214: 289-297.

331. Cywes-Bentley C, Skurnik D, Zaidi T, Roux D, Deoliveira RB, et al. (2013) Antibody to a conserved antigenic target is protective against diverse prokaryotic and eukaryotic pathogens. Proc Natl Acad Sci U S A 110: E2209-2218.

332. Farlow J, Wagner DM, Dukerich M, Stanley M, Chu M, et al. (2005) Francisella tularensis in the United States. Emerg Infect Dis 11: 1835-1841.

333. Jarrett CO, Deak E, Isherwood KE, Oyston PC, Fischer ER, et al. (2004) Transmission of Yersinia pestis from an infectious biofilm in the flea vector. J Infect Dis 190: 783-792.

334. Hopla CE, Durden LA, Keirans JE (1994) Ectoparasites and classification. Rev Sci Tech 13: 985-1017.

335. Modise T, Ryder C, Mane SP, Bandara AB, Jensen RV, et al. (2012) Genomic comparison between a virulent type A1 strain of Francisella tularensis and its attenuated O-antigen mutant. J Bacteriol 194: 2775-2776.

336. Melillo A, Sledjeski DD, Lipski S, Wooten RM, Basrur V, et al. (2006) Identification of a Francisella tularensis LVS outer membrane protein that confers adherence to A549 human lung cells. FEMS Microbiol Lett 263: 102-108.

337. Park KM, So JS (2000) Altered cell surface hydrophobicity of lipopolysaccharide-deficient mutant of Bradyrhizobium japonicum. J Microbiol Methods 41: 219-226.

338. Kempf M, Eveillard M, Deshayes C, Ghamrawi S, Lefrancois C, et al. (2012) Cell surface properties of two differently virulent strains of Acinetobacter baumannii isolated from a patient. Can J Microbiol 58: 311-317.

339. Nakao R, Ramstedt M, Wai SN, Uhlin BE (2012) Enhanced biofilm formation by Escherichia coli LPS mutants defective in Hep biosynthesis. PLoS One 7: e51241.

340. Lee YW, Jeong SY, In YH, Kim KY, So JS, et al. (2010) Lack of O-polysaccharide enhances biofilm formation by Bradyrhizobium japonicum. Lett Appl Microbiol 50: 452-456.

341. Murphy K, Park AJ, Hao Y, Brewer D, Lam JS, et al. (2014) Influence of O polysaccharides on biofilm development and outer membrane vesicle biogenesis in Pseudomonas aeruginosa PAO1. J Bacteriol 196: 1306-1317.

342. Davey ME, Duncan MJ (2006) Enhanced biofilm formation and loss of capsule synthesis: deletion of a putative glycosyltransferase in Porphyromonas gingivalis. J Bacteriol 188: 5510-5523.

343. Lees-Miller RG, Iwashkiw JA, Scott NE, Seper A, Vinogradov E, et al. (2013) A common pathway for O-linked protein-glycosylation and synthesis of capsule in Acinetobacter baumannii. Mol Microbiol 89: 816-830.

344. Hug I, Feldman MF (2011) Analogies and homologies in lipopolysaccharide and glycoprotein biosynthesis in bacteria. Glycobiology 21: 138-151.

345. Gerke C, Kraft A, Sussmuth R, Schweitzer O, Gotz F (1998) Characterization of the N-acetylglucosaminyltransferase activity involved in the biosynthesis of the

Staphylococcus epidermidis polysaccharide intercellular adhesin. J Biol Chem 273: 18586-18593.

APPENDIX

A1 Supplemental reference images

Figures are derived from the as yet unpublished dissertation work of Cheryl Ryder.

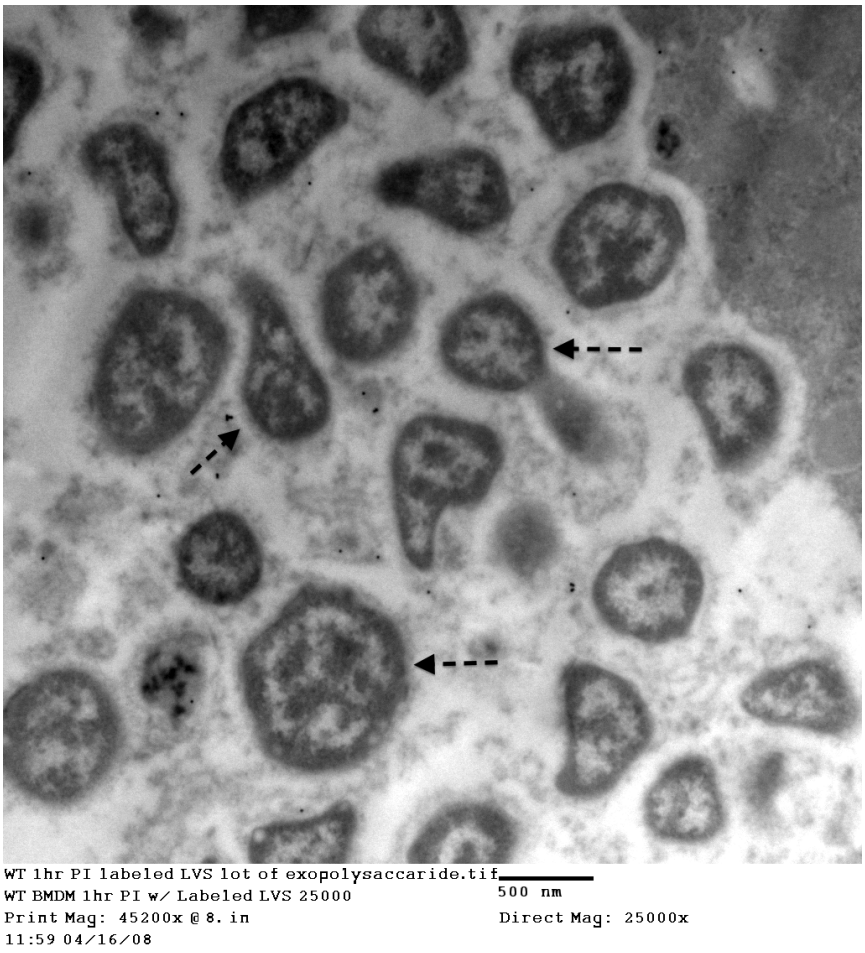

Figure A1 Multiple *Francisella* LVS in BMDM vacuole with CLC material evident.

BMDM infected with LVS (selected cells indicated by dotted arrow) 1 hour post-infection and negatively stained with uranyl acetate. Visualized with TEM, 31500x magnification. Multiple LVS cells inside a vacuole of an infected BMDM. Vesicular CLC material is evident surrounding all LVS cells.

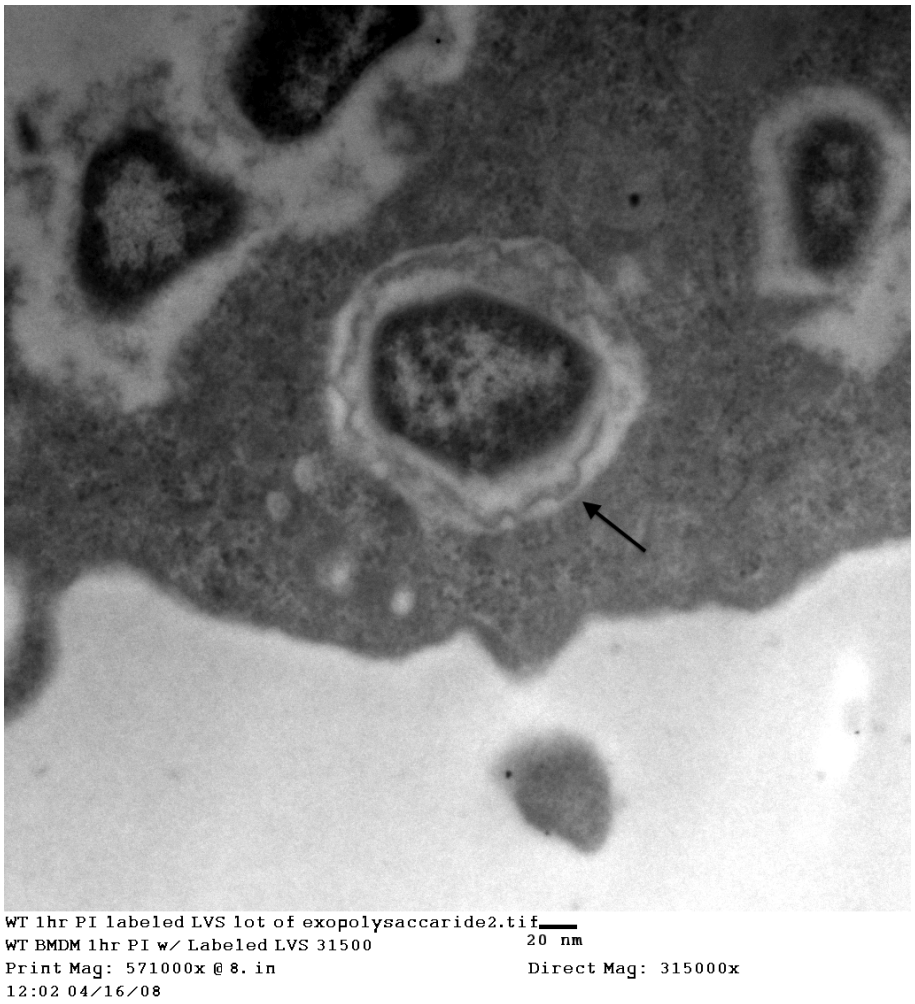

Figure A2 ***Francisella*** **LVS in BMDM vacuole with CLC material evident.** BMDM infected with LVS 1 hour post-infection and negatively stained with uranyl acetate. Visualized with TEM, 31500x magnification. LVS cell with CLC vesicular material (indicated by arrow) surrounding the cell inside a vacuole.